UNIVERSITAT POLITÈCNICA DE VALÈNCIA

DEPARTAMENTO DE TECNOLOGÍA DE ALIMENTOS
CENTRO DE RECONOCIMIENTO MOLECULAR
Y DESARROLLO TECNOLÓGICO

Use of silica supports for enhancing the stability of folates and developing antimicrobial agents

Submitted by

María Ruiz Rico

PhD Supervisors:

Prof. José Manuel Barat Baviera
Dr. María Dolores Marcos Martínez
Dr. Édgar Pérez Esteve

Valencia, October 2016

JOSÉ MANUEL BARAT BAVIERA, PhD in Food Technology and Professor at the *Universitat Politècnica de València*, MARÍA DOLORES MARCOS MARTÍNEZ, PhD in Chemistry and Lecturer at the *Universitat Politècnica de València,* and ÉDGAR PÉREZ ESTEVE, PhD in Food Technology

CERTIFY:

That the work *"***Use of silica supports for enhancing the stability of folates and developing antimicrobial agents"** has been developed by María Ruiz Rico under their supervision in the Departamento de Tecnología de Alimentos and the Centro de Reconocimiento Molecular y Desarrollo Tecnológico (IDM) of the *Universitat Politècnica de València*, as a Thesis Project in order to obtain the degree of PhD in Food Technology at the *Universitat Politècnica de València.*

Valencia, October 2016.

Prof. José Manuel Barat Baviera   Dr. Mª Dolores Marcos Martínez   Dr. Édgar Pérez Esteve

Acknowledgements

Agradecimientos

Resumen

La presente tesis doctoral, que lleva por título "Uso de soportes de sílice para la mejora de la estabilidad de los folatos y el desarrollo de agentes antimicrobianos", se centra en el desarrollo y evaluación de nuevos sistemas inteligentes basados en el uso de nano- y micropartículas de sílice como soporte inorgánico para la encapsulación o inmovilización de dos tipos de compuestos de interés para la industria alimentaria: vitaminas y antimicrobianos.

El primer capítulo muestra el efecto de la encapsulación de ácido fólico y 5-formiltretahidrofolato en micropartículas mesoporosas de sílice funcionalizadas con poliaminas sobre la bioaccessibilidad y estabilidad de ambos vitámeros. Por una parte, el uso de este soporte híbrido orgánico-inorgánico permite modular la liberación de la vitamina en función del pH del medio (inhibición de la liberación a pH ácido -estómago- y liberación controlada a pH neutro -intestino-) en sistemas *in vitro*. Así mismo, el soporte mesoporoso es capaz de proteger a la vitamina frente a la degradación tras la exposición a diversos agentes externos, como el pH, la temperatura o la luz. Además, la incorporación de ácido fólico encapsulado a zumos de frutas (manzana y naranja) ha permitido estudiar la capacidad moduladora y protectora del sistema de liberación en una matriz alimentaria real. Este estudio ha demostrado que el soporte funcionalizado con poliaminas no sólo es capaz de mantener el ácido fólico en el interior de los poros tras la incorporación a los zumos y modular correctamente la liberación del mismo tras la simulación de una digestión *in vitro*, sino que también es capaz de proteger la vitamina tras la simulación del procesado y almacenamiento de los zumos. Por tanto, el sistema de liberación propuesto puede ser una excelente alternativa a la fortificación directa para mantener la vitamina estable durante la producción y almacenamiento de los alimentos, así como para modificar la bioaccesibilidad del ácido fólico a lo largo del tracto gastrointestinal.

Resumen

En el segundo capítulo se describe el desarrollo de diferentes agentes antimicrobianos, basados en la combinación de compuestos activos orgánicos con diversos materiales de sílice. Para ello, se han usado dos metodologías diferentes: la encapsulación del agente antimicrobiano en los poros de las partículas mesoporosas de sílice, y la inmovilización del compuesto activo sobre la superficie de las partículas de sílice. El efecto de la encapsulación sobre la mejora de las propiedades antimicrobianas de un compuesto ha sido estudiado determinando la actividad antimicrobiana de ácido caprílico libre y encapsulado en nanopartículas mesoporosas tipo MCM-41 frente a diversas bacterias patógenas presentes en alimentos. Los resultados de los ensayos *in vitro* de susceptibilidad bacteriana y la determinación del daño celular mediante microscopia muestran que el nanodispositivo mantiene las propiedades antimicrobianas respecto al ácido caprílico libre. El efecto de la inmovilización de un compuesto activo sobre la superficie de un soporte en la mejora de sus propiedades antimicrobianas ha sido estudiado con dos tipos de moléculas diferentes: poliaminas (usadas como puerta molecular en el sistema de liberación de folatos) y aceites esenciales. En ambos casos la inmovilización del compuesto bioactivo incrementa entre 1-100 veces el poder antimicrobiano de las moléculas libres tanto en ensayos *in vitro*, como en ensayos en alimentos reales (zumos de frutas y leche pasteurizada) donde se ha comprobado que los compuestos inmovilizados tienen un efecto bacteriostático a lo largo del período de almacenamiento mientras que concentraciones equivalentes de compuesto libre permiten el crecimiento del microorganismo.

En resumen, se puede concluir que en la presente tesis se ha evaluado la versatilidad de los materiales de sílice para solventar dos de los grandes problemas de la industria alimentaria: alteración de compuestos bioactivos durante el procesado del alimento y la pérdida de la eficacia de los sistemas antimicrobianos actuales. Así, los dispositivos desarrollados podrían ser usados como métodos alternativos a los sistemas tradicionales de encapsulación o a los tratamientos tradicionales para asegurar la inocuidad de los alimentos.

Resum

La present tesi doctoral, que porta per títol "Ús de suports de sílice per a la millora de l'estabilitat dels folats i el desenvolupament d'agents antimicrobians", es centra en el desenvolupament i avaluació de nous sistemes intel·ligents basats en l'ús de nano- i micropartícules de sílice com a suport inorgànic per a l'encapsulació o immobilització de dos tipus de compostos d'interès per a la indústria alimentària: vitamines i antimicrobians.

El primer capítol mostra l'efecte de l'encapsulació d'àcid fòlic i 5-formiltretahidrofolat en micropartícules mesoporoses de sílice funcionalitzades amb poliamines sobre la bioaccessibilitat i estabilitat d'ambdós vitàmers. D'una banda, l'ús d'aquest suport híbrid orgànic-inorgànic permet modular l'alliberament de la vitamina en funció del pH del medi (inhibició de l'alliberament a pH àcid –estómac- i alliberament controlat a pH neutre –intestí-) en sistemes *in vitro*. Així mateix, el suport mesoporós és capaç de protegir a la vitamina enfront de la degradació després de l'exposició a diversos agents externs, com el pH, la temperatura o la llum. A més, la incorporació d'àcid fòlic encapsulat a sucs de fruites (poma i taronja) ha permès estudiar la capacitat moduladora i protectora del sistema d'alliberament en una matriu alimentària real. Aquest estudi ha demostrat que el suport funcionalitzat amb poliamines no sols és capaç de mantindre l'àcid fòlic a l'interior dels porus després de la incorporació als sucs i modular correctament l'alliberament del mateix després de la simulació d'una digestió *in vitro*, sinó que també és capaç de protegir la vitamina després de la simulació del processat i emmagatzemament dels sucs. Per tant, el sistema d'alliberament proposat pot ser una excel·lent alternativa a la fortificació directa per mantindre la vitamina estable durant de la producció i emmagatzemament dels aliments, així com per modificar la bioaccessibilitat de l'àcid fòlic al llarg del tracte gastrointestinal.

Resum

En el segon capítol es descriu el desenvolupament de diferents agents antimicrobians, basats en la combinació de compostos actius orgànics amb diversos materials de sílice. Per a això, s'han usat dues metodologies diferents: l'encapsulació de l'agent antimicrobià en els porus de les partícules mesoporoses de sílice, i la immobilització del compost actiu sobre la superfície de les partícules de sílice. L'efecte de l'encapsulació sobre la millora de les propietats antimicrobianes d'un compost ha sigut estudiat determinant l'activitat antimicrobiana d'àcid caprílic lliure i encapsulat en nanopartícules mesoporoses tipus MCM-41 enfront de diversos bacteris patògens presents en aliments. Els resultats dels assajos *in vitro* de susceptibilitat bacteriana i la determinació del dany cel·lular per mitjà de microscòpia mostren que el nanodispositiu manté les propietats antimicrobianes respecte a l'àcid caprílic lliure. L'efecte de la immobilització d'un compost actiu sobre la superfície d'un suport en la millora de les seues propietats antimicrobianes ha sigut estudiat amb dues tipus de molècules diferents: poliamines (usades com a porta molecular en el sistema d'alliberament de folats) i olis essencials. En ambdós casos la immobilització del compost bioactiu incrementa entre 1-100 vegades el poder antimicrobià de les molècules lliures tant en assajos *in vitro*, com en assajos en aliments reals (sucs de fruites i llet pasteuritzada) on s'ha comprovat que els compostos immobilitzats tenen un efecte bacteriostàtic al llarg del període d' emmagatzemament mentre que concentracions equivalents de compost lliure permeten el creixement del microorganisme.

En resum, es pot concloure que en la present tesi s'ha avaluat la versatilitat dels materials de sílice per a resoldre dos dels grans problemes de la indústria alimentària: alteració de compostos bioactius durant el processat de l'aliment i la pèrdua de la eficàcia dels sistemes antimicrobians actuals. Així, els dispositius desenvolupats podrien ser usats com a mètodes alternatius als sistemes tradicionals d'encapsulació o els tractaments tradicionals per assegurar la innocuïtat dels aliments.

Abstract

The present PhD thesis, entitled "Use of silica supports for enhancing the stability of folates and developing antimicrobial agents", focuses on the development and evaluation of new smart systems based on the use of silica nano- and microparticles as inorganic supports for the encapsulation or immobilization of two compounds types of interest to the food industry: vitamins and antimicrobials.

The first chapter shows the effect of encapsulation of folic acid and 5-formyltetrahydrofolate in mesoporous silica microparticles functionalized with polyamines on the bioaccessibility and stability of both vitamers. The use of this hybrid organic-inorganic support allows the modification of the delivery of the vitamin dependent on the pH of the medium (inhibition of the release at an acidic pH, e.g. stomach, controlled release at a neutral pH, e.g. intestine) in *in vitro* systems. Also, the mesoporous support can protect the vitamin against degradation after exposure to external agents, such as pH, temperature or light. Furthermore, the incorporation of encapsulated folic acid into fruit juices (apple and orange) allowed us to study the modulating and protective capability of the delivery system in a real food matrix. This study has demonstrated that the amine-functionalized support is able to not only maintain folic acid inside pores after its incorporation into juices and to properly modify the delivery of the vitamin after simulated *in vitro* digestion, but to also protect the vitamin after the simulating the processing and storage of juices. Therefore, the proposed delivery system could be an excellent alternative to direct fortification in order to maintain vitamin stability during food production and storage, and to modify folic acid bioaccessibility along the gastrointestinal tract.

The second chapter describes development of different antimicrobial agents based on the combination of organic active compounds with diverse silica materials. To this end, two different methodologies have been used: encapsulation of the antimicrobial agent in the pores of mesoporous silica

particles, and immobilization of the active compound on the surface of silica particles. The effect of encapsulation on the enhancement of the antimicrobial properties of a compound has been studied by evaluating the antimicrobial activity of free and MCM-41 nanoparticles encapsulated caprylic acid against diverse pathogen food-borne bacteria. The results of the *in vitro* bacterial susceptibility assays and the determination of cellular damage by microscopy show that the nanodevice maintains antimicrobial properties in relation to the free caprylic acid. The effect of the immobilization of an active compound on the surface of a support on the improvement of its antimicrobial properties has beem studied with two types of different molecules: polyamines (used as a molecular gate in the folates delivery system) and essential oils. In both cases, immobilization of the bioactive compound increases the antimicrobial effect of free molecules between 1- and 100-fold in the *in vitro* assays and in real food systems (fruit juices and pasteurized milk), in which immobilized compounds have a bacteriostatic effect during storage, while the equivalent free compound concentrations allow microbial growth.

In summary, it is concluded that the present thesis has evaluated the versatility of silica materials to solve two of the biggest problems in the food industry: alteration of active compounds during food processing and current antimicrobial systems losing of efficacy. Thus the developed devices may be used as alternative methods to traditional encapsulation systems or traditional food safety treatments.

TABLE OF CONTENTS

1. PREAMBLE

1. PREAMBLE

This PhD thesis forms part of the projects "***Improvement of the stability and control release of biomolecules by using microcapsules functionalized with molecular gates*** (AGL2012-39597-C02-01)" and "***Use of biocompatible supports for the development of new antimicrobials and controlled release systems*** (AGL2015-70235-C2-1-R)", funded by the 2013-2016 and 2016-2019 National Research Plan of the Spanish Ministry of Economy and Competitiveness, respectively.

Protecting bioactive molecules is a most interesting subject in food technology. The functional activity of bioactive molecules can be drastically reduced *in vivo* due to transformations during processing, conservation, and even during digestion. In addition, some bioactive molecules are not compatible with the food matrix because of issues of solubility or organoleptic properties.

In this context, the main objective of the project "***Improvement of the stability and control release of biomolecules by using microcapsules functionalized with molecular gates***" was to enhance the bioaccessibility and stability of bioactive substances of nutritional interest by encapsulation in gated materials. These gated materials contain an inorganic support (mesoporous silica particles) that acts as a container for biomolecules and a switchable "gate-like" ensemble capable of being "open" or "closed" when certain external stimuli are applied to thus, allow the controlled release of the biomolecule.

This first project has led to new research lines based on the limitations or findings that arose while it was underway. These shortcomings are the achievement of the zero release of the bioactive compound, the difficulty of achieving capsules which are economic and stable enough to withstand processing, storage and/or food intake, and the possibility of encapsulating large molecules. Studies into the potential toxicity of the gated material on bacterial

viability have allowed the potential antimicrobial effect of these particles to be noted.

Therefore, the main objective of the second project, "***Use of biocompatible supports for the development of new antimicrobials and controlled release systems***", was to develop particles with antimicrobial activity by anchoring naturally-occurring antimicrobials, and to develop new and cheaper smart delivery systems based on hybrid materials for controlled release in the digestive tract.

The doctoral thesis entitled "Use of silica supports for enhancing the stability of folates and developing antimicrobial agents" is the second doctoral thesis undertaken within this framework.

2. OBJECTIVES

2. OBJECTIVES

The main objective of this PhD thesis was to enhance the stability of folates by encapsulation in gated materials based on porous silica supports functionalized with polyamines, and to develop new antimicrobial agents based on the attachment of bioactive molecules to the surface of silica particles.

To meet the main objective, the present thesis was divided into two different approaches with the following specific objectives:

a. ***Toward the enhancement of folates stability through silica supports.*** This was addressed to evaluate the protective effect and controlled release capability of mesoporous silica particles on folates encapsulation.

I. To synthesize and characterize smart delivery systems capable of delivering large amounts of folates with a minimum amount of support.

II. To assess the capability of the developed smart delivery systems to modulate folates delivery according to pH (i.e. hinder releases at an acidic pH and allow the sustained release at a neutral pH).

III. To evaluate the stability of free and entrapped folates against different environmental stimulus.

b. ***Toward the development of new antimicrobial agents based on silica supports.*** This was addressed to create antimicrobial supports by encapsulation, and by anchoring bioactive and naturally-occurring antimicrobial molecules in silica particles.

IV. To design, synthesize, characterize and apply new antimicrobial particles.

V. To assess the antibacterial activity of new antimicrobial agents *in vitro* and in real food systems, and to compare the inhibitory effect with free bioactive antimicrobial compounds.

3. GENERAL INTRODUCTION[1]

[1]General Introduction is based on the book chapter: Pérez-Esteve, É., Ruiz-Rico, M., Martínez-Máñez, R., & Barat, J.M. (2016). Mesoporous silica particles as encapsulation and delivery systems for food ingredients and nutraceuticals. In: Sen, S., & Pathak, Y. (Eds) Nanotechnology in Nutraceuticals: Production to Consumption. CRC Press. *In press*

1. Mesoporous silica particles as systems for the encapsulation and delivery of food ingredients and nutraceuticals

Mesoporous silica particles (MSPs) are structures of silicon dioxide (SiO_2) arranged so that they are able to create pores between 2 and 50 nm (Zhao, 2006). The first described porous silica with a uniform pore size, called folded sheet mesoporous materials (FSM-16), was reported by Kuroda and co-workers in 1990 (Yanagisawa et al., 1990). A few years later, in 1992, researchers of the Mobil Company reported the synthesis of a family of mesoporous silica materials called M41S (Beck et al., 1992) that include hexagonal MCM-41, cubic MCM-48, and lamellar MCM-50.

In 2001, Vallet-Regí and co-workers explored properties of MSPs for controlling the delivery of bioactive molecules. In that case, they reported the encapsulation and controlled release of ibuprofen from MCM-41 (Vallet-Regí et al., 2001). Since then, MSPs have witnessed an exponential increase in the number of applications and they have been used not only in the controlled release of drugs for biomedical applications, but also of nutrients, antioxidants, antimicrobials, peptides, aromas, or enzymes, among others, for food applications (Hisamatsu et al., 2012; Izquierdo-Barba et al., 2009a; Pérez-Esteve et al., 2015; Popova et al., 2014; Veith et al., 2004). Given the potential use of these particles in a myriad of applications, it is not surprising that research concerning the use of MSPs is one of the hottest areas in nanobiotechnology (Tang et al., 2012).

Among the number of characteristics exhibited by MSPs that allow their utilization as supports for the encapsulation and delivery of food ingredients the following are the most important.

- *High loading capacity*⸺MSPs exhibit in their structure a large number of mesopores that confers to the particles high specific surface areas (700-1000 $m^2\ g^{-1}$) and a great loading capacity also related to large pore sizes (2-10 nm), specific pore volumes (0.6-1 $cm^3\ g^{-1}$) and total surface (1000 $cm^2\ g^{-1}$) (Colilla et al., 2013). Pore size and specific pore volume are

essential to encapsulate a sufficiently high amount of a certain bioactive component efficiently until it needs to be delivered.

- *Programmable pore size and well defined structure*—In contrast to most porous minerals that show disordered pores with a broad size distribution and irregular shapes, MSPs display ordered mesopores with a narrow size distribution (Charnay et al., 2004). The capacity to tailor the pore diameter during the particle synthesis allows a precise control of the release rate of the payload molecule. Generally, a small pore size conducts to low release rates, while a pore enlargement increases release rates. In fact, depending on the pore size (in uncapped MSPs) drug release can occur in a wide period such as minutes, hours or days.

- *Two functional surfaces*—MSPs have two different functional surfaces: the internal surface (i.e. cylindrical pores) and the external surface (i.e. exterior particle surface). This characteristic allows the selective functionalization of the internal and/or external surfaces with different organic groups (Slowing et al., 2008).

- *Zero-release*—One appealing concept of MSPs as delivery carriers is the possibility to develop gated nanodevices exhibiting "zero premature release". These materials are prepared by reacting molecular or supramolecular caps with a free silanol group of the surface of the particles previously loaded with a particular cargo. The caps or "gates" can then be opened and the cargo delivered at-will upon the application of a given stimulus (Coll et al., 2013). This zero-release behavior allows the possibility to preserve functional properties as well as modulate the bioaccessibility of the cargo molecules during food production, storage, or digestion. In particular, MSPs capped with organic molecules acting as molecular gates that inhibit the release of their cargo triggered by specific stimuli (e.g. pH, enzymes, surfactant, etc.) are presented in this chapter. See Section 2.3.3. for details.

- *Stability against chemical, biological and thermal attack*⸺In their structure, MSPs show thick walls (i.e. 1.5-3 nm). Due to this characteristic, MSPs have significant advantage compared to most general organic carriers (liposomes, micelles, capsules), being stable against chemical, biological and thermal attack (El Mourabit et al., 2012; He & Shi, 2011; Tischer & Wedekind, 1999).

- *Generally recognized as safe composition*⸺Silicon dioxide (SiO_2) is "Generally Recognized as Safe" (GRAS) by Food and Drug Administration (FDA) regulations in U.S. and New Zealand. It is also an authorized additive in Europe and achieves E-551 classification (Contado et al., 2013). In food industry, synthetic amorphous silica has been used for many years to clear beers and wines, as an anticaking agent to maintain the flow properties of powder products, as a carrier agent for flavorings and aromas, and to thicken pastes. Moreover, silica, such as aerosil, is a widely used pharmaceutical excipient (Charnay et al., 2004).

- *Biocompatibility*⸺Application of MSPs as encapsulation carriers requires biocompatibility and low toxicity. Although it is hard to draw conclusive conclusions about biocompatibility and toxicity of MSPs, it has been reported, from *in vitro* and *in vivo* studies, that MSPs are generally well tolerated by both, cells and superior animals (He et al., 2009; Kupferschmidt et al., 2013). Moreover, it has so been reported that the use of mesoporous silica microparticles functionalized in their surface with biocompatible organic molecule improves the biocompatibility of MSPs as supports for the encapsulation of food ingredients and nutraceuticals (Tang et al., 2012).

- *Improved dissolution rate of poorly water-soluble molecules*⸺Well-ordered porous structure of MSPs can control the crystallinity of bioactive molecules in the solid dispersion system. It leads to a much improved dissolution rate that increases the dissolution properties of poorly water-soluble molecules. One of the molecules that has been demonstrated an

increased solubility rate after encapsulation in ordered mesoporous silica particles is the commonly known antioxidant resveratrol (Quan et al., 2012).

- *Protects its cargo against degradation*⸺MSPs have the ability to protect their entrapped cargo against oxidation, enzymatic degradation or denaturation induced by pH or temperature (Arcos & Vallet-Regí, 2013). Among bioactive molecules that have been protected from the environment via the encapsulation in MSPs highlight enzymes (Zhao et al., 2013), or the flavonoid quercetin (Berlier et al., 2013).

- *Food matrix compatibility*⸺It is considered that a delivery system suitable for a particular application should be compatible with the food or beverage matrix, without causing any adverse effects on product appearance, flavor, texture, mouth feel or shelf life. In spite of the importance of this aspect, as far as we know, there is only one publication dealing with the establishment of the influence of MSPs in physical properties of the food matrix (Pérez-Esteve et al., 2014). In this work we demonstrated that mechanical properties of the gels filled with bare or functionalized MSPs remained or improved with the addition of MSPs depending on the particle size, surface functionalization and particle concentration. Large particles or small concentration resulted in a small absolute number of particles embedded in the matrix, having as a result a minimum modification of textural properties. Small particles or high volume fractions reinforced protein networks and increased Young's modulus and fracture properties. Moreover, keeping in mind that MSPs have a high load capacity, when bioactive compounds exhibit functional properties at very low concentrations, it is presumed that the amount of loaded MSPs needed to release an adequate concentration of the component might be very low. In these cases it is foreseen that physicochemical features of the matrix incorporating MSPs should not be affected.

2. Preparation of delivery systems based on functionalized MSPs

2.1. Synthesis of the MSPs

The preparation of MSP-based delivery systems starts with the synthesis of the porous silica support. The synthesis of MSPs is achieved via supramolecular self-assembly (also called soft-templating) employing two basic elements: (1) a structure-directing agent (template) whose function is to direct the construction of the high-ordered (crystalline) porous scaffold and (2) a polymeric precursor that self-organizes around the template and, upon polymerization, build up the final rigid structure (Pal & Bhaumik, 2013).

The synthesis starts with the hydrolysis and condensation, in aqueous solution, of the inorganic siliceous precursor (e.g. tetraethyl orthosilicate, sodium metasilicate) around surfactant micelles (e.g. *N*-cetyltrimethylammonium bromide (CTABr)) (Qiao et al., 2009). The mesoporous inorganic scaffold obtained in these conditions presents cylindrical unidirectional empty channels of approximately 3 nm of diameter (when CTABr is used as surfactant) arranged in a uniform two-dimensional (2D) hexagonal p6m distribution (Landry et al., 2001). The synthesis can be performed either in acidic or basic conditions, and the source of silica can be fumed silica, sodium silicate, or a tetra-alkyl oxide of silane (Trewyn et al., 2007). The final mesoporous material is obtained after removing the surfactant template using either solvent extraction or aerobic high temperature calcination (500 °C - 600 °C) (Grudzienk et al., 2006). Figure 1 schematically represents this procedure.

According to this model, small changes in the reaction conditions (i.e. reaction time, temperature, pH, ionic strength, the type of silicate precursors or co-surfactants, surfactant and co-cation types and concentration, postsynthesis treatment) (Beck et al., 1992; Cho et al., 2001; Khushalani et al., 1995; Kruk et al., 2002; Lei et al., 2004; Muth et al., 2001; Nishiyama et al., 2003; Sayari & Hamoudi, 2001) make possible to modify important final features of the porous silica supports. These changes may produce other types of mesoporous silica such as

folding sheet materials (FSM) (Yanagisawa et al., 1990), hexagonal mesoporous silica (HMS) (Tanev & Pinnavaia, 1995), Santa Barbara amorphous silica (SBA-15) (Zhao et al., 1998a; Zhao et al., 1998b), Technische Universiteit Delft material (TUD-1) (Jansen et al., 2001), Universidad Valencia material (UVM-7) (el Haskouri et al., 2002), nanoporous folic-acid templated material (NFM-1) (Zhou & Garcia-Bennet, 2010), anionic-templated mesoporous silica material (AMS-6) (Garcia-Bennett et al., 2004), Korea Advanced Institute of Science and Technology material (KIT-6) (Kim et al., 2005) and an extensive diversity of hollow silica spheres (Cao et al., 2013; Li et al., 2004).
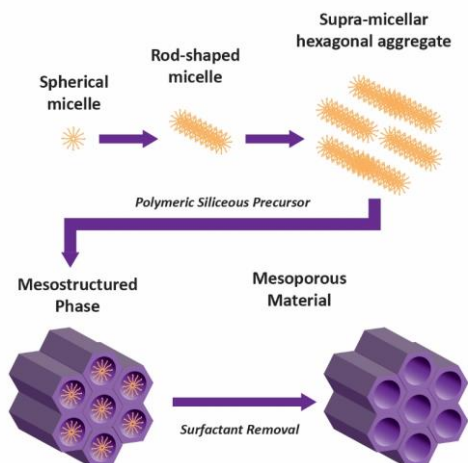
Figure 1. Schematic representation of the synthesis of mesoporous silica particles by structure-directing agents.

2.2. Loading of the MSPs with the payload molecule

Utilization of MSPs for delivery of food ingredients and nutraceutical requires that the bioactive molecule enters efficiently into the pores, limiting or avoiding the confining of the cargo in the external surface. The maximum incorporation of the molecule in the voids of the MSPs is important because even quite small fractions of payload on the particle surface (surface fraction) can significantly change the delivery profile and lead to erroneous results (Salonen et al., 2008).

Despite of the presumable simplicity of the cargo loading, achieving a successful loading of the payload in the voids of the MSPs requires taking into account different considerations such us the ratio among the payload molecule size and the textural properties of the porous material (pore size and specific pore volume), solubility of the cargo in the loading solution, viscosity of the payload or the solution, temperature, pH, time, potential chemical reactivity of the cargo and MSPs, and loading method. The most important factors are described below.

2.2.1.   Ratio between guest molecule and pore size

The adsorption of bioactive molecules into mesoporous silica is governed by size and charge selectivity. One of the most important conditions to guarantee that one molecule (food ingredient or nutraceutical) can be entrapped in a MSP is to be sure that the molecule is smaller than the pore size of the support (Arcos et al., 2013). Other factors determining the adsorption and the release kinetics of a bioactive compound in a certain media are pore length and pore ordering (Burguete et al., 2012; Izquierdo-Barba et al., 2009b), particle morphology (Manzano et al., 2008), surface area (Balas et al., 2006), the macroscopic form (Izquierdo-Barba et al., 2009a) and the modification or functionalization of the silica surface with functional groups (Nieto et al., 2008).

Pore size of the most common MSPs ranges from 1-6 nm while pore volume ranges from 0.3-1.5 cm^3 g^{-1}. These sizes are sufficient for the encapsulation of a large number of food ingredients and nutraceuticals such as antioxidants, antimicrobials, flavors, vitamins, bioactive peptides, bioactive lipids, oligosaccharides and probiotics. In fact, some of these molecules have already been encapsulated in different MSP (see Section 4 for details).

Despite the importance of ensuring a minimum pore size for efficient encapsulation of the target molecule within the pore of the mesoporous material, it cannot be excessive. Pore size and porosity are important not only for cargo loading, but they also have an effect in the release of the payload from the MSPs.

When the size of the pore diameter and cargo molecule are similar, a sustained release favored by the size confinement effect is obtained. In contrast, the loaded drug can be released at a relatively high rate when the pore size of MSPs is much larger than that of cargo (He & Shi, 2011). In the same line, when the pore diameter is higher than the molecular gate, a leakage of the guest molecule is produced. Having this in mind, porous material should be large enough to be able to incorporate the payload into their pores, but small enough to provide both an adequate mass transfer rate and a satisfactory protection of the loaded molecule.

2.2.2. Solvent selection

Despite the payload molecules can be introduced in some cases in a liquid (molten) state, they are normally introduced dissolved in a solution once dissolved in a proper solvent. The viscosity of the payload or the solution containing the payload should be low in order to enable uniform distribution of the payload into the pore structure of the MSPs (Santos, 2014). Thus, a wrong choice of solvent could totally hinder drug loading (Charnay et al, 2004; Salonen et al., 2008).

2.2.3. Loading method

The process of loading a payload molecule into MSPs can be performed using various methods (Figure 2). The use of one or another is mostly conditioned by the solubility of the payload molecule, its temperature stability, and its cost.
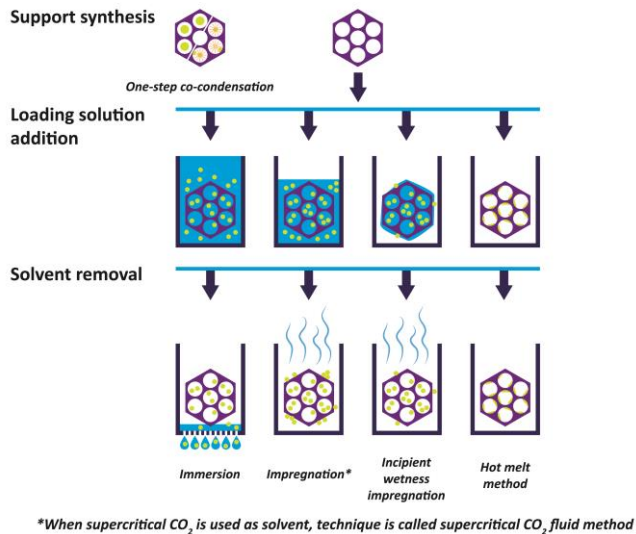
Figure 2. Schematic representation of different loading methods. (Adapted from Santos, H.A., ed., 2014, Porous Silicon for Biomedical Applications, Cambridge: Woodhead Publishing.).

2.2.3.1. One-step co-condensation process

This first method to load bioactive molecules into MSPs, also known as one-pot synthesis and loading, consists of the addition of the payload molecule to the synthesis mixture. In this manner, the payload acts at the same time as cargo and structure directing agent. As the payload is present in the media during the silica condensation, the molecules can be encapsulated either into the channels of mesostructured silica or into the polymer-silica assembled capsules. This method has been applied for the encapsulation of folic acid (Zhou & Garcia-Bennett, 2010) or oleic acid (Han et al., 2011), resulting in new materials known as NFM-1 and a kind of hollow silica spheres. Using this approach, up to 100% of the cargo can be incorporated into the mesoporous silica (Izquierdo-Barba et al., 2009b). However, only few molecules with the capacity of being used as a structure directing agent and at the same time remaining unaltered in the presence of the synthesis conditions can be loaded by this method. Due to these limitations, most of the

molecules are loaded into the mesoporous silica support after the extraction of the structure-directing agent (following strategies).

2.2.3.2. Immersion method

The most simple, reproducible, and widely used method for loading guest molecules into template-free MSPs is the so-called immersion method. This method consists of dissolving an excess of payload molecules in a suitable solvent followed by the immersion of the porous material in the solution. The payload molecule fills the pores at the same velocity and concentration as the loading liquid. In addition to the adsorbed payload, some molecules exist in a dissolved state in the pores. The loading process can take several hours. After the adsorption, solvent is removed by filtration or evaporation, while the payload remains in the pores. The immersion method has many advantages such as the loading can be performed at room temperature making it suitable for the loading sensitive molecules (i.e. most of vitamins, antioxidants). Moreover, the payload molecule is not exposed to a harsh chemical environment. Despite these advantages, this method cannot be used (or is not recommended) for insoluble or poorly soluble cargos (Mellaerts et al., 2008; Salonen et al., 2008; Limnell et al., 2011; Santos, 2014).

2.2.3.3. Impregnation method

A different loading approach involves the use of the impregnation method. In this method the loading solution is added to a thin layer of carrier and allowed to infuse through capillary action into the pores while the solvent is evaporated. The main advantage of the impregnation method is that it is easy to control the amount of the drug that is loaded in the carrier. Furthermore, the drug is efficiently loaded. This method is thus recommended for loading highly expensive payload molecules. However, a disadvantage is that this method sorts out by exhibiting a high uniformity of the molecules loading and a high facility to create a crystalline surface of the cargo on the surface of the carrier (Salonen et al., 2008;

Santos, 2014). The remaining of payload on the external surface of particles is especially disadvantageous for delivery of poorly soluble active molecules because the slow dissolution of the molecules on the external surface prevents access of the release medium to the pores (Riikonen, 2012).

2.2.3.4. Incipient wetness impregnation method

A variation of the impregnation method is known as incipient wetness impregnation. In this method, void space of the MSPs is filled with a precise amount of highly concentrated loading solution, avoiding in this way the time-consuming equilibration and the filtration step (Mellaerts et al., 2008). In incipient wetness impregnation, high cargo concentrations or repeated impregnations are required in order to achieve a high loading (Santos, 2014).

2.2.3.5. Hot melt method

A particular case of incipient wetness impregnation method is commonly known as the hot melt method. In this solvent-free procedure, the payload is heated along with the adsorbent to a temperature above the melting point and the system is cooled (Madieh et al., 2007). Despite the effectiveness in the loading of different molecules (i.e. essential oils) (Bernardos et al., 2015), the high temperature stability and the low viscosity of the payload limit the use of this technique in most applications. In addition, the probability of undesired reactions between the porous material and the payload molecules is increased at elevated temperatures (Santos, 2014).

2.2.3.6. Supercritical CO_2 fluid method

Novel strategies to load bioactive molecules in mesoporous silica particles include the use of supercritical fluid techniques (i.e. CO_2). Above its critical temperature and critical pressure, CO_2 is a liquid with high diffusivity and high dissolving capacity able to make poorly water-soluble molecules go into the deeper pore canals of the MSPs. Using this procedure, an improved loading

capacity and a prolonged releasing time of poorly water-soluble molecules can be achieved (Li-Hong et al., 2013).

2.3. Functionalization of MSPs to create capped-MSPs

To be a perfect food ingredient and nutraceutical carrier, MSPs should exhibit a zero release of their cargo during food production, food storage, and food digestion. This can be achieved via surface functionalization of the MSPs. One important feature of the structure of MSPs is their high concentration of structural defects in the form of silanol (Si-OH) groups. Silanol groups readily react, for instance, with trialkoxysilane derivatives (e.g. $(R'O)_3$-Si-R-) resulting in the preparation of a large number of different functionalized "hybrid materials" (Vinu et al., 2005).

2.3.1. Methods to functionalize MSPs

There are two general approaches to functionalize MSPs commonly known as "co-condensation" and "grafting".

2.3.1.1. Co-condensation

Co-condensation, also called one-pot synthesis, consists of the formation of the MSPs in presence of the desired functional group (usually a trialkoxyorganosilane). In this manner, organic functionalities are direct components of the silica matrix resulting in a homogeneous distribution of the functional groups in the final support. Because functional groups are part of the structure as well as structure directing agents, templates must be removed by extraction because calcination would destroy the grafted organic moieties. Extending the co-condensation approach to bridged organosilicon precursors of the type $(R'O)_3Si–R–Si(OR')_3$ results in the formation of periodic mesoporous organosilicas (PMOs) (Brühwiler, 2010). In general, the degree of mesoscopic order of the products decreases with increasing concentration of $(R'O)_3SiR$ in the

reaction mixture, which ultimately leads to totally disordered products. Moreover, an increase in concentration of the incorporated organic groups can lead to a reduction in the pore diameter, pore volume, and specific surface areas. These methodological disadvantages limit the use of co-condensation method in some applications.

2.3.1.2. Grafting

An alternative method to synthesize organically functionalized mesoporous silica phases is the postsynthetic method, also often referred to as grafting. In this method, functional groups are introduced after the formation of the mesoporous silica, either before or after removal of the structure-directing agent. Introduced in this way, the functional groups do not compromise the mesoscopic order of the silica support. This method exploits the abundant silanol groups present on the mesoporous silica surface. The result is an inhomogeneous surface coverage of the R species near the entries to the mesoporous channels and on the exterior surfaces (Brühwiler, 2010; Huh et al., 2003). A schematic representation of both main possibilities for the functionalization of MSPs is shown in Figure 3.
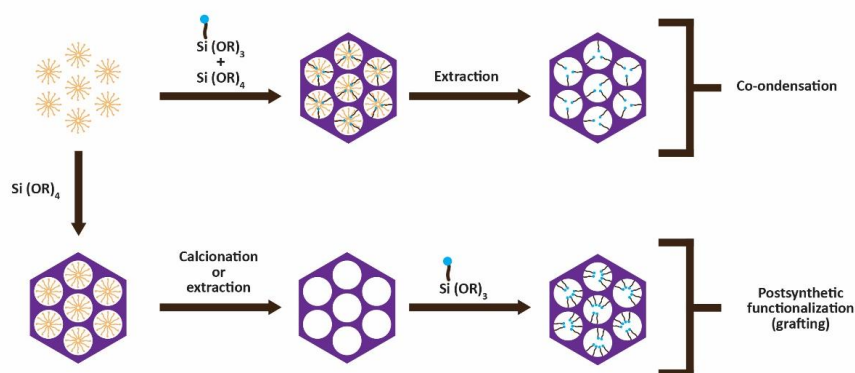

Figure 3. A schematic representation of functionalization procedures on MSPs. (Adapted from Brühwiler, D., 2010, Postsynthetic functionalization of mesoporous silica, Nanoscale, 2, 887–892).

2.3.2.   Capped-MSPs: definition and properties

Organic or bioorganic molecules included in the mesoporous materials with the objective of control the release of a guest molecule as function of a particular stimulus are commonly known as molecular gates (Figure 4). These can be defined as nanoscopic supramolecular-based devices, attached to certain porous supports, that can control mass transport, which is triggered by a target external stimulus that can control the state of the gate (closed or open) *ad lib* (Aznar et al., 2009b).

Capped MSPs are then based in the use of a suitable inorganic support acting as a nanocontainer (for loading the cargo) and a switchable gate-like ensemble capable of being opened or closed upon the application of certain external stimuli. A schematic representation of a gate-like superstructure is shown in Figure 4. Both components -support and gate- are important, and their selection determines the controlled release performance of the hybrid material. In particular, depending on the type of the applied stimulus, it is possible to modify the properties of the anchored molecules (i.e. polarity, conformation, size, interaction with other species, bond hydrolysis, etc.), which in turn results in a control of the delivery.

Among different molecules/supramolecules employed as molecular gates controlling the opening/closing of pore entrances of MSPs are inorganic nanoparticles (Aznar et al., 2009a; Lai et al., 2003), polymers (Bernardos et al., 2012; Liu et al., 2008), and large supramolecular assemblies (Agostini et al., 2012b; Mondragón et al., 2014; Nguyen et al., 2007). Prepared systems are able to respond to a range of stimuli such as pH (Angelos et al., 2008; Casasús et al, 2004; Popat et al., 2012; Zheng et al., 2014), light (Knežević et al., 2011; Mal et al., 2003), redox potential (Hernandez et al., 2004; Liu et al., 2008; Nguyen et al., 2007), temperature (de la Torre et al., 2014) and biomolecules (e.g. enzymes, antibodies, nucleotides, etc.) (Bernardos et al., 2009; Climent et al., 2009; Climent et al., 2010; Mas et al., 2013). Among them, only some capping systems and stimuli are appropriate in food applications.
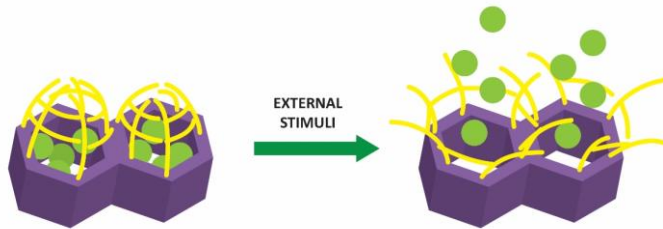
Figure 4. Representation of a nanoscopic molecular gate system working principle.

There are a number of requirements for a molecule/biomolecule to be used as a molecular gate in the preparation of functionalized MSPs as delivery systems for food ingredients and nutraceuticals. Some of the most important attributes are the following:

1. The molecule should be able to be anchored to the surface of the MSP (i.e. covalently, electrostatically) and to remain unaltered until the triggering stimulus is present.
2. Ideally, a molecular gate should be large enough to block the pores avoiding leakage of the cargo during processing or storage.
3. The molecule should respond against a stimulus present in the gastrointestinal tract (e.g. changes in pH in the stomach and intestine; presence of specific enzymes such as amylase, lipase, protease, etc.), an environmental stimulus (important in packaging containing MSPs), or a stimulus derived from the presence of microorganisms (important in the delivery of specific antimicrobials).
4. The molecular gate should be fabricated using GRAS molecules to avoid toxicological and legislative issues.
5. The coating contributed by the functionalization with the molecule acting as a molecular gate should be compatible with the food matrix, preventing problems of solubility, precipitation, or phase separation.

2.3.3. Strategies to develop capped-MSPs responsive to stimuli present in the gastrointestinal tract

One strategy to develop delivery systems containing molecular gates able to retain biomolecules in the voids of MSPs until an adequate stimulus in the gastrointestinal tract is present consists of the preparation of pH-responsive MSPs. To this purpose, it is possible to anchor polyamines in the outer surface of the silica support since protonation/deprotonation processes of polyamines grafted into the pore outlets of MSPs modify their structural conformation (Casasús et al., 2004). At acid pH, Coulombic repulsions between protonated amino groups hinders cargo delivery (gate closed) while at neutral pH, unprotonated amines tend to interact to each other favoring pore access (gate open). Figure 5 illustrates this gate mechanism.

Other strategies to develop delivery systems based on capped-MSPs for food applications involve the use of immediate primary source of energy molecules (carbohydrates, protein, etc.) or nucleotides as molecular gates. When anchored to the outlets of the mesoporous inorganic scaffold, these molecules have demonstrated the capability to hinder the delivery of the payload until digestive enzymes break down the capping molecule and the cargo is released. One of the first examples of MSPs capped with a molecular gate able to deliver its cargo in the presence of digestive enzymes (i.e. saccharases) was described by Bernardos et al. (2009). The system consisted of a MCM-41 support functionalized with lactose through a silane derivative. Cargo delivery from aqueous suspensions was negligible because of the formation of a dense disaccharide network in with the lactose groups was most likely linked through hydrogen-bonding interaction around the pore outlets. In contrast, in the presence of the enzyme galactosidase, the hydrolysis of the β1-4 bonds in the lactose moiety conducted to the release of the entrapped payload (Figure 5b).
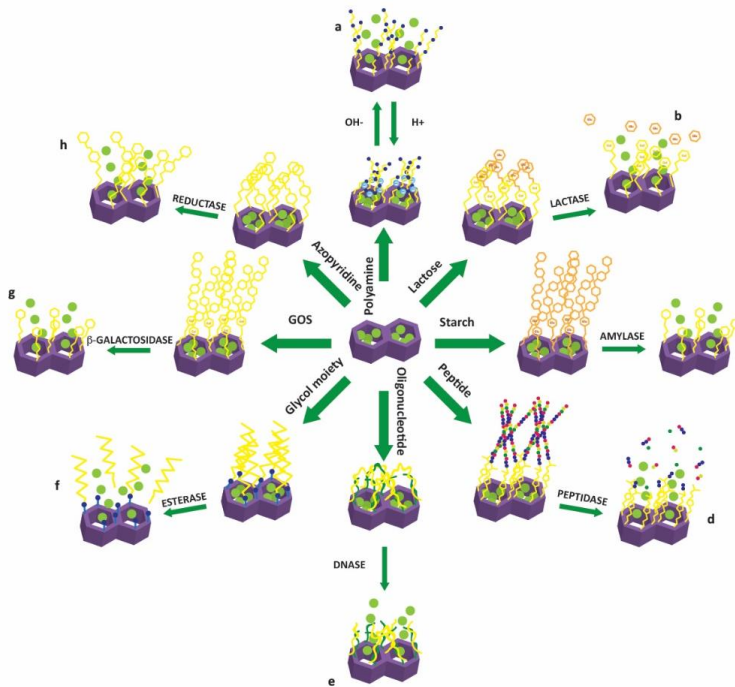
Figure 5. Graphical representation of selected delivery systems based on MSPs functionalized with molecules acting as molecular gates and the corresponding triggering stimulus. (a) pH, (b) presence of lactase, (c) presence of pancreatine, (d) presence of protease, (e) presence of DNAse, (f) presence of esterase, (h) presence of β-galactosidase, (i) presence of azo-reductase.

In a further attempt, the same authors functionalized the surface of a loaded MCM-41 support with three different commercially available hydrolyzed starches (Glucidex 47, 39 and 29) via the derivatization of the starch with an alkoxysilane (Bernardos et al., 2010). Cargo release was achieved by enzymatic hydrolysis in the presence of pancreatin (an enzyme cocktail containing pancreatic amylase) (Figure 5c). Moreover, a clear control of the delivery rate was found by employing hydrolyzed starches with different dextrose equivalent values. The lesser the hydrolysis of starch was, the lower the delivery rate. These results showed how it

was possible to design different delivery profiles by selecting the degree of hydrolysis of the starch.

The use of peptide sequences grafted to the pore outlets of mesoporous silica nanoparticles by using click chemistry reaction have also demonstrated great effect to hamper cargo release, whereas delivery was triggered in the presence of a protease (Figure 5d) (Coll et al., 2011). Oligonucleotide chains have also been used to design capped-MSPs triggered in the presence of DNAse I (Figure 5e) (Zhu et al., 2011; Zhang et al., 2014).

Finally, enzymes secreted from colonic microflora have also proved to be suitable for triggering the release of active molecules from capped MSPs. In particular, galacto-oligosaccharides, ester glycol moieties, and azopyridine derivatives have been used as caps in smart delivery systems triggered in the presence of esterases (Figure 5f), β-galactosidases (Figure 5g), and azo-reductases (Figure 5h), respectively (Agostini et al., 2012a, Agostini et al., 2012c, Mas et al., 2013). A more extensive review of hybrid organic–inorganic systems for the controlled release of biomolecules in the gastrointestinal tract has been recently published (Pérez-Esteve et al., 2016).

3. Encapsulation of food ingredients and nutraceuticals in MSPs

The preceding sections described general methods for the fabrication of MSPs and how they can be used as encapsulation systems. In the following sections, examples of delivery systems based on bare or functionalized MSPs for the encapsulation of food ingredients and nutraceuticals are provided and discussed. Examples have been classified in different categories (vitamins, phytochemicals, bioactive peptides, antimicrobials, aromas and enzymes) according to the chemical structure or function of the encapsulated molecule.

2.4. Encapsulation of vitamins

Vitamins are a group of nutrients essential for human growth and development. They are not produced by the body (or produced in a very low quantity). Hence, all vitamin requirements must be provided by natural or fortified food. Despite the fact that a number of food fortified with vitamins are available in the market, not all of them ensure that the vitamin is going to be bioavailable for the human body. The reason is clear, both, water-soluble and oil-soluble vitamins, exhibit very low stability in the presence of heat, ultraviolet light, and metal ions. Moreover, as it is presumable, oil-soluble vitamins are incompatible with a number of water-based products. To solve these problems, vitamin encapsulation is seen as a promising strategy due to its demonstrated capacities to improve molecules stability and nutrient bioavailability. In this section, specific details about vitamins that have been encapsulated in MSPs, the preparation process of these encapsulation systems as well as the benefits of encapsulation of water-soluble and oil-soluble vitamins in MSPs are provided.

2.4.1. Encapsulation of water-soluble vitamins

2.4.1.1. Riboflavin

One of the first examples involving the use of MSPs for the encapsulation and controlled delivery of vitamins in pure water was reported by Bernardos et al., (2009). These authors employed MCM-41 as inorganic support and riboflavin as payload molecule. Riboflavin (vitamin B2) plays important roles in energy metabolism by interconverting $NAD^+/NAD(H)$ and $NADP^+/NADPH$ couples in several dehydrogenase reactions. This vitamin is required in the metabolism of amino acids, fatty acids and carbohydrates. Riboflavin is really stable to heat and other processing operations but degrades easily in the presence of light (Zhuge & Klopfenstein, 1986). With the goal of protecting the vitamin from environmental degradation these authors encapsulated the vitamin in MCM-41 microparticles functionalized on the external surface with a suitable polyamine (i.e., the organosiloxane derivative 3-[2-(2-aminoethylamino)ethylamino]propyl-

trimethoxysilane). The system showed an extraordinary ability to control the delivery of the vitamin as a function of the pH of the media mediated by the change of the conformation of the amines as a function of pH (see section 2.3.3.). It allowed the development of orally applicable delivery systems designed to have the particular ability to protect the cargo from the environment as the vitamin is only released at neutral pH (i.e., intestine where the vitamin is absorbed).

2.4.1.2. Niacin

Niacin (vitamin B3) is indispensable for conversion of dietary proteins, fats, and carbohydrates into usable energy. Insufficient niacin in the diet can cause nausea, skin and mouth lesions, anemia, headaches, and tiredness. Stability of niacin is excellent in the presence of heat, light, air, and alkali, but it is altered in the presence of other micronutrients such as minerals, especially at high temperatures (Zhuge et al., 1986). The encapsulation of niacin has been achieved by using mesoporous silica hollow microspheres by employing the covalent grafting method (Kapoor et al., 2010). In this particular case, the encapsulation procedure consisted of the derivation of niacin into a vitamin B3 precursor that was polymerized inside the hollow microspheres resulting in a high loading efficiency. The vitamin was sustainably released in the presence of simulated gastric fluid. Moreover, toxicology studies performed on rats revealed that the proposed niacin deliver system did not exhibit any harmful effect.

2.4.1.3. Ascorbic acid

Another water-soluble vitamin successfully encapsulated in porous silica particles is ascorbic acid (vitamin C). Ascorbic acid is a common enzymatic cofactor in mammals used in the synthesis of collagen and it enhances the availability and absorption of iron from non-heme iron sources. A severe deficiency of this vitamin causes scurvy. As a molecule, ascorbate is a powerful reducing agent capable of rapidly scavenging a number of reactive oxygen species (ROS). As a consequence, it is very unstable during processing and storage due to

oxidation processes. In a recent study by Rashidi et al. (2013) ascorbic acid was efficiently encapsulated in MSPs with 2.44 nm of pore size with a loading efficiency of 3.22 mg of the vitamin per gram of particle. The *in vitro* release of the vitamin in simulated digestion fluids (gastric and intestinal) showed a bust release during the first 30 minutes. The bust release was more acute in the case of intestinal fluid (basic pH). After 30 min a sustained release occurred in both cases.

2.4.2. *Encapsulation of lipid-soluble vitamins*

2.4.2.1. β-carotene

β-carotene is the most important precursor of vitamin A. Once in the liver β-carotene is converted into two molecules of vitamin A. This vitamin is important for growth and development, for the maintenance of the immune system and for good vision. Food enrichment with vitamin A is complex due to the poor bioavailability of the vitamin and its sensitivity to oxygen in air, especially in the presence of light and heat. With the objective of improving β-carotene bioavailability and stability, Clifford et al. (2008) encapsulated *trans*-β-carotene in MSPs. In the synthesis, cetyl trimethyl ammonium bromide micelles were loaded with *trans*-β-carotene molecules. Then, the filled micelles were coated with the silica precursor to form particles under acidic condition. Comparing the stability of free and encapsulated *trans*-β-carotene it was proved that encapsulation of β-carotene by non-covalent interaction improved the photostability of the vitamin over days. Loaded MSPs also showed an extraordinary capability to control the release of the vitamin, thus improving its bioavailability.

2.4.2.2. α-tocopherol

Encapsulation of vitamin E (α-tocopherol) in MSPs has been studied by different research groups. α-Tocopherol is the most biologically active form of vitamin E. The major role of vitamin E is to protect polyunsaturated fatty acids (PUFA) from oxidation. It acts as an antioxidant in the lipid phase of cell

membranes. Due to its powerful antioxidant power, its use as replacer of synthetic antioxidants in food formulations and food packaging has been proposed in the last years. However, as occurs with most of the vitamins, tocopherols are very sensitive to light, oxygen and heat.

In a study on α-tocopherol encapsulation, the influence of the texture properties of different MSPs (i.e., C12-MCM-41, C16-MCM-41 and SBA-15) and amorphous silica as well as the influence of different solvents such as *n*-heptane, cyclohexane, *n*-butanol and ethanol on the encapsulation efficiency of the vitamin were studied (Chandrasekar et al., 2005). Results showed that vitamin E adsorption capacity depends on the solvent used, the specific surface area, and the specific pore volume of the adsorbent. C16-MCM-41 showed the highest adsorption capacity as compared to other silica materials. The adsorption from *n*-heptane was significantly higher compared to those from the non-polar solvent cyclohexane and polar solvents such as *n*-butanol and ethanol.

More recently, Gargiulo et al. (2013) proposed the encapsulation of α-tocopherol in SBA-15 and its use as an alternative antioxidant for polymer protection during processing and also as an additive for active packaging systems. The preparation of this encapsulation system started with the synthesis of an amine-modified SBA-15 via co-condensation reactions. Then the solid was impregnated with a solution of α-tocopherol in ethanol. Loading efficiencies of about 0.42 g of tocopherol per gram of silica were found. Finally, tocopherol-loaded SBA-15 particles were added to low-density polyethylene films. Results showed that encapsulation had an influence not only in the release kinetics of the antioxidant, but also in the antioxidant activity. α-Tocopherol antioxidant effectiveness was higher when adsorbed on modified SBA-15 than when free.

2.5. Encapsulation of phytochemicals

Phytochemicals are a large group of plant-derived compounds hypothesized to be responsible for health promotion and disease prevention conferred from diets high in fruits, vegetables, beans, cereals, and plant-based beverages such as tea and wine (Arts & Hollman, 2005). In accordance, interest to include phytochemicals in the formulation of food has increased in recent years. However, their incorporation into food is limited due to a very low solubility and high environmental instability. The following lines review the possibilities of encapsulation of phytochemicals in mesoporous silica carriers to solve problems associated with their use as food ingredients or nutraceuticals.

2.5.1. Polyphenols

Polyphenols are a family of naturally-occurring compounds characterized by possessing at least one aromatic ring bearing one or more hydroxyl substituents (i.e., flavonoids, phenolic acids, stilbenes, curcuminoids, lignans, etc.). They are found largely in fruits, vegetables, cereals, and beverages. Epidemiological studies and associated meta-analyses strongly suggest that long-term consumption of diets rich in plant polyphenols offer protection against development of cancers, cardiovascular diseases, diabetes, osteoporosis, and neurodegenerative diseases (Pandey & Rizvi, 2009). These health effects attributed to polyphenols depend on the consumed amount and on their bioavailability.

2.5.1.1. Wine polyphenols

It is well known that wine is a product very rich in polyphenols. Phenolic compounds present in wine in the soluble state contribute to the wine's color, aroma, flavor, astringency, bitterness, hardness, and stability. The use of MSPs to concentrate wine polyphenols, being then used as a nutraceutical product, has been proposed. According to Cotea et al. (2012) SBA-15 materials are able to retain efficiently molecules of quercetin (concentrated 4900 times) and *cis-*

resveratrol (concentrated 1400 times) from wine. Other molecules retained in a lesser but reasonable quantity were *trans*-resveratrol, catechin, epicatechin, rutin, and phenolic acids (meta- and para-hydroxybenzoic, vanillic, caffeic, syringic, salicylic and para-coumaric acids).

2.5.1.2. Quercetin

Flavonols such as quercetin are a group of bioactive molecules with high antioxidant effect whose use in the formulation of nutraceuticals is limited by their unfavorable physicochemical properties, especially their very poor water solubility and low stability. A study comprising the use of the mesoporous silica MCM-41 functionalized with octyl groups (to vary the hydrophobic/hydrophilic character of the surface) reported the benefits of the quercetin encapsulation to improve quercetin stability over the time when exposed to UV irradiation (Berlier et al., 2013). Moreover, compared to other encapsulation systems (i.e., liposomes, nanostructures or cyclodextrins) quercetin-loaded MCM-41 showed high loading values and a remarkable efficiency of encapsulation. Similar results were found by Sapino et al. (2014). In this study, the authors reported the protective effect of quercetin encapsulation in aminopropyl functionalized mesoporous silica nanoparticles against UV-induced degradation. Concretely, at a concentration 60 μM the antioxidant and chemopreventive properties of quercetin-loaded MSPs was more effective than quercetin alone.

2.5.1.3. Resveratrol

Resveratrol is a potential antioxidant with strong antiinflammatory and antiproliferative properties, which can be found in grapes, nuts, fruits and red wine. It is really poorly soluble and extremely photosensitive, which limits its beneficial therapeutic effects. Encapsulation of resveratrol in MSPs to achieve an improved dissolution rate (Quan et al., 2012) and a better chemical stability (Popova et al., 2014) has been recently reported. In the study of Quan and co-workers (2012), resveratrol encapsulated in ordered mesoporous silica particles

exhibited an enhanced release behavior compared to the non-encapsulated molecules. The efficiency of encapsulation to improve the solubility of the molecule was attributed to the capability of the mesoporous particle to keep the molecule in the amorphous conformation, which exhibits a better solubility than the crystalline phase. In the study reported by Papova and co-workers (2014), resveratrol encapsulated in silica-based spherical mesoporous MCM-41 showed high loading efficiencies of 40-46%, improved solubility compared to the free resveratrol, and chemical stabilization.

2.5.1.4. Curcumin

Curcumin, is a yellow pigment extracted from *Curcuma longa* commonly used as a spice and a food-coloring agent. This polyphenol exhibits excellent antioxidant, anti-inflammatory, anticarcinogenic and anti-tumor *in vitro* activity. *In vivo* bioactive activity of curcumin is limited because of its low absorption when administrated orally. In a study carried out by Clifford et al. (2008) curcumin was encapsulated in MSPs with pores of 4 nm with a loading efficiency of 44 mg g^{-1}. The encapsulated curcumin showed an extraordinary sustained release profile and an improved photostability.

2.5.2. *Organosulfurs*

Organosulfurs (e.g., allicin, diallyl disulfide, diallyl sulphide, allixin, etc.) are a family of volatile compounds found in *Allium* vegetables (garlic, onion, leek, chive) with high proved antibiotic, antioxidant and anticancer activity. The main problem of these compounds for their use in the formulation of functional foods is their distinctive pungent flavor and aroma, a matter that can be dismissed or eliminated through encapsulation. In this context, we have demonstrated the possibility to encapsulate garlic extracts (rich in allicin and diallyl disulphide) in capped-MSPs to improve their stability and to decrease the aromatic perception of the molecule (Acosta et al., 2014). In our study, the carrier systems consisted of MCM-41 solids functionalized in the outer surface with linear polyamines and

with hydrolyzed starch, both acting as molecular gates. Due to the excellent performance of both carrier systems to enhance the stability of the active molecules as well as decreasing the distinctive aroma, the carriers were incorporated in nylon nanofibers by electrospinning. The nanofibers containing the particles impregnated with the garlic extract conserved the same release and protective properties than the particles by themselves. The proposed encapsulation system could be employed in the formulation of food or in the formulation of active packages.

2.5.3. Glucosinolates

Glucosinolates are a family of natural compounds found in cruciferous vegetables such as broccoli and cabbage. Glucosinolates (e.g., allylisothiocyanate) show great antibacterial efficacy against bacteria such as *Escherichia coli*, *Staphylococcus aureus*, *Proteus vulgaris*, *Pseudomonas fragi*, and *Pseudomonas aeruginosa* in vapor phase. After complete evaporation of the active molecule, the antimicrobial effect disappears. To control the volatility of the allylisothiocyanate, Park et al. (2012) encapsulated the molecules in two types of MSPs exhibiting different textural properties: MCM-41 (pore diameter 2.4 nm) and SBA-15 (7.2 nm). Despite encapsulation efficiencies being very high in both types of supports (ca. 95%), the release behavior and the capability to inhibit bacterial growth were really different. While SBA-15 showed a burst release of 80% of available allylisothiocianate in the first 24 h achieving lethal doses against selected bacteria and fungi, release from MCM-41 was retarded due to more narrow pores that resulted in a delayed reduction of bacteria counts.

2.6. Encapsulation of bioactive peptides

Bioactive peptides are fragments of protein naturally encrypted in their primary sequence that are released during gastrointestinal digestion or food processing and that confer bioactive functions beyond basic nutritional benefits (i.e., antihypertensive, antioxidant, anticancer, antimicrobial, immunomodulatory and cholesterol-lowering effects). The main challenge of using bioactive peptides as nutraceuticals is to preserve their structure during food processing, digestion and adsorption in order for them to enter in their proper conformation to the bloodstream at a significant level. Some bioactive peptides show bitter flavor that hinders the application of protein hydrolysates into functional food products. Encapsulation in MSPs as a delivery mechanism can be used to overcome these challenges by protecting them against the gastrointestinal environment (acid pH and proteolytic enzymes), masking undesired sensory properties, and enhancing absorption of bioactive peptide-based products.

Most of the examples of using MSPs for the encapsulation of bioactive peptides include antimicrobial peptides as payload molecules. Antimicrobial peptides, also called host defense peptides, are part of the innate immune response found among all classes of life. After development of recombinant DNA technologies by which peptides are produced in large amounts with high purity and in a relative economic way, interest in using these peptides as therapeutic agents and food preservatives is growing rapidly. Despite these advantages, their use is limited because of reduced half-lives, a lack of specificity, and the required high doses. Bearing this in mind, targeted encapsulation and delivery achieved by capped-MSPs can fulfil the objective of achieving the intake of total quantities sufficiently low to be innocuous for the consumer but that locally are high enough to be lethal for the infectious agent (Urbán et al., 2012). In this respect, Izquierdo-Barba et al., (2009a) reported the encapsulation of the antimicrobial peptide LL-37 on mesoporous silica by the one-pot evaporation-induced self-assembly method. The loaded support was then functionalized with 3-mercaptopropyltrimethoxysilane to decrease the release kinetics of LL-37. The

final loaded and functionalized supports improved the stability of the antimicrobial agent, as well as displayed an efficient antimicrobial effect against both gram-positive *S. aureus* and gram-negative *E. coli.*

Besides antimicrobial peptides, Liu et al. (2011) reported the use of two encapsulation systems based on periodic mesoporous organosilicas (pore size 2.6 and 2.8 nm) for entrapping small molecular weight peptides. More recently, Luo et al. (2015) prepared a controlled deliver system to encapsulate bone-forming peptide derived from bone morphogenetic protein-7 (BMP-7) into the mesoporous silica nanoparticles, obtaining a slow-release system for osteogenic factor delivery. These results suggest that MSPs are able to entrap bioactive peptides, and a number of future applications can be envisioned.

2.7. Encapsulation of food flavors and aroma

Flavor, defined as a combination of taste, smell and/or trigeminal stimuli, is one of the most important characteristics of a food product that conditions consumers' acceptance (Firestein, 2001). In this manner, aroma molecules can be among the most valuable ingredients in any food formula. In general, aromas have a low molecular weight (often between 100 and 250 g mol^{-1}) and can be classified as hydrocarbons, alcohols, aldehydes, ketones, esters, acids, and sulphides (Zuidman & Heinrich, 2010). Even small amounts of some aroma substance can be expensive, and because they are usually delicate and volatile, preserving them is often a top concern of food manufacturers (Madene et al., 2006). Encapsulation of aroma allows obtaining aromatic capsules that are easy to handle, that improve the stability of the molecules, and that allow a controlled delivery. These properties are desired for both pleasant aromas that reduce their evaporation rate and elongate their flavoring power and for bad aromas that can be masked due to encapsulation. As far as we know, no systems of flavor encapsulation in MSPs for specific utilization in food applications have been reported. However, model aroma molecules such as ethyl butanoate, ethyl

hexanoate, ethyl octanoate, and ethyl decanoate have demonstrated to be easily entrapped through silica, providing sustained delivery profiles (Veith et al., 2004).

2.8. Encapsulation of enzymes

Specificity of enzyme catalysts promise improvements in many applications in industries regarding the production of sugar and corn syrups, dairy, baking products, alcohol drinks, meat tenderness, and cheese ripening. However, the short lifetime of enzymes presently limit their usefulness. In this context, encapsulation is providing new opportunities to prolong enzyme shelf life and to use existing enzyme activities in new applications where they are not used due to problems of instability or incompatibility.

One of the works that better describes the effect of enzyme encapsulation for their use in food applications is the study reported by Hisamatsu et al. (2012). In this study, the authors encapsulated α-amylase in different mesoporous silica materials. Amylases are predominantly applied during the processing of raw materials containing starch. In the production of syrups, amylases transform maize or potato starch into sugars. In bakery, amylases "predigest" the starch and improve starch hydrolysates utilization by yeasts. Finally, in production of beers or spirits, amylases hydrolase starch into sugars that can be easily fermented into alcohol.

Hisamatsu and co-workers (2012) evaluated the efficiency of different supports (i.e., several folded sheet mesoporous silica (FSM), a cubic mesoporous silica (KIT-6) and two SBA-15) that differed morphologically in terms of particle shape, pore size, and pore structure to encapsulate α-amylase. Results showed that encapsulated α-amylase increases with increasing pore size in the following order: SBA-15 < KIT-6 < FSM. In a second part of the study, α-amylase activity was measured by determining the quantity of starch remaining after incubating the silica loaded with amylases with a starch solution at 37 °C. These assays concluded that the conformation of α-amylase appeared to be better conserved in FSM than

in KIT-6 or SBA-15. Finally, the effect of encapsulation in the protection of enzyme activity after heat treatment at 90 °C revealed that α-amylase encapsulated in FSMs retained over 70% enzyme activity, even after a 60 min heat treatment, whereas α-amylase encapsulated in SBA-15 lost almost all activity after 10 min of heat treatment, similar to the activity loss observed in free α-amylase. Despite the fact that in this study SBA-15 support exhibited the worst α-amylase encapsulation properties, it has been demonstrated that the encapsulation of cellulase in SBA-15 supports of 8.9 nm in diameter improves the thermal stability with respect to the free enzyme. Moreover, encapsulated cellulase maintains high enzyme activity even after 4 weeks of storage at room temperature (Takimoto et al., 2008).

Another enzyme that has been efficiently encapsulated in MSPs is lipase. Concretely, encapsulation of lipase in mesoporous silica yolk–shell spheres enhanced its thermal stability in a 90%, compared to free lipase that loses its activity after thermal treatment at 70 °C for 2 h (Zhao et al., 2013).

These findings point out the importance of an adequate silica support to maximize the loading, the stability, and thus the catalytic effect of a specific enzyme.

4. Conclusions and future perspectives

Encapsulation of food ingredients and nutraceuticals in mesoporous silica particles has the potential to solve some of the requests of the food industry. Reported MSPs-based encapsulation systems are able to improve bioavailability of bioactive molecules by increasing their solubility or by delivering the molecule in a concrete place of the gastrointestinal tract, to mask their odor and taste, to reduce its volatility, to improve their compatibility with the food matrix and also to protect bioactive molecules from environment during production, storage and digestion. These properties are summarized in Figure 6.

Despite these reported advantages, application of MSPs in the agri-food sector (such as occur in other nanostructured materials) is still viewed as challenging. On the one hand, the definition of nanostructurated materials and nanoparticles is a changing and disharmonised concept. These definitions, apart from being technical, affect regulatory aspects and food labeling. On the other hand, validated methods for *in situ* detection and characterization of nanomaterials in complex food matrices should be developed. These methods should ideally include techniques and equipment that are present at laboratories. Moreover, the lack of validated information about the possible toxicity (short and long term ingestion) as well as precise knowledge about the absorption, distribution, metabolism, and excretion of these materials makes it difficult to assess the safe daily intake of these supports. In this context, regulatory bodies should provide specific regulations and criteria to be followed when evaluating the safety of MSPs to be used in food applications or when launching a new product containing nanostructurated particles to the market.

Until these gaps are overcome, generalizations, doubts or insecurities will be the main obstacle to the utilization of these reported encapsulation systems in the food sector, despite the large number of potential applications.
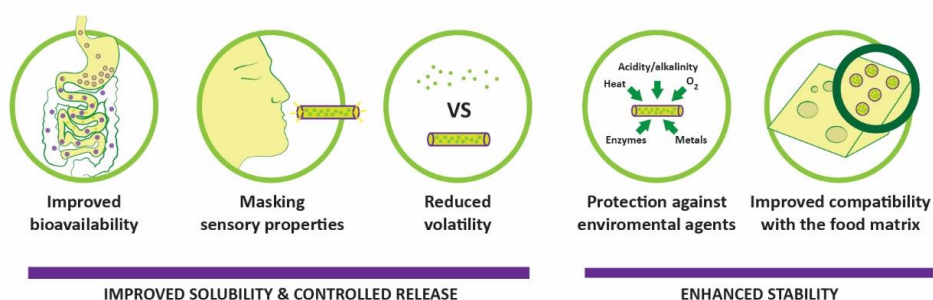

Figure 6. Representation of different applications of mesoporous silica particles as encapsulation and delivery systems for food ingredients and nutraceuticals.

References

Acosta, C., Pérez-Esteve, E., Fuenmayor, C.A., Benedetti, S., Cosio, M.S., Soto, J., Sancenón, F., Mannino, S., Barat, J.M., Marcos, M.D, & Martínez-Máñez, R. (2014). Polymer composites containing gated mesoporous materials for on-command controlled release. *ACS Applied Materials & Interfaces*, *6*(9), 6453-6460.

Agostini, A., Mondragón, L., Bernardos, A., Martínez-Máñez, R., Marcos, M.D., Sancenón, F., Soto, J., Costero, A.M., Manguan-García, C., Perona, R., Moreno-Torres, M., Aparicio-Sanchis, R., & Murguía, J.R. (2012a). Targeted cargo delivery in senescent cells using capped mesoporous silica nanoparticles. *Angewandte Chemie*, *51*(42), 10556-10560.

Agostini, A., Mondragón, L., Coll, C., Aznar, E., Marcos, M.D., Martínez-Máñez, R., Sancenón, F., Soto, J., Pérez-Payá, E., & Amorós, P. (2012b). Dual enzyme-triggered controlled release on capped nanometric silica mesoporous supports. *ChemistryOpen*, *1*(1), 17-20.

Agostini, A., Mondragón, L., Pascual, L., Aznar, E., Coll, C., Martínez-Máñez, R., Sancenón, F., Soto, J., Marcos, M.D., Amorós, P., Costero, A.M., Parra, M., & Gil, S. (2012c). Design of enzyme-mediated controlled release systems based on silica mesoporous supports capped with ester-glycol groups. *Langmuir*, *28*(41), 14766-14776.

Angelos, S., Yang, Y.W., Patel, K., Stoddart, J.F., Zink, J.I. (2008) pH-responsive supramolecular nanovalves based on cucurbit[6]uril pseudorotaxanes. *Angewandte Chemie*, *120*(12), 2254-2258.

Arcos, D., & Vallet-Regí, M. (2013). Bioceramics for drug delivery. *Acta Materialia*, *61*(3), 890-911.

Arts, I.C., & Hollman, P.C. (2005). Polyphenols and disease risk in epidemiologic studies. *The American Journal of Clinical Nutrition, 81*(1), 317S-325S.

Aznar, E., Marcos, M.D., Martínez-Máñez, R., Sancenón, F., Soto, J., Amorós, P., & Guillem, C. (2009a). pH-and photo-switched release of guest molecules from mesoporous silica supports. *Journal of the American Chemical Society*, *131*(19), 6833-6843.

Aznar, E., Martínez-Máñez, R., & Sancenón, F. (2009b). Controlled release using mesoporous materials containing gate-like scaffoldings. *Expert Opinion on Drug Delivery, 6*(6), 643-655.

Balas, F., Manzano, M., Horcajada, P., & Vallet-Regí, M. (2006). Confinement and controlled release of bisphosphonates on ordered mesoporous silica-based materials. *Journal of the American Chemical Society*, *128*(25), 8116-8117.

Beck, J.S., Vartuli, J.C., Roth, W.J., Leonowicz, M.E., Kresge, C.T., Schmitt, K.D., Chu, C.T.W., Olson, D.H., Sheppard, W., McCullen, S.B., Higgins, J.B., & Schlenker, J.L. (1992). A new family of mesoporous molecular sieves prepared with liquid crystal templates. *Journal of the American Chemical Society*, *114*(27), 10834-10843.

Berlier, G., Gastaldi, L., Ugazio, E., Miletto, I., Iliade, P., & Sapino, S. (2013). Stabilization of quercetin flavonoid in MCM-41 mesoporous silica: positive effect of surface functionalization. *Journal of Colloid and Interface Science, 393,* 109-118.

Bernardos, A., Aznar, E., Marcos, M.D., Martínez-Máñez, R., Sancenón, F., Soto, J., Barat, J.M., & Amorós, P. (2009). Enzyme-responsive controlled release using mesoporous silica supports capped with lactose. *Angewandte Chemie*, *121*(32), 5998-6001.

Bernardos, A., Marina, T., Žáček, P., Pérez-Esteve, É., Martínez-Mañez, R., Lhotka, M., Kouřimská, L., Pulkrábek, J., & Klouček, P. (2015). Antifungal effect of essential oil components against

Aspergillus niger when loaded into silica mesoporous supports. *Journal of the Science of Food and Agriculture, 95,* 2824–2831.

Bernardos, A., Mondragon, L., Aznar, E., Marcos, M.D., Martínez-Máñez, R., Sancenón, F., Soto, J., Barat, J.M., Pérez-Payá, E., Guillem, C., & Amorós, P. (2010). Enzyme-responsive intracellular controlled release using nanometric silica mesoporous supports capped with "saccharides". *ACS Nano*, *4*(11), 6353-6368.

Bernardos, A., Mondragón, L., Javakhishvili, I., Mas, N., de la Torre, C., Martínez-Máñez, R., Sancenón, F., Barat, J.M., Hvilsted, S., Orzaez, M., Pérez-Payá, E., & Amorós, P. (2012). Azobenzene polyesters used as gate-like scaffolds in nanoscopic hybrid systems. *Chemistry-A European Journal*, *18*(41), 13068-13078.

Burguete, P., Beltrán, A., Guillem, C., Latorre, J., Pérez-Pla, F., Beltrán, D., & Amorós, P. (2012). Pore length effect on drug uptake and delivery by mesoporous silicas. *ChemPlusChem, 77*(9), 817-831.

Brühwiler, D. (2010). Postsynthetic functionalization of mesoporous silica. *Nanoscale, 2*, 887-892.

Chandrasekar, G., Vinu, A., Murugesan, V., & Hartmann, M. (2005) Adsorption of vitamin E on mesoporous silica molecular sieves. *Studies in Surface Science and Catalysis, 158,* 1169-1176.

Cao, Z., Yang, L., Yan, Y., Shang, Y., Ye, Q., Qi, D., Ziener, U., Shan, G., & Landfester, K. (2013). Fabrication of nanogel core–silica shell and hollow silica nanoparticles via an interfacial sol–gel process triggered by transition-metal salt in inverse systems. *Journal of colloid and interface science*, *406*, 139-147.

Casasús, R., Marcos, M.D., Martínez-Máñez, R., Ros-Lis, J.V., Soto, J., Villaescusa, L.A., Amorós, P., Beltrán, D., Guillem, C., & Latorre, J. (2004). Toward the development of ionically controlled nanoscopic molecular gates. *Journal of the American Chemical Society*, *126*(28), 8612-8613.

Charnay, C., Begu, S., Tourne-Peteilh, C., Nicole, L., Lerner, D.A., & Devoisselle, J. M. (2004). Inclusion of ibuprofein in mesoporous templated silica: Drug loading and release property. *European Journal of Pharmaceutics and Biopharmaceutics, 57*, 533-540.

Cho, E-B., Kwon, K-W., & Char, K. (2001). Mesoporous organosilicas prepared with PEO-containing triblock copolymers with different hydrophobic moieties. *Chemistry of Materials, 13*(11), 3837-3839.

Clifford, N.W., Iyer, K.S., & Raston, C.L. (2008). Encapsulation and controlled release of nutraceuticals using mesoporous silica capsules. *Journal of Materials Chemistry*, *18*(2), 162-165.

Climent, E., Martínez-Máñez, R., Sancenón, F., Marcos, M.D., Soto, J., Maquieira, A., & Amorós, P. (2010). Controlled delivery using oligonucleotide-capped mesoporous silica nanoparticles. *Angewandte Chemie, 49*(40), 7281-7283.

Climent, E., Bernardos, A., Martínez-Máñez, R., Maquieira, A., Marcos, M.D., Pastor-Navarro, N., Puchades, R., Sancenón, F., Soto, J., & Amorós, P. (2009). Controlled delivery systems using antibody-capped mesoporous nanocontainers. *Journal of the American Chemical Society*, *131*(39).

Colilla, M., González, B., & Vallet-Regí, M. (2013). Mesoporous silica nanoparticles for the design of smart delivery nanodevices. *Biomaterials Science*, *1*(2), 114-134.

Coll, C., Bernardos, A., Martínez-Máñez, R., & Sancenón, F. (2013) Gated silica mesoporous supports for controlled release and signaling applications. *Accounts of Chemical Research*, 46(2), 339-349.

Coll, C., Mondragón, L., Martínez-Máñez, R., Sancenón, F., Marcos, M.D., Soto, J., Amorós, P., & Pérez-Payá, E. (2011). Enzyme-mediated controlled release systems by anchoring peptide sequences on mesoporous silica supports. *Angewandte Chemie International Edition*, *50*(9), 2138-2140.

Contado, C., Ravani, L., & Passarella, M. (2013). Size characterization by sedimentation field flow fractionation of silica particles used as food additives. *Analytica Chimica Acta*, *788*, 183-192.

Cotea, V.V., Luchian, C.E., Bilba, N., & Niculaua, M. (2012). Mesoporous silica SBA-15, a new adsorbent for bioactive polyphenols from red wine. *Analytica Chimica Acta, 732*, 180-1855.

de la Torre, C., Agostini, A., Mondragón, L., Orzáez, M., Sancenón, F., Martínez-Máñez, R., Marcos, M.D., Amorós, P., & Pérez-Payá, E. (2014). Temperature-controlled release by changes in the secondary structure of peptides anchored onto mesoporous silica supports. *Chemical Communications*, *50*(24), 3184-3186.

El Haskouri, J., de Zárate, D.O., Guillem, C., Latorre, J., Caldés, M., Beltrán, A., Beltrán, D., Descalzo, A.B., Rodríguez-López, G., Martínez-Máñez, R., Marcos, M.D., & Amorós, P. (2002). Silica-based powders and monoliths with bimodal pore systems. *Chemical Communications*, (4), 330-331.

El Mourabit, S., Guillot, M., Toquer, G., Cambedouzou, J., Goettmann, F., & Grandjean, A. (2012). Stability of mesoporous silica under acidic conditions. *RSC Advances, 2,* 10916-10924.

Firestein, S. (2001). How the olfactory system makes sense of scents. *Nature*, *413*(6852), 211-218.

Garcia-Bennett, A., Terasaki, O., Che, S., & Tatsumi, T. (2004) Structural investigations of AMS-n mesoporous materials by transmission electron microscopy. *Chemistry of Materials, 16*(5), 813-821.

Gargiulo, N., Attianese, I., Buonocore, G.G., Caputo, D., Lavorgna, M., Mensitieri, G., & Lavorgna, M. (2013). α-Tocopherol release from active polymer films loaded with functionalized SBA-15 mesoporous silica. *Microporous and Mesoporous Materials, 167*, 10-15.

Grudzien, R.M., Grabicka, B.E., & Jaroniec, M. (2006). Effective method for removal of polymeric template from SBA-16 silica combining extraction and temperature-controlled calcination. *Journal of Materials Chemistry*, *16*(9), 819-823.

Han, L., Gao, C., Wu, X., Chen, Q., Shu, P., Ding, Z., & Che, S. (2011). Anionic surfactants templating route for synthesizing silica hollow spheres with different shell porosity. *Solid State Sciences,* 13(4), 721-728.

He, Q., & Shi, J. (2011). Mesoporous silica nanoparticle based nano drug delivery systems: synthesis, controlled drug release and delivery, pharmacokinetics and biocompatibility. *Journal of Materials Chemistry, 21*, 5845-5855.

He, Q., Zhang, Z., Gao, Y., Shi, J., & Li, Y. (2009). Intracellular localization and cytotoxicity of spherical mesoporous silica nano- and microparticles. *Small*, *5*(23), 2722-2729.

Heikkilä, T., Salonen, J., Tuura, J., Hamdy, M.S., Mul, G., Kumar, N., Salmi, T., Murzin, D.Y., Laitinen, L., Kaukonen, A.M., Hirvonen, J., & Lehto, V.P. (2007). Mesoporous silica material TUD-1 as a drug delivery system. *International Journal of Pharmaceutics*, *331*(1), 133-138.

Hernandez, R., Tseng, H.R., Wong, J.W., Stoddart, J.F., & Zink, J.I. (2004). An operational supramolecular nanovalve. *Journal of the American Chemical Society*, *126*(11), 3370-3371.

Hisamatsu, K., Shiomi, T., Matsuura, S.I., Nara, T.Y., Tsunoda, T., Mizukami, F., & Sakaguchi, K. (2012). α-Amylase immobilization capacities of mesoporous silicas with different morphologies and surface properties. *Journal of Porous Materials*, *19*(1), 95-102.

Huh, S., Wiench, J.W., Yoo, J-C., Pruski, M., & Lin V.S-Y. (2003). Organic functionalization and morphology control of mesoporous silicas via a co-condensation synthesis method. *Chemistry of Materials, 15*, 4247-4256.

Inagaki, S., Fukushima, Y., & Kuroda, K. (1993). Synthesis of highly ordered mesoporous materials from a layered polysilicate. *Chemical Communications, 8*, 680-682.

Izquierdo-Barba, I., Vallet-Regí, M., Kupferschmidt, N., Terasaki, O., Schmidtchen, A., & Malmsten, M. (2009a). Incorporation of antimicrobial compounds in mesoporous silica film monolith. *Biomaterials. 30*(29), 5729-5736.

Izquierdo-Barba, I., Sousa, E., Doadrio, J.C., Doadrio, A.L., Pariente, J.P., Martínez, A., Babonneau, F., & Vallet-Regí, M. (2009b). Influence of mesoporous structure type on the controlled delivery of drugs: release of ibuprofen from MCM-48, SBA-15 and functionalized SBA-15. *Journal of sol-gel science and technology*, *50*(3), 421-429.

Jansen, J.C., Shan, Z., Marchese, L., Zhou, W., v d Puil, N., & Maschmeyer, T. (2001). A new templating method for three-dimensional mesopore networks. *Chemical Communications*, (8), 713-714.

Kaneda, M., Tsubakiyama, T., Carlsson, A., Sakamoto, Y., Ohsuna, T., & Terasaki, O. (2002). Structural study of mesoporous MCM-48 and carbon networks synthesized in the spaces of MCM-48 by electron crystallography. *The Journal of Physical Chemistry B*, *106*(6), 1256-1266.

Kapoor, M.P., Vinu, A., Fujii, W., Kimura, T., Yang, Q., Kasama, Y., Yanagi, M., & Juneja, L.R. (2010). Self-assembly of mesoporous silicas hollow microspheres via food grade emulsifiers for delivery systems. *Microporous and Mesoporous Materials*, *128*(1), 187-193.

Knežević, N.Ž., Trewyn, B.G., & Lin, V.S.Y. (2011). Light-and pH-responsive release of doxorubicin from a mesoporous silica-based nanocarrier. *Chemistry-A European Journal*, *17*(12), 3338-3342.

Khushalani, D., Kuperman, A., Ozin, G.A., Tanaka, K., Coombs, N., Olken, M.M., & Garcés, J. (1995). Metamorphic materials: Restructuring siliceous mesoporous materials. *Advanced materials*, *7*(10), 842-846.

Kim, T.W., Kleitz, F., Paul, B., & Ryoo, R. (2005). MCM-48-like large mesoporous silicas with tailored pore structure: facile synthesis domain in a ternary triblock copolymer-butanol-water system. *Journal of the American Chemical Society, 127*(20), 7601-7610.

Kruk, M., Jaroniec, M., Antochshuk, V., & Sayari, A. (2002). Mesoporous silicate-surfactant composites with hydrophobic surfaces and tailored pore sizes. *The Journal of Physical Chemistry B, 106*(39), 10096-10101.

Kupferschmidt, N., Xia, X., Labrador, R.H., Atluri, R., Ballell, L., & Garcia-Bennett, A.E. (2013). *In vivo* oral toxicological evaluation of mesoporous silica particles. *Nanomedicine, 8*(1), 57-64.

Lai, C.Y., Trewyn, B.G., Jeftinija, D.M., Jeftinija, K., Xu, S., Jeftinija, S., & Lin, V.S.A. (2003). Mesoporous silica nanosphere-based carrier system with chemically removable CdS

nanoparticle caps for stimuli-responsive controlled release of neurotransmitters and drug molecules. *Journal of the American Chemical Society, 125*(15), 4451-4459.

Landry, C.C., Tolbert, S.H., Gallis, K.W., Monnier, A., Stucky, G.D., Norby, P., & Hanson, J.C. (2001). Phase transformations in mesostructured silica/surfactant composites. Mechanisms for change and applications to materials synthesis. *Chemistry of materials*, *13*(5), 1600-1608.

Lei, J., Fan, J., Yu, C., Zhang, L., Jiang, S., Tu, B., & Zhao, D. (2004) Immobilization of enzymes in mesoporous materials: controlling the entrance to nanospace. *Microporous and Mesoporous Materials, 73*(6), 121–128.

Li, Z.Z., Wen, L.X., Shao, L., & Chen, J.F. (2004). Fabrication of porous hollow silica nanoparticles and their applications in drug release control. *Journal of Controlled Release*, *98*(2), 245-254.

Li-hong, W., Xin, C., Hui, X., Li-li, Z., Jing, H., Mei-juan, Z., Jie, L., Yi, L., Jin-wen, L., Wei, Z., & Gang, C. (2013). A novel strategy to design sustained-release poorly water-soluble drug mesoporous silica microparticles based on supercritical fluid technique. *International Journal of Pharmaceutics*, *454*(1), 135-142.

Limnell, T., Santos, H.A., Mäkilä, E., Heikkilä, T., Salonen, J., Murzin, D.Y., Kumar, N., Laaksonen, T., Peltonen, L., & Hirvonen, J. (2011). Drug delivery formulations of ordered and nonordered mesoporous silica: comparison of three drug loading methods. *Journal of Pharmaceutical Sciences*, *100*(8), 3294-3306.

Liu, F., Yuan, P., Wan, J.J., Qian, K., Wei, G.F., Yang, J., Liu, B.H., Wang, Y.H., & Yu, C.Z. (2011). Periodic mesoporous organosilicas with controlled pore symmetries for peptides enrichment. *Journal of nanoscience and nanotechnology*, *11*(6), 5215-5222.

Liu, R., Zhao, X., Wu, T., & Feng, P. (2008). Tunable redox-responsive hybrid nanogated ensembles. *Journal of the American Chemical Society*, *130*(44), 14418-14419.

Luo, Z., Deng, Y., Zhang, R., Wang, M., Bai, Y., Zhao, Q., Lyu, Y., Wei, J., & Wei, S. (2015). Peptide-laden mesoporous silica nanoparticles with promoted bioactivity and osteo-differentiation ability for bone tissue engineering. *Colloids and Surfaces B: Biointerfaces*, *131*, 73-82.

Ma, Z., Bai, J., Wang, Y., & Jiang, X. (2014). Impact of shape and pore size of mesoporous silica nanoparticles on serum protein adsorption and RBCs hemolysis. *ACS Applied Materials & Interfaces, 6*(4), 2431–2438.

Madene, A., Jacquot, M., Scher, J., & Desobry, S. (2006). Flavour encapsulation and controlled release–a review. *International Journal of Food Science & Technology*, *41*(1), 1-21.

Madieh, S., Simone, M., Wilson, W., Mehra, D. & Augsburger, L. (2007). Investigation of drug-porous adsorbent interactions in drug mixtures with selected porous adsorbents. *Journal of Pharmaceutical Sciences*, *96*(4), 851-863.

Mellaerts, R., Jammaer, J.A., Van Speybroeck, M., Chen, H., Humbeeck, J.V., Augustijns, P., Van den Mooter, G., & Martens, J.A. (2008). Physical state of poorly water soluble therapeutic molecules loaded into SBA-15 ordered mesoporous silica carriers: a case study with itraconazole and ibuprofen. *Langmuir*, *24*(16), 8651-8659.

Mal, N.K., Fujiwara, M., & Tanaka, Y. (2003). Photocontrolled reversible release of guest molecules from coumarin-modified mesoporous silica. *Nature*, *421*(6921), 350-353.

Manzano, M., Aina, V., Arean, C.O., Balas, F., Cauda, V., Colilla, M., Delgado, M.R., & Vallet-Regi, M. (2008). Studies on MCM-41 mesoporous silica for drug delivery: effect of particle morphology and amine functionalization. *Chemical Engineering Journal*, *137*(1), 30-37.

Mas, N., Agostini, A., Mondragón, L., Bernardos, A., Sancenón, F., Marcos, M.D., Martínez-Máñez, R., Costero, A.M., Gil, S., Merino-Sanjuán, M., Amorós, P., Orzáez, M., & Pérez-Payá, E. (2013). Enzyme-responsive silica mesoporous supports capped with azopyridinium salts for controlled delivery applications. *Chemistry-A European Journal*, *19*(4), 1346-1356.

Mondragón, L., Mas, N., Ferragud, V., de la Torre, C., Agostini, A., Martínez-Máñez, R., Sancenón, F., Amorós, P., Pérez-Payá, E., & Orzáez, M. (2014). Enzyme-Responsive Intracellular-Controlled Release Using Silica Mesoporous Nanoparticles Capped with ε-Poly-L-lysine. *Chemistry-A European Journal*, *20*(18), 5271-5281.

Muth, O., Schellbach, C., & Fröba, M. (2001). Triblock copolymer assisted synthesis of periodic mesoporous organosilicas (PMOs) with large. *Chemical Communications*, (19), 2032-2033.

Nieto, A., Balas, F., Colilla, M., Manzano, M., & Vallet-Regí, M. (2008). Functionalization degree of SBA-15 as key factor to modulate sodium alendronate dosage. *Microporous and Mesoporous Materials*, *116*(1), 4-13.

Nishiyama, N., Tanaka, S., Egashira, Y., Oku, Y., & Ueyama, K. (2003) Vapor-phase synthesis of mesoporous silica thin films. *Chemistry of Materials, 15*(4), 1006-1011.

Nguyen, T.D., Liu, Y., Saha, S., Leung, K.C.F., Stoddart, J.F., & Zink, J.I. (2007). Design and optimization of molecular nanovalves based on redox-switchable bistable rotaxanes. *Journal of the American Chemical Society*, *129*(3), 626-634.

Pal, N., & Bhaumik, A. (2013). Soft templating strategies for the synthesis of mesoporous materials: Inorganic, organic–inorganic hybrid and purely organic solids. *Advances in colloid and interface science*, *189*, 21-41.

Pandey, K.B., & Rizvi, S.I. (2009). Plant polyphenols as dietary antioxidants in human health and disease. *Oxidative Medicine and Cellular Longevity, 2*(5), 270–278.

Park, S-Y., Barton, M., & Pendleton, P. (2012) Controlled release of allyl isothiocyanate for bacteria growth management. *Food Control Volume, 23*(2), 478-484.

Pérez-Esteve, É., Fuentes, A., Coll, C., Acosta, C., Bernardos, A., Amorós, P., Marcos, M.D., Sancenón, F., Martínez-Máñez, R., & Barat, J.M. (2015). Modulation of folic acid bioaccessibility by encapsulation in pH-responsive gated mesoporous silica particles. *Microporous and Mesoporous Materials*, *202*, 124-132.

Pérez-Esteve, É., Ruiz-Rico, M., Martínez-Máñez, R., & Barat, J.M. (2016a). Mesoporous silica-based supports for the controlled and targeted release of bioactive molecules in the gastrointestinal tract. *Journal of Food Science*, *80*(11), E2504-E2516.

Pérez-Esteve, É., Oliver, L., García, L., Nieuwland, M., de Jongh, H.H., Martínez-Máñez, R., & Barat, J.M. (2014). Incorporation of mesoporous silica particles in gelatine gels: Effect of particle type and surface modification on physical properties. *Langmuir*, *30*(23), 6970-6979.

Popat, A., Liu, J., Lu, G.Q. M., & Qiao, S.Z. (2012). A pH-responsive drug delivery system based on chitosan coated mesoporous silica nanoparticles. *Journal of Materials Chemistry*, *22*(22), 11173-11178.

Popova, M., Szegedi, A., Mavrodinova, V., Tušar, N.N., Mihály, J., Klébert, S., Benbassat, N., & Yoncheva, K. (2014). Preparation of resveratrol-loaded nanoporous silica materials with different structures. *Journal of Solid State Chemistry*, *219*, 37-42.

Qiao, Z.A., Zhang, L., Guo, M., Liu, Y., & Huo, Q. (2009). Synthesis of mesoporous silica nanoparticles via controlled hydrolysis and condensation of silicon alkoxide. *Chemistry of Materials*, *21*(16), 3823-3829.

Quan, G.L., Chen, B., Wang, Z.H., Wu, H., Huang, X.T., Wu, L.N., & Wu, C.B. (2012) Improving the dissolution rate of poorly water-soluble resveratrol by the ordered mesoporous silica. *Acta Pharmaceutica Sinica, 47*(2), 239-243.

Rashidi, L., Vasheghani-Farahani, E., Rostami, K., Gangi, F., & Fallahpour, M. (2013) Mesoporous silica nanoparticles as a nanocarrier for delivery of vitamin C. *Iranian Journal of Biotechnology, 11*(4), 209-213.

Riikonen, J. (2012). Modification, characterization and applications of mesoporous silicon-based drug carriers. *Solid state: processes and analysis, 45,* 1-72.

Santos, H.A. (Ed.). (2014). *Porous silicon for biomedical applications*. Cambridge: Woodhead Publishing Elsevier.

Salonen, J., Kaukonen, A.M., Hirvonen, J., & Lehto, V. P. (2008) Mesoporous silicon in drug delivery applications. *Journal of Pharmaceutical Sciences, 97*(2), 632-653.

Sapino, S., Ugazio, E., Gastaldi, L., Miletto, I., Berlier, G., Zonari, D., & Oliaro-Bosso, S. (2015) Mesoporous silica as topical nanocarriers for quercetin: characterization and *in vitro* studies. *European Journal of Pharmaceutics and Biopharmaceutics, 89,* 116-125.

Sayari, A., & Hamoudi, S. (2001) Periodic mesoporous silica-based organic-inorganic nanocomposite materials. *Chemistry of Materials, 13*(10), 3151-3168.

Slowing, I.I., Vivero-Escoto, J.L., Wu, C.W., & Lin, V.S.Y. (2008). Mesoporous silica nanoparticles as controlled release drug delivery and gene transfection carriers. *Advanced drug delivery reviews*, *60*(11), 1278-1288.

Tang, F., Li, L., & Chen, D. (2012). Mesoporous silica nanoparticles: synthesis, biocompatibility and drug delivery. *Advanced Materials*, *24*(12), 1504-1534.

Takimoto, A., Shiomi, T., Ino, K., Tsunoda, T., Kawai, A., Mizukami, F., & Sakaguchi, K. (2008). Encapsulation of cellulase with mesoporous silica (SBA-15). *Microporous and Mesoporous Materials*, *116*(1), 601-606.

Tanev, P.T., & Pinnavaia, T.J. (1995). A neutral templating route to mesoporous molecular sieves. *Science*, *267*(5199), 865-867.

Tischer, W., & Wedekind, F. (1999). Immobilized enzymes: methods and applications. In: *Biocatalysis - from discovery to application* (pp. 95-126). Springer Berlin Heidelberg.

Trewyn, B.G., Slowing, I.I., Giri, S., Chen, H.T., & Lin, V.S. (2007). Synthesis and functionalization of a mesoporous silica nanoparticle based on the sol-gel process and applications in controlled release. *Accounts of Chemical Research, 40*(9), 846-853.

Urbán, P., Valle-Delgado, J.J., Moles, E., Marques, J., Díez, C., & Fernàndez-Busquets, X. (2012). Nanotools for the delivery of antimicrobial peptides. *Current Drug Targets, 13*(9), 1158-1172.

Vallet-Regí, M., Ramila, A., del Real, R.P., & Perez-Pariente, J. (2001). A new property of MCM-41: drug delivery system. *Chemistry of Materials, 13,* 308-311.

Veith, S.R., Hughes, E., & Pratsinis, S.E. (2004). Restricted diffusion and release of aroma molecules from sol-gel-made porous silica particles. *Journal of Controlled Release*, *99*(2), 315-327.

Vinu, A., Hossain, K.Z., & Ariga, K. (2005). Recent advances in functionalization of mesoporous silica. *Journal of Nanoscience and Nanotechnology*, *5*(3), 347-371.

Yanagisawa, T., Shimizu, T., Kuroda, K., & Kato, C. (1990). The preparation of alkyltrimethylammonium-kanemite complexes and their conversion to microporous materials. *Bulletin of the Chemical Society of Japan, 63*(4), 988-992

Zhang, G., Yang, M., Cai, D., Zheng, K., Zhang, X., Wu, L., & Wu, Z. (2014). Composite of functional mesoporous silica and DNA: an enzyme-responsive controlled release drug carrier system. *ACS applied materials & interfaces*, *6*(11), 8042-8047.

Zhao, X.S. (2006). Novel porous materials for emerging applications. *Journal of Materials Chemistry, 16*, 623-625.

Zhao, D.Y., Feng, J.L., Huo, Q.S., Melosh, N., Fredrickson, G.H., Chmelka, B.F., & Stucky, G.D. (1998a). Triblock copolymer syntheses of mesoporous silica with periodic 50 to 300 angstrom pores. *Science, 279,* 548–552.

Zhao, D., Huo, Q., Feng, J., Chmelka, B.F., & Stucky, G.D. (1998b). Nonionic triblock and star diblock copolymer and oligomeric surfactant syntheses of highly ordered, hydrothermally stable, mesoporous silica structures. *Journal of the American Chemical Society*, *120*(24), 6024-6036.

Zhao, Z.Y., Liu, J., Hahn, M., Qiao, S., Middelberg, A.P., & He, L. (2013). Encapsulation of lipase in mesoporous silica yolk–shell spheres with enhanced enzyme stability. *RSC Advances*, *3*(44), 22008-22013.

Zheng, Q., Lin, T., Wu, H., Guo, L., Ye, P., Hao, Y., Guo, Q., Jiang, J., Fu, F., & Chen, G. (2014). Mussel-inspired polydopamine coated mesoporous silica nanoparticles as pH-sensitive nanocarriers for controlled release. *International journal of pharmaceutics*, *463*(1), 22-26.

Zhou, C., & Garcia-Bennett, A.E. (2010). Release of folic acid in mesoporous NFM-1 silica. *Journal of Nanoscience and Nanotechnology, 10*(11), 7398-7401.

Zhu, Y., Meng, W., & Hanagata, N. (2011). Cytosine-phosphodiester-guanine oligodeoxynucleotide (CpG ODN)-capped hollow mesoporous silica particles for enzyme-triggered drug delivery. *Dalton Transactions*, *40*(39), 10203-10208.

Zhuge, Q., & Klopfenstein, C.F. (1986). Factors affecting storage stability of vitamin A, riboflavin, and niacin in a broiler diet premix. *Poultry Science*, *65*(5), 987-994.

Zuidam, N.J., & Heinrich, E. (2010). In: *Encapsulation of aroma* (pp. 127-160). Springer New York.

4. CHAPTER 1. Toward the enhancement of folates stability through silica supports

4.1. Introduction

1. Chemical classification and appearance

Folate is a generic term for a water-soluble vitamin B including naturally-occurring folates with different states of oxidation. They all originate from the main structure of pteroylmonoglutamic acid which is commonly known as folic acid (FA) and does not occur in nature. FA is suggested to be the most stable type of the folate group and is commercially used in dietary supplements and fortified food (Fukuwatari et al., 2009). This basic heterocyclic structure is composed of a pteridine ring connected by a methylene bond to a residue of p-amino benzoic acid and a glutamate moiety (Araújo et al., 2011; Fukuwatari et al., 2009). Folates are the reduced forms of FA and differ in state of oxidation of the pteridine ring, the one-carbon substitutions like methyl and formyl groups of the pteridine ring, and the number of conjugated glutamyl moieties (Verlinde et al., 2009).

Natural folates can be found in green leafy vegetables, citrus fruits, beans, cereals, liver, egg yolk, yeast, milk, and fermented dairy products (Gujska et al., 2009; Indrawati et al., 2004; Ngyuen et al., 2003; Scott et al., 2000). The amount and composition of folates varies in food, and therefore a distribution of appearing folates cannot be generalized. Most folates are in the form of polyglutamates (90%) and a small amount is in form of monoglutamates (10%). The most dominant naturally-occurring folate derivatives are 5-methyltetrahydrofolate, 5-formyltetrahydrofolate, and 10-formyltetrahydrofolate, as well as their oxidation products 10-formyldihydrofolate, 5,10-methenyltetrahydrofolate and 10-formylfolic acid (Jägerstad & Jastrebova, 2013; Verlinde et al., 2009).

2. Role in human nutrition

Folate intake is essential for human body and cannot be synthesized *de novo* by the organism. They prevent cardiovascular diseases, Alzheimer, atherosclerosis, colon and colorectal cancer, and birth defects during pregnancy (Choi & Mason, 2002; Clarke et al., 1998; Hoag et al., 1997; Lucock, 2000; Pitkin, 2007; Stover, 2004). Folates are needed for their role as coenzyme in nucleic acids and amino acids (methionine from homocysteine) synthesis and for the oxidation and reduction of one-carbon units required for normal metabolism and regulation (Wagner, 1995). It is recommended a daily intake of 200-400 µg folates per day for adults and an additional 400 µg folates per day in pregnant women (ESCO, 2009). An adequate folate status should be obtained from food or dietary supplements (Gujska et al., 2009).

The absorption process of folates takes place in the jejunum where are directly taken in by mucosal cells once the cleavage of polyglutamate chains by carboxypeptidase enzyme (Melse-Boonstra et al., 2004). The synthetic vitamin (FA) is a monoglutamate and therefore shows a higher bioavailability (FAO/WHO, 2001). After absorption, FA has to be enzymatically transformed into the biologically active folate (5-methyltetrahydrofolate).

High doses of natural folates hinder the uptake of folate into cells by not cleaving the polyglutamate moieties. In contrast, excessive intake of FA is not regulated by enzymes and it can appear unaltered in the bloodstream (Scott et al., 2000).

The accumulation of unmetabolized FA in blood (higher than upper tolerance intake of 1 mg/day) may stimulate tumor growth, mask vitamin B12 deficiency which causes neurological defects, and reduce the efficacy of drugs used in rheumatoid arthritis or psoriasis treatment (ESCO, 2009; Kim, 2007; Scott et al., 2000). However, the need of folic acid or folates for human body is indisputable. Then, the folate intake should be a balancing act to assure that the required level is given but not overdosed by consuming supplements or fortified food.

3. Stability

Folates are widely distributed in food but they are in relative low quantity, and they can be affected, among other factors, by pH, temperature, pressure, light and antioxidants.

The folates stability at different pH values depends on the acidity or alkalinity of the aqueous solution and the presence of antioxidants such as ascorbic acid or mercaptoethanol (De Brouwer et al., 2007). Folic acid and folates have shown good stability in the range between pH 4 and pH 10, and fast degradation below or above this range in absence of antioxidants (Jastrebova et al., 2013; Yakubu & Muazu, 2010).

Solid folic acid is crystalline at room temperature, but under thermal stress it suffers great degradation at 200 °C resulting in an amorphous product. FA decomposes in three steps: the first reaction corresponds to the loss of the glutamic acid moiety from the FA structure, followed by the loss of the amide, and then the pteridine decomposes at 270 °C (Vora et al., 2002). Otherwise, dissolved FA and folates are stable at 100 °C for several hours but their stability is highly pH-dependent with substantially degradation at low pH (Cheung et al., 2008; De Brouwer et al., 2007). The presence of antioxidants also takes place an important role in the thermal degradation of folates (Nguyen et al., 2003).

Folates and FA are photosensitive compounds which are degraded by visible and ultraviolet light in aqueous solution (Ball, 2005). Diverse studies have shown total degradation of FA after some hours of irradiation (Akhtar et al., 2003; Off et al., 2005; Yakubu & Muazu, 2010) and higher stability of natural folates (Fukuwatari et al., 2009). FA showed higher stability in alkaline media than under acidic conditions (Akhtar et al., 2003). The degradation takes place due to the cleavage of the bond between C9-N10, and then the excision of the p-teridin moiety from p-aminobenzoylglutamate (Akhtar et al., 2003; Off et al., 2005). This oxidative degradation generates an enamine compound due to dehydrogenation

of FA by a free radical. This intermediate form irreversible breaks the bond between the C9-N10 which causes the final decay in the separation of the pteridine moiety from the p-aminobenzoylglutamate (Akhtar et al., 2003; Off et al., 2005).

4. Encapsulation systems

Although folate intake is indispensable, some studies have reported that high doses of FA may promote some neoplasia and mask symptoms of vitamin B12 deficiency (Crider et al., 2011; Wright et al., 2007). Recent studies suggest that these negative side effects might be related to the presence of unmetabolized FA in blood because of the reduced enzyme activity (Lucock & Yates, 2009). Therefore, it is of interest to create a dosage form which can fully guarantee controlled release of the vitamin and thus bioavailability at the site of action, and protect the vitamin from degradation.

Micro- and nanoencapsulation of folic acid and derivatives in organic delivery supports have been recently developed for food fortification. Diverse studies have microencapsulated this vitamin using polysaccharides or proteins through spray-drying (de Britto et al., 2012; Liu et al., 2012; Madziva et al., 2006; Shrestha et al., 2012; Tomiuk et al., 2012), and electrospinning (Aceituno-Medina et al., 2015; Bakhshi et al., 2013). Some of these delivery systems have been incorporated to food products and they have exhibited the improvement of folates stability. In the studies of Liu et al. (2012) and Tomiuk et al. (2012), 5-methyltetrahydrofolate was co-encapsulated with sodium ascorbate and added to flour. Breads made with fortified flour presented high recoveries of the vitamin after bread baking and storage. Madziva et al. (2006) encapsulated folic acid in alginate-pectin capsules and incorporated them in milk to produce Cheddar cheese resulting in improved stability during production and ripening period. Other food processing operation tested was the extrusion of starch with microencapsulated 5-methyltetrahydrofolate. Analysis of fortified extrudate powder showed the

enhancement of the encapsulated vitamin stability, in comparison to its free form, mainly at elevated extrusion temperatures (Shrestha et al., 2012). Despite the protective effect, none of these systems were able to control the release of the vitamin along the time. Thus, their consumption could provoke peaks of absorption and related implications in health.

On the other hand, it has been recently presented a smart delivery system based on amine-functionalized mesoporous silica particles to dosage FA along a simulated digestion process to hinder its release during its pass through the stomach and gradually deliver the cargo during its pass through the intestine (Pérez-Esteve et al., 2015). The loading of this delivery support was optimized to release a large amount of the vitamin (95 µg FA/mg solid). In this manner, the higher recommended dietary intakes in human nutrition, established for pregnant women in 600 µg per day of folates could be reached by an oral administration of only ca. 4 mg of particles, which is a remarkable low amount. After that, different silica materials (hollow silica shells, MCM-41, SBA-15, UVM-7) were used to study the influence of particle morphology, pore size, and pore volume of the silica support on the loading efficiency and FA release profile (Pérez-Esteve et al., 2016). Results showed higher FA release for SBA-15 particles and hollow silica shells than MCM-41 or UVM-7. However, having in mind the most sustained release profile, microparticles of MCM-41 were proposed as the most convenient support for modulating the bioaccessibility of FA along the pass through the small intestine. Despite their capability to modulate FA bioaccessibility, the possible protective effect of these particles against main prodegradative factors is unknown.

Thus, the first chapter of this thesis is focused on the evaluation of the protective effect of mesoporous silica particles against degradation processes occurring in folic acid and folates during food processing and human digestion.

References

Aceituno-Medina, M., Mendoza, S., Lagaron, J. M., & López-Rubio, A. (2015). Photoprotection of folic acid upon encapsulation in food-grade amaranth (*Amaranthus hypochondriacus L*.) protein isolate–Pullulan electrospun fibers. *LWT-Food Science and Technology, 62*(2), 970-975.

Akhtar, M.J., Khan, M.A., & Ahmad, I. (2003). Identification of photoproducts of folic acid and its degradation pathways in aqueous solution. *Journal of Pharmaceutical and Biomedical Analysis, 31*(3), 579-588.

Araújo, M.M., Marchioni, E., Bergaentzle, M., Zhao, M., Kuntz, F., Hahn, E., & Villavicencio, A.L.C.H. (2011). Irradiation stability of folic acid in powder and aqueous solution. *Journal of Agricultural & Food Chemistry, 59*(4), 1244–1248.

Ball, G. F. M. (2005). In: *Vitamins in Foods, Analysis, Bioavailability and Stability*. CRC, Boca Raton.

Bakhshi, P.K., Nangrejo, M.R., Stride, E., & Edirisinghe, M. (2013). Application of electrohydrodynamic technology for folic acid encapsulation. *Food and Bioprocess Technology, 6*(7), 1837-1846.

Cheung, R.H.F., Morrison, P.D., Small, D.M., & Marriott, P.J. (2008). Investigation of folic acid stability in fortified instant noodles by use of capillary electrophoresis and reversed-phase high performance liquid chromatography. *Journal of Chromatography A, 1213*(1), 93-99.

Choi, S.W., & Mason, J.B. (2002). Folate status: effects on pathways of colorectal carcinogenesis. *The Journal of Nutrition, 132*, 2413–2418.

Clarke, R., Smith, A.D., Jobst, K.A., Refsum, H., Sutton, L. &. Ueland, P.M. (1998). Folate, vitamin B_{12}, and serum total homocysteine levels in confirmed Alzheimer disease. *Formerly Archives of Neurology 55*(11), 1449-1455.

Crider, K.S., Bailey, L.B., &. Berry, R.J. (2011). Folic acid food fortification - Its history, effect, concerns, and future directions. *Nutrients 3*(3), 370–384.

de Britto, D., de Moura, M.R., Aouada, F.A., Mattoso, L.H., & Assis, O. B. (2012). N, N, N-trimethyl chitosan nanoparticles as a vitamin carrier system. *Food hydrocolloids, 27*(2), 487-493.

De Brouwer, V., Zhang, G.F., Storozhenko, S., Van Der Straeten, D., & Lambert, W. E. (2007). pH stability of individual folates during critical sample preparation steps in prevision of the analysis of plant folates. *Phytochemical Analysis 18*(6), 496-508.

ESCO (EFSA's Scientific Cooperation) (2009). Report on analysis of risks, benefits of fortification of food with folic acid, 17-99.

Food and Agriculture Organization/ Word Health Organization (FAO/WHO) (2001). Human vitamin and mineral requirements - Chapter 4: folate and folic acid. Report of a joint FAO/WHO expert consultation, 53–63.

Fukuwatari, T., Fujita, M., & Shibata, K. (2009). Effects of UVA irradiation on the concentration of folate in human blood. *Bioscience, Biotechnology, and Biochemistry, 73*(2), 322-327.

Gujska, E., Michalak, J., & Klepacka, J. (2009). Folates stability in two types of rye breads during processing and frozen storage. *Plant Foods for Human Nutricion, 64*(2), 129-134.

Hoag, S.W., Ramachandruni, H., & Shangraw, R.F. (1997). Failure of prescription prenatal vitamin products to meet USP standards for folic acid dissolution. Six of nine vitamin products tested failed to meet USP standards for folic acid dissolution. *Journal of the American Pharmaceutical Association 37*(4), 397–400.

Indrawati, Arroqui, C., Messagie, I., Nguyen, M. T., Loey, A., & Hendrickx, M. (2004). Comparative study on pressure and temperature stability of 5-methyltetrahydrofolic acid in model systems and in food products. *Journal of Agricultural and Food Chemistry, 52*(3), 485-492.

Jastrebova, J., Axelsson, M., Strandler, H.S., & Jägerstad, M. (2013). Stability of dietary 5-formyl-tetrahydrofolate and its determination by HPLC: a pilot study on impact of pH, temperature and antioxidants on analytical results. *European Food Research and Technology 237*(5), 747–754.

Jägerstad, M., & Jastrebova, J. (2013). Occurence, stability, and determination of formyl folates in foods. *Journal of Agricultural and Food Chemistry, 61*, 9758–9768.

Kim, Y.I. (2007) Folic acid fortification and supplementation - good for some but not so good for others. *Nutrition Reviews, 65*(11), 504–511.

Liu, Y., Green, T.J., Wong, P., & Kitts, D.D. (2012). Microencapsulation of L-5-methyltetrahydrofolic acid with ascorbate improves stability in baked bread products. *Journal of Agricultural and Food Chemistry, 61*(1), 247-254.

Lucock, M. (2000). Folic acid: nutritional biochemistry, molecular biology, and role in disease processes. *Molecular Genetics and Metabolism, 71*, 121–138.

Lucock, M., & Yates, Z. (2009). Folic acid fortification: a double-edged sword. *Current Opinion in Clinical Nutrition & Metabolic Care*, *12*(6), 555-564.

Madziva, H., Kailasapathy, K., & Phillips, M. (2006). Evaluation of alginate–pectin capsules in Cheddar cheese as a food carrier for the delivery of folic acid. *LWT-Food Science and Technology, 39*(2), 146-151.

Melse-Boonstra, A., West, C.E., Katan, M.B., Kok, F.J., & Verhoef, P. (2004). Bioavailability of heptaglutamyl relative to monoglutamyl folic acid in healthy adults. *The American Journal of Clinical Nutrition, 79*, 424-429.

Nguyen, M.T., Indrawati, & Hendrickx, M. (2003). Model studies on the stability of folic acid and 5-methyltetrahydrofolic acid degradation during thermal treatment in combination with high hydrostatic pressure. *Journal of Agricultural and Food Chemistry, 51*(11), 3352–3357.

Off, M. K., Steindal, A. E., Porojnicu, A. C., Juzeniene, A., Vorobey, A., Johnsson, A., & Moan, J. (2005). Ultraviolet photodegradation of folic acid. *Journal of Photochemistry and Photobiology B: Biology, 80*(1), 47-55.

Pérez-Esteve, É., Fuentes, A., Coll, C., Acosta, C., Bernardos, A., Amorós, P., Marcos, M. D., Sancenón, F., Martínez-Máñez, R., & Barat, J. M. (2015). Modulation of folic acid bioaccessibility by encapsulation in pH-responsive gated mesoporous silica particles. *Microporous and Mesoporous Materials*, *202*, 124-132.

Pérez-Esteve, É., Ruiz-Rico, M., de la Torre, C., Villaescusa, L. A., Sancenón, F., Marcos, M. D., Amorós, P., Martínez-Máñez, R., & Barat, J. M. (2016). Encapsulation of folic acid in different silica porous supports: A comparative study. *Food Chemistry*, *196*, 66-75.

Pitkin, R.M. (2007). Folate and neural tube defects. *The American Journal of Clinical Nutrition, 85*, 285–288.

Scott, J., Rébeillé, F., & Fletcher, J. (2000). Folic acid and folates: the feasibility for nutritional enhancement in plant foods. *Journal of the Science of Food and Agriculture, 80*(7), 795-824.

Shrestha, A. K., Arcot, J., & Yuliani, S. (2012). Susceptibility of 5-methyltetrahydrofolic acid to heat and microencapsulation to enhance its stability during extrusion processing. *Food chemistry, 130*(2), 291-298.

Stover, P.J. (2004). Physiology of folate and vitamin B_{12} in health and disease. *Nutrition Reviews 62*(6), 3–12.

Tomiuk, S., Liu, Y., Green, T. J., King, M. J., Finglas, P. M., & Kitts, D. D. (2012). Studies on the retention of microencapsulated L-5-methyltetrahydrofolic acid in baked bread using skim milk powder. *Food chemistry, 133*(2), 249-255.

Verlinde, P.H.C.J., Oey, I., Deborggraeve, W.M., Hendrickx, M.E., & Loey, A.M. (2009) Mechanism and related kinetics of 5-methyltetrahydrofolic acid degradation during combined high hydrostatic pressure–thermal treatments. *Journal of Agricultural & Food Chemistry, 57*(15), 6803–6814.

Vora, A., Riga, A., Dollimore, D., & Alexander, K. S. (2002). Thermal stability of folic acid. *Thermochimica Acta, 392,* 209-220.

Wagner, C. (1995). In: *Biochemical role of folate in cellular metabolism*. Bailey, L.B. (Ed), Folate in Health and Disease. New York: Marcel Dekker.

Wright, A.J., Dainty, J.R., & Finglas, P.M. (2007). Folic acid metabolism in human subjects revisited: potential implications for proposed mandatory folic acid fortification in the UK. *British Journal of Nutrition, 98*(04), 667-675.

Yakubu, S.; & Muazu, J. (2010). Effects of variables on degradation of folic acid. *Der Pharmacia Sinica, 1*(3), 55-58.

4.2. Protective effect of mesoporous silica particles on encapsulated folates

María Ruiz-Rico,[a*] Hanna Daubenschüz,[a] Édgar Pérez-Esteve,[a] María D. Marcos,[b,c] Pedro Amorós,[d] Ramón Martínez-Máñez,[b,c] and José M. Barat[a]

[a]Grupo de Investigación e Innovación Alimentaria, Departamento de Tecnología de Alimentos. Universitat Politècnica de València. Camino de Vera s/n, 46022, Spain
[b]Centro de Reconocimiento Molecular y Desarrollo Tecnológico (IDM), Unidad Mixta Universitat Politècnica de València - Universidad de Valencia. Departamento de Química Universitat Politècnica de València, Camino de Vera s/n, 46022, Valencia, Spain
[c]CIBER de Bioingeniería, Biomateriales y Nanomedicina (CIBER-BBN)
[d]Institut de Ciència dels Materials (ICMUV), Universitat de València, P.O. Box 2085, 46071, Valencia, Spain

Abstract

Mesoporous silica particles (MSPs) are considered suitable supports to design gated materials for the encapsulation of bioactive molecules. Folates are essential micronutrients which are sensitive to external agents that provoke nutritional deficiencies. Folates encapsulation in MSPs to prevent degradation and to allow their controlled delivery is a promising strategy. Nevertheless, no information exists about the protective effect of MSPs encapsulation to prevent their degradation. In this work, 5-formyltetrahydrofolate (FO) and folic acid (FA) were entrapped in MSPs functionalized with polyamines, which acted as pH-dependent molecular gates. The stability of free and entrapped vitamins after acidic pH, high temperature and light exposure was studied. The results showed the degradation of FO after high temperature and acidic pH, whereas entrapped FO displayed enhanced stability. Free FA was degraded by light, but MSPs stabilized the vitamin. The obtained results point toward the potential use of MSPs as candidates to enhance stability and to improve the bioavailability of functional biomolecules.

Keywords: 5-formyltetrahydrofolate; controlled release; encapsulation; folic acid; mesoporous silica particles; stability

1. Introduction

In the last years hybrid organic–inorganic materials have attracted considerable interest due to the combination of the beneficial characteristic of organic chemistry and material science in order to develop smart nanodevices. Among different hybrid solids, mesoporous silica particles (MSPs) offer several unique features that allow the design of gated materials for controlled release and sensing/recognition protocols (Aznar et al., 2016). The first family of MSPs called MCM was described in the early 1990s by the Mobil Corporation Laboratories. This family of silica supports include different porous silica exhibiting hexagonal (MCM-41), cubic (MCM-48) and lamellar (MCM-50) pore shapes. After these developments, new ordered materials (i.e. MSU, KIT, FDU, AMS, SBA…) with a wide range of textural properties have been described by different authors (Trewyn et al., 2007). MSPs possess broadly advantageous properties such as biocompatibility, thermal and chemical stability, huge loading capacity, high surface areas, tunable morphologies and pore sizes, as well as facile functionalization of surfaces and pores (Li et al., 2012; Pérez-Esteve et al., 2014; Popat et al., 2011; Slowing et al., 2008; Song & Yang, 2015). The surface functionalization of MSPs for the development of gated materials allows that the delivery of the cargo stored in the inorganic support can be triggered by applying selected external stimulus (Aznar et al., 2016). Furthermore, it is considered that the inorganic framework can effectively protect the payload molecules from enzymatic degradation or denaturation caused by environmental changes (Song & Yang, 2015). However, there are few studies in the literature about the protective effect of MSPs on the stability of biomolecules in biological solutions.

The functionalized MSPs have been used to encapsulate drugs mainly for the biomedical field, but also to encapsulate bioactive molecules for other sectors such as food technology. Different food ingredients and nutraceuticals including vitamins (Bernardos et al., 2008; Clifford et al., 2008; Kapoor et al., 2010; Pérez-Esteve et al., 2015; Rashidi et al., 2011), antioxidants (Cotea et al., 2012; Popoya et al., 2014), antimicrobials (Bernardos et al., 2015; Izquierdo-Barba et al., 2009;

Ruiz-Rico et al., 2015), aromas (Veith et al., 2004) or enzymes (Hisamatsu et al., 2012) have been entrapped in gated mesoporous materials. Most studies have been focused on the development and optimization of the encapsulation systems for controlled delivery, but it is expected that the MPSs may be able to enhance the stability of the entrapped bioactive compound.

Water-soluble vitamins, like folates, are labile compounds in the presence of environmental agents, such as extreme pH values or high temperatures (Ball, 2005). As folates are essential for the human body and cannot be synthesized *de novo* by the organism, this indispensable vitamin needs to be obtained from food or dietary supplements (Gujska et al., 2009). Thus the stability of this vitamin after storage and processing in food products or supplements should be taken into account. Loss of the biochemical activity of natural folates can occur during harvest, storage and food processing (Joint FAO & WHO, 2001; Indrawati et al., 2004). In general, pH, temperature, pressure, light and antioxidants, among others, can affect the stability of the natural folates and the synthetic folic acid (FA) (Vora et al., 2002; Akhtar et al., 2003; Nguyen et al., 2003; Off et al., 2005; Fukuwatari et al., 2009; Yakubu & Muazu, 2010; Jastrebova et al., 2013). FA, with a fully oxidized pteridine ring system, exhibits greater stability than folates. Among folates, large differences in stability exist in susceptibility to oxidative degradation, and 5-formyltetrahydrofolate (FO) is the most stable (Butz et al., 2004). Moreover, the stability of folates is influenced by pH and oxygen, which provokes their oxidation (Jastrebova et al., 2013; Wu et al., 2010). The inclusion of antioxidant compounds, such as ascorbic acid (AA) or mercaptoethanol, is required to prevent the destruction of labile folates from thermal exposure and photodegradation during food processing (Ball, 2005; Indrawati et al., 2004; Juzeniene et al., 2009).

Bearing in mind these factors, it is of interest to create folates encapsulation systems which can ensure the required dose and fully guarantee the stability and bioavailability of this vitamin. Therefore, the objective of this study was the encapsulation of FO and FA in a mesoporous silica support (MCM-41)

functionalized with amines to create a system to be used in orally delivered applications, and to study the stability of entrapped vitamins to test the efficacy of the MCM-41 support as a protector against external agents, such as acidic pH, high temperature and light.

2. Materials and methods

2.1. Chemicals

Tetraethylorthosilicate (TEOS), *N*-cetyltrimethylammonium bromide (CTABr), sodium hydroxide (NaOH), triethanolamine (TEAH₃), *N*-(3-trimethoxysilylpropyl)diethylenetriamine (N3), sodium phosphate monobasic (NaH₂PO₄), sodium phosphate dibasic (Na₂HPO₄) and tetrabutylammonium hydrogen sulfate (TBAHS) were provided by Sigma–Aldrich (Madrid, Spain). 5-formyltetrahydrofolate (FO) and folic acid (FA) were purchased from Schircks Laboratories (Jona, Switzerland). Acetonitrile HPLC grade was provided by Scharlab (Barcelona, Spain).

2.2. Mesoporous silica particles synthesis

Synthesis of microparticulated MCM-41 particles was carried out following the so-called "atrane route", where CTABr was used as the structure-directing agent. A molar ratio, fixed at 7 TEAH₃: 2 TEOS: 0.52 CTABr: 0.5 NaOH: 180 H₂O. CTABr, was added to a TEAH₃ and NaOH solution, which contained TEOS at 118 °C. After dissolving CTABr in the solution, water was slowly added along with vigorous stirring at 70 °C to form a white suspension. This mixture was aged at 100 °C for 24 h. Following synthesis, the solid was recovered, washed with deionized water and dried at 70 °C. The as-synthesized microparticles were calcined at 550 °C in an oxidant atmosphere for 5 h to remove the template phase (Bernardos et al., 2015).

2.3. Synthesis of encapsulated folates

The design of the encapsulation system was based on a previous work, in which FA was entrapped in a MSP functionalized with amines to deliver FA during a simulated digestion process (Pérez-Esteve et al., 2015). Dissolutions of FO and FA (10 mg/mL) were prepared in distilled water and phosphate-buffered saline (PBS), respectively. Solutions were added to 300 mg of MCM-41 in 3 addition cycles (1.5 mL per cycle). After each addition cycle, solids were dried at 37 °C to remove water content. After loading and drying, solids were collected and functionalized with 1.29 mL of N3 using different media; i.e. acetonitrile (**E-FO**) or acetate buffer at pH 2 (**E-FA**). The final mixtures were stirred for 5.5 h at room temperature, isolated by vacuum filtration, washed with 300 mL of water adjusted to pH 2, and dried at room temperature for 24 h.

2.4. Characterization of solids

Powder X-ray diffraction (PXRD), transmission electron microscopy (TEM), N_2 adsorption–desorption isotherms and zeta potential were used to characterize the synthesized materials. PXRD was performed in a BrukerD8 Advance diffractometer using CuKα radiation (Bruker, Coventry, UK). For the TEM analysis, particles were dispersed in dichloromethane and sonicated for 2 min to preclude aggregates. The suspension was then deposited onto copper grids coated with a carbon film (Aname SL, Madrid, Spain). The MSPs samples were imaged by JEOL JEM-1010 (JEOL Europe SAS, Croissy-sur-Seine, France) at an acceleration voltage of 80 kV. The single-particle size was estimated by averaging the measured size values of 50 particles. The N_2 adsorption–desorption isotherms were recorded with a Micrometrics ASAP2010 automated sorption analyzer (Micromeritics Instrument Corporation, Norcross, USA). Samples were degassed at 90 °C in vacuum overnight. Specific surface areas were calculated from the adsorption data within the low pressure range by the BET model. Pore size was determined following the BJH method. To determine the zeta potential of the materials, a

Zetasizer Nano ZS (Malvern Instruments, UK) was employed. Samples were dispersed in water at a concentration of 1 mg/mL. Before taking each measurement, samples were sonicated for 2 min to preclude aggregation. The zeta potential was calculated from the particle mobility values by applying the Smoluchowski model. The average of five recordings was reported as the zeta potential. Measurements were taken at 25 °C in triplicate.

2.5. Release studies

Delivery studies were conducted to test the release capacity of the encapsulation system and to confirm the functionality of the gates to modulate the release of vitamins according to the pH of the medium (closed gates at pH 2, opened gates at pH 7.5). To determine the release of FO and FA from the amine-gated mesoporous support (**E-FO** and **E-FA**), 10 mg of the solids was placed in 25 mL of PBS at pH 2 and pH 7.5. At certain time points (0, 2, 5, 15, 30, 60, 120, 180 min), aliquots were separated, the suspension was filtered and the solution was analyzed by HPLC.

2.6. Stability assays

The influence of diverse external agents, such as acidic pH, high temperature and light, on the stability of the free and entrapped vitamin was studied. Free FO and FA were treated, whenever possible, as the encapsulated vitamin in order to ensure reproducibility. In order to simulate not only the 3 day-loading (72 h drying at 37 °C) of the particles with the vitamin, but also a further 24-h drying period after functionalization, compounds in their free form were incubated for 96 h at 37 °C. The stability assays with the free vitamin were all conducted with these incubated samples (**F-FO** and **F-FA**).

For the stability assays, 4 mg of the entrapped vitamins (**E-FO** and **E-FA**) and the correspondent amounts of the free forms (ca. 0.02 mg for FO and ca. 0.3 mg

for FA) were dissolved in 10 mL of PBS (pH 2 or pH 7.5). All the stability experiments were performed in triplicate. The vitamin recoveries were presented by assuming the percentage recovered under optimal conditions to be 100% (pH 7.5, no treatment).

2.6.1. pH stability

These experiments were carried out to study the stability and solubility of vitamins at different pH values; e.g., the acidic pH at which FO and FA exhibited very low solubility (Jastrebova et al., 2013; Wu et al., 2010). These assays allow us to confirm the mechanism of polyamines as molecular gates due to the transformation of amines (open gate at a neutral/basic pH) into polyammonium groups (closed gate at an acidic pH).

Firstly, the recovery of free compounds under different pH conditions (pH 1, 2, 3, 4, 5, 6, 7, 8, 9, 10) was examined. Depending on the pH value, PBS was adjusted with H_2SO_4 and NaOH 1 M according to Wu et al. (2010). Then the correspondent volume of a stock solution of vitamins was added. After stirring samples for 1 h, they were taken for the HPLC analysis. The second part of the pH assays was conducted to test the stability behavior of vitamins after neutralization and to prove the functionality of ascorbic acid and the pH-responsive gated support to protect vitamins. The encapsulated vitamins were mixed with PBS (pH 2), stirred for 1 h and samples were taken. pH was adjusted to neutral pH with NaOH 5 M and vitamins were released. The same procedure was carried out with the free forms in the presence or absence of ascorbic acid.

2.6.2. Temperature stability

Temperature experiments were performed in an autoclave. Free vitamins were dissolved in PBS (pH 7.5) and equivalent amounts of encapsulated vitamin were suspended in PBS (pH 2) to keep the gates closed, and to then undergo the

sterilization process. Treatment was conducted at 121 °C and 1 bar at different times: 5, 10, 15 min. After treatment, vessels were cooled in an ice bath before taking samples to be analyzed. The encapsulated samples were released by adjusting the pH of the suspension from pH 2 to a neutral pH. Delivery was done as previously described.

2.6.3. Light stability

Two different light sources (visible and ultraviolet (UV) lamps) were used in the stability assays. Samples were prepared in their free forms (dissolved in PBS pH 7.5) and the impact of ascorbic acid as an antioxidant (0.1% AA dissolved in PBS) was partially examined. Experiments were conducted on encapsulated vitamins in PBS (pH 2) and were adjusted to pH 7.5 after the experiments, as reported above. All the samples were kept inside closed transparent borosilicate glass vessels (Ø 24 mm, h 45 mm) for different times in order to simulate an indirect light-induced stress, which can actually occur in real food products. Release of vitamins was conducted as explained above.

2.7. Folate and folic acid quantification

FO and FA were determined by reversed-phase HPLC following the method described by Pérez-Esteve et al. (2015). The HPLC instrument consisted in a Hitachi LaChrom Elite liquid chromatograph (Hitachi Ltd., Tokyo, Japan), equipped with an auto-sampler (module L-2200) and an UV detector (model L-2400). A Kromaphase 100 C18 (250 mm × 4.6 mm i.d., 5 µm particle size analytical column) (Scharlab, Barcelona, Spain) was used for separations. The wavelength of the UV detector was set at 280 nm. The mobile phase consisted in (A) 0.125 mM of NaH_2PO_4, 0.875 mM of Na_2HPO_4 and 0.4 mM of TBAHS in water and (B) an acetonitrile-mobile phase A 65:35 (v/v). The gradient program was: the mobile phase was run isocratically for the first 5 min with 90% A and 10% B. The percentage of B was linearly increased to reach 36% at 15 min and 60% at 30 min.

The percentage of B was lowered linearly to the original composition in 5 min, and remained under the initial conditions for 5 min. FO and FA were quantified according to the external standard method, in which a calibration curve of the peak area was used against the compound concentration.

2.8. Data analysis

Statistical data processing was performed using Statgraphics Centurion XVI (Statpoint Technologies, Inc., Warrenton, VA, USA). The influence of the different factors on the release and stability of the vitamin was analyzed by one-way analysis of variance (One-way ANOVA). The LSD procedure (least significant difference) was used to test for the differences between means at the 5% significance level.

3. Results and discussion

3.1. Synthesis and material characterization

FO and FA were encapsulated in the MSPs that contained gate-like ensembles as devices for controlled delivery applications. In this work, diethylenetriamine moiety was chosen as the capping ensemble given its proven properties to control the delivery of cargo molecules from the voids of MSPs in response to changes in pH (Bernardos et al., 2008; Casacús et al., 2008; Pérez-Esteve et al., 2015). In a first step, the support was synthesized by using CTABr as a structure director agent and TEOS as a silica source. After removing the surfactant by calcination the starting MCM-41 support was obtained. The pores of MCM-41 were loaded with FO and FA. To obtain the final materials (**E-FO** and **E-FA**), the loaded solids were reacted with *N*-(3-trimethoxysilylpropyl)diethylenetriamine.

The different supports were characterized by standard techniques. The X-ray patterns of solids MCM-41 as synthesized (a), calcined (b), loaded with FO and functionalized with amines (c) and loaded with FA and functionalized with amines

(d) can be found in Fig. 1. Curve a shows the expected four peaks of a hexagonal ordered array indexed as (1 0 0), (1 1 0), (2 0 0) and (2 1 0) Bragg reflections. A significant shift in the (1 0 0) reflection in the PXRD spectrum of the MCM-41 calcined sample is clearly seen on curve b, which corresponds to a cell contraction related to the condensation of silanols in the calcination step. Curves c and d show that reflections (1 1 0), (2 0 0) and (2 1 0) were lost, probably due to a reduced contrast, which can be attributed to the presence of FO or FA in the pores, and to the anchored N3 molecule. Nevertheless, the existence of the (1 0 0) peak in the PXRD patterns in all cases indicated that the process of pore loading with FO and FA, and functionalization did not basically modify the typical porosity of the mesoporous MCM-41 scaffold.
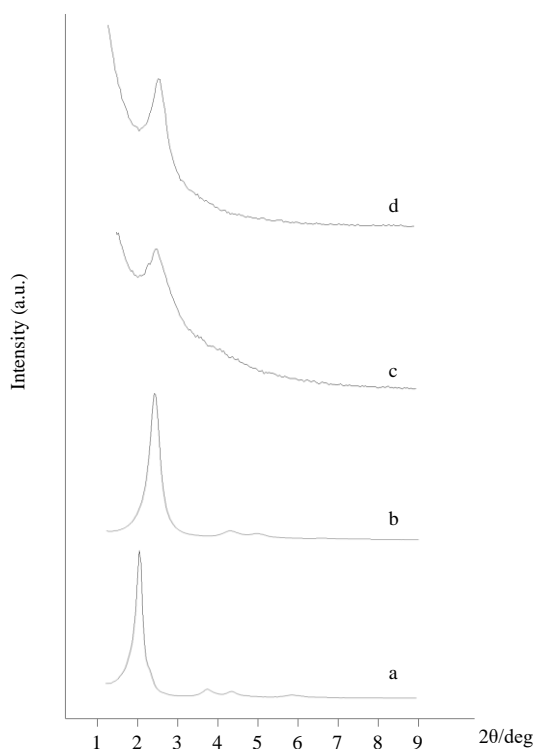

Figure 1. Powder X-ray patterns of the solids (a) MCM-41 as-synthesized, (b) MCM-41 calcined, (c) **E-FO** and (d) **E-FA**.

In addition to PXRD patterns, Fig. 2 shows FESEM and TEM images of the different bare and functionalized materials. By means of FESEM observation, characterization of the shape and size of the particles was performed. MCM-41 microparticles showed a size in the microscale and irregular morphology. The comparison of the images before and after loading with FO and FA and functionalization with N3 allowed concluding that neither loading nor functionalization significantly modified the external surface suggesting a complete encapsulation of the vitamins in the support. After loading with FO and FA and functionalization with polyamines, the MCM-41 mesostructure was also confirmed by the TEM images (Fig. 2). The particles are irregular in shape, with a particle size of 708 ± 102, 779 ± 131 and 752 ± 89 nm for bare calcined MCM-41, **E-FO** and **E-FA**, respectively. Moreover, the typical channels of the mesoporous matrix are seen as alternate black and white stripes, or as a pseudo hexagonal array of pore voids.
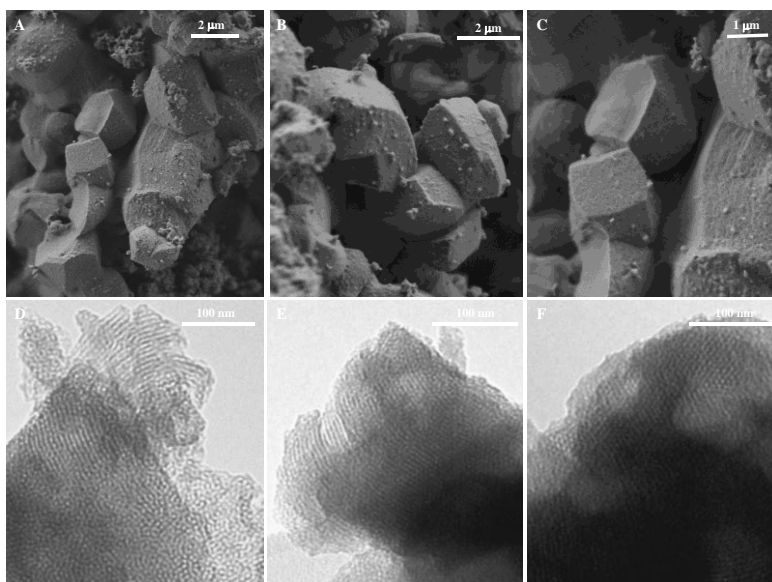

Figure 2. Characterization of particle size, particle shape and pore system by means of FESEM (A-C) and TEM (D-F). (A, D) calcined MCM-41; (B, E) **E-FO** and (C, F) **E-FA**.

The N$_2$ adsorption–desorption isotherms of the starting MCM-41 calcined material, and of the loaded and functionalized solids, can be found in Fig. 3. The MCM-41 material curve shows a well-defined adsorption step at intermediate P/P$_0$ values, which corresponds to a type IV isotherm that is typical of mesoporous materials. The isotherms of **E-FO** and **E-FA** show mesoporous system curves with partially filled mesopores. The entrapment of FA in mesopores seemed more efficient than FO, and in exactly the same way as the release studies, which showed greater FA release.
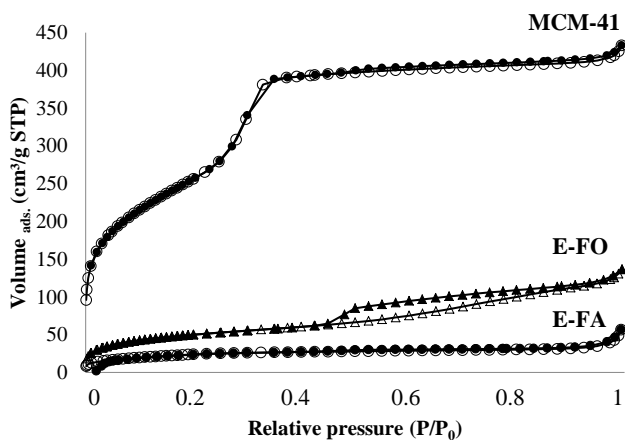

Figure 3. Nitrogen adsorption-desorption isotherms for MCM-41 mesoporous material, **E-FO** and **E-FA** materials.

Table 1 displays the change in the structural properties of the starting material after the loading and functionalization processes. The values of specific surface, pore volume and pore size in **E-FO** and **E-FA** indicate significant pore blocking and the subsequent absence of appreciable mesoporosity due to the incorporation of vitamins into the mesopores, as well as a reduced surface area because of the attachment of amine gates.

Table 1. Analytical and structural parameters from N_2 adsorption-desorption isotherms.

	SBET (m^2/g)	Pore volume (cm^3/g)	Pore size (nm)
MCM-41	932.61	0.46	2.72
E-FA	88.75	0.06	-
E-FO	183.39	0.19	-

Functionalization efficiency was verified by the zeta potential determinations of bare MCM-41, MCM-41 loaded with FO/FA, and MCM-41 loaded and functionalized with amines. Bare particles revealed an average negative zeta potential of −31 mV. After loading particles with FO/FA, the zeta potential changed slightly to values of ca. −30 mV. Yet after functionalization with N3, the zeta potential changed positively to values of ca. 50 mV for **E-FO** and **E-FA**, which confirmed the attachment of amines to the particle surface.

3.2. Release studies

The release studies confirmed the mechanism of the amine-gated MSPs to modulate vitamin release according to the pH of the medium. The pH-dependent releases of the encapsulated FO and FA are shown in Fig. 4. Gates were largely closed at pH 2 and the vitamin was barely detected, which confirmed that vitamin delivery was hindered by the combination of the low solubility of the vitamins under acidic conditions, the effect of the amines anchored to the surface of MSPs and the polyammonium groups-anionic species interaction. At an acidic pH, polyamines were transformed into polyammonium groups, which adopted a rigid-like conformation due to Coulombic repulsions and coordinate anions (phosphates present in solution), which blocked pores and avoided vitamin release (Bernardos et al., 2008; Casasús et al., 2008).
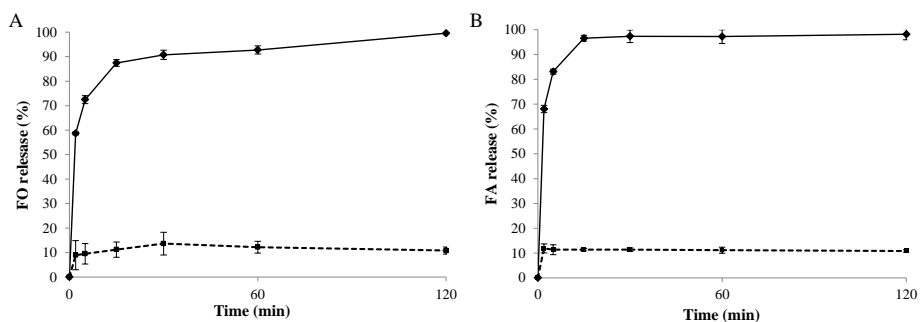
Figure 4. Release profiles of vitamin from the pores of **E-FO** (A) and **E-FA** (B) in PBS at pH 2.0 (dotted lines) and pH 7.5 (solid lines). Values are Means ± SD, n = 3.

In contrast, FO and FA showed a progressive release among time at pH 7.5. After 2 h, maximum vitamin releases were obtained at pH 7.5, with 41.9 ± 7.2 mg FO/g solid for **E-FO** and 84.3 ± 7.8 mg FA/g solid for **E-FA**. The maximum released amounts were used to calculate the equivalent amount of solids needed in the stability assays to make a comparison between the free and encapsulated FO and FA. A sustained release was produced because polyamines were less protonated at a neutral pH, and the Coulombic repulsion between them and the affinity for anions significantly reduced. These effects, along with increased vitamin solubility, allowed the delivery of FO and FA from pores. This pH-responsive delivery effect has been suggested to be suitable for releasing vitamins in the gastrointestinal tract (closed gates in the stomach, opened gates in the intestine) (Pérez-Esteve et al., 2015). Encapsulation was also expected to protect vitamins from degradation after exposure to environmental agents (*vide infra*).

3.3. Stability assays

The influence of diverse external agents related to food processing or storage, such as pH, temperature and light, on the stability of free 5-formyltetrahydrofolate and folic acid (**F-FO** and **F-FA**) and the corresponding entrapped vitamins (**E-FO** and **E-FA**) was studied.

3.3.1 pH

The study of the effect of pH on the stability of FO and FA at different pH values was conducted in two steps. In the first step, water solutions of free FA and FO were adjusted to different pHs and stirred for 1 h before being analyzed by HPLC. Fig. 5 shows the detected concentrations of FA and FO (in terms of recovery) in the aqueous solutions under all the study conditions (i.e. pH 1–10).
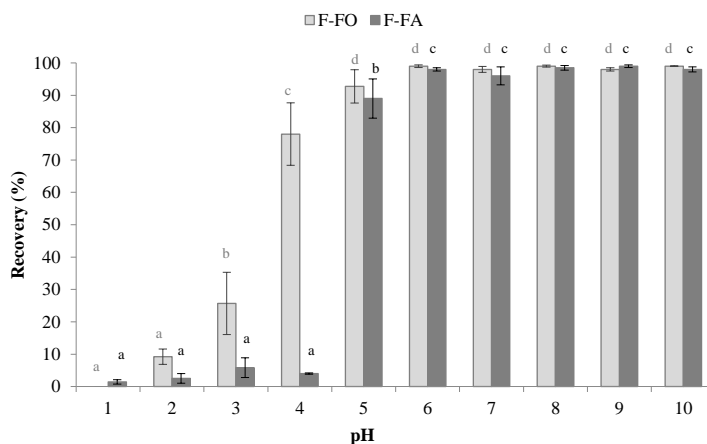

Figure 5. F-FO and **F-FA** recoveries at different pH values. Different letters in the bars indicate statistically significant differences (p<0.05) from levels of pH. Values are Means ± SD, n = 3.

As observed, recoveries reached values of ca. 100% from pH 5 to 10, which confirms the stability of both molecules at these pH values. Below this pH range, the concentrations of both molecules lowered. The FO concentration in water gradually lowered from ca. pH 4 to pH 1, whereas this effect was observed for FA below ca. pH 3.

The drop in the recovery of FO and FA at an acidic pH can be explained by three phenomena: (a) loss of solubility; (b) interconversion into other derivatives; (c) oxidative degradation. Folates are slightly soluble at an acidic pH, and are

highly soluble under neutral/basic conditions due to the protonation and deprotonation of molecules in aqueous environments (Wu et al., 2010). In addition to oxidative degradation, FO can nonenzymatically interconvert with 5,10-methenyltetrahydrofolate through changes in pH, temperature and oxygen (De Brouwer et al., 2007). 5,10-methenyltetrahydrofolate is formed by the acidification of 5-formyltetrahydrofolate because one molecule of water is lost (dehydration), which leads to the cyclization of the molecule in a reversible manner. The equilibrium gradually shifts toward 5,10-methenyltetrahydrofolate, and its formation becomes faster the lower pH becomes (Jägerstad & Jastrebova, 2013).

Bearing all these factors in mind, which could explain loss of recovery at an acidic pH, in a second step, experiments were run to determine the amount of vitamins lost at an acidic pH. In them aqueous solutions of free FA and FO were adjusted to pH 2, stirred for 1 h and then pH was adjusted to 7.5 before the HPLC analysis. The percentage of vitamins determined at pH 2 and after neutralization to pH 7.5 is shown in Fig. 6A, where almost no recovery of vitamins is detected after stirring them for 1 h at pH 2 (which agrees with Fig. 5). However, the vitamins reappeared with a percentage of ca. 40% for **F-FO** and of ca. 72% for **F-FA** after neutralizing the pH. **F-FA** gave higher values after adjusting to the neutral value than free FO, but none of them achieved complete recovery. Some studies have revealed that FA might not be soluble at a low pH (Pérez-Esteve et al., 2015), but other authors have reported its degradation at an acidic pH (Yakubu & Muazu, 2010). The natural folate showed less stability at an acidic pH than FA, probably due to degradation (Jägerstad & Jastrebova, 2013).
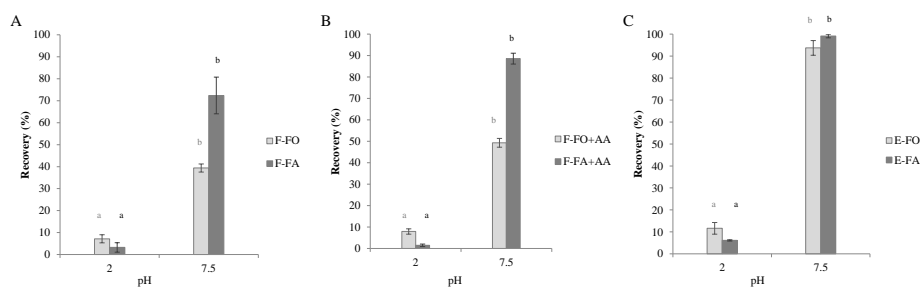
Figure 6. FO and FA recoveries after pH changes for free vitamins (A), free vitamins in presence of ascorbic acid (B) and encapsulated vitamins (C). Different letters in the bars indicate statistically significant differences ($p<0.05$) from levels of pH. Values are Means ± SD, n = 3.

Similar studies to those shown above have been conducted in the presence of ascorbic acid (AA), and their results are shown in Fig. 6B. This antioxidant was included because previous studies have demonstrated that its incorporation increases folate stability as oxidation reactions are prevented (De Brouwer et al., 2007). As for the vitamins supplemented with AA, the **F-FO** concentration only slightly increased (from 40% in the absence of AA to 50%). However, AA remarkably influenced the stability of **F-FA**, and revealed a recovery of almost 90%.

Lastly, the effect of pH changes on the encapsulated vitamins was studied in order to prove the protective function of the support. As shown in Fig. 6C, minor vitamin recoveries took place at pH 2. When pH was adjusted to 7.5, **E-FO** and **E-FA** were almost fully detectable with a recovery of 94% and 99%, respectively. Both encapsulated vitamins were highly preserved in the acidic environment by the pH-responsive gated material. As a result, the highly protective function of the MSPs functionalized with amines at a low pH was evidenced by both vitamins. This approach better improved the stability of vitamins than the strategy reported to enhance the stability of natural folates (addition of antioxidants). Neither the free form nor the vitamins supplemented with AA were as stable at an acidic pH as they were inside the pores of MSPs.

3.3.2. Temperature

Previous experiments conducted with vitamins dissolved in PBS at temperatures below 100 °C had no impact on their stability (data not shown). In order to investigate the impact of higher temperatures on the vitamins, a study was carried out by simulating sterilization conditions (121 °C, 1 bar) at different times. The temperature assays performed in the autoclave are presented in Fig. 7. The results showed that encapsulated folate did not significantly reduce vitamin content at various exposure times. In contrast, **F-FO** revealed a significant loss of ca. 27% after 15 min, probably due to the formation of interconversion products (Jastrebova et al., 2013). With FA, no significant differences were obtained for both the **E-FA** and **F-FA** results. These results are in accordance with previous studies that have reported good FA stability after thermal exposure in the solid state and with dissolution (Nguyen et al., 2003; Vora et al., 2002). Synthetic vitamin has been suggested to be the most stable type in the folate group because of its oxidized p-teridin ring (Scott et al., 2000). The thermostability of FA and FO has been previously reported as being similar at a neutral pH (Indrawati et al., 2004). The results obtained with the encapsulated vitamins revealed that entrapped FO could bear up under thermal pressure exposure and greater stability after proving FO encapsulation. However, encapsulated FA could also resist the burden of thermal pressure as well as its free form.
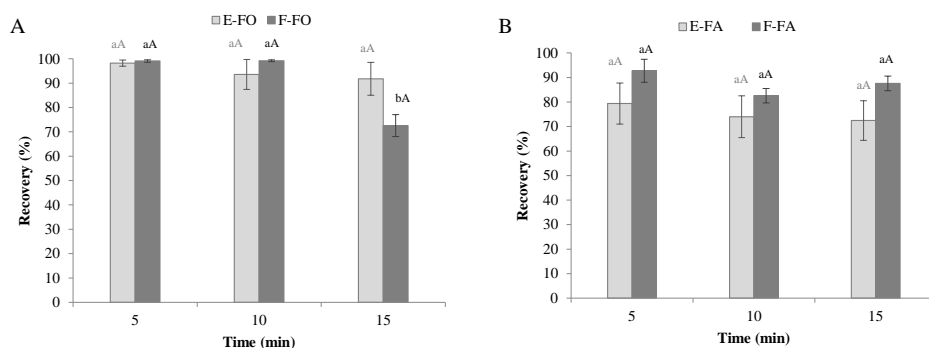
Figure 7. Influence of temperature exposure on the stability of encapsulated (E-) and free (F-) FO (A) and FA (B) vitamins. Different letters in the bars indicate statistically significant differences (p<0.05) from levels of time exposure (small letters) and differences between the encapsulated FO/FA or in their free form (capital letters). Values are Means ± SD, n = 3.

3.3.3. Light

Previous articles, which have reported the influence of various light sources on the degradation of synthetic FA, have investigated the impact of visible and UV light on both vitamins (Akhtar et al., 2003). Preliminary experiments revealed no or very little degradation after 6 h (data not shown). Therefore, assays were carried out from 8 h to 16 h.

Visible light assays were conducted with a lamp, which generated visible light with an intensity ca. 8 mW/cm^2. The results obtained from visible light experiments are presented in Fig. 8. The good stability of FO (Fig. 8A) after light exposure was evidenced. Neither **F-FO** nor **E-FO** showed degradation during visible light exposure.

With FA (Fig. 8B), **F-FA** showed considerable loss after 8 h of visible light exposure, with a remaining averaged amount of 40%. Gradual reduction of **F-FA** was detected up to 12 h irradiation, with a low value of 12%, and total degradation occurred after 16 h with an average remaining amount of 3%.

Conversely, **E-FA** was well-protected by the functionalized support and a non-significant decrease was detected.
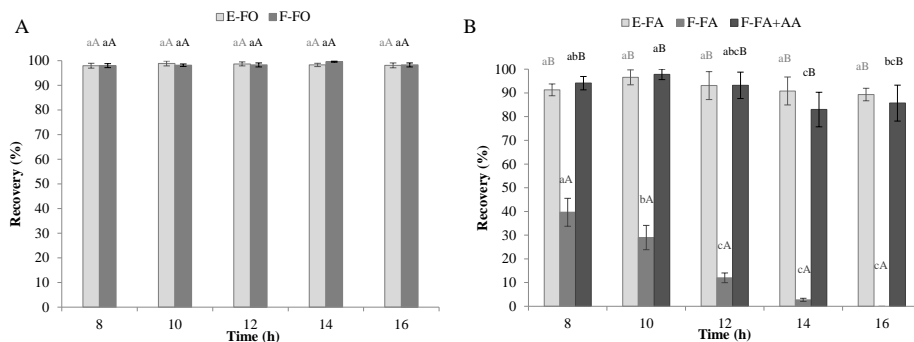

Figure 8. Influence of visible light exposure on the stability of encapsulated (E-) and free (F-) FO (A) and FA (B) in presence or not of ascorbic acid. Different letters in the bars indicate statistically significant differences (p<0.05) from levels of visible light exposure (small letters) and differences between the encapsulated FO/FA or in their free form (capital letters). Values are Means ± SD, n = 3.

Given **F-FA**'s tendency to be degraded by light in solution, the effect of antioxidant AA was also evaluated as a strategy to improve stability and to confirm the mechanism of degradation (i.e. oxidation). Free FA dissolution supplemented with AA showed marginal fluctuation after 16 h of visible light exposure, but appeared to stabilize FA substantially in the same way as the encapsulation system.

Fig. 9 shows the free and encapsulated FO and FA recoveries after UV light exposure with an estimated intensity of 4 mW/cm^2. The results revealed that **E-FO** and **F-FO** exhibited good stability under UV light (Fig. 9A). Hence natural folate was highly stable in both the free and encapsulated forms. FA stability was affected by UV light (Fig. 9B) and **F-FA** showed losses after 8 h of UV exposure. As in the visible light assays, the impact of AA enhanced the good stability of the

synthetic vitamin and demonstrated more effective protection than the mesoporous system after 16 h of light exposure.
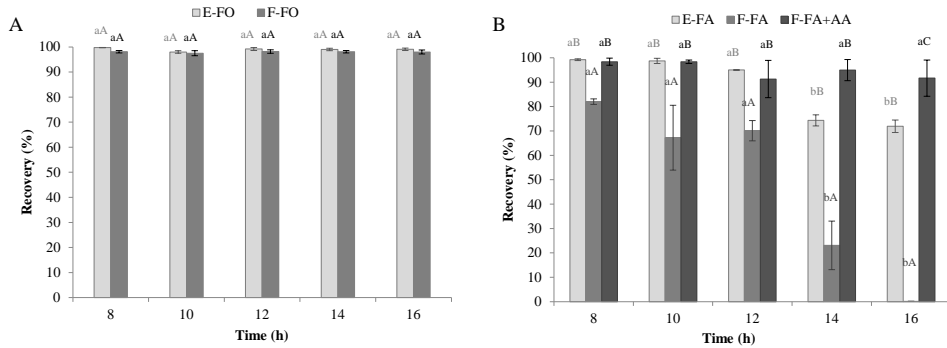

Figure 9. Influence of UV light exposure on the stability of encapsulated (E-) and free (F-) FO (A) and FA (B) in presence or not of ascorbic acid. Different letters in the bars indicate statistically significant differences ($p < 0.05$) from levels of visible light exposure (small letters) and differences between the encapsulated FO/FA or in their free form (capital letters). Values are Means ± SD, n = 3.

Summing up the two light experiments, it was noted that FO did not degrade under either visible light exposure or UV light stress, but FA was susceptible to visible and UV light exposure. However, the mesoporous system was able to efficiently protect the vitamin and stability was greatly enhanced.

This study simulated indirect light-induced stress and, therefore, intensities until degradation occurred. We were unable to compare these results with previous studies as they all used direct exposures (Akhtar et al., 2003; Fukuwatari et al., 2009; Off et al., 2005). Even though it has been suggested to be considerably more stable at pH 7.5 than in acidic media (Yakubu & Muazu, 2010), we detected complete oxidative degradation after 16 h of visible light and UV exposure. Akhtar et al. (2003) suggested the mechanism of this oxidative degradation as they hinted at degradation being produced in the C9–N10 position. Aqueous solution can form various radiolytic products, which initiate

oxidative dehydrogenation and lead to an enamine compound. This intermediate form is highly susceptible in acidic media and can undergo fast degradation. In alkaline media, this decomposition process has been proposed to take place more slowly, but it also led to irreversible cleavage between C9 and N10 bonding after 16 h of light exposure. This caused final decay in the separation of the p-teridin moiety from p-aminobenzoylglutamate (Akhtar et al., 2003; Off et al., 2005).

Encapsulated FA, which was solved in PBS (pH 2) in the stability assays, showed good stability. Not even the degradation-favorable acidic surrounding could hardly affect **E-FA** compared to the free form. Apart from successful FA improvement through encapsulation, antioxidant AA enhanced stability in the same way. Compared to the well-known protective mechanism of antioxidants [38], the protective function of the mesoporous support has not been reported to date, and the stabilizing mechanism remains unclear. Although it is fully accepted that MSPs show very little absorption within the visible and ultraviolet range (Hornebecq et al., 2003; Weiping & Lide, 1997), enhanced encapsulated vitamin recovery was confirmed herein. The possible role of MSPs as a stability enhancer could hinder access to weak points (C9–N10 bonding) by entrapping the vitamin in mesopores in such a way that conformational transformations of the molecule are avoided.

4. Conclusions

The successful entrapment of natural FO and synthetic FA in pH-responsive MSPs and the controlled release of the compounds that mimic the gastrointestinal tract were accomplished herein. The ability of MSPs to protect vitamins after environmental degradation was clearly evidenced. The stability assays revealed that encapsulated FO and FA were effectively protected against degradation at an acidic pH compared to their free from. The sterilization studies showed that encapsulation allowed vitamins to withstand thermal exposure and enhanced their stability. The results obtained after exposure to visible and UV

light displayed good stability for free FO, which was not influenced by encapsulation, but improved FA stability after entrapment in MSPs. When considering the protective effect of MSPs against external agents and acidic stomach conditions, and progressive delivery with time under the intestinal conditions, the FO- and FA-loaded supports proposed herein can be considered promising potential systems as supplements for food systems.

References

Akhtar, M. J., Khan, M. A., & Ahmad, I. (2003). Identification of photoproducts of folic acid and its degradation pathways in aqueous solution. *Journal of Pharmaceutical and Biomedical Analysis, 31*(3), 579-588.

Aznar, E., Oroval, M., Pascual, L., Murguía, J. R., Martínez-Máñez, R., & Sancenón, F. (2016). Gated materials for on-command release of guest molecules. *Chemical Reviews, 116*, 561–718.

Ball, G. F. M. (2005). In: *Vitamins in Foods, Analysis, Bioavailability and Stability*. CRC, Boca Raton.

Bendich, A., Machlin L. J., Scandurra O., Burton, G. W., & Wayner D. D. M. (1986). The Antioxidant Role of Vitamin C. *Advances in Free Radical Biology & Medicine*, *2*(2), 419-444.

Bernardos, A., Aznar, E., Coll, C., Martínez-Mañez, R., Barat, J. M., Marcos, M. D., Sancenón, F., Benito, A., & Soto, J. (2008). Controlled release of vitamin B2 using mesoporous materials functionalized with amine-bearing gate-like scaffoldings. *Journal of Controlled Release, 131*, 181-189.

Bernardos, A., Marina, T., Žáček, P., Pérez-Esteve, E., Martínez-Mañez, R., Lhotka, M., Kourimská, L., Pulkrávek, J., & Klouček, P. (2015). Antifungal effect of essential oil components against *Aspergillus niger* when loaded into silica mesoporous supports. *Journal of the Science of Food and Agriculture, 95*, 2824–2831**.**

Butz, P., Serfert, Y., Garcia, A. F., Dieterich, S., Lindauer, R., Bognar, A., & Tauscher, B. (2004). Influence of high-pressure treatment at 25 °C and 80 °C on folates in orange juice and model media. *Journal of Food Science, 69*(3), SNQ117-SNQ121.

Casasús, R., Climent, E., Marcos, M. D., Martínez-Máñez, R., Sancenón, F., Soto, J., Amorós, P., Cano, J., & Ruiz E. (2008). Dual aperture control on pH- and anion-driven supramolecular nanoscopic hybrid gate-like ensembles. *Journal of the American Chemical Society, 130*(6), 1903-1917.

Clifford, N. W., Iyer, K. S., & Raston, C. L. (2008). Encapsulation and controlled release of nutraceuticals using mesoporous silica capsules. *Journal of Materials Chemistry*, *18*(2), 162-165.

Cotea, V. V., Luchian, C. E., Bilba, N., & Niculaua, M. (2012). Mesoporous Silica SBA-15, a new adsorbent for bioactive polyphenols from red wine. *Analytica Chimica Acta, 732,* 180-1855.

De Brouwer, V., Zhang, G. F., Storozhenko, S., Van Der Straeten, D., & Lambert, W. E. (2007). pH stability of individual folates during critical sample preparation steps in prevision of the analysis of plant folates. *Phytochemical Analysis, 18*(6), 496-508.

Fukuwatari, T., Fujita, M., & Shibata, K. (2009). Effects of UVA irradiation on the concentration of folate in human blood. *Bioscience, Biotechnology and Biochemistry, 73*(2), 322-327.

Gujska, E., Michalak, J., & Klepacka, J. (2009). Folates stability in two types of rye breads during processing and frozen storage. *Plant Foods for Human Nutricion, 64*(2), 129-134.

Hisamatsu, K., Shiomi, T., Matsuura, S. I., Nara, T. Y., Tsunoda, T., Mizukami, F., & Sakaguchi, K. (2012). α-Amylase immobilization capacities of mesoporous silicas with different morphologies and surface properties. *Journal of Porous Materials*, *19*(1), 95-102.

Hornebecq, V., Antonietti, M., Cardinal, T., & Treguer-Delapierre, M. (2003). Stable silver nanoparticles immobilized in mesoporous silica. *Chemistry of Materials, 15*(10), 1993-1999.

Indrawati, Arroqui, C., Messagie, I., Nguyen, M. T., Loey, A., & Hendrickx, M. (2004). Comparative study on pressure and temperature stability of 5-methyltetrahydrofolic acid in model systems and in food products. *Journal of Agricultural and Food Chemistry, 52*(3), 485-492.

Izquierdo-Barba, I., Vallet-Regí, M., Kupferschmidt, N., Terasaki, O., Schmidtchen, A., & Malmsten, M. (2009). Incorporation of antimicrobial compounds in mesoporous silica film monolith. *Biomaterials*, *30*(29), 5729-5736.

Jägerstad, M., & Jastrebova, J. (2013). Occurrence, stability, and determination of formyl folates in foods. *Journal of Agricultural and Food Chemistry, 61*(41), 9758-9768.

Jastrebova, J., Axelsson, M., Strandler, H. S., & Jägerstad, M. (2013). Stability of dietary 5-formyl-tetrahydrofolate and its determination by HPLC: a pilot study on impact of ph, temperature and antioxidants on analytical results. *European Food Research and Technology*, *237*(5), 747-754.

Joint FAO & WHO (2001). *FAO/WHO Expert Consultation on Human Vitamin and Mineral Requirements*. Food and Nutrition Division, FAO Rome, 53-63.

Juzeniene, A., Tam, T. T. T., Iani, V., & Moan, J. (2009). 5-Methyltetrahydrofolate can be photodegraded by endogenous photosensitizers. *Free Radical Biology & Medicine, 47*(8), 1199-1204.

Kapoor, M. P., Vinu, A., Fujii, W., Kimura, T., Yang, Q., Kasama, Y., Yanagi, M, & Juneja, L. R. (2010). Self-assembly of mesoporous silicas hollow microspheres via food grade emulsifiers for delivery systems. *Microporous and Mesoporous Materials, 128*(1), 187-193.

Li, Z., Barnes, J. C., Bosoy, A., Stoddart, J. F., & Zink, J. I. (2012). Mesoporous silica nanoparticles in biomedical applications. *Chemical Society Reviews, 41*(7), 2590-2605.

Nguyen, M. T., Oey, I., Verlinde, P., van Loey, A., & Hendrickx, M. (2003). Model studies on the stability of folic acid and 5-methyltetrahydrofolic acid degradation during thermal treatment in combination with high hydrostatic pressure. *Journal of Agricultural and Food Chemistry, 51*(11), 3352-3357.

Off, M. K., Steindal, A. E., Porojnicu, A. C., Juzeniene, A., Vorobey, A., Johnsson, A., & Moan, J. (2005). Ultraviolet photodegradation of folic acid. *Journal of Photochemistry and Photobiology B: Biology, 80*(1), 47-55.

Pérez-Esteve, E., Fuentes, A., Coll, C., Acosta, C., Bernardos, A., Marcos, M. D., Martínez-Máñez, R., & Barat, J.M. (2015). Modulation of folic acid bioaccesibility by encapsulation in pH-responsive gated mesoporous silica particles. *Microporous and Mesoporous Materials,* 202, 124-132.

Pérez-Esteve, E., Oliver, L., García, L., Nieuwland, M., de Jongh, H. H., Martínez-Máñez, R., & Barat, J. M. (2014). Incorporation of mesoporous silica particles in gelatine gels: effect of particle type and surface modification on physical properties. *Langmuir, 30*, 6970-6979.

Popat, A., Hartono, S. B., Stahr, F., Liu, J., Qiao, S. Z., & Lu, G. Q. (2011). Mesoporous silica nanoparticles for bioadsorption, enzyme immobilisation, and delivery carriers. *Nanoscale, 3*(7), 2801-2181.

Popova, M., Szegedi, A., Mavrodinova, V., Tušar, N. N., Mihály, J., Klébert, S., Benbassat, N., & Yoncheva, K. (2014). Preparation of resveratrol-loaded nanoporous silica materials with different structures. *Journal of Solid State Chemistry*, *219*, 37-42.

Rashidi, L., Vasheghani-Farahani, E., Rostami, K., Gangi, F., & Fallahpour, M. (2013). Mesoporous silica nanoparticles as a nanocarrier for delivery of vitamin C. *Iranian Journal of Biotechnology*, *11*(4), 209-213.

Ruiz-Rico, M., Fuentes, C., Pérez-Esteve, É., Jiménez-Belenguer, A. I., Quiles, A., Marcos, M. D., Martínez-Máñez, R., & Barat, J. M. (2015). Bactericidal activity of caprylic acid entrapped in mesoporous silica nanoparticles. *Food Control*, *56*, 77-85.

Scott, J., Rébeillé, F., & Fletcher, J. (2000). Folic acid and folates: the feasibility for nutritional enhancement in plant foods. *Journal of the Science of Food and Agriculture, 80*(7), 795-824.

Slowing, I. I., Vivero-Escoto, J. L., Wu, C. W., & Lin, V. S. Y. (2008). Mesoporous silica nanoparticles as controlled release drug delivery and gene transfection carriers. *Advanced Drug Delivery Reviews, 60,* 1278-1288.

Song, N., & Yang, Y. W. (2015). Molecular and supramolecular switches on mesoporous silica nanoparticles. *Chemical Society Reviews, 44,* 3474-3504.

Trewyn, B. G., Giri, S., Slowing, I. I., & Lin, V. S. Y. (2007). Mesoporous silica nanoparticle based controlled release, drug delivery, and biosensor systems. *Chemical Communications,* 3236-3245.

Veith, S. R., Hughes, E., & Pratsinis, S. E. (2004). Restricted diffusion and release of aroma molecules from sol-gel-made porous silica particles. *Journal of Controlled Release*, *99*(2), 315-327.

Vora, A., Riga, A., Dollimore, D., & Alexander, K. S. (2002). Thermal stability of folic acid. *Thermochimica Acta, 392,* 209-220.

Weiping, C., & Lide, Z. (1997). Synthesis and structural and optical properties of mesoporous silica containing silver nanoparticles. *Journal of Physics: Condensed Matter, 9*(34), 7257.

Wu, Z., Li, X., Hou, C., & Qian, Y. (2010). Solubility of folic acid in water at pH values between 0 and 7 at temperatures (298.15, 303.15, and 313.15) K. *Journal of Chemical & Engineering Data, 55*(9), 3958-3961.

Yakubu, S.; & Muazu, J. (2010). Effects of variables on degradation of folic acid. *Der Pharmacia Sinica, 1*(3), 55-58.

4.3. Protection of folic acid through encapsulation in mesoporous silica particles included in fruit juices

María Ruiz-Rico[a*], Édgar Pérez-Esteve[a], María J., Lerma-García[a], María D. Marcos[b,c], Ramón Martínez-Máñez[b,c], José M. Barat[a]

[a] Grupo de Investigación e Innovación Alimentaria, Departamento de Tecnología de Alimentos. Universitat Politècnica de València. Camino de Vera s/n, 46022, Valencia, Spain
[b] Centro de Reconocimiento Molecular y Desarrollo Tecnológico (IDM), Unidad Mixta Universitat Politècnica de València - Universitat de València. Departamento de Química. Universitat Politècnica de València, Camino de Vera s/n, 46022, Valencia, Spain
[c] CIBER de Bioingeniería, Biomateriales y Nanomedicina (CIBER-BBN)

Abstract

Folic acid (FA) is a synthetic vitamin commonly used for food fortification. However, its vulnerability to processing and storage implies loss of efficiency, which would induce over-fortification by processors to obtain a minimum dose upon consumption. Recent studies have indicated potential adverse effects of FA overdoses, and FA protection during processing and storage could lead to more accurate fortification. In addition, sustained vitamin release after consumption would help improve its metabolism. The objective of this work was to study controlled FA delivery and stability in fruit juices to reduce potential over-fortification risks by using gated mesoporous silica particles (MSPs). The obtained results indicated that FA encapsulation in MSPs significantly improved its stability and contributed to controlled release after consumption by modifying vitamin bioaccessibility. These results confirmed the suitability of MSPs as support for controlled release and protection of bioactive molecules in food matrices in different food production and storage stages.

Keywords: bioaccessibility modification; folic acid; fruit juice; mesoporous silica particles; stability.

1. Introduction

The generic term ''folates'' refers to a group of naturally-occurring B vitamins essential for the human body. An adequate folate status provides health benefits by preventing birth defects during pregnancy and cardiovascular diseases (Hoag et al., 1997), Alzheimer's disease (Clarke et al., 1998) or colorectal cancer (Stover, 2004). The European Food Safety Authority (EFSA) recommends a daily intake of 200-400 µg folate/day for adults, and an additional intake of 400 µg for women of childbearing age (ESCO, 2009).

Folates are present in diverse food products, including liver, egg yolk, green vegetables, certain beans, citrus fruits, and cereal products (Ball, 2005). However, folate intake is strongly influenced by the degradation of its vitamers during food processing. Hence folic acid (FA), a synthetic form of the vitamin, is commonly used for folate supplementation and food fortification thanks to its reported enhanced bioaccessibility and stability. Food fortification should guarantee the FA concentration indicated on the label until the expiry date, which usually entails having to add large amounts of the vitamin (up to 50%) to compensate for the losses that occur during processing and/or storage (Frommherz et al., 2014). The folates degradation process depends on several factors, such as high temperature, light, low pH, oxygen and overall food composition (Fukuwatari et al., 2009; Jastrebova et al., 2013; Nguyen et al., 2003). Some studies have reported a marked deviation of FA content from the labeled values of fortified foods (Frommherz et al., 2014; Lebiedzińska et al., 2008), which can result in health risks. In particular, FA, which requires metabolic activation before it can function, appears unmetabolized in the bloodstream when the tolerable upper intake level of 1 mg/day (EFSA, 2006) is exceeded. Unmetabolized FA has been associated with some neoplasia, cognitive damage among seniors due to the masking of vitamin B12 deficiency, and also to the reduced efficacy of anti-folate drugs used to treat rheumatoid arthritis or psoriasis (Crider et al., 2011; ESCO, 2009).

Considering the importance of FA for human health, its vulnerability to external agents and the potential risks associated with excessive intake, FA encapsulation could be an opportunity to diminish its degradation and improve its bioavailability. Diverse micro- and nanoencapsulation systems have been recently reported for folates fortification based on organic encapsulation supports (Aceituno-Medina et al., 2013; Bakhshi et al., 2013; Madziva et al., 2006; Shrestha et al., 2012; Tomiuk et al., 2012). Some proposed systems have improved the stability of this vitamin in different food matrices and food processing. However, these systems present some instability during processing or ingestion processes, a poor ability to control the FA rate release or provide targeted delivery (Pérez-Esteve et al., 2015b). As an alternative, inorganic encapsulation systems, such as mesoporous silica particles (MSPs), can be useful in food fortification thanks to large loading capacity, biocompatibility, stability during digestion conditions and controlled release capability (Aznar et al., 2016, Li, et al., 2012; Pérez-Esteve et al., 2016; Slowing et al., 2008; Song & Yang, 2015). Despite some toxicological limitations need to be overcome before starting to use MSP as smart delivery systems in food industry, several studies have assessed the impact of MSPs. Diverse and contradictory results have been observed in some cells or animals treated with MSPs, but the use of functionalized mesoporous silica microparticles seems a good strategy to minimize the risks associated with using MSPs as supports to develop smart delivery systems (Pérez-Esteve et al., 2015b).

In this scenario, we previously reported the design and synthesis of a smart FA delivery system capable of controlling and modifying the FA release in different digestion steps (Pérez-Esteve et al., 2015a). As a step forward, the present work aimed to evaluate the protective effect of MSPs in relation to FA stability under real food industry conditions. To accomplish this goal, the bioaccessibility and stability of FA encapsulated into a MCM-41 silica support functionalized with amines that acted as molecular gates was investigated after its incorporation into fruit juices. Apple and orange juices were selected as model food systems for their low pH, which should hinder the delivery of the vitamin, and because different

amounts of protective active ingredients were present, such as ascorbic acid. In order to establish the influence of MSPs encapsulation, the stability of free and entrapped FA against processing and storage agents, such as high temperature, light and juice composition, was investigated. As far as we know, this is the first study dealing with the protective effect of MSPs on the stability of biomolecules in real food systems.

2. Materials and methods

2.1. Chemicals

Tetraethylorthosilicate (TEOS), *N*-cetyltrimethylammonium bromide (CTABr), sodium hydroxide (NaOH), triethanolamine (TEAH₃), *N*-(3-trimethoxysilylpropyl)diethylenetriamine (N3) and phosphoric acid were provided by Sigma-Aldrich (Madrid, Spain). FA was purchased from Schircks Laboratories (Jona, Switzerland). Acetonitrile HPLC grade was provided by Scharlab (Barcelona, Spain). Two types of fruit juices (apple and orange) were purchased from local supermarkets. The composition of these juices is shown in Table 1. HPLC analysis revealed a concentration of folic acid below the limit of quantification in both juices. Juices were stored at 4 °C until analyzed.

Table 1. Main nutrients and pH values from apple and orange juices.

	Apple juice	Orange juice
Carbohydrates (g/100 mL)	11.3	9.9
Proteins (g/100 mL)	0.1	0.7
Fats (g/100 mL)	0.1	0.1
Vitamin C (mg/100 mL)	-	40
pH	3.53	3.64

2.2. Synthesis of encapsulated folic acid (**E-FA**)

Synthesis of microparticulated MCM-41 was carried out using CTABr as the structure-directing agent and TEOS as the silica source, and a molar ratio fixed at 7 TEAH$_3$:2 TEOS:0.52 CTABr:0.5 NaOH:180 H$_2$O. CTABr was added to a TEAH$_3$ and NaOH solution that contained TEOS at 118 °C. Then water was slowly added, with vigorous stirring at 70 °C. A white suspension was formed after a few minutes of stirring. This mixture was aged in an autoclave at 100 °C for 24 h. The resulting powder was collected by filtration. Then it was washed with distilled water and ethanol and dried at 70 °C. The as-synthesized solid was calcined at 550 °C for 5 h to remove the template phase (Bernardos et al., 2008).

FA was loaded in the calcined MCM-41 microparticles by the impregnation method described by Pérez-Esteve et al. (2015a). FA (10 mg/mL) dissolved in phosphate-buffered saline (PBS) was added to 300 mg of MCM-41 in three addition cycles (1.5 mL per cycle). After each addition cycle, the solid was dried at 37 °C to remove water content. After loading and drying, the solid was functionalized with 1.29 mL of N3 in acetate buffer at pH 2. The final mixture was stirred for 5.5 h at room temperature, isolated by vacuum filtration, washed with 300 mL of acetate buffer at pH 2, and dried at room temperature for 24 h.

2.3. Characterization of supports

Powder X-ray diffraction (PXRD), transmission electron microscopy (TEM), field emission scanning electron microscopy (FESEM), N$_2$ adsorption-desorption isotherms and zeta potentials were used to characterize the synthesized materials. PXRD was performed in a BrukerD8 Advance diffractometer using CuKα radiation (Bruker, Coventry, UK). FESEM images were acquired with a Zeiss Ultra 55 (Carl Zeiss NTS GmbH, Oberkochen, Germany) and observed in the secondary electron mode. For the TEM analysis, particles were dispersed in dichloromethane and deposited onto copper grids coated with a carbon film (Aname SL, Madrid, Spain). Imaging of the MSPs samples was performed with a JEOL JEM-1010 (JEOL

Europe SAS, Croissy-sur-Seine, France) at an acceleration voltage of 80 kV. Single-particle size was estimated by averaging the measured size values of 50 particles. The N_2 adsorption-desorption isotherms were recorded with a Micrometrics ASAP2010 automated sorption analyzer (Micromeritics Instrument Corporation, Norcross, USA). Samples were degassed at 90 °C in vacuum overnight. Specific surface areas were calculated from the adsorption data within the low pressure range by the BET model. Pore size was determined following the BJH method. Zeta potential measurements were taken by a Zetasizer Nano ZS (Malvern Instruments, U.K.). Samples were dispersed in water at a concentration of 1 mg/mL. The zeta potential was calculated from the particle mobility values by applying the Smoluchowski model. Measurements were taken at 25 °C in triplicate.

2.4. Release and bioaccessibility studies

The release kinetics of **E-FA** in fruit juices was performed to assess the capability of the polyamines to hinder vitamin release at the juice's natural pH (pH ca. 3.5), and to evaluate if juice composition had any influence on vitamin delivery when the gate was open (pH 7.5). Moreover, the release studies allowed us to calculate the maximum FA release from 1 mg of support in both juices. In a typical experiment, 10 mg of the solid **E-FA** were placed in 25 mL of the corresponding juice. The same procedure was carried out with the juices neutralized with NaOH 5 M to simulate the pH after reaching the small intestine, where folic acid should be delivered by its absorption and body assimilation. At certain time points (0, 2, 5, 15, 30, 60, 120, 180 and 240 min), aliquots were separated, centrifuged, filtered, and the solution was analyzed by HPLC to establish the amount of released FA.

FA bioaccessibility from fruit juices was determined by simulating human digestion according to Versantvoort et al. (2005). For these assays, 4 mg of **E-FA** or the equivalent amount of free FA (**F-FA**, 0.3 mg) were suspended in 10 mL of

apple or orange juice. The *in vitro* digestion procedure started by adding 6 mL of simulated saliva and the incubation of the mixture for 5 min at 37 °C. Then 12 mL of gastric juice were added and the sample was maintained with stirring at 37 °C for 2 h. Lastly, 12 mL of duodenal juice, 6 mL of bile and 2 mL of bicarbonate solution (1M) were added simultaneously, and the mixture was incubated for 2 h. At certain time points (0, 2, 5, 10, 60, 115, 120, 135, 150, 180 and 240 min), aliquots were taken and centrifuged. Supernatants were filtered and analyzed by HPLC to determine FA concentrations. All the chemicals for the digestive fluids were provided by Sigma-Aldrich (Madrid, Spain).

2.5. Stability assays

Stability experiments were run to establish the influence of diverse parameters, such as temperature, light and food composition on free and entrapped FA stability during the shelf life of juices.

In a typical experiment, 4 mg of the entrapped vitamin (**E-FA**) or equivalent amount of free form (**F-FA**, 0.3 mg), were dissolved in 10 mL of fruit juice. For all the stability assays (thermostability, photostability and shelf life experiments) the free folic acid was previously incubated (37 °C, 96 h) in order to simulate the loading and functionalization process of the entrapped vitamin.

In order to determine thermostability of free and entrapped vitamin, **E-FA** and **F-FA** were added to the fruit juices' insight opaque containers (Ø 24 mm, h 45 mm) and subjected to thermal treatment at 121°C and 1 bar at different times (5, 10 and 15 min). After treatment, samples were cooled in an ice bath and FA was released from the MCM-41 voids before quantification. For the photostability experiments two light sources, visible (intensity ca. 8 mW/cm²) and ultraviolet (intensity ca.4 mW/cm²) lamps, were used. **E-FA** and **F-FA** were incorporated into the fruit juices and kept inside closed transparent borosilicate glass vessels (Ø 24 mm, h 45 mm). Samples were placed under visible and ultraviolet (UV) lamps for different times (16, 18, 20, 22 and 24 h) to simulate an indirect light-induced

exposure of the food products. Shelf life experiments were carried out to study the influence of juice composition on vitamin stability during the storage period. Free (**F-A**) and encapsulated (**E-FA**) FA were added to the corresponding juice inside the opaque containers and samples were maintained refrigerated at 4 °C for 28 days. Samples were analyzed by HPLC on certain days (0, 7, 14, 21 and 28 days). Before the analysis in all cases, samples were adjusted to neutral pH and stirred at 37 °C for 2 h to solubilize (**F-FA-**containing samples) or release (**E-FA-**containing samples) the FA vitamin before the HPLC analysis. All the stability experiments were performed in triplicate. The control solutions, with the same amount of entrapped and free FA, at pH 7.5 with no treatment, were also studied for comparison purposes. Vitamin recoveries after treatments were calculated as the ratio between FA content in treated and control juices (non-exposed to light, heat or acid media).

2.6. Folic acid quantification

FA was determined by reversed-phase HPLC according to the method described by Johansson et al. (2005) with some modifications. The HPLC instrument consisted of a Hitachi LaChrom Elite liquid chromatograph (Hitachi Ltd., Tokyo, Japan) equipped with an auto-sampler (module L-2200) and UV detector (model L-2400). A Kromaphase 100 C18 (250 mm x 4.6 mm i.d., 5-µm particle size analytical column) (Scharlab, Barcelona, Spain) was used for separations. The wavelength of the UV detector was set at 280 nm. The mobile phase consisted of (A) 30 mM potassium phosphate buffer at pH 2.3 and (B) acetonitrile. The gradient program was isocratic for 10 min with 90% A and 10% B. FA was quantified according to the external standard method (since no matrix effect was observed) using a calibration curve of the peak area against the compound concentration. For all samples, the applicability of this method was evaluated by performing a recovery study. For this purpose, juice samples were fortified with FA at three different concentration levels. In all cases, recovery values, which were estimated from measured versus added amounts of FA, were

close to 100%. Thus, the results obtained demonstrated the applicability of the proposed methodology for the accurate determination of FA in juice samples.

2.7. Data analysis

Data were statistically processing using Statgraphics Centurion XVI (Statpoint Technologies, Inc., Warrenton, VA, USA). The influence of different factors on the release and stability of the vitamin was analyzed by a one-way analysis of variance (One-way ANOVA). The LSD (least significant difference) procedure was used to test the differences between means at the 5% significance level.

3. Results and discussion

3.1. Synthesis and material characterization

FA was entrapped in MCM-41 microparticles functionalized with diethylenetriamine moieties (solid **E-FA**), which acts as capping systems to control payload delivery at a neutral pH, but was able to hinder the delivery of the cargo at an acidic pH. This pH-responsive capping system has already been reported by some of us (see Bernardos et al., 2008; Casacús et al., 2008; Pérez-Esteve et al., 2015a).

The final **E-FA** support was characterized by standard techniques. The X-ray patterns of MCM-41 solids as synthesized (A), calcined (B) and loaded with FA and functionalized with polyamines (C) are shown in Figure 1. The PXRD of MCM-41 as synthesized (curve a) shows the expected four peaks of a hexagonal-ordered array indexed as (1 0 0), (1 1 0), (2 0 0) and (2 1 0) Bragg reflections. After calcination (curve b), a significant shift of the (1 0 0) reflection was clearly observed, which relates to cell contraction by the condensation of silanols in the calcination step. The loading and functionalization (curve c) produced the loss of reflections (1 1 0), (2 0 0) and (2 1 0) However, the fact that a (1 0 0) peak appeared in the PXRD patterns in all the solids clearly indicates that the pore loading and

functionalization process did not modify mesoporous MCM-41 scaffolding to a large extent. In addition, FESEM and TEM analysis were used to characterize the shape and size of the solids and the particle mesostructure (Figure 2). The MCM-41-based particles were irregular in shape, while the size of particles was 853±67 and 862±59 nm for bare calcined MCM-41 and **E-FA**, respectively.
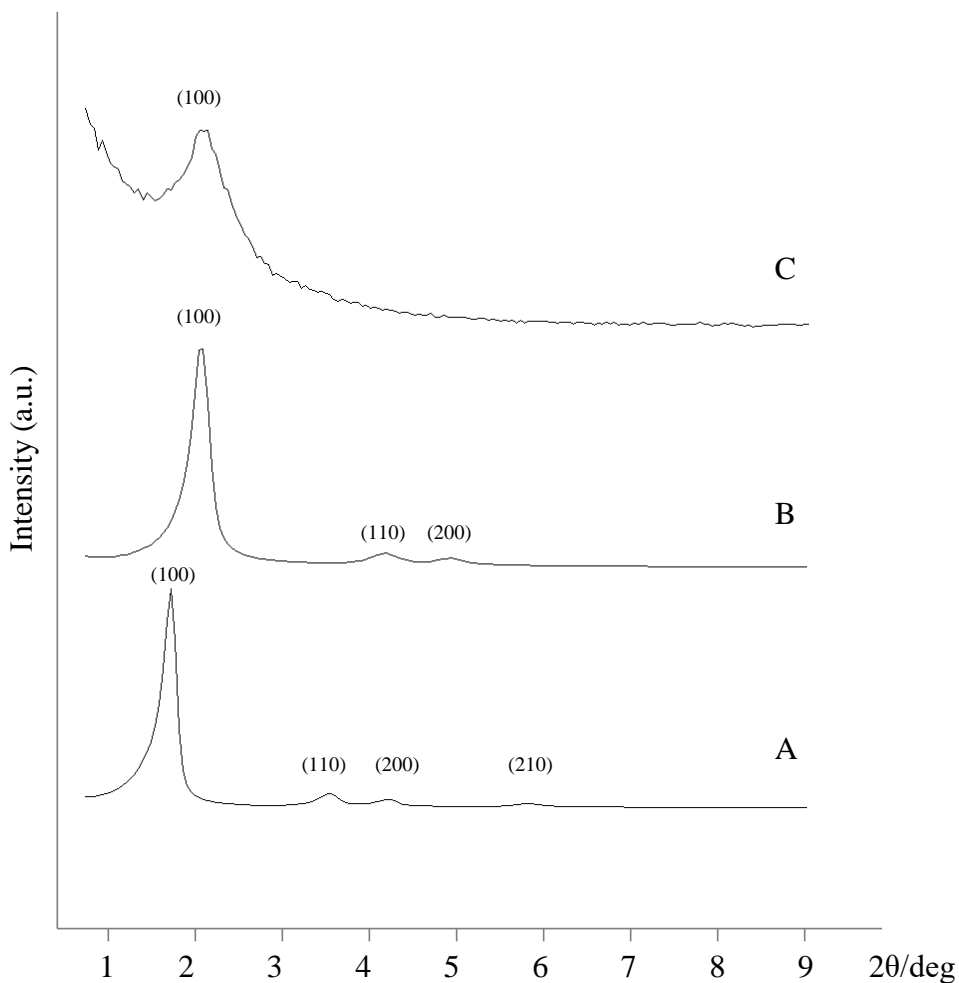

Figure 1. Powder X-ray patterns of the solids (A) MCM-41 as-synthesized, (B) MCM-41 calcined, and (C) **E-FA**.
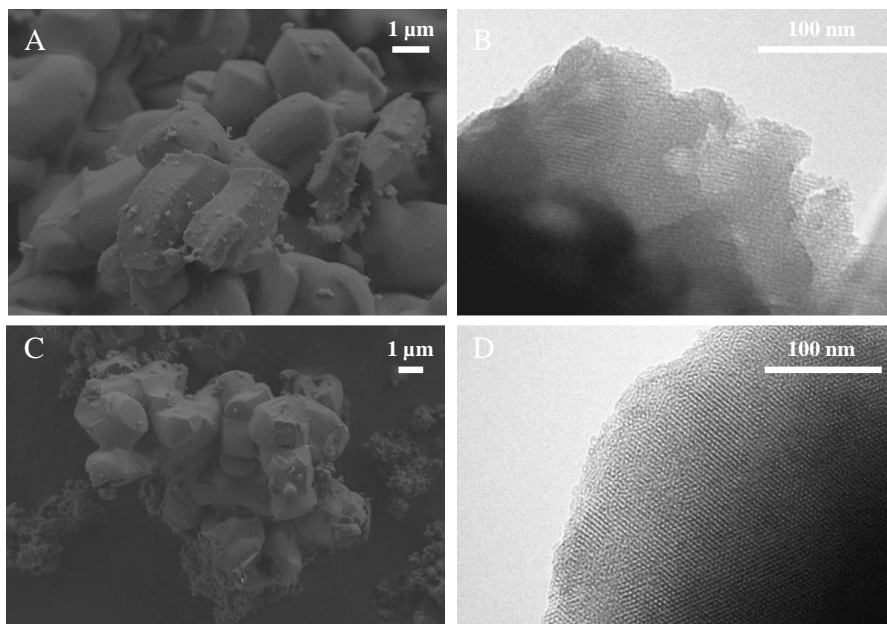
Figure 2. FESEM and TEM images of MCM-41 calcined (A, B) and **E-FA** (C, D).

The N_2 adsorption-desorption isotherms of the MCM-41 calcined material and **E-FA** are shown in Figure 3. The calcined MCM-41 material showed a type IV isotherm, which is typical of mesoporous supports. In contrast, **E-FA** displayed the characteristic curves of supports with filled mesopores. The calculated pore size (2.98 nm), pore volume (0.467 cm^3/g) and specific surface area (1075.36 m^2/g) of the starting MCM-41 material clearly reduced in **E-FA** (pore volume 0.058 cm^3/g and specific surface area 124.21 m^2/g) due to cargo loading and external functionalization.

The functionalization process was also verified by zeta potential determinations of the bare MCM-41 and MCM-41 loaded with FA and amine-functionalized (**E-FA**). The starting particles showed a zeta potential of -23 mV, which changed to +54 mV for **E-FA**. This is in agreement with the presence of amines in the final solid.
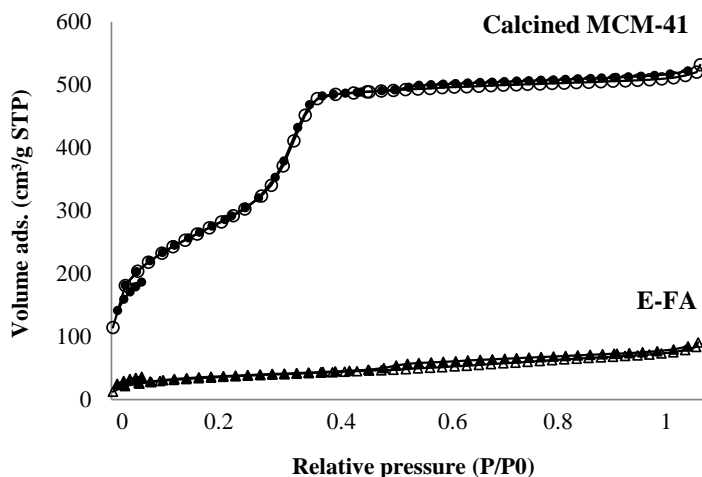
Figure 3. Nitrogen adsorption-desorption isotherms for calcined MCM-41 mesoporous material and **E-FA** support.

3.2. Juice fortification with entrapped FA

New strategies for food fortification are based on FA encapsulation in order to improve both the stability and bioavailability of the added vitamin in food products. Some FA encapsulation strategies based on food-grade nanoencapsulation systems based on chitosan nanoparticles (de Britto et al., 2012), alginate nanoparticles (Bakhshi et al., 2013) or amaranth protein-based electrospun fibers (Aceituno-Medina et al., 2015) have been described in recent years. Moreover, Pérez-Esteve et al. (2015a) developed a new FA delivery system based on MSPs capped with amines to assess the modulation of vitamin release and bioaccessibility in *in vitro* assays. Herein the latter pH-responsive delivery support was incorporated into apple and orange juice to study its release behavior in real food systems. Fruit juices were chosen because they are liquid drinks commonly used as vehicles for FA fortification (Sherstha et al., 2012). The reported amount of endogenous folates are 0.3 µg/100 g and 25 µg/100 g for apple and orange juice, respectively (Vahteristo et al., 2002). More importantly,

orange juice is rich in ascorbic acid, while apple juice only contains a small amount of this vitamin (Gardner et al., 2000). Besides its nutritional importance, ascorbic acid is considered significant because its content guarantees the presence of other nutrients, and it is usually added to process orange juice in recommended values of around 40 mg/100 mL (Esteve et al., 2005).

3.2.1. FA release profile in juices

Release studies were carried out to confirm the ability of the amine-gated **E-FA** support to control vitamin release according to the pH of food. The pH-dependent releases of the encapsulated FA in the apple and orange juices are shown in Figure 4. Delivery profiles exhibited the typical progression, which has already been found in the work of Pérez-Esteve et al. (2015a) in PBS at pH 2 and pH 7.5. As this figure depicts, delivery from **E-FA** was largely inhibited at the typical pH of fruit juices (pH 3.5) and only 10% FA release values were detected with time. This allowed us to confirm that vitamin delivery from **E-FA** was hindered by the combination of low FA solubility at a low pH and the gating effect of the polyamines anchored to the surface of MSPs due to electrostatic repulsions, and also to the interaction between the polyammonium moieties and anionic species present in juices. Polyamines are transformed into polyammonium groups at an acidic pH by adopting a rigid-like conformation due to Coulombic repulsions, and are able to interact with anions via electrostatic forces, which result in the capping of pores and cargo release inhibition (Bernardos et al., 2008). Conversely, sustained FA release with time was observed in neutralized fruit juices (pH 7.5). At a neutral pH, delivery took place because FA solubility increased and polyamines were less protonated, which reduced Coulombic repulsion and affinity for anions. The delivery profile of the entrapped vitamin from **E-FA** in fruit juices at a neutral pH was similar to that obtained in a buffer solution (Pérez-Esteve et al., 2015a). So it can be concluded that the matrix composition of fruit juices had no significant influence on the delivery functionality of the gated support. Maximum vitamin release at a neutral pH was achieved in less than 2 h with an

average value of 83.9±6.2 mg FA/g (a similar delivered amount was found for both juices). This was much higher than for other previously described FA encapsulation systems, such as that obtained by Madziva et al. (2006), which allowed maximum FA encapsulation of 3.6 μg/g in alginate-pectin capsules. The maximum release amount of FA was used to calculate the equivalent amount of entrapped and free FA needed in the stability assays (*vide infra*).
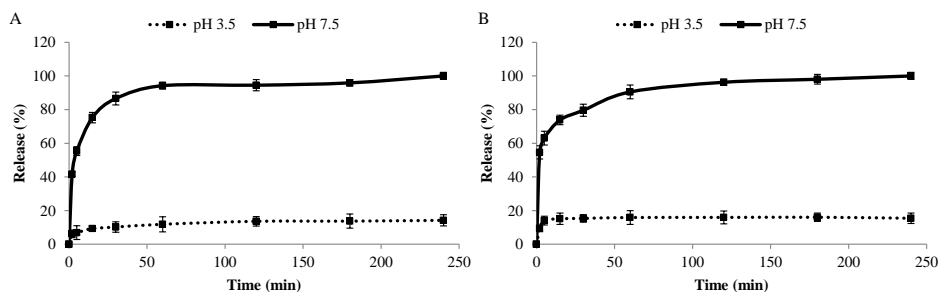
Figure 4. Release profiles of the vitamin from the pores of **E-FA** in apple (A) and orange juice (B) at pH 3.5 (dotted lines) and pH 7.5 (solid lines).

3.2.2.   FA bioaccessibility during in vitro digestion of juices

The pH-responsive delivery of FA from the amine-gated MSPs (solid **E-FA**) suggested that it is suitable for vitamin release in the gastrointestinal tract (closed gates in the stomach and opened gates in the intestine). Therefore, bioaccessibility of the vitamin during the simulated digestion of fruit juices was investigated. Figure 5 shows the behavior of entrapped (**E-FA**) and free (**F-FA**) FA in different *in vitro* digestion stages. As we can see, a small amount of FA was detected in the juices that contained free or entrapped FA in the buccal and stomach stages (2 h). The oral phase was too short to solubilize and/or release the vitamin, and the low pH of the gastric phase inhibited FA release and solubilization. In contrast, **E-FA** and **F-FA** displayed different behaviors in the intestinal stage. The bioaccessibility of free FA rapidly increased after adding

intestinal juices. With apple juice, free FA recovery did not reach 100% of the vitamin added because of degradation after exposure to acidic pH according to the shelf life stability results (*vide infra*). Conversely, sustained vitamin delivery from **E-FA** was observed in the digestion phase for both juices. In apple juice, progressive FA release after adding intestinal juices was detected and the maximum release took place at ca. 240 min. With orange juice, FA release was faster and a 100% release was observed after ca. 180 min of digestion. This suggests that apple juice better controls vitamin release than orange juice, and the differences in delivery rates were most likely due to differences in the food composition (Table 1). Overall these studies demonstrated that **E-FA** can protect FA in early digestion stages, but progressive FA release in the intestine can occur (where it is absorbed). This could allow the metabolic activation of the entire vitamin and could prevent the potential risks associated with presence of unmetabolized FA in the bloodstream.

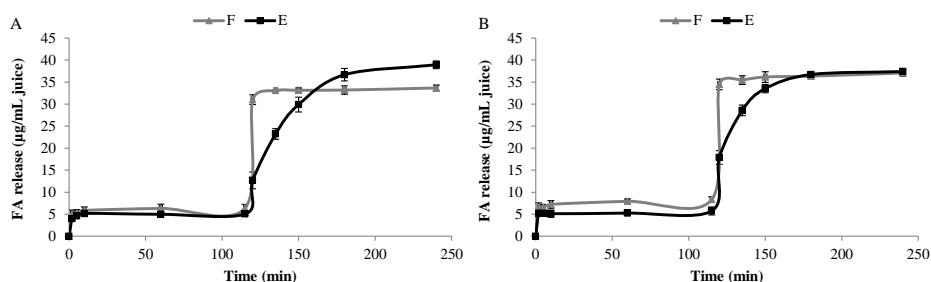**Figure 5**. Bioaccessibility of **F-FA** (gray lines) and **E-FA** (black lines) during an *in vitro* digestion procedure in apple (A) and orange (B) juice.

3.3. *Stability assays*

Besides folates encapsulation and the controlled release from the **E-FA** support, some studies have reported the ability of encapsulation systems to enhance the stability of entrapped vitamers after food production and storage.

Based on this idea, the stability of entrapped (**E-FA**) and free (**F-FA**) FA incorporated into fruit juices after simulating food production and storage processes was further studied.

3.3.1.   *Temperature stability*

Heat treatment is a key step in food processing to ensure the microbiological food safety in different food production and storage stages. The impact of high temperature on the stability of encapsulated (**E-FA**) and non-encapsulated (**F-FA**) FA was studied by simulating the sterilization conditions (121 °C, 1 bar) at different times. Figure 6 shows the recoveries of FA (FA present in the solution) from **E-FA** and **F-FA** in the apple (A) and orange (B) juices after heat treatment. With apple juice, entrapped FA showed significantly better stability than the free vitamin at the different exposure times ($p < 0.05$). Heat treatment led to major free FA loss of between 34% and 42% due to the high temperature and acidic pH combination. According to the literature, FA is considered stable at 100 °C for several hours within the 5.0–12.0 pH range, but becomes increasingly unstable as pH goes below 5.0 (Ball, 2005). In contrast, when **E-FA** and **F-FA** were added to orange juice, excellent FA recovery was observed at different times. Typical FA recovery values of 81-91% and 81-85% for the encapsulated (**E-FA**) and non-encapsulated (**F-FA**) vitamin were respectively observed (Fig. 6B). This improved FA stability in orange juice compared with apple juice is most likely related to presence of ascorbic acid in citrus juice, which has been reported to strongly protect folates against pressure and heat treatments (Butz et al., 2004; Liu et al., 2012).

These results demonstrated that encapsulation in MSPs enhanced FA stability. A simulated sterilization process has revealed the protective effect of MSPs on the vitamin's thermostability, mainly for the apple juice samples in which ascorbic acid content is negligible (Fig. 6A). Other encapsulation systems have obtained similar results in previous studies after different food processing treatments. The

processing of bread flour fortified with folates has resulted in a 20-30% FA loss (Gujska & Majewska, 2005; Johansson et al., 2002). However, the microencapsulation of folates significantly improved their stability during the course of bread making, while toasting obtained similar recoveries to those obtained when sodium ascorbate was added. Furthermore, co-encapsulating the reducing agent with folates provided better vitamin recovery after baking and greater stability during storage than the free compound (Liu et al., 2012; Tomiuk et al., 2012). Shrestha et al. (2012) encapsulated 5-methyltetrahydrofolic acid by spray-drying and exposed microcapsules to extrusion (100-150 °C) to obtain enhanced folate stability (84–94.5% retention) compared to the free form (65.3–83.2%) in all the extruded products.
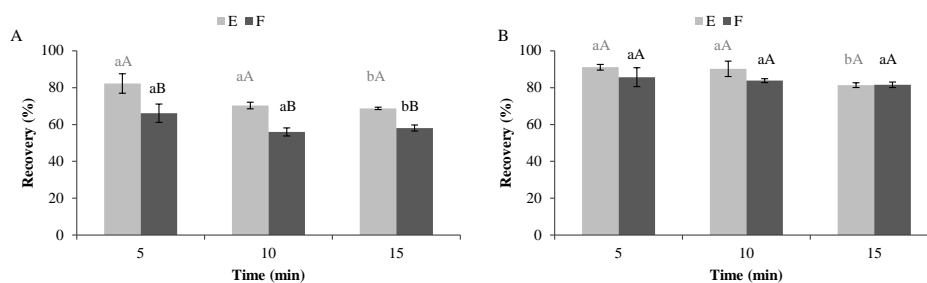
Figure 6. Influence of temperature exposure on the stability of encapsulated (**E-FA**) and free (**F-FA**) vitamin incorporated to apple (A) and orange (B) juices. Different letters in the bars indicate statistically significant differences (p<0.05) from levels of time exposure (small letters) and differences between encapsulated or free FA (capital letters). Values are Means ± SD, n = 3.

3.3.2. Light stability

Folic acid is photosensitive to visible or ultraviolet light, which results in the cleavage of the bond between C9-N10, and then the excision of the p-teridin moiety from p-aminobenzoylglutamate (Akhtar et al., 2003). In this section, free

(**F-FA**) and encapsulated (**E-FA**) FA were added to apple and orange juices, and were exposed to visible and UV light. Recoveries were compared with those of the non-irradiated samples. The preliminary experiments revealed no or very little degradation after 14 h of treatment (data not shown), so assays were ran from 16 h to 24 h. Figure 7 displays the different degradation profiles of the vitamin after exposure to visible light in apple juice (A) and orange juice (B). FA, when added as **F-FA**, progressively declined over time and with a maximum degradation of ca. 76% after 24 h for the apple juice samples. The FA from **E-FA** underwent a similar degradation rate to **F-FA**, but recoveries were significantly greater in all the samples, which confirmed the protective effect of the encapsulation system. In contrast, neither the free nor encapsulated FA included in the orange juice showed degradation during visible light exposure. The high antioxidant (ascorbic acid) content in this food system was most likely responsible for the high FA stability against oxidative photodegradation (Ball, 2005).

The stability behavior of the FA from **E-FA** and **F-FA** was similar after ultraviolet light exposure. With apple juice (Fig. 7C), the FA concentration decreased over time and non-significant differences were found between encapsulated and non-encapsulated FA, which obtained only 44% and 36% of the FA originally contained in the samples, respectively. In orange juice, the vitamin displayed better stability behavior (Fig. 7D). Despite the fact that the FA included in orange juice displayed slight degradation during the exposure time, after 24 h of irradiation more than 73% and 83% of the vitamin had been recovered for **E-FA** and **F-FA**, respectively. Nevertheless, the protective action of the mesoporous silica support against photodegradation was evidenced when ascorbic acid was absent. The mechanism of action was not clear, but enhanced stability could be a result of confining the vitamin in the mesopores of the silica support, which hindered the oxidation of the C9-N10 bond (Song & Yang, 2015).
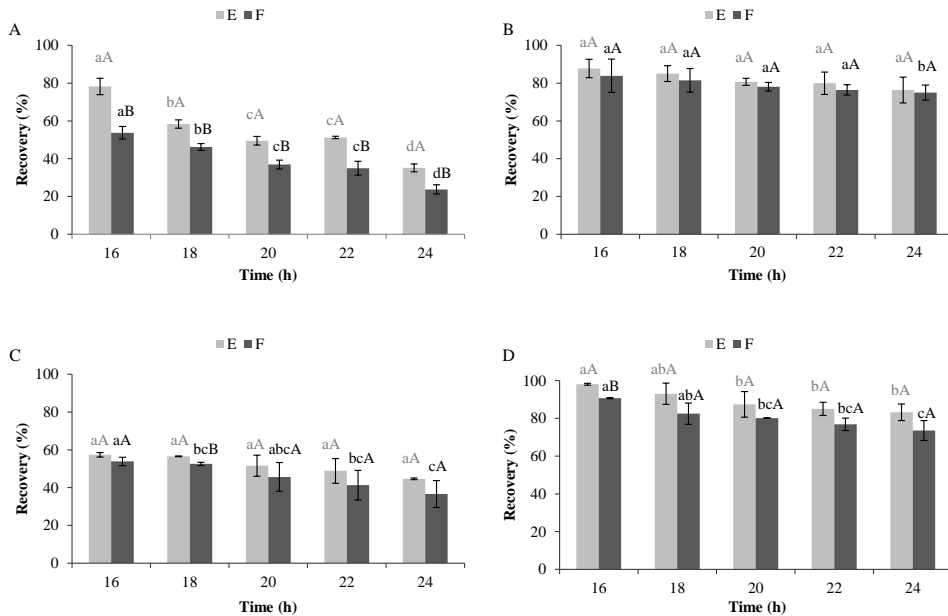
Figure 7. Influence of visible (A, B) and ultraviolet (C, D) light exposure on the stability of encapsulated (**E-FA**) and free (**F-FA**) vitamin incorporated to apple (left) and orange (right) juices. Different letters in the bars indicate statistically significant differences (p<0.05) from levels of time exposure (small letters) and differences between encapsulated or free FA (capital letters). Values are Means ± SD, n = 3.

3.3.3. Composition influence throughout shelf life

Another factor that could affect FA stability was the composition of foodstuffs during the storage period. The shelf life of fruit juices has been established to be around 1 month when considering them to be refrigerated pasteurized juices (Öhrvik & Witthöft, 2008). Figure 8 presents the stability of FA when encapsulated (**E-FA**) and non-encapsulated (**F-FA**) in apple (A) and orange juice (B) throughout storage time (0, 7, 14, 21 and 28 days). FA added in the **F-FA** form brought about a significant decrease in the recoveries of both juices, but the degradation profile differed according to juice type. With apple juice, the free vitamin was quickly degraded with an obtained recovery of 90% at at day 0 according to previous

studies due to oxidative degradation (De Brouwer et al., 2007). Moreover, FA recovery diminished to values of 77% after 28 days of refrigerated storage. However, **F-FA** added to orange juice was almost fully detectable with a 98% recovery on day 0. After the storage period (28 days), a slight decrease was observed with final FA recovery values of ca. 80%. These results are in accordance with previous studies, which have demonstrated a significant decrease in FA concentration (46%) during a 12-month period in fortified fruit juices, which indicates FA instability in an aqueous acidic matrix (Frommherz et al., 2014; Yakubu & Muazu, 2010). A higher degradation rate was obtained in month one due to a reaction with oxygen, which was eventually exhausted (Frommherz et al., 2014). Some other studies have considered orange juice a proper matrix to contain FA due to high ascorbic acid content (De Brouwer et al., 2007; Öhrvik & Witthöft, 2008) which can also be potentially lost during storage (Esteve et al., 2005). Kabasakalis et al. (2000) reported ascorbic acid degradation in commercial fruit juices and showed complete antioxidant loss when containers were opened for consumption and stored refrigerated for 31 days. Therefore, alternatives to the presence of ascorbic acid are needed to maintain FA content in fruit juices.
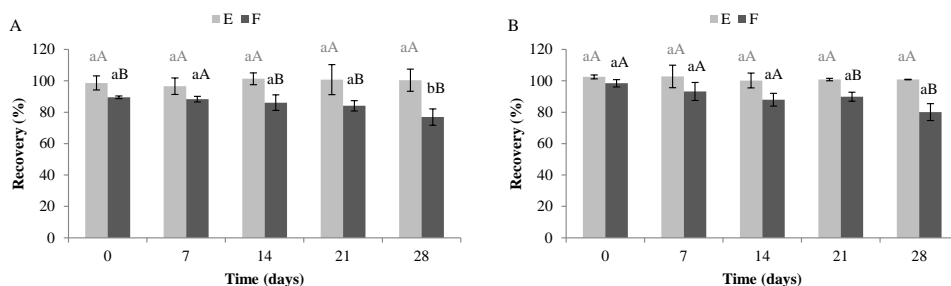

Figure 8. Stability of encapsulated (**E-FA**) and free (**F-FA**) vitamin incorporated to apple (A) and orange (B) juices during the shelf life period. Different letters in the bars indicate statistically significant differences (p<0.05) from levels of time exposure (small letters) and differences between the encapsulated or free FA (capital letters). Values are Means ± SD, n = 3.

As depicted in Figure 8, FA recoveries reached values of ca. 100% in all cases when **E-FA** was used, which indicates the good stability of the encapsulated vitamin in the acidic environment of these fruit juices. These results confirmed the suitability of MSPs as a support for FA encapsulation and protection in fortified juices in the same way as for other reported encapsulation systems (Madziva et al., 2006).

4. Conclusions

A smart delivery system of FA based on amine-gated MSPs has been successfully applied to improve both FA bioaccessibility and stability after being incorporated into fruit juices. The pH-responsive delivery effect of the functionalized support conferred the vitamin protection during food production simulation, as well as its controlled release under digestion conditions. A simulated *in vitro* digestion of fortified juices showed that entrapped FA was protected in the buccal and gastric stages, and that vitamin bioaccessibility was modified by the amine-gated MSPs in the intestinal stage, which would prevent unmetabolized synthetic FA being present in the bloodstream. Moreover, fortified juices were exposed to different environmental agents, which led to improved FA stability when the pH-responsive **E-FA** mesoporous support was used, particularly when ascorbic acid was absent. This preservation strategy could allow a smaller amount of FA needed for food fortification and could reduce the potential risks associated with high exposure to the vitamin. The impact of different processing and storage factors on FA stability has been individually evaluated herein. Bearing in mind these findings, we suggest considering MSPs to be smart delivery systems for the encapsulation, protection and controlled release of different food-related bioactive molecules in diverse food systems.

Acknowledgements

References

Aceituno-Medina, M., Mendoza, S., Lagaron, J. M., & López-Rubio, A. (2015). Photoprotection of folic acid upon encapsulation in food-grade amaranth (*Amaranthus hypochondriacus L.*) protein isolate–pullulan electrospun fibers. *LWT-Food Science and Technology, 62*(2), 970-975.

Akhtar, M.J., Khan, M.A., & Ahmad, I. (2003). Identification of photoproducts of folic acid and its degradation pathways in aqueous solution. *Journal of Pharmaceutical and Biomedical Analysis, 31*(3), 579-588.

Aznar, E., Oroval, M., Pascual, L., Murguía, J. R., Martínez-Máñez, R., & Sancenón, F. (2016). Gated materials for on-command release of guest molecules. *Chemical Reviews, 116,* 561–718.

Bakhshi, P.K., Nangrejo, M.R., Stride, E., & Edirisinghe, M. (2013). Application of electrohydrodynamic technology for folic acid encapsulation. *Food and Bioprocess Technology, 6*(7), 1837-1846.

Ball, G.F.M. (2005). *Vitamins in foods, analysis, bioavailability and stability*. Taylor & Francis, Boca Raton, FL.

Bernardos, A., Aznar, E., Coll, C., Martínez-Mañez, R., Barat, J.M., Marcos, M.D., Sancenón, F., Benito, A., & Soto, J. (2008). Controlled release of vitamin B2 using mesoporous materials functionalized with amine-bearing gate-like scaffoldings. *Journal of Controlled Release, 131*, 181-189.

Butz, P., Serfert, Y., Garcia, A.F., Dieterich, S., Lindauer, R., Bognar, A., & Tauscher, B. (2004). Influence of high-pressure treatment at 25 °C and 80 °C on folates in orange juice and model media. *Journal of Food Science, 69*(3), SNQ117-SNQ121.

Casasús, R., Climent, E., Marcos, M.D., Martínez-Máñez, R., Sancenón, F., Soto, J., Amorós, P., Cano, J., & Ruiz E. (2008). Dual Aperture Control on pH- and Anion-Driven Supramolecular Nanoscopic Hybrid Gate-like Ensembles. *Journal of the American Chemical Society 130*(6), 1903-1917.

Clarke, R., Smith, A.D., Jobst, K.A., Refsum, H., Sutton, L. &. Ueland, P.M. (1998). Folate, vitamin B_{12}, and serum total homocysteine levels in confirmed Alzheimer disease. *Formerly Archives of Neurology 55*(11), 1449-1455.

Crider, K.S., Bailey, L.B., &. Berry, R.J. (2011). Folic acid food fortification - Its history, effect, concerns, and future directions. *Nutrients 3*(3), 370–384.

de Britto, D., de Moura, M.R., Aouada, F.A., Mattoso, L.H., & Assis, O. B. (2012). N, N, N-trimethyl chitosan nanoparticles as a vitamin carrier system. *Food hydrocolloids, 27*(2), 487-493.

De Brouwer, V., Zhang, G.F., Storozhenko, S., Van Der Straeten, D., & Lambert, W. E. (2007). pH stability of individual folates during critical sample preparation steps in prevision of the analysis of plant folates. *Phytochemical Analysis 18*(6), 496-508.

EFSA (2006). Tolerable upper intake levels for vitamins and minerals, 51-58.

ESCO (EFSA's Scientific Cooperation) (2009). Report on analysis of risks, benefits of fortification of food with folic acid, 17-99.

Esteve, M.J., Frígola, A., Rodrigo, C., & Rodrigo, D. (2005). Effect of storage period under variable conditions on the chemical and physical composition and colour of Spanish refrigerated orange juices. *Food and Chemical Toxicology, 43*(9), 1413-1422.

Frommherz, L., Martiniak, Y., Heuer, T., Roth, A., Kulling, S. E., & Hoffmann, I. (2014). Degradation of folic acid in fortified vitamin juices during long term storage. *Food chemistry, 159*, 122-127.

Fukuwatari, T., Fujita, M., &. Shibata, K. (2009). Effects of UVA irradiation on the concentration of folate in human blood. *Bioscience Biotechnology Biochemistry 73*(2), 322–327.

Gardner, P.T., White, T.A., McPhail, D.B., & Duthie, G.G. (2000). The relative contributions of vitamin C, carotenoids and phenolics to the antioxidant potential of fruit juices. *Food Chemistry, 68*(4), 471-474.

Gujska, E., & Majewska, K. (2005). Effect of baking process on added folic acid and endogenous folates stability in wheat and rye breads. *Plant Foods for Human Nutrition, 60*(2), 37-42.

Hoag, S.W., Ramachandruni, H., &. Shangraw, R.F. (1997). Failure of prescription prenatal vitamin products to meet USP standards for folic acid dissolution. Six of nine vitamin products tested failed to meet USP standards for folic acid dissolution. *Journal of the American Pharmaceutical Association 37*(4), 397–400.

Jastrebova, J., Axelsson, M., Strandler, H.S., & Jägerstad, M. (2013). Stability of dietary 5-formyl-tetrahydrofolate and its determination by HPLC: a pilot study on impact of pH, temperature and antioxidants on analytical results. *European Food Research and Technology 237*(5), 747–754.

Johansson, M., Witthöft, C.M., Bruce, Å., & Jägerstad, M. (2002). Study of wheat breakfast rolls fortified with folic acid. *European Journal of Nutrition, 41*(6), 279-286.

Johansson, M., Jastrebova, J., Grahn, A., & Jägerstad, M. (2005). Separation of dietary folates by gradient reversed-phase HPLC: comparison of alternative and conventional silica-based stationary phases. *Chromatographia, 62*(1-2), 33-40.

Kabasakalis, V., Siopidou, D., & Moshatou, E. (2000). Ascorbic acid content of commercial fruit juices and its rate of loss upon storage. *Food Chemistry, 70*(3), 325-328.

Lebiedzińska, A., Dbrowska, M., Szefer, P., & Marszałł, M. (2008). High-performance liquid chromatography method for the determination of folic acid in fortified food products. *Toxicology mechanisms and methods, 18*(6), 463-467.

Li, Z., Barnes, J.C., Bosoy, A., Stoddart, J.F., &. Zink, J.I. (2012). Mesoporous silica nanoparticles in biomedical applications. *Chemical Society Reviews, 41*(7), 2590-2605.

Liu, Y., Green, T.J., Wong, P., & Kitts, D.D. (2012). Microencapsulation of L-5-methyltetrahydrofolic acid with ascorbate improves stability in baked bread products. *Journal of Agricultural and Food Chemistry, 61*(1), 247-254.

Madziva, H., Kailasapathy, K., & Phillips, M. (2006). Evaluation of alginate–pectin capsules in Cheddar cheese as a food carrier for the delivery of folic acid. *LWT-Food Science and Technology, 39*(2), 146-151.

Nguyen, M.T., Oey, I., Verlinde, P., van Loey, A., &. Hendrickx, M. (2003). Model studies on the stability of folic acid and 5-methyltetrahydrofolic acid degradation during thermal treatment in combination with high hydrostatic pressure. *Journal of Agricultural and Food Chemistry 51*(11), 3352–3357.

Öhrvik, V., & Witthöft, C. (2008). Orange juice is a good folate source in respect to folate content and stability during storage and simulated digestion. *European Journal of Nutrition, 47*(2), 92-98.

Pérez-Esteve, E., Fuentes, A., Coll, C., Acosta, C., Bernardos, A., Marcos, M.D., Martínez-Máñez, R., & Barat, J.M. (2015a). Modulation of folic acid bioaccesibility by encapsulation in pH-responsive gated mesoporous silica particles. *Microporous and Mesoporous Materials, 202*, 124-132.

Pérez-Esteve, É., Ruiz-Rico, M., Martínez-Máñez, R., & Barat, J.M. (2015b). Mesoporous silica-based supports for the controlled and targeted release of bioactive molecules in the gastrointestinal tract. *Journal of Food Science, 80*(11), E2504-E2516.

Shrestha, A. K., Arcot, J., & Yuliani, S. (2012). Susceptibility of 5-methyltetrahydrofolic acid to heat and microencapsulation to enhance its stability during extrusion processing. *Food Chemistry, 130*(2), 291-298.

Slowing, I.I., Vivero-Escoto, J.L., Wu, C.W., Lin, V.S.Y. (2008). Mesoporous silica nanoparticles as controlled release drug delivery and gene transfection carriers. *Advanced Drug Delivery Reviews, 60*, 1278-1288.

Song, N., & Yang, Y.W. (2015). Molecular and supramolecular switches on mesoporous silica nanoparticles. *Chemical Society Reviews, 44*(11), 3474-3504.

Stover, P.J. (2004). Physiology of folate and vitamin B_{12} in health and disease. *Nutrition Reviews 62*(6), 3–12.

Tomiuk, S., Liu, Y., Green, T. J., King, M. J., Finglas, P. M., & Kitts, D. D. (2012). Studies on the retention of microencapsulated L-5-methyltetrahydrofolic acid in baked bread using skim milk powder. *Food Chemistry, 133*(2), 249-255.

Vahteristo, L., Kariluoto, S., Bärlund, S., Kärkkäinen, M., Lamberg-Allardt, C., Salovaara, H., & Piironen, V. (2002). Functionality of endogenous folates from rye and orange juice using human *in vivo* model. *European Journal of Nutrition, 41*(6), 271-278.

Versantvoort, C.H., Oomen, A.G., Van de Kamp, E., Rompelberg, C.J., & Sips, A.J. (2005). Applicability of an *in vitro* digestion model in assessing the bioaccessibility of mycotoxins from food. *Food and Chemical Toxicology, 43*(1), 31-40.

Yakubu, S. & Muazu, J. (2010). Effects of variables on degradation of folic acid. *Der Pharmacia Sinica 1*(3), 55-58.

5. CHAPTER 2. Toward the development of new antimicrobial agents based on silica supports

5.1. Introduction[2]

Nanomaterials have emerged in the microbiological area because of their unique physicochemical properties (chemical stability, size, surface area and possibility of functionalization) which allow the antimicrobial effect to be improved.

New technologies to prevent spoilage and to guarantee the safety of food products have been developed because resistant microorganisms and inadequate traditional antimicrobial methods have extended. Inappropriate use of chemical preservatives can lead to resistant microorganisms and can provide them with favorable conditions to emerge, spread and persist (Capeletti et al., 2014). Bacterial resistance can be resolved by exploring antimicrobial nanomaterials, to which microbial pathogens might not be able to develop resistance, as well as novel nanosized supports for efficient antimicrobial compounds delivery (Huh & Kwon, 2011). Furthermore, current methods used in the food industry to inhibit microbial growth affect the quality properties of food (thermal treatment), or are related to toxicological problems (traditional additives) (Zengin et al., 2011). As a result, consumers demand alternative methods to inhibit microorganisms in food, while maintaining the quality and safety of the food product. A novel approach for the inhibition of microbial growth could be the application of nanomaterials, which could be: responsible for antimicrobial activity because of their composition, structure or size, such as metallic nanoparticles; or can be used as antimicrobial carriers that allow the encapsulation or attachment of antimicrobial molecules to protect them from degradation, such as food-grade

---

[2] Introduction is based on the book chapter: Ruiz-Rico, M., Pérez-Esteve, E., & Barat, J.M. Use of nanotechnology as an antimicrobial tool in the food sector. . In: Dhawan, A., Shanker, R., Singh, S., Kumar, A. (Ed.) Nanobiotechnology: Human Health and the Environment. CRC Press, *In press*

nanoencapsulation systems (nanoemulsions, microemulsions, liposomes, solid lipid nanoparticles or nanofibres) or inorganic encapsulation systems (zeolites, clays or mesoporous silica particles). Antimicrobial nanoparticles help reduce toxicity by overcoming resistance and lower costs compared to conventional antimicrobial agents. Nanosized carriers are also able to improve bioavailability and the inhibitory effect of antimicrobial biomolecules (Huh & Kwon, 2011).

1. Nanoencapsulation systems

Microbial inhibition has been traditionally achieved by adding chemical antimicrobial agents or preservatives. Despite their effectiveness, the continuous use of antimicrobials may result in resistant strains appearing (EFSA, 2013), and in some toxicity problems (Zengin et al., 2011). Therefore, consumers demand alternative antimicrobials, such as natural products and/or new administration forms, which help lower concentrations of doses (Gyawali & Ibrahim, 2014). Although naturally-occurring antimicrobial compounds have particularly attracted much attention, the number of compounds allowed by regulations to be used in foods is very limited. So making better use of available approved antimicrobial compounds is necessary and, for this reason, research has focused on developing technologies, such as nanoencapsulation systems, to improve the functionality of food antimicrobials (Weiss et al., 2009).

Naturally-occurring antimicrobial compounds include plant metabolites such as essential oils, free fatty acids or phytochemicals (i.e. curcuminoids, organosulfurs), animal enzymes or proteins, and microorganism-based bacteriocins. Among existing antimicrobial compounds, encapsulation of essential oils (EOs) to protect bioactive substances from environmental stress, to mask undesirable sensory properties of EOs and to achieve the controlled release of the antimicrobial compounds at the site of action has been broadly reported. These lipophilic extracts of bioactive compounds have displayed antimicrobial activity against several pathogen and food-borne microorganisms. Inhibitory activity has

been attributed to their phenolic compounds and their interaction with microbial cell membranes, which cause leakage of ions and cytoplasmic content, and thus lead to cellular breakdown (Burt, 2004). The direct application of EOs in food products has several limitations due to their strong sensory properties (odor and flavor), high volatility, poor solubility and potential toxicity. The concentration of an essential oil needed to inhibit microbial growth in a food system is higher than in *in vitro* studies because of not only interactions with food components (Jo et al., 2015), but also difficulties in their dispersion in the food water phase (Weiss et al., 2009). Therefore, nanoencapsulation systems help lower the concentration of EOs and reduce their incorporation into food with a different polarity which, in turn, helps improve the balance between food sensory properties and antimicrobial efficacy, and to enhance stability, protection from environmental stress and to prevent interactions with food components (Gaysinsky et al., 2005; Liang et al., 2012).

Other biomolecules with proved antimicrobial activity are proteins and enzymes. These hydrophilic compounds are fragile, and even small conformational changes may reduce their activity. Therefore, stabilization of peptides or enzymes through entrapment in nanoencapsulation systems may be a potential alternative to protect antimicrobials from denaturation by proteolysis and dilution effects, and to enhance their efficacy and stability for food applications. As a result of entrapments in the confined environment of nanopores, the molecular motions of water molecules are modified. Consequently, biochemical reaction rates lower and the stabilization of biological materials during storage reduces (Balcão et al., 2013). Encapsulation of antimicrobial proteins in organic vesicles may offer several advantages, such as: reducing the affinity between the antimicrobial compound and non-target components, which could imply undesired interactions; protecting protein from inhibitors or unfavorable conditions; or cutting the risk of emergence of resistant strains (Mozafari et al., 2008). However, the main limitation of the entrapment of antibacterial peptides in lipid carriers is the ability of these compounds to interact

with liposomal membranes and to disrupt them. So the entrapment process and the lipid composition of matrices should be optimized to minimize this disadvantage (Laridi et al., 2003).

When selecting supports for encapsulating antimicrobial compounds, two principal approaches can be chosen: organic nanoencapsulation systems based on food-grade nanoparticles and inorganic nanoencapsulation systems such as zeolites, nanoclays or mesoporous silica particles.

2. Organic nanoencapsulation systems

Organic nanoencapsulation systems are based on food-grade nanoparticles (NPs), which are particles that exist naturally or have been manufactured within the nanosize range from food compatible sources like chitosan, lecithin, alginate, arabic and xanthan gum, proteins, etc. (Hannon et al., 2015). These supports have different structures and properties that allow the entrapment of varied bioactive compounds and offer considerable advantages of usage. Liquids substances can be handled since solids, smell or taste can be masked in a food product, sensitive compounds can be protected, and delivery can be controlled and targeted (Gomes et al., 2011). Figure 1 shows current nanostructured encapsulation systems, which include liposomes, solid lipid nanoparticles, nanoemulsions, microemulsions, and nanofibers (Weiss et al., 2009). Among these nanoencapsulation systems, there are particles that exceed the size range for NPs. Notwithstanding, the scientific community now considers these systems to be nanoencapsulation systems due to the encapsulation concept of small molecules. In our opinion, this nomenclature may be confusing and standard definitions are needed.
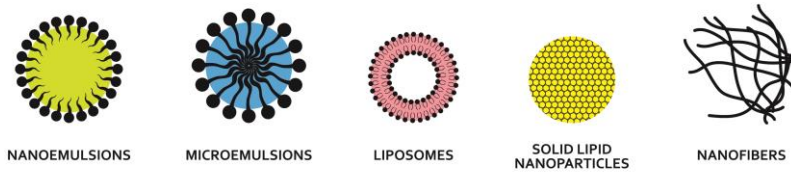
Figure 1: Schematic representation of different food-grade encapsulation systems.

3. Inorganic nanoencapsulation systems

Inorganic nanoencapsulation systems are characterized by a well-organized regular system of channels or pores that allow the entrapment of bioactive molecules. Different inorganic containers have been described to encapsulate and control the release of bioactive compounds, such as zeolites, nanoclays or mesoporous silica particles. Zeolites and clays are aluminosilicate solids organized into different three-dimensional frameworks with adequate features (simple manufacturing, low-cost and biocompatibility) that act as delivery systems. However according to the literature, mesoporous silica particles are the most important carriers for entrapping and delivering bioactive compounds in a sustained manner. Therefore, this section focuses on these mesoporous materials.

Compared to organic encapsulation systems, MSPs are more rigid (higher thermal and chemical stability, and more resistant to changes in pH, ion concentrations or pressure) supports that can protect cargoes from chemical and biological (enzymatic or microbial) degradation (Tao, 2014; Song & Yang, 2015).

MSPs are considered biocompatible materials for microbial populations in the literature. For instance, the study by Wehling et al. (2013) investigated the effect of silica particles with sizes between 15 and 500 nm on bacterial viability. The results determined that particles displayed no inhibitory properties independently of their particle size. Other research works, which have assessed the antibacterial

effect of loaded nanoparticles, have shown that unloaded supports display no inhibitory activity against the studied microorganisms (Izquierdo-Barba et al., 2009; Mas et al., 2013; Wang et al., 2014). Nevertheless, when MSPs are loaded and/or functionalized with antimicrobial compounds, they can be used as antimicrobial materials in different applications.

3.1. Antimicrobial loaded MSPs

The incorporation of antimicrobial compounds into the pores of MSPs has been reported in recent years as an efficient strategy to create antimicrobial agents. The study of Izquierdo-Barba et al. (2009) reports the encapsulation of the antimicrobial peptide LL-37 and chlorhexidine in a mesoporous silica monolith, and achieved controlled release by attaching thiol groups to the silica surface. Both loaded particles showed bactericidal activity against gram-positive and gram-negative bacteria, but the particles loaded with chlorhexidine displayed high toxicity according to the hemolysis, lactate dehydrogenase release and cell proliferation assays. In another study, nitroimidazole PA-824, with high anti-tubercular activity, was entrapped in MSPs and its solubility and, thus its bioavailability, improved. However, antibacterial activity was no greater than the effect of the free compound. Lack of improved activity could be due to difficulties in releasing nitroimidazole from the MSPs produced by molecules, which could interfere with the cellular environment (Xia et al., 2014).

The encapsulation of natural antimicrobial compounds in mesoporous supports has also been recently described. Allyl isothiocyanate is a natural antibacterial compound that can be added to food, but problems with its volatility, pungency and poor water solubility exist (Siahaan et al., 2013). Encapsulation of this compound in MSPs and its controlled release has been achieved according to pore size distribution, and antibacterial properties remained after adsorption and desorption processes (Park et al., 2011; Park & Pendleton, 2012; Park et al., 2012). Siahaan et al. (2013) compared the suitability

of MCM-41 and dried algae *Laminaria japonica* as carriers of allyl isothiocyanate. Their results revealed that loading was achieved in both delivery vectors, despite the MCM-41 support allowed higher adsorption and desorption, and consequently, greater bacteriostatic activity.

Along the same lines, Bernardos et al. (2015) reported the entrapment of some EOs components (carvacrol, cinnamaldehyde, eugenol and thymol) in MCM-41 and β-cyclodextrin in order to control the volatility of the bioactive compounds. The *in vitro* antifungal activity of the free and encapsulated EOs components against *Aspergillus niger* was established. The results revealed that carvacrol and thymol in MCM-41 displayed remarkably enhanced antifungal properties compared to free or β-cyclodextrin-encapsulated compounds. The antifungal activity of silica-entrapped carvacrol and thymol maintained antifungal activity and inhibited fungal growth after 30 days of incubation. This clearly contrasts with corresponding compounds when alone or encapsulated in β-cyclodextrin, which were unable to display antifungal properties to such an extent.

Besides natural organic molecules such as EO components, organosulfur compounds and fatty acids, encapsulation of antibiotics, such as amoxicillin, gentamicin, erythromycin, vancomycin, rifampicin, linezolid and tetracycline in the MSPs also allows the preparation of novel biopesticides (Doadrio et al., 2004; Capeletti et al., 2014; Li et al., 2010, Molina-Manso et al., 2012; Vallet-Regí et al., 2004). Amoxicillin has been entrapped in bare MSPs (Vallet-Regí et al., 2004) and then 3-aminopropyl trimethoxysilane and 3-chloropropyltriethoxysilane have been functionalized on MSPs surface (Li et al., 2010). It was also possible to modulate the delivery of the antibiotic by functionalization, while release was based on the diffusion mechanism. These studies have revealed that an *in vitro* controlled release of amoxicillin in mesoporous material has advantages over traditional administration forms (capsules, tablets), where antibiotic release is faster and not controlled. Xue & Shi (2004) studied gentamicin encapsulation in an SBA-15 solid functionalized with a poly (DL-lactide-co-glycolide) (PLGA). This

hybrid support produced an initial burst release for 1 day, followed by a sustained release over a 5-week period due to polymer degradation. Another functionalization strategy for controlled delivery has been evaluated by Doadrio et al. (2006), who studied the functionalization of SBA-15 with hydrophobic groups (octyl and octadecyl groups) to control erythromycin release. This functionalization produced reduced loading and induced slower delivery kinetics because of the support's diminished wettability. More recently, entrapment of vancomycin, rifampicin and linezolid in SBA-15 has been evaluated against a strain of *S. aureus,* which produced biofilms. This support was able to release high antibiotic concentrations in the initial stage of experiments, with concentrations well over the breakpoints (Molina-Manso et al., 2012). Capeletti et al. (2014) reported the use of silica nanospheres to entrap tetracycline and found that antibacterial activity was produced in the presence of the antibiotic in the support's pores.

3.2. Antimicrobial functionalized MSPs

As mentioned above, MSPs not only have voids capable of entrapping active compounds, but also present a large surface capable of reacting with organic molecules. This process is commonly known as functionalization. Antimicrobial functionalized MSPs are particles that display antimicrobial properties because of the effect of molecules that are attached to the surface of supports. This approach to create antimicrobial devices is really new and in accordance there are very few references of this type of antimicrobial MSPs found in the literature.

MSPs coated with didodecyldimethylammonium bromide (DDAB) showed strong antimicrobial activity against bacteria, yeast, molds, and viruses. The nanoparticles coated with quaternary ammonium cationic surfactant had a lower minimum inhibitory concentration than that obtained for free DDAB. This improvement may be due to differences in the size, charge density and the stiffness of both formulations, which may have an impact on their interaction with

biological systems. It has also been reported that coated MSPs can be reused without losing their antimicrobial activity, and that DDAB did not show leaching. Thus the antimicrobial effect is mediated mainly by contact (Botequim et al., 2012).

In a later study, Li & Wang (2013) reported lysozyme-coated mesoporous silica nanoparticles (Lys-MSNs) to be antibacterial agents that exhibit efficient antibacterial activity against *E. coli* both *in vitro* and *in vivo,* and had low cytotoxicity and negligible hemolytic side effects. Bacterial growth was 5-fold lower for Lys-MSNs than that of free lysozyme (Lys) *in vitro*. These particles were able to reduce the microorganism by two orders of magnitude using an intestine-infected mouse model compared to the untreated group. This enhanced antibacterial efficacy originated from the Lys corona, and presented a multivalent interaction between the Lys of the functionalized nanoparticles and peptidoglycans of the bacterial walls. This multivalent interaction increased the local Lys concentration on the surface of cell walls, which produced the hydrolysis of peptidoglycans and damaged the bacterial cell wall.

The use of particles functionalized with an antibiotic has been recently studied by Qi et al. (2013). They investigated the development of vancomycin-modified mesoporous silica nanoparticles (Van-MSNs) for targeting and killing gram-positive bacteria on macrophage-like cells. Vancomycin shows specific hydrogen bonding interactions towards the terminal D-alanyl-D-alanine moieties of gram-positive bacteria, as well as inhibited bacterial cell wall synthesis capability. The vancomycin corona on Van-MSNs provided multivalent interactions and enhanced specific recognition towards gram-positive bacteria. The high local vancomycin concentration on surfaces enabled NPs to strongly immobilize on the cell walls of *S. aureus,* which resulted in a significant inhibition effect on cell wall synthesis. Van-MSNs also showed a weak recognition with gram-negative bacteria, which was attributed to the non-specific electrostatic interactions between Van-MSNs and the negatively charged bacterial membranes. Detectable non-specific binding of Van-MSNs with macrophage-like cells was not observed.

Pędziwiatr-Werbicka et al. (2014) synthesized novel silicates using silylated natural fatty acids as co-condensing reagents to produce functionalized MSPs. Different mono- and bis-silylated fatty acid precursors were used to modify the SBA-15 structure. The obtained functionalized materials displayed pronounced hydrophobicity owing to the presence of fatty length chains. The antimicrobial activity of fatty acid tethered silicates at different concentrations was evaluated. The result revealed that the inhibitory effect was sensitive to the nature of the fatty acid precursor, which reached a maximum inhibition of 50% compared to the control samples.

3.3. Antimicrobial loaded and functionalized MSPs

The combination of both previously described mechanisms, loading and functionalizing MSPs, could well be another effective system against microbial growth. This section presents reported studies that have used an antimicrobial compound entrapped in supports functionalized on their external surface with antimicrobial molecules. The presence and activity of both compounds enhance them synergistically. A schematic representation of antimicrobials loaded and functionalized MSPs is offered in Figure 2. As this figure illustrates, the interaction between the coating of MSPs and bacteria allowed cargo release and, thus, cell damage and microorganism death due to the combined effect of attached and entrapped molecules.

Figure 2. Representation of the synergistic effect of loaded and functionalized MSPs.

One of the examples found in the literature is the development of MSPs loaded with peracetic acid (PAA) and silver NPs that decorate the structure of particles and have a strong synergistic bactericidal effect on antibiotic-resistant and biofilm-forming *S. aureus* (Carmona et al., 2012). Minimum reduction was observed for PAA- or Ag-loaded materials, which indicates limited antimicrobial action of the released compounds when used alone. Conversely when the Ag-PAA-SBA-15 samples were used in bactericidal tests, a clear synergistic effect was observed with total bacteria inhibition. The synergic effect was probably produced by a de-aggregation effect on the biofilm caused by PAA increasing the exposed surface of the bacteria susceptible to being affected by Ag^+ ions, and the amplified Ag^+ production was likely due to the accelerated dissolution of Ag NPs.

Another example is the study of Mas et al. (2013), in which MCM-41 nanoparticles were loaded with vancomycin and capped with ε-poly-L-lysine (ε-PL). The developed NPs showed enhanced ε-PL toxicity against gram-negative bacteria. ε-PL is a cationic polymer with antimicrobial activity against gram-negative bacteria, while vancomycin is an antibiotic that has an inhibitory effect against gram-positive bacteria, as mentioned above. ε-PL attached to NPs, which was positively charged, was bound to the negatively charged cell wall to induce bacterial wall damage, and allowed entrapped vancomycin to gain access to the cell. The achieved antibacterial activity indicated a strong synergistic effect when the nanoformulation was used.

4. Final remarks

Nanostructured materials exhibit unique physicochemical properties that offer the opportunity for creating new technologies for manufacturing, packaging and storage of food products (Dasgupta et al., 2015). Nanoscalar delivery systems allow the encapsulation or attachment of antimicrobial compounds with high volatility or poor solubility, which protect them from environmental degradation. Nanoencapsulation systems also have a good loading capacity that allow

antimicrobial inhibitory concentrations to lower, as well as the controlled or stimuli-responsive delivery of the antimicrobial compound at the site of action. Figure 3 summarizes the most relevant features of each of the described nanoscalar delivery system, demonstrating the advantages of using MSPs in the development of a new generation of antimicrobials for food aplications in comparision to the use of organic systems.

Carrier		Remarkable features
	NANOEMULSIONS	Slightly turbid Increased bioavailability and controlled delivery Tendency to breakdown Susceptible to chemical degradation
	MICROEMULSIONS	Transparent High stability Increased bioavailability
	LIPOSOMES	Biocompatibility Easy functionalization Increased bioavailability
	SOLID LIPID NANOPARTICLES	High stability Increased bioavailability
	NANOFIBERS	Mechanical performance Entrapment of other encapsulation systems
	MESOPOROUS SILICA PARTICLES	High stability Controlled release Easy functionalization Delivery in the site of action

Figure 3. Overview of the features of different nanoencapsulation systems.

References

Balcão, V.M., Costa, C.I., Matos, C.M., Moutinho, C.G., Amorim, M., Pintado, M.E., Gomes, A.P., Vila, M.M., & Teixeira, J.A. (2013). Nanoencapsulation of bovine lactoferrin for food and biopharmaceutical applications. *Food Hydrocolloids, 32*, 425-431.

Bernardos, A., Marina, T., Žáček, P., Pérez-Esteve, E., Martínez-Mañez, R., Lhotka, M., Kourimská, L., Pulkrávek, J., & Klouček, P. (2015). Antifungal effect of essential oil components against *Aspergillus niger* when loaded into silica mesoporous supports. *Journal of the Science of Food and Agriculture, 95,* 2824–2831.

Botequim, D., Maia, J., Lino, M.M.F., Lopes, L.M.F., Simoes, P.N., Ilharco, L.M., & Ferreira, L. (2012). Nanoparticles and surfaces presenting antifungal, antibacterial and antiviral properties. *Langmuir, 28*(20), 7646-7656.

Burt, S. (2004). Essential oils: Their antimicrobial properties and potential applications in food – A review. *International Journal of Food Microbiology, 94*, 223–253.

Capeletti, L.B., de Oliveira, L.F., Gonçalves, K.D.A., de Oliveira, J.F.A., Saito, Â., Kobarg, J., & Cardoso, M.B. (2014). Tailored Silica-Antibiotic Nanoparticles: Overcoming Bacterial Resistance with Low Cytotoxicity. *Langmuir, 30*, 7456–7464.

Carmona, D., Lalueza, P., Balas, F., Arruebo, M., & Santamaría, J. (2012). Mesoporous silica loaded with peracetic acid and silver nanoparticles as a dual-effect, highly efficient bactericidal agent. *Microporous and Mesoporous Materials, 161*, 84-90.

Dasgupta, N., Ranjan, S., Mundekkad, D., Ramalingam, C., Shanker, R., & Kumar, A. (2015). Nanotechnology in agro-food: from field to plate. *Food Research International, 69*, 381-400.

Doadrio, A.L., Sousa, E.M.B., Doadrio, J.C., Pérez Pariente, J., Izquierdo-Barba, I., & Vallet-Regí, M. (2004). Mesoporous SBA-15 HPLC evaluation for controlled gentamicin drug delivery. Journal of *Controlled Release, 97*(1), 125-132.

Doadrio, J.C., Sousa, E.M., Izquierdo-Barba, I., Doadrio, A.L., Perez-Pariente, J., & Vallet-Regí, M. (2006). Functionalization of mesoporous materials with long alkyl chains as a strategy for controlling drug delivery pattern. *Journal of Materials Chemistry, 16*(5), 462-466.

EFSA (2013). The European Union Summary Report on antimicrobial resistance in zoonotic and indicator bacteria from humans, animals and food in 2011. *EFSA Journal, 11*(5), 3196-3359. (http://www.efsa.europa.eu/en/efsajournal/pub/3196.htm). [30/07/2015]

Gaysinsky, S., Davidson, P.M., Bruce, B.D., & Weiss, J. (2005). Growth inhibition of *Escherichia coli* O157:H7 and *Listeria monocytogenes* by carvacrol and eugenol encapsulated in surfactant micelles. *Journal of Food Protection, 68*(12), 2559–2566.

Gomes, C., Moreira, R.G., & Castell-Perez, E. (2011). Poly (DL-lactide-co-glycolide) (PLGA) nanoparticles with entrapped trans-cinnamaldehyde and eugenol for antimicrobial delivery applications. *Journal of Food Science, 76*(2), 16-24.

Gyawali, R. & Ibrahim, S.A. (2014). Natural products as antimicrobial agents. *Food Control, 46*, 412-429.

Hannon, J.C., Kerry, J., Cruz-Romero, M., Morris, M., & Cummins, E. (2015). Advances and challenges for the use of engineered nanoparticles in food contact materials. *Trends in Food Science & Technology, 43*(1), 43-62.

Huh, A.J., & Kwon, Y.J. (2011). "Nanoantibiotics": a new paradigm for treating infectious diseases using nanomaterials in the antibiotics resistant era. *Journal of Controlled Release, 156*(2), 128-145.

Izquierdo-Barba, I., Vallet-Regí, M., Kupferschmidt, N., Terasaki, O., Schmidtchen, A., & Malmsten, M. (2009). Incorporation of antimicrobial compounds in mesoporous silica film monolith. *Biomaterials, 30*(29), 5729-5736.

Jo, Y.J., Chun, J.Y., Kwon, Y.J., Min, S.G., Hong, G.P., Choi, M.J. (2015). Physical and antimicrobial properties of trans-cinnamaldehyde nanoemulsions in water melon juice. *LWT - Food Science and Technology, 60*, 444-451.

Laridi, R., Kheadr, E.E., Benech, R.O., Vuillemard, J.C., Lacroix, C., & Fliss, I. (2003). Liposome encapsulated nisin Z: optimization, stability and release during milk fermentation. *International Dairy Journal, 13*, 325-336.

Li, L.L., & Wang, H. (2013). Enzyme-coated mesoporous silica nanoparticles as efficient antibacterial agents *in vivo*. *Advanced Healthcare Materials, 2(10)*, 1351-1360.

Li, Z., Su, K., Cheng, B., & Deng, Y. (2010). Organically modified MCM-type material preparation and its usage in controlled amoxicillin delivery. *Journal of Colloid and Interface Science, 342*(2), 607-613.

Liang, R., Xu, S., Shoemaker, C.F., Li, Y., Zhong, F., & Huang, Q. (2012). Physical and antimicrobial properties of peppermint oil nanoemulsions. *Journal of Agricultural and Food Chemistry, 60*, 7548–7555.

Mas, N., Galiana, I., Mondragón, L., Aznar, E., Climent, E., Cabedo, N., Sancenón, F., Murguía, J.R., Martínez-Máñez, R., Marcos, M.D., & Amorós, P. (2013). Enhanced efficacy and broadening of antibacterial action of drugs via the use of capped mesoporous nanoparticles. *Chemistry-A European Journal, 19*(34), 11167-11171.

Molina-Manso, D., Manzano, M., Doadrio, J.C., Del Prado, G., Ortiz-Pérez, A., Vallet-Regí, M., Gómez-Barrena, E., & Esteban, J. (2012). Usefulness of SBA-15 mesoporous ceramics as a delivery system for vancomycin, rifampicin and linezolid: a preliminary report. *International Journal of Antimicrobial Agents, 40*(3), 252-256.

Mozafari, M.R., Johnson, C., Hatziantoniou, S., & Demetzos, C. (2008). Nanoliposomes and their applications in food nanotechnology. *Journal of Liposome Research, 18*, 309–327.

Park, S.Y., & Pendleton, P. (2012). Mesoporous silica SBA-15 for natural antimicrobial delivery. *Powder Technology, 223*, 77-82.

Park, S.Y., Barton, M., & Pendleton, P. (2011). Mesoporous silica as a natural antimicrobial carrier. *Colloids and Surfaces A: Physicochemical and Engineering Aspects, 385*(1), 256-261.

Park, S.Y., Barton, M., & Pendleton, P. (2012). Controlled release of allyl isothiocyanate for bacteria growth management. *Food Control, 23*(2), 478-484.

Pędziwiatr-Werbicka, E., Miłowska, K., Podlas, M., Marcinkowska, M., Ferenc, M., Brahmi, Y., Katir, N., Majoral, J.P., Felczak, A., Boruszewka, A., Lisowska, K., Bryszewska, M., & El Kadib, A. (2014). Oleochemical-Tethered SBA-15-Type Silicates with Tunable Nanoscopic Order, Carboxylic Surface, and Hydrophobic Framework: Cellular Toxicity, Hemolysis, and Antibacterial Activity. *Chemistry-A European Journal, 20(31)*, 9596-9606.

Qi, G., Li, L., Yu, F., & Wang, H. (2013). Vancomycin-modified mesoporous silica nanoparticles for selective recognition and killing of pathogenic gram-positive bacteria over macrophage-like cells. *ACS applied materials & interfaces, 5(21)*, 10874-10881.

Siahaan, E.A., Meillisa, A., Woo, H. C., Lee, C.W., Han, J.H., & Chun, B.S. (2013). Controlled release of allyl isothiocyanate from brown algae Laminaria japonica and mesoporous silica MCM-41 for inhibiting food-borne bacteria. *Food Science and Biotechnology, 22*(1), 19-24.

Song, N., & Yang, Y. W. (2015). Molecular and supramolecular switches on mesoporous silica nanoparticles. *Chemical Society Reviews, 44*(11), 3474-3504.

Tao, Z. (2014). Mesoporous silica-based nanodevices for biological applications. *RSC Advances, 4*(36), 18961-18980.

Vallet-Regí, M., Doadrio, J.C., Doadrio, A.L., Izquierdo-Barba, I., & Pérez-Pariente, J. (2004). Hexagonal ordered mesoporous material as a matrix for the controlled release of amoxicillin. *Solid State Ionics, 172*(1), 435-439.

Wang, L., He, H., Zhang, C., Sun, L., Liu, S., & Yue, R. (2014). Excellent antimicrobial properties of silver-loaded mesoporous silica SBA-15. *Journal of Applied Microbiology, 116*(5), 1106-1118.

Wehling, J., Volkmann, E., Grieb, T., Rosenauer, A., Maas, M., Treccani, L., Rezwan, K. (2013). A critical study: Assessment of the effect of silica particles from 15 to 500 nm on bacterial viability. *Environmental Pollution, 176*, 292-299.

Weiss, J., Gaysinsky, S., Davidson, M., & McClements, D.J. (2009). Nanostructured encapsulation systems: food antimicrobials. *Global issues in food science and technology, 1*, 425-479.

Xia, X., Pethe, K., Kim, R., Ballell, L., Barros, D., Cechetto, J., Jeon, H., Kim, K., & Garcia-Bennett, A. E (2014). Encapsulation of anti-tuberculosis drugs within mesoporous silica and intracellular antibacterial activities. *Nanomaterials, 4*, 813-826.

Xue, J.M., & Shi, M. (2004). PLGA/mesoporous silica hybrid structure for controlled drug release. *Journal of Controlled Release, 98*(2), 209-217.

Zengin, N., Yüzbaşıoğlu, D., Ünal, F., Yılmaz, S., & Aksoy, H. (2011). The evaluation of the genotoxicity of two food preservatives: sodium benzoate and potassium benzoate. *Food and Chemical Toxicology, 49*(4), 763-769.

5.2. Bactericidal activity of caprylic acid entrapped in mesoporous silica nanoparticles

María Ruiz-Rico[a*], Cristina Fuentes[a], Édgar Pérez-Esteve[a], Ana I. Jiménez-Belenguer[b], Amparo Quiles[c], María D. Marcos[d,e], Ramón Martínez-Máñez[d,e], José M. Barat[a]

[a] Grupo de Investigación e Innovación Alimentaria. Departamento de Tecnología de Alimentos, Universitat Politècnica de València. Camino de Vera s/n, 46022, Valencia, Spain

[b] Departamento de Biotecnología, Universitat Politècnica de València. Camino de Vera s/n, 46022, Valencia, Spain

[c] Grupo de Microestructura y Química de Alimentos. Departamento de Tecnología de Alimentos, Universitat Politècnica de València. Camino de Vera s/n, 46022, Valencia, Spain

[d] Centro de Reconocimiento Molecular y Desarrollo Tecnológico (IDM), Unidad Mixta Universitat Politècnica de València – Universitat de València. Departamento de Química, Universitat Politècnica de València, Camino de Vera s/n, 46022, Valencia, Spain

[e] CIBER de Bioingeniería, Biomateriales y Nanomedicina (CIBER-BBN)

Abstract

Development of nanotechnologies to improve the functionality of natural antimicrobials for food applications has received much attention in recent years. Mesoporous silica particles, such as MCM-41, have been recently proposed as smart delivery devices capable of loading and releasing large amounts of cargo. In this study, the antimicrobial activity of caprylic acid entrapped in MCM-41 nanoparticles against *Escherichia coli*, *Salmonella enterica*, *Staphylococcus aureus* and *Listeria monocytogenes* was tested and compared with the bactericidal effect of free caprylic acid using the macrodilution method. The minimum bactericidal concentration for free caprylic acid was established to be below 18.5 mM for *S. aureus* and *L. monocytogenes* and within the 18.5–20 mM range for *E. coli* and *S. enterica*. Moreover, caprylic acid – loaded nanoparticles showed a total inhibition of the growth within the 18.5–20 mM range for the tested bacteria, and therefore the antimicrobial activity was preserved. Transmission electron microscopy images revealed that bacteria treatment with the caprylic acid-loaded nanoparticles generated disruption of cell envelope and leakage of cytoplasmic content, which resulted in cell death. We believe that caprylic acid encapsulation in nanoparticles MCM-41 can provide an effective system for potential applications in food safety in the food industry due to the possible controlled release of fatty acid and the masking of its unpleasant organoleptic properties.

Keywords: Caprylic acid-loaded nanoparticles; antimicrobial activity; minimum bactericidal concentration; encapsulation.

1. **Introduction**

   Antimicrobial agents are chemical compounds that are able to either inhibit the growth or inactivate pathogenic or spoilage microorganisms when present in or added to foods, food packaging, food contact surfaces or food processing environments (Weiss et al., 2009). Despite the effectiveness of these compounds, the continuous use of antimicrobials may result in the appearance of resistant strains (EFSA, 2013). Thus consumers are concerned about the safety of synthetic preservatives used in food. Consequently, demand for natural products or new administration forms that allow the concentrations of traditional antimicrobials to lower is increasing (Gyawali & Ibrahim, 2014; Weiss et al., 2009).

   In particular, natural antimicrobial agents have attracted much attention. However, the numbers of compounds allowed by regulations to be used in foods is very limited. Therefore it is necessary to make better use of available approved antimicrobial compounds and, for this reason, research has focused on developing technologies to help improve the functionality of food antimicrobials (Weiss et al., 2009).

   Among various natural antimicrobial compounds, lipids, such as fatty alcohols, free fatty acids (FFAs) and monoglycerides of fatty acids, are known to be potent antimicrobial agents against enveloped viruses, bacteria and fungi (Chang et al., 2010; Hirazawa et al., 2001). The antibacterial mechanisms of action of FFAs are still not completely understood, but the prime target seems to be the bacterial cell membrane via targeting various essential processes that occur within and on the membrane. In fact it is known that FFAs disrupt the electron transport chain and oxidative phosphorylation, inhibit enzyme activity, impair nutrient uptake, generate peroxidation and auto-oxidation degradation products, or directly lyse bacterial cells (Chang et al., 2010; Desbois and Smith, 2010; Hirazawa et al., 2001, Skrivanová et al., 2008; Solís de los Santos et al., 2010). In this context caprylic acid (CA), also known as octanoic acid, is an eight-carbon chain-length saturated FFA with reported antimicrobial activity. CA is found in the breast milk of various mammals and is a minor component of coconut oil and palm kernel oil (Chang et

al., 2010; Hirazawa et al., 2001; Jang & Rhee, 2009). It is a food-grade compound classified and generally recognized as safe (GRAS) by the U.S. Food and Drug Administration, and is also considered safe by the Joint FAO/WHO Expert Committee on Food Additives when used as flavor (JECFA, 2000). For instance the effectiveness of free CA against food-borne pathogens, *Escherichia coli*, *Listeria monocytogenes*, *Cronobacter* spp., and *Salmonella* spp. in food has been reported (Chang et al., 2010; Choi et al., 2013; Jang & Rhee, 2009; Nair et al., 2004; Vasudevan et al., 2005). Despite such evidence, the application or supplementation of food products with CA has disadvantages for its sensorial properties, such as an unpleasant rancid-like smell and taste (Hulankova et al., 2013), and diminished antimicrobial activity due to interactions with food constituents (Kabara et al., 1972). A suitable approach to address these problems can be the use of encapsulation supports which may allow FFAs to maintain their properties and increase stability against external agents. In fact nano-encapsulation has been reported to overcome some difficulties that emerge when applying antimicrobial compounds in their free form. Besides, reduction of particle size can improve delivery properties, solubility, residence time and absorption of bioactive compound through cells (Sozer & Kokini, 2009). Therefore, some problems such as complex mass transport phenomena, interaction with food constituents or alteration of functionality due to physical and chemical food processes (Weiss et al., 2009) can be prevented.

Current nanostructured encapsulation systems for food applications are based on nanoemulsions, microemulsions, solid-lipid nanoparticles, micelles and liposomes (Sozer & Kokini, 2009). One alternative to these nanostructured systems is mesoporous silica particles (MSPs). As supports for encapsulation and controlled release, MSPs such as MCM-n (Mobil Composition of Matter), exhibit unique features, such as high stability, biocompatibility, non-apparent toxicity, large load capacity and the possibility of including gate-like scaffoldings on the external surface (Al Shamsi et al., 2010; Aznar et al., 2009; Coll et al., 2013, Manzano & Vallet-Regí, 2010; Pérez-Esteve et al., 2014; Slowing et al., 2008; Suh

et al., 2009). Encapsulation of natural antimicrobial compounds in this type of particles has been recently reported (Park et al., 2012; Park & Pendleton, 2012), and it offers promising results as a delivery support.

The purpose of this study was to evaluate the antimicrobial activity of caprylic acid entrapped in mesoporous silica nanoparticles against some food-borne pathogens such as *E. coli*, *Salmonella enterica*, *Staphylococcus aureus* and *L. monocytogenes*, and to study the morphological changes produced in the bacteria treated with the MCM-41 CA-loaded nanoparticles.

2. Materials and methods

2.1. Chemicals

Tetraethylorthosilicate (TEOS), *N*-cetyltrimethylammonium bromide (CTABr), sodium hydroxide (NaOH) and caprylic acid (CA) were provided by Sigma (Sigma-Aldrich Química S.L., Madrid, Spain). N-hexane HPLC grade was supplied by Scharlau (Barcelona, Spain).

2.2. Mesoporous silica particles synthesis

Nanoparticulated MCM-41 particles were synthesized by following the procedure described by Bernardos et al. (2010). The molar ratio of the reagents was fixed at 1 TEOS:0.1 CTABr:0.27 NaOH:1000 H_2O. NaOH was added to the CTABr solution and the solution temperature was adjusted to 95 °C. TEOS was then added dropwise to the surfactant solution. The mixture was allowed to stir for 3 h to yield a white precipitate. After the synthesis the solid was recovered, washed with deionized water and air-dried at room temperature. The as-synthesized nanoparticles were calcined at 550 °C in an oxidant atmosphere for 5 h to remove the template phase (**N0**).

*2.3. Synthesis of **N1***

In a typical synthesis, 200 mg of free-template solid (**N0**) were suspended in a solution of 5.7 g of CA in 19 mL of n-hexane in a round-bottomed flask. The mixture was stirred for 24 h at room temperature to achieve maximum loading in the MCM-41 scaffolding pores. The loaded nanoparticles (**N1**) were isolated by vacuum filtration and dried at room temperature for 24 h.

2.4. Materials characterization

The starting MSP (**N0**) and CA-loaded MSP (**N1**) were characterized by standard techniques: transmission electron microscopy (TEM), particle size distribution (PSD) and zeta potential (ζ). For the TEM analysis, MSPs were dispersed in dichloromethane and sonicated for 2 min to preclude aggregates. The suspension was deposited onto copper grids coated with carbon film (Aname SL, Madrid, Spain). Imaging of the MSPs samples was done using a JEOL JEM-1010 (JEOL Europe SAS, France), operating at an acceleration voltage of 80 kV. Single particle size was estimated by averaging the measured size values of 50 particles. Microscopy studies were completed by determining the size distribution of the solids dispersed in Tryptic Soy Broth (TSB) by Dynamic Light Scattering (DLS). The measurements were conducted at 25 °C using a Malvern Zetasizer Nano ZS instrument (Malvern Instruments, UK). All measurements were performed in triplicate on previously sonicated highly dilute dispersions. The zeta potential of the different solids dispersed in TSB was measured in Zetasizer Nano ZS equipment (Malvern Instruments, UK). Samples were prepared at a concentration of 1 mg mL−1 and the measurement was taken at 20 °C. Before taking each measurement, samples were sonicated for 2 min to preclude aggregation. The zeta potential was calculated from the particle mobility values by applying the Smoluchowski model. The average of five recordings was reported as the zeta potential.

2.5. Caprylic acid release studies

The CA release studies of **N1** were performed to evaluate the release kinetics of CA from the solid and to determine the maximum amount of CA delivered by 1 mg of particle. In a typical experiment 10 mg of **N1** were placed in 10 mL of TSB in triplicate. The mixture was maintained under stirring at 4 °C, 20 °C or 37 °C for 5 h. At a given time (0.08, 0.25, 0.5, 0.75, 1.5, 2, 3 and 5 h), the suspensions were centrifuged to remove the solid, and the pH of the supernatant was brought down to the pH below the pK_a of the fatty acid (pK_a=4.9). In order to extract CA, 5 mL of n-hexane were added to the aqueous solution. After phase separation, the upper layer containing CA was removed and transferred to a fresh vial, and the extraction process was repeated 3 times. The organic phase was dried under a N_2 stream and solubilized with 8 mL of 5% (v/v) H_2SO_4/CH_3OH. The vial containing CA was incubated at 70 °C for 30 min. After cooling down the vial to room temperature, the reaction was quenched by adding 2 mL of water. The final extraction was conducted by adding 5 mL of n-hexane. The upper layer containing the CA methyl ester derivative was removed to a new vial for analysis.

2.6. Caprylic acid determination

CA concentration was determined by GC–MS according to the method described by Han et al. (2011), but with some modifications. GC–MS was done in a gas chromatography instrument (mod. 6890N, Agilent Technologies Ltd., CA, USA) with an autoinjector (mod. 7683B) coupled to a quadruple mass detector (mod. 5975). Gas chromatographic separation was carried out by injecting 1 µL of the samples into an HP-5 ms capillary column (30 m × 0.25 mm × 0.25 µm, Agilent J&W) in the splitless mode. Helium carrier gas was set at a constant flow rate of 1.0 mL min^{-1}. The optimized temperature programme was as follows: column temperature was held at 90 °C for 1 min; temperature rose from 90 °C to 219 °C at 15 °C min^{-1}, and was held at 219 °C for 2 min. Then the temperature rose from 219 °C to 290 °C at 25 °C min^{-1} and was held for 5 min. The injection temperature

was maintained at 280 °C. The ion source temperature was 200 °C, and the full scan mode was used within the 50–400 m z^{-1} range at 0.4 s/scan velocity.

2.7. Microbiological analysis

2.7.1. Culture media

Plate Count agar and TSB were used to grow bacteria and to prepare inoculums. Selective media were used for each studied microorganism to detect contamination during the study. Tryptone Bile x-glucuronide agar, Brilliant Green agar, Baird Parker agar base supplemented with sterile egg yolk tellurite emulsion, and Palcam agar base supplemented with polymyxin B, acriflavine and ceftazidime, were used to grow *E. coli*, *S. enterica*, *S. aureus* and *L. monocytogenes*, respectively.   All the media were provided by Scharlau (Barcelona, Spain).

2.7.2. Bacterial culture

The *E. coli* (CECT 1103), *S. enterica* (CECT 915), *S. aureus* (CECT 240) and *L. monocytogenes* (CECT 936) strains were obtained from the Colección Española de Cultivos Tipo (CECT) in Valencia (Spain). Bacterial stocks were stored at 4 °C in a solid medium before use. Bacteria cells were grown aerobically in TSB at 37 °C for 24 h.

2.7.3. Antimicrobial susceptibility assays of CA

The antimicrobial susceptibility of CA was studied using the macrodilution method of the Clinical and Laboratory Standards Institute (CLSI, 2007), but with some modifications. A wide range of concentrations of between 5 and 100 mM of CA, dispersed in nutrient broth, was tested according to previous references of FFA inhibitory activity (Bergsson et al., 2001; Chang et al., 2010; Nair et al., 2004;

Nobmann et al., 2009; Vasudevan et al., 2005). To achieve final concentrations in test tubes, different volumes of CA (between 8 and 158 µL) were added to 10 mL of TSB. Test tubes were inoculated with 10 µL of inoculum (Section 2.7.2) and incubated with orbital stirring (150 rpm) at 37 °C for 48 h. All the treatments were done in triplicate.

Bactericidal activity was quantified by preparing serial dilutions of the incubation mixtures and plating them on selective agar at 24 h and 48 h of incubation. Plates were incubated at 37 °C for 24 h (gram-negative) and 48 h (gram-positive microorganisms), and the colony-forming units per milliliter (CFUs mL^{-1}) were determined. These values were logarithmically transformed and expressed as log CFU mL^{-1}. Control positive values were used to quantify the growth inhibition of the diverse study conditions and to calculate the percentage of growth reduction.

2.7.4. Effect of the MCM-41 matrix on bacterial viability

The bacterial viability of microorganisms was tested with different concentrations of nanoparticles (**N0**) suspended in nutrient broth. These concentrations (1, 2.5, 5 and 10 mg mL^{-1}) fell within the range of the amount of loaded solid required to perform the antimicrobial susceptibility assays. To achieve the final particle concentrations, 0.04, 0.1, 0.2 and 0.4 mL of 250 mg mL^{-1} of particle stock suspension were added to 10 mL of TSB in test tubes. They were inoculated with 10 µL of inoculum (Section 2.7.2) and incubated with orbital stirring (150 rpm) at 37 °C for 24 h. All the treatments were done in triplicate. To determine bacterial viability, CFUs were counted by plating serial dilutions of bacterial suspensions on selective agar, followed by incubation at 37 °C for 24–48 h according to the studied microorganism.

*2.7.5. Antimicrobial susceptibility assays of the CA-loaded **N1***

The antimicrobial activity of the CA-loaded nanoparticles **N1** was tested using the CA concentrations of 15, 18.5, 20, 22.5 and 25 mM, established according to the preliminary test results (Section 2.7.3). The required amount of solids was calculated from the CA concentration actually released, determined by GC–MS (Sections 2.5 and 2.6) and the different concentrations of nanoparticles tested were 1.65, 2.04, 2.20, 2.48 and 2.75 mg mL^{-1} TSB. Test tubes were inoculated with 10 µL of inoculum (Section 2.7.2) and were incubated under orbital stirring (150 rpm) at 37 °C for 48 h. All the treatments were done in triplicate. To quantify bactericidal activity, serial dilutions of the incubation mixtures were plated on selective agar at 24 h and 48 h of incubation, followed by the appropriate incubation conditions explained above. CFUs were calculated, logarithmically transformed and expressed as log CFU mL^{-1}. Control positive values were used to quantify the percentage of growth reduction for the different test conditions.

In all the microbiological assays, a positive control (test tube containing inoculum and nutrient broth with neither CA nor MSPs) and a negative control (test tube containing CA or MSPs and nutrient broth without bacteria) were included. The positive control indicated the bacterial growth profile in the absence of an antimicrobial compound, while the negative control confirmed the absence of contamination of MSPs.

2.8. Detection of morphological changes in bacteria cells

To study the morphological changes in *L. monocytogenes* cells caused by **N1**, TEM was employed in this study. The TEM specimens were prepared by the following procedure: the cells treated by unloaded particles (**N0**) and CA-loaded nanoparticles (**N1**) were collected at the end of treatment by vacuum filtration (0.45 µm) performed under sterile conditions. Pellets were collected and fixed with 25 g L^{-1} glutaraldehyde solution for 24 h at 4 °C and post-fixed with 20 g L^{-1}

osmium tetroxide solution for 1.5 h. Cells were centrifuged and the pellet was collected after each step of the process.

After the above process ended, cells were stabilized by mixing them with a low gelling temperature agarose solution (3%, p/v) at 30 °C, which facilitates fixation and embedding prior to TEM observations (Ortuño et al., 2014). Next the cells inserted into solidified agar were cut into cubes (1 mm^3). These cubes were fixed with 25 g L^{-1} glutaldehyde solution, post-fixed with 20 g L^{-1} osmium tetroxide solution, dehydrated with 30 g L^{-1}, 50 g L^{-1}, 70 g L^{-1} ethanol and 100 g L^{-1}, contrasted with uranyl acetate solution (20 g L^{-1}) and embedded in epoxy resin (Durcupan, Sigma–Aldrich, St. Louis, MO, USA). The obtained blocks were cut using a Reichter-Jung ULTRACUT ultramicrotome (Leica Mycrosystems, Wetzlar, Germany). The obtained ultrathin sections (0.1 μm) were collected in copper grids and stained with 20 g L^{-1} acetate uranile and 40 g L^{-1} lead citrate to be observed under a Philips EM 400 Transmission Electronic Microscope (Eindhoven, Holland) at 80 kV.

2.9. Data analysis

Statistical data processing was performed with Statgraphics Centurion XVI (Statpoint Technologies, Inc., Warrenton, VA, USA). An analysis of variance (One-way ANOVA) was done to evaluate the effect of the CA concentration and exposure time on the reduction of the growth of the studied microorganisms. The LSD (least significant difference) procedure was utilized to test for differences between averages at the 5% significance level.

3. Results and discussion

3.1 Inhibitory activity of free caprylic acid

The antimicrobial activity of free CA was tested to establish the minimum bactericidal concentration (MBC) – the lowest concentration of a compound that gives rise to a reduction of 99.9% of the initial bacterial inoculum – of CA in a nutrient broth against different microorganisms. Fig. 1 shows the growth reduction (%) of the tested microorganisms in the presence of free CA concentrations between 5 and 100 mM after the 24-h incubation. The study was maintained to 48 h of incubation and no significant differences in the growth inhibition results were found (data not shown). As seen in Fig. 1A, *E. coli* growth was completely inhibited by free CA at a concentration that was equal to or higher than 20 mM. At non-bactericidal concentrations, reduced microorganism growth was observed in 23.012 ± 0.004% and 34.786 ± 0.006% for 18.5 mM and 15 mM, respectively. Microbial growth was not affected by the 12 mM and 5 mM concentrations. It was thus established that the MBC fell within the 18.5–20 mM range for this microorganism.

The established MBC for *E. coli*, in the presence of CA, in this study was lower than the values described by other authors. Nair et al. (2004) found that a 25 mM CA concentration led to a reduction of 2 logarithmic cycles of *E. coli* O157:H7 growth after incubation at 37 °C for 24 h, and total inhibition was achieved with a combination of low temperatures (4 °C and 8 °C) and CA 50 mM in a study of microbial inhibition in milk. Another study was performed with alfalfa seeds (Chang et al., 2010), in which a more marked reduction in *E. coli* was reported using an FFA concentration of 25 mM in 0.75 logarithmic cycles after 12 h of treatment.

The differences between our results and those reported by other authors might be due to the chosen bacterial strain, studied temperature and matrix effect. In food, the presence of certain molecules such as proteins can produce the formation of complexes with CA, which hampers CA in performing its

antimicrobial activity (Kabara et al., 1972). In such cases, higher antimicrobial doses are required to achieve the same effect on microbial growth.
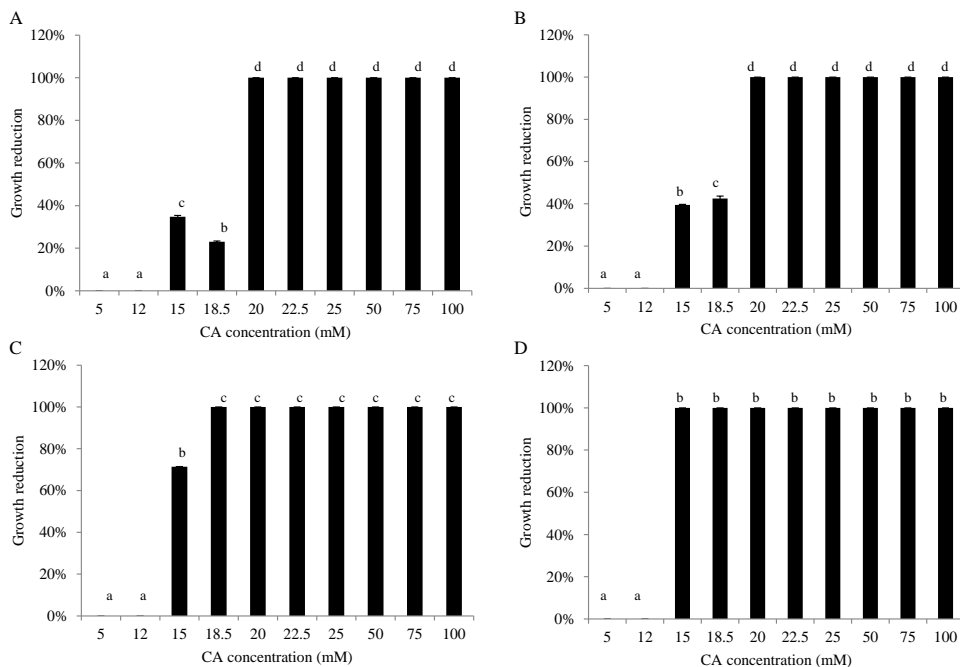
Figure 1. Reduction of microbial growth (%) of *E. coli* (A), *S. enterica* (B), *S. aureus* (C) and *L. monocytogenes* (D) with free CA at 24 h of treatment. The same letters in the bars indicate homogeneous group membership (p<0.05). (Means and standard deviations, n = 3).

CA affected *S. enterica* growth, with MBC falling within the same range as in the E. coli assays (18.5–20 mM), as shown in Fig. 1B. These MBC values are lower than other previously reported. In the study of Chang et al. (2010), *Salmonella* spp. populations on alfalfa seeds reduced to below 0.6 logarithmic cycles within 6 h of exposure to CA 75 mM, and maximum *Salmonella* spp. reductions of 1.28 and 2.3 logarithmic cycles were achieved at the 25 mM and the 50 mM CA

concentration, respectively. However, Choi et al. (2013) studied the antimicrobial activity of CA and other compounds against *S. enterica* serovar Typhimurium in reconstituted infant formula, and established that the microorganism was inactivated in the presence of CA 40 mM at 40 °C for 10 min. The differences between these results may be due to the above-mentioned effect of different variables. However, the study of Vasudevan et al. (2005), performed in a nutrient medium, found that the 50 mM CA concentration reduced *Salmonella* Enteritidis by approximately 5 log CFU mL^{-1} after a 1-min incubation and showed complete pathogen inactivation at 24 h.

As seen in Fig. 1C, the inhibition of *S. aureus* growth was greater than that of gram-negative bacteria. Different concentrations can be divided into three groups to show complete inhibition (18.5–100 mM), partial inhibition (15 mM) or no reduction (5–12 mM). The MBC of CA was lower than for *E. coli* and *S. enterica*, and fell within the 15–18.5 mM range. These results are similar to those obtained in the study of Bergsson et al. (2001), who used culture broth. In this study, the CA 10 mM concentration gave rise to a slightly inhibitory effect on *S. aureus* after a 10-min incubation at 37 °C.

L. monocytogenes was the microorganism that was most affected by free CA (Fig. 1D). Complete inhibition of bacteria occurred at concentrations between 15 and 100 mM, so the MBC would be between 12.5 mM and 15 mM. These results agree with the study of Nobmann et al. (2009), which established a minimum inhibitory concentration of 5 mM for *Listeria innocua* and of ≥5 mM for different *L. monocytogenes* strains after incubation for 18 h in nutrient broth at 35 °C. A study of antimicrobial susceptibility of CA in milk (Nair et al., 2004) reported only a reduction of 3 logarithmic cycles after a 24-h incubation at 37 °C using the CA 25 mM concentration.

Free CA proved more effective against gram-positive microorganisms as it reduced *L. monocytogenes* growth to below the limit of detection for a concentration of between 15 mM and 100 mM (MBC < 15 mM), and obtained an MBC within the 15–18.5 mM range for *S. aureus*. The MBC for the tested gram-

negative bacteria fell within a slightly higher range, with values between 18.5 mM and 20 mM. These results coincide with those of other studies, which showed that the antimicrobial activity of CA was greater against gram-positive bacteria (Nieman, 1954; Nobmann et al., 2009; Thormar et al., 1987) than against gram-negative microorganisms. These differences in microbial susceptibility can be attributed to differences in the structure and permeability of the bacterial cell membrane between gram-positive (thick layer of peptidoglycan) and gram-negative microorganisms (thick layer of peptidoglycan and outer membrane with lipopolysaccharides) (Hajipour et al., 2012; Nair et al., 2004).

The MBCs obtained for each microorganism were used to establish the range of concentrations in the study conducted with the CA-loaded MSPs.

3.2 Synthesis and characterization of the CA-loaded mesoporous support

In a first step of the work, the starting MCM-41 support was synthesized following well-known procedures using *N*-ctyltrimetylammonium (CTABr) as a structure director agent and tetraethylorthosilicate (TEOS) as a silica source. After removal the surfactant by calcination the starting MCM-41 support was obtained (**N0**). Then, the pores of the MCM-41 support were loaded with CA (**N1**).

3.2.1 Characterization of mesoporous silica particles

Solids **N0** and **N1** were characterized by standard techniques. The mesoporous structure of **N0** after calcination was clearly confirmed by TEM (see Fig. 2). From these studies it is as also observed that the size and morphology of the CA-loaded **N1** nanoparticles was very similar to that found for **N0** indicating that the loading process did not affected to the characteristics of the mesoporous support. Fig. 2 also shows the typical mesoporosity of the nanoparticles as alternate black and white stripes.
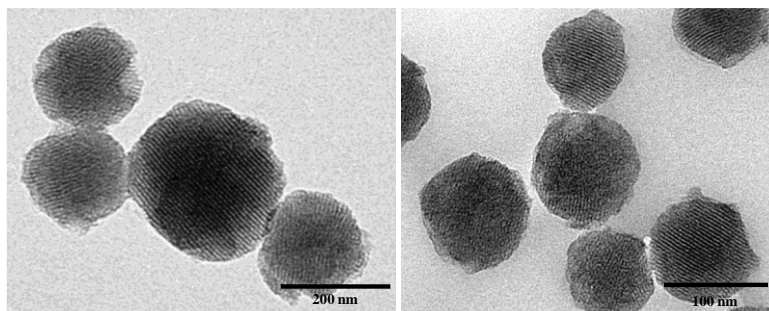
Figure 2. TEM images of inorganic MCM-41 nanoparticle calcined matrix **N0** (left) and CA-loaded support **N1** (right).

Besides porosity, the morphologic analysis with TEM allowed to calculate the size of nanoparticles (see Table 1). Moreover particles size was also determined by light diffraction studies (Table 1). In addition, Table 1 also displays the zeta potential determined for the **N0** and **N1** nanoparticles.

Table 1. Particle size of the different MCM-41 particles determined by TEM (dry) or Light Scattering (dispersed in TSB), and the zeta potential (Means and standard deviations).

Particle	Particle size (µm)		Zeta potential (mV)
	TEM	DLS	
N0	0.088 ± 0.013	0.154 ± 0.033	-17.05 ± 2.30
N1	0.114 ± 0.0183	0.156 ± 0.048	-14.68 ± 0.92

As Table 1 shows nanoparticles **N0** and **N1** exhibited sizes that fell within the range of ca. 100 nm, according to the TEM analysis. In contrast, when light scattering was used, size values of ca. 160 nm were found. This difference must be related with the different media used in both techniques; i.e. vacuum in TEM versus TSB for light scattering. This result suggested that there was some interaction between the nanoparticles and the TBS medium that resulted in a size

increment. This interaction may be explained if taking into account that the nanoparticles are negatively charged (see zeta potential values in Table 1) and that interaction with positively charged species in the TBS medium are highly probable. This is in agreement with studies of García-Saucedo et al. (2011). Interaction effects depend on the isoelectric point of particles, the charge and molecular structure of the organic compound, and the pH of dispersions.

3.2.2 Characterization of CA release

CA release kinetics were performed at 4 °C, 20 °C and 37 °C to check the effect of temperature on the release behavior of CA from **N1**. The release profile of CA from **N1** in a nutrient broth suspension at 37 °C is shown in Fig. 3. Progressive controlled delivery was produced during the first assay hours. The maximum release was achieved after 3 h. Moreover from the release studies we calculated that **N1** nanoparticles suspended in TSB are able to release 9.08 ± 0.24 mmol CA g^{-1} solid. This value was used later (*vide infra*) to calculate the required quantity of CA-loaded MSP (**N1** solid) to be dispersed in the nutrient broth to achieve the objective concentrations for the antimicrobial susceptibility assays described in Section 2.7.5. Results of release studies carried out at refrigeration (4 °C) and room temperature (20 °C) showed that content of CA released at refrigeration or room temperature was ca. 30% lower than CA released at 37 °C, meaning that temperature affects the release kinetics of the fatty acid. However, at these temperatures, the growth of the tested bacteria is limited. In general, the growth rate of the studied microorganisms is between 5 °C and 40 °C and that the growth rate is double for each 10 °C increase (McKinney, 2004). Thus, the antimicrobial activity of CA-loaded **N1** nanoparticles was checked at 37 °C in order to evaluate the effect of encapsulated CA on bacterial viability in the optimal growth conditions (see Section 3.4).
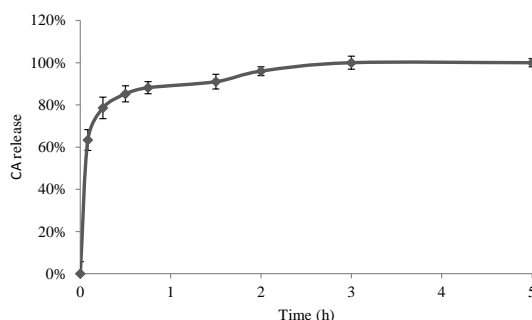
Figure 3. Release profile of CA from **N1** solid in TSB at 37 °C (Means and standard deviations, n=3).

3.3. Effect of the mesoporous silica matrix on bacterial viability

To test the effect of the mesoporous silica matrix on bacteria, the bacterial viability of the microorganisms was tested with nanoparticles (**N0**) at concentrations of 1–10 mg mL^{-1} suspended in nutrient broth. In all cases, the 100% survival of microorganisms, compared with the positive controls, indicated that the treatment with unloaded particles did not affect the microbial growth of any bacteria. These results are in accordance with the data obtained in the study performed by Wehling et al. (2013), which investigated the effect of silica particles on bacterial viability, whose size was between 15 and 500 nm. These authors established that particles displayed no inhibitory properties independently of their particle size. Besides bacterial viability assays, TEM images of the bacteria treated with **N0** were obtained (see Section 3.5). In these images, the treated bacteria did not show irreversible cell damaging, which means that the unloaded solid (**N0**) is innocuous itself under the tested conditions.

3.4 Antimicrobial activity of CA-loaded **N1** nanoparticles

According to the results obtained in Section 3.1, the range of concentrations in the antimicrobial assays of the CA-loaded **N1** was established to be 15–25 mM. The inhibitory effect of the CA-loaded **N1** nanoparticles against *E. coli*, *S. enterica*,

S. aureus and *L. monocytogenes* at 24 h and 48 h of incubation at 37 °C is shown in Fig. 4.

As Fig. 4A illustrates, *E. coli* growth was affected by **N1** solids at concentrations of between 20 mM and 25 mM, and total inhibition was accomplished. The non-bactericidal concentrations, 15 mM and 18.5 mM, were divided into two statistically different groups where the higher the concentration, the lower the growth of the microorganism. Thus the MBC of the N1 particles fell within the 18.5–20 mM range for this microorganism.
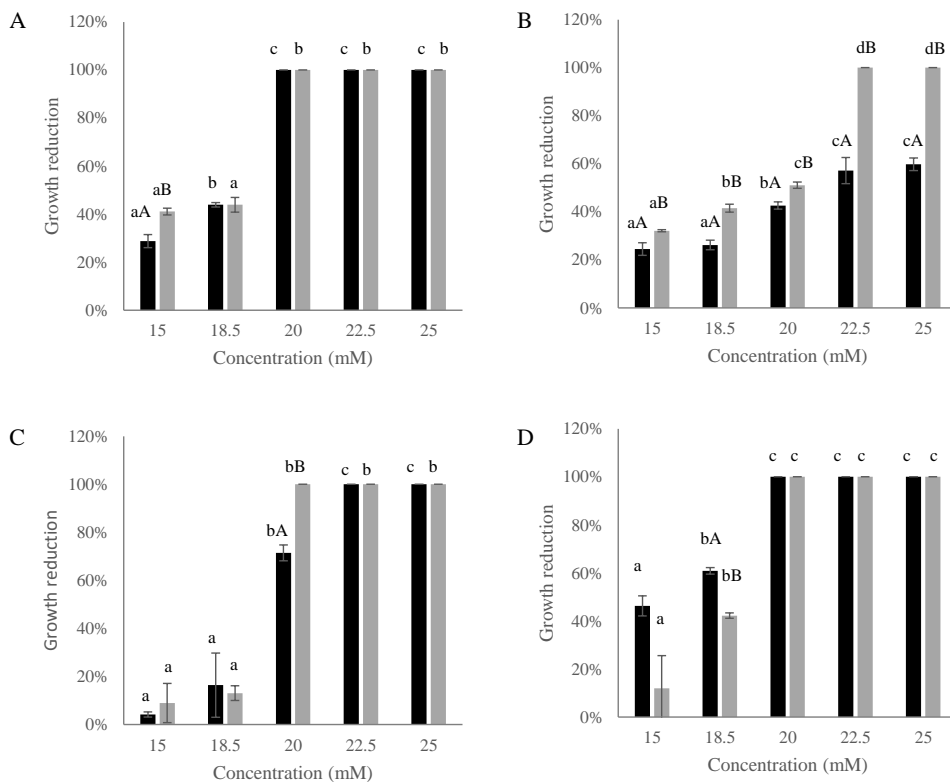

Figure 4. Reduction of microbial growth (%) of *E. coli* (A), *S. enterica* (B), *S. aureus* (C) and *L. monocytogenes* (D) with **N1** solids at 24 h (black) and 48 h (grey) of treatment. Different letters in the bars indicate statistically significant differences (p<0.05) from levels of

concentration (small letters) and exposure time (capital letters). (Means and standard deviations, n=3).

The loaded nanoparticles displayed a completely different behavior with *S. enterica* (Fig. 4B) if compared with other studied bacteria. None of the concentrations of the **N1** solids was bactericidal to *S. enterica* 24 h after incubation. In this case reductions of 59.81 ± 0.03% and 57.13 ± 0.05% were obtained at a concentration of 25 mM and 22.5 mM, respectively. At 48 h (grey bars), four statistically different groups of the concentration levels reached an MBC within the 20–22.5 mM range. These results indicate that the inhibitory effect of **N1** was slower for *S. enterica* than for the rest of microorganisms. Since free CA had a similar effect on *S. enterica* than on *E. coli*, it can be stated that both gram-negative bacteria have similar sensitivity to the bactericidal action of CA. Thus, the differences in the action of **N1** against this bacterium could only be related to different release kinetics of CA when *S. enterica* is in the media. Some previous workers have recently demonstrated that *Salmonella* spp. exhibits higher attachment and adhesion strength on surfaces than other similar strains such as *E. coli* (Abban et al., 2012; Zhang et al., 2014). This adhesion tendency could create aggregates among the aggregative fimbriae of the cells -responsible of the bacterial attachment- and the nanoparticles. The aggregates formed between the bacteria and the nanoparticles could hamper the release of the fatty acid, and as a consequence, to slow the microbial action of CA.

The counts of *S. aureus* (Fig. 4C) were completely inhibited by the loaded nanoparticles at the 22.5 mM and 25 mM concentrations and were slightly affected by the 15 mM and 18.5 mM concentrations. An MBC of 20–22.5 mM was calculated in this case. Significant differences were observed for treatment time levels at the 20 mM concentration, which resulted in an increased MBC within the 18.5–20 mM range at the 48 h incubation time.

The bactericidal effect of **N1** solids for *L. monocytogenes* (Fig. 4D) was 18.5–20 mM at different treatment times, and this result fell within the same range as the *E. coli* and *S. aureus* assays. Otherwise, lower concentrations further reduced

microbial growth at the incubation time of 24 h than at 48 h, and statistically differences were shown for this factor at the 18.5 mM concentration.

When comparing the effect of free CA and CA-loaded nanoparticles, it was stated that the antibacterial activity of the free and entrapped CA against *E. coli* growth fell within the same range (18.5–20 mM) for both conditions. However, free fatty acid more effectively reduced the population for *S. enterica*, *S. aureus* and *L. monocytogenes*. Despite the slight variances of antibacterial activity for free CA and CA-loaded nanoparticles, that may be related with particular differences in CA delivery from **N1** in the presence of the different bacteria, the results indicated that mesoporous silica nanoparticles are suitable reservoirs for CA encapsulation and control delivery for bactericidal applications.

Thus, the proposed system was able to maintain the antimicrobial activity despite the encapsulation. This property allows the incorporation of CA-loaded nanoparticles into matrices were the final flavor or taste is important (Hulankova et al., 2013) or into matrixes where CA could interact with food constituents dismissing its antimicrobial activity (Kabara et al., 1972). Moreover, the obtained results open the possibility to create gated mesoporous silica particles loaded with CA to be used in on-command delivery applications. The presence of silanol groups on the surface of the MSPs offers the possibility of functionalize their surface with organic molecules, generally called molecular gates, able to block or allow the release of the cargo under the presence of target stimuli. These molecular gates have been proposed by different authors to develop carriers for smart stimuli-responsive delivery in the gastrointestinal tract with response to biological stimuli such as pH or enzymes including amylases, proteases or gut microflora enzymes (Pérez-Esteve et al., 2015; Popat et al., 2014; Mas et al., 2013).

*3.5 Morphological changes in Listeria monocytogenes treated with unloaded (**N0**) and CA-loaded (**N1**) nanoparticles*

Fig. 5 depicts the TEM images of the typical rod-shaped morphology of untreated *L. monocytogenes* cells, showing the intracellular organization with a complete cytoplasm and inner material surrounded by an intact cell membrane and cell wall (Fig. 5A–B). The bacteria cells grown in the presence of unloaded nanoparticles (**N0**) are seen in Fig. 5C and D. In this case the cell wall and cell membrane appeared to be complete, but slightly modified, as the cytoplasm content inside cells showed empty regions. These cavities might be due to the aggregation or precipitation of internal cell components, or to the removal of part of the cytoplasmic content, which were seen outside the bacteria (Fig. 5D). Despite these changes, bacterial viability was not affected by the presence of nanoparticles at any of the tested concentrations (see Section 3.3) suggesting that bacteria could probably be able to repair cell damage and to maintain its viability. These results are in accordance with the conclusions drawn by Wehling et al. (2013), in which silica particles of different sizes (15, 50 and 500 nm) had no effect on the viability of diverse bacteria strains.

The TEM images of the cells treated with CA-loaded **N1** nanoparticles at the 25 mM concentration of fatty acid are included in Fig. 5E and F. **N1** treatment produced severe effects on the morphology of the bacteria and disrupted the cell envelope integrity, along with leakage of cellular contents. These observations are clearly in agreement with cell viability reduction described above.

According to several authors the mechanism of action of CA on bacteria cells is based on the alteration of the different essential processes occurring at the cell envelope (Bergsson et al., 2001, Chang et al., 2010 and Desbois and Smith, 2010), which results in microorganism inhibition. CA in particular, and FFAs in general, are known to create pores that may penetrate the cell membrane, this induces portions of the lipid bilayer to be released and disruption of membrane permeability takes place (Choi et al., 2013).
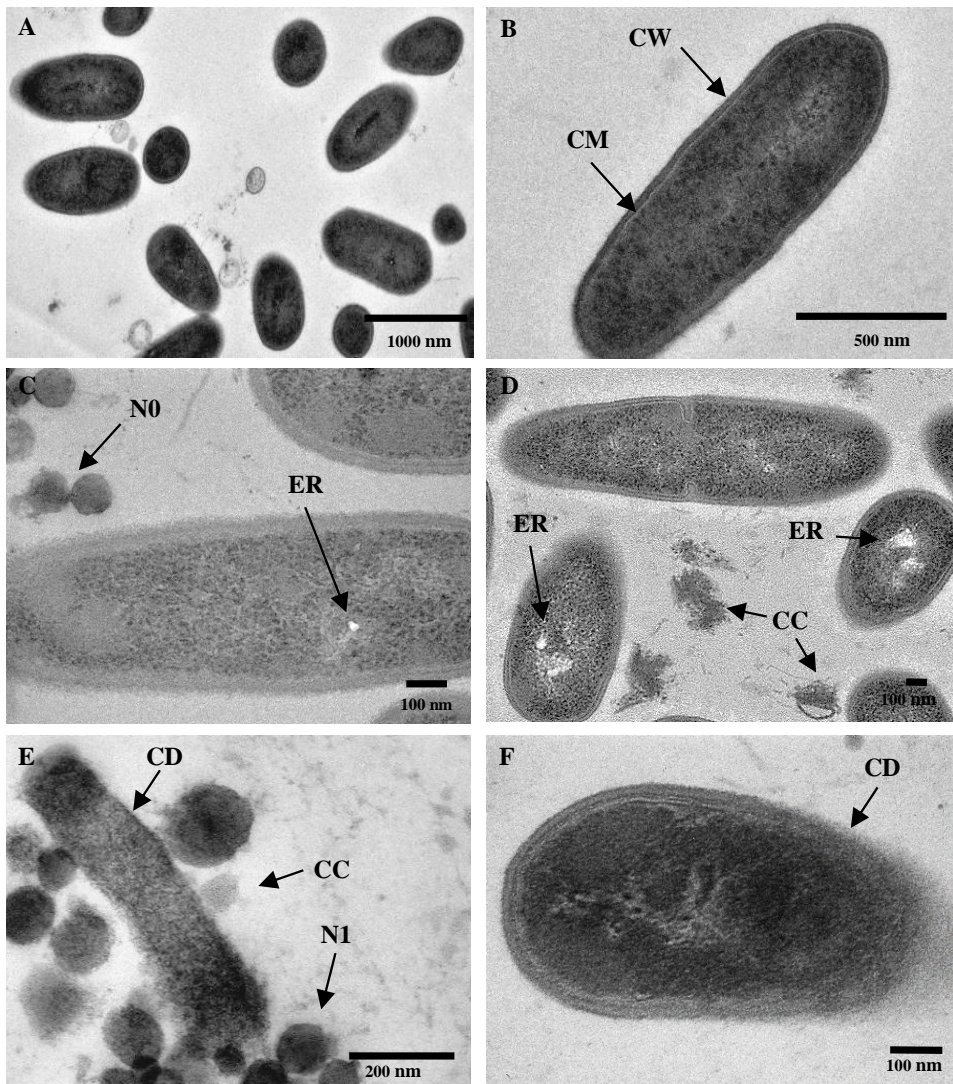
Figure 5. TEM micrographs by ultrathin sectioning of *L. monocytogenes*. Images A-B show untreated cells; images C-D show cells in the presence of nanoparticles **N0**; images E-F show cells treated with CA-loaded nanoparticles **N1**. CW: cell wall; CM: cell membrane; ER: empty regions; CC: cytoplasmic content; CD: cell wall and membrane damage.

4. Conclusions

In recent years, consumers demand natural products or new administration forms that allow the concentrations of traditional antimicrobials to lower to prevent bacterial resistance. This study has demonstrated the effectiveness of CA as an antimicrobial compound using a nano-encapsulated formulation based in the use of silica mesoporous supports. Free CA was more effective against gram-positive microorganisms and provided MBC values within the 12–15 mM range. For gram-negative bacteria free CA gave MBC values between 18.5 mM and 20 mM depending on the bacteria. This study has also shown the suitability of MSPs to entrap CA and to maintain its antimicrobial activity. In fact CA-loaded MSPs proved to be an appropriate support for CA encapsulation with MBC falling within the 18.5–20 mM range. TEM studies confirmed the inhibitory effect to be the result of cellular damage. The obtained results confirm the potential usefulness of CA entrapped in mesoporous supports to inhibit microbial growth with some added advantages such as the masking of the unpleasant flavor of the fatty acid, avoiding the interaction of the active principle with food matrix, or allowing the development of smart delivery system for the release of the antimicrobial compound in the site of action after incorporation of molecular gates in the supports. We believe that nano-encapsulation of FFAs may be an appealing option for the design of new bactericidal formulations that may found applications in some fields including the food industry.

References

Abban, S., Jakobsen, M., & Jespersen, L. (2012). Attachment behavior of *Escherichia coli* K12 and *Salmonella* Typhimurium P6 on food contact surfaces for food transportation. *Food microbiology, 31*(2), 139-147.

Al Shamsi, M., Al Samri, M.T., Al-Salam, S., Conca, W., Shaban, S., Benedict, S., Tariq, S., Biradar, A.V., Penefsky, H.S., Asefa, T., & Souid, A.K. (2010). Biocompatibility of calcined mesoporous silica particles with cellular bioenergetics in murine tissues. *Chemical Research in Toxicology, 23*, 1796-1805.

Aznar, E., Martínez-Máñez, R., & Sancenón, F. (2009). Controlled release using mesoporous materials containing gate-like scaffoldings. *Expert Opinion on Drug Delivery, 6*, 643-655

Bergsson, G., Arfinnson, J., Steingrinsson, O., & Thormar, H. (2001). Killing of Gram-positive cocci by fatty acids and monoglycerides. *APMIS Journal, 109*, 670-678.

Bernardos, A., Mondragón, L., Aznar, E., Marcos, M.D., Martínez-Máñez, R., Sancenón, F., Soto, J., Barat, J.M., Pérez-Payá, E., Guillem, C., & Amorós, P. (2010). Enzyme-responsive intracellular controlled release using nanometric silica mesoporous supports capped with 'saccharides'. *ACS nano, 4*(11), 6353-6368.

CLSI (2007). Performance standards for antimicrobial susceptibility testing; seventeenth informational supplement. *Clinical and Laboratory Standards Institute*, M100-S17, 27 (1).

Chang, S., Redondo-Solano, M., & Thippareddi, H. (2010). Inactivation of *Escherichia coli* O157:H7 and *Salmonella* spp. on alfalfa seeds by caprylic acid and monocaprylin. *International Journal of Food Microbiology, 144*, 141-146.

Choi, M.J., Kim, S.A., Lee, N.Y., & Rhee, M.S. (2013). New decontamination method based on caprylic acid in combination with citric acid or vanillin for eliminating *Cronobacter sakazakii* and *Salmonella enterica* serovar Typhimurium in reconstituted infant formula. *International Journal of Food Microbiology, 166*, 499-507.

Coll, C., Bernardos, A., Martínez-Máñez, R., & Sancenón F. (2013). Gated silica mesoporous supports for controlled release and signaling applications. *Accounts of Chemical Research, 46*, 339-349.

Desbois, A.P., & Smith, V.J. (2010). Antibacterial free fatty acids: activities, mechanisms of action and biotechnological potential. *Applied Microbiology and Biotechnology, 85*, 1629-1642.

EFSA (2013). The European Union Summary Report on antimicrobial resistance in zoonotic and indicator bacteria from humans, animals and food in 2011. *EFSA Journal, 11*(5), 3196-3359. (http://www.efsa.europa.eu/en/efsajournal/pub/3196.htm). [30/06/2014]

García-Saucedo, C., Field, J. A., Otero-Gonzalez, L., & Sierra-Álvarez, R. (2011). Low toxicity of HfO_2, SiO_2, Al_2O_3 and CeO_2 nanoparticles to the yeast, *Saccharomyces cerevisiae*. *Journal of Hazardous Materials, 192*(3), 1572-1579.

Gyawali, R., & Ibrahim, S.A. (2014). Natural products as antimicrobial agents. *Food Control, 46*, 412-429.

Hajipour, M.J., Fromm, K.M., Ashkarran, A.A., Jimenez de Aberasturi, D., Ruiz de Larramendi, I., Rojo, T., Serpooshan, V., Parak, W.J., & Mahmoudi, M. (2012). Antibacterial properties of nanoparticles. *Trends in Biotechnology, 30*(10), 499-511.

Han, L.D., Xia, J.F., Liang, Q.L., Wang, Y., Wang, Y.M., Hu, P., Li, P., & Luo, G.A. (2011). Plasma esterified and non-esterified fatty acids metabolic profiling using gas chromatography-mass

spectrometry and its application in the study of diabetic mellitus and diabetic nephropathy. *Analytica Chimica Acta, 689*(1), 85-91.

Hirazawa, N., Oshima, S., & Hata, K. (2001a). *In vitro* assessment of the antiparasitic effect of caprylic acid against several fish parasites. *Aquaculture, 200,* 251-258.

Hirazawa, N., Oshima, S., Hara, T., Mitsuboshi, T., & Hata, K. (2001b). Antiparasitic effect of medium-chain fatty acids against the ciliate *Cryptocaryon irritans* infestation in the red sea bream *Pagrus major*. *Aquaculture, 198*, 219-228.

Hulankova, R., Borilova, G., & Steinhauserova, I. (2013). Combined antimicrobial effect of oregano essential oil and caprylic acid in minced beef. *Meat Science, 95,* 190-194.

Jang, H.I., & Rhee, M.S. (2009). Inhibitory effect of caprylic acid and mild heat on Cronobacter spp. (*Enterobacter sakazakii*) in reconstituted infant formula and determination of injury by flow cytometry. *International Journal of Food Microbiology, 133*, 113-120.

JECFA (Joint FAO & WHO Expert Committee on Food Additives) (2000). Evaluation of certain food additives and contaminants. *World Health Organization technical report series 896*, 1.

Kabara, J.J., Swieczkowski, D.M., Conley, A.J., & Truant, J.P. (1972). Fatty acids and derivatives as antimicrobial agents. *Antimicrobial Agents Chemotherapy, 2*(1), 23-28.

Manzano, M., & Vallet-Regí, M. (2010). New developments in ordered mesoporous materials for drug delivery. *Journal of Materials Chemistry, 20*, 5593-5604.

Mas, N., Agostini, A., Mondragón, L., Bernardos, A., Sancenón, F., Marcos, M.D., Martínez-Máñez, R., Costero, A.M., Gil, S., Merino-Sanjuán, M., Amorós, P., Orzáez, M., & Pérez-Payá, E. (2013). Enzyme-Responsive Silica Mesoporous Supports Capped with Azopyridinium Salts for Controlled Delivery Applications. *Chemistry-A European Journal, 19*(4), 1346-1356.

McKinney R.E. (2004). *Environmental pollution control microbiology: a fifty-year perspective*. CRC Press.

Nair, M.K.M., Vasudevan, P., Hoagland, T., & Venkitanarayanan, K. (2004). Inactivation of *Escherichia coli* O157:H7 and *Listeria monocytogenes* in milk by caprylic acid and monocaprylin. *Food Microbiology, 21*, 611-616.

Nieman, C. (1954). Influence of trace amounts of fatty acids on the growth of microorganisms. *Bacteriological Reviews, 18*(2), 147-163.

Nobmann, P, Smith, A., Dunne, J., Henehan, G., & Bourke, P. (2009). The antimicrobial efficacy and structure activity relationship of novel carbohydrate fatty acid derivatives against *Listeria* spp. and food spoilage microorganisms. *International Journal of Food Microbiology, 128*, 440-445.

Ortuño, C., Quiles, A., & Benedito, J. (2014). Inactivation kinetics and cell morphology of *E. coli* and *S. cerevisiae* treated with ultrasound-assisted supercritical CO_2. *Food Research International, 62*, 955-964.

Park, S.Y., & Pendleton, P. (2012). Controlled release of allyl isothiocyanate for bacteria growth management. *Food control, 23*, 478-484.

Park, S.Y., Barton, M., & Pendleton, P. (2012). Mesoporous silica SBA-15 for natural antimicrobial delivery. *Powder Technology, 223*, 77-82.

Pérez-Esteve, E., Oliver, L., García, L., Nieuwland, M., de Jongh, H. H., Martínez-Máñez, R., & Barat, J. M. (2014). Incorporation of Mesoporous Silica Particles in Gelatine Gels: Effect of Particle Type and Surface Modification on Physical Properties. *Langmuir, 30*, 6970-6979.

Pérez-Esteve, E., Fuentes, A., Coll, C., Acosta, C., Bernardos, A., Amorós, P., Marcos, M.D., Sancenón, F., Martínez-Máñez, R., & Barat, J.M. (2015). Modulation of folic acid bioaccessibility by encapsulation in pH-responsive gated mesoporous silica particles. *Microporous and Mesoporous Materials, 202*, 124-132.

Popat, A., Jambhrunkar, S., Zhang, J., Yang, J., Zhang, H., Meka, A., & Yu, C. (2014). Programmable drug release using bioresponsive mesoporous silica nanoparticles for site-specific oral drug delivery. *Chemical Communications, 50*(42), 5547-5550.

Skrivanová, E., Molatová, Z., & Marounek, M. (2008). Effects of caprylic acid and triacylglycerols of both caprylic and capric acid in rabbits experimentally infected with enteropathogenic *Escherichia coli* O103. *Veterinary Microbiology, 126*, 372-376.

Slowing, I.I., Vivero-Escoto, J.L., Wu, C.W., & Lin, V.S.Y. (2008). Mesoporous silica nanoparticles as controlled release drug delivery and gene transfection carriers. *Advanced Drug Delivery Reviews, 60*, 1278-1288.

Solís de los Santos, F., Hume, M., Venkitanarayanan, K., Donoghue, A.M., Hanning, I., Slavik, M.F., Aguiar, V.F., Metcalf, J.H., Reyes-Herrera, I., Blore, P.J., & Donoghue, D.J. (2010). Caprylic acid reduces enteric campylobacter colonization in market-aged broiler chickens but does not appear to alter cecal microbial populations. *Journal of Food Protection, 73*(2), 251-257.

Sozer, N., & Kokini, J.L. (2009). Nanotechnology and its applications in the food sector. *Trends in Biotechnology, 27*(2), 82-89.

Suh, W.H., Suslick, K.S., Stucky, G.D., & Suh, Y.H. (2009). Nanotechnology, nanotoxicology and neuroscience. *Progress in Neurobiology, 87*, 133-170.

Thormar, H., Isaacs, C.E., Brown, H.R., Barshatzky, M.R., & Pessolano, T. (1987). Inactivation of enveloped viruses and killing cells by fatty acids and monoglycerides. *Antimicrobial Agents and Chemoterapy, 31*, 27-31.

Vasudevan, P., Marek, P., Nair, M.K.M., Annamalai, T., Darre, M., Khan, M., & Venkitanarayanan, K. (2005). *In Vitro* Inactivation of *Salmonella* Enteritidis in Autoclaved Chicken Cecal Contents by Caprylic acid. *Poultry Science Association, 14*(1), 122-125.

Wehling, J., Volkmann, E., Grieb, T., Rosenauer, A., Maas, M., Treccani, L., & Rezwan, K. (2013). A critical study: Assessment of the effect of silica particles from 15 to 500 nm on bacterial viability. *Environmental Pollution, 176*, 292-299.

Weiss, J., Gaysinsky, S., Davidson, M., & McClements, J. (2009). Nanostructured encapsulation systems: food antimicrobials. *In IUFoST world congress book: Global issues in food science and technology*, 425-479.

Zhang, M., Yang, F., Pasupuleti, S., Oh, J.K., Kohli, N., Lee, I.S., Perez, K., Verkhoturov, S.V., Schweikert, E.A., Jayaraman, A., Cisneros-Zevallos, L. & Akbulut, M. (2014). Preventing adhesion of *Escherichia coli* O157: H7 and *Salmonella* Typhimurium LT2 on tomato surfaces via ultrathin polyethylene glycol film. *International Journal of Food Microbiology, 185*, 73-81.

5.3. Towards the development of powerful antimicrobial "nanobullets" based on functionalized mesoporous silica particles

María Ruiz-Rico[a*], Édgar Pérez-Esteve[a], Cristina de la Torre[b,c], Ana I. Jiménez-Belenguer[d], Amparo Quiles[e], María D. Marcos[b,c], Ramón Martínez-Máñez[b,c], José M. Barat[a]

[a] Grupo de Investigación e Innovación Alimentaria. Departamento de Tecnología de Alimentos, Universitat Politècnica de València. Camino de Vera s/n, 46022, Valencia, Spain

[b] Instituto Interuniversitario de Investigación de Reconocimiento Molecular y Desarrollo Tecnológico (IDM), Unidad Mixta Universitat Politècnica de València – Universitat de València. Departamento de Química, Universitat Politècnica de València, Camino de Vera s/n, 46022, Valencia, Spain

[c] CIBER de Bioingeniería, Biomateriales y Nanomedicina (CIBER-BBN)

[d] Departamento de Biotecnología, Universitat Politècnica de València. Camino de Vera s/n, 46022, Valencia, Spain

[e] Grupo de Microestructura y Química de Alimentos. Departamento de Tecnología de Alimentos, Universitat Politècnica de València. Camino de Vera s/n, 46022, Valencia, Spain

Abstract

The treatment of bacterial infections by using new agents is a current strategy to manage the antibiotic resistance crisis. In the search of a new generation of antimicrobials, nanotechnology has an important role to play. In the present work we demonstrate the capability of silica nanoparticles to concentrate organic molecules on their large surface and to act as an antimicrobial "nanobullets". The developed antimicrobial device consist of MSNs functionalized with polyamines, which confer particles a highly positively charged surface due to protonation of amines in aqueous environments, being able to disrupt the bacterial cell wall. Surface concentration of organic groups is so effective that amine-functionalized MSNs were 100 times more effective in killing *Listeria monocytogenes* bacteria than free polyamines. This novel approach for the creation of antimicrobial nanodevices opens the possibility to put in value the antimicrobial power of natural molecules that have been discarded because of its low antimicrobial power.

Keywords: amine corona; bactericidal activity; *Listeria monocytogenes*; mesoporous silica nanoparticles; surface functionalization.

1. Introduction

Bacterial infection is one of the most serious in the development of foodborne illnesses and thus in global public health. To fight against pathogen and alterative microflora, an indiscriminate use of pesticides, food preservatives and antibiotics have been used in recent years, yielding as a consequence the apparition of a growing number of resistant strains (Capeletti et al., 2014). In this scenario, the development of novel antibacterial systems as an alternative to classical antibiotics is an urgent need, and nanotechnology, the manipulation of matter at an atomic and molecular level, is viewed as an excellent opportunity to achieve it.

While some natural antibacterial materials, such as zinc and silver owe their antimicrobial power to their capacity to generate reactive oxygen species (ROS) species able to interact with bacteria cell membrane, other such as TiO_2 and ZnO owe it to the size reduction which increases the surface per volume ratio or a given mass of particle modifying the mechanism by which the nanoparticle or the nanostructured material interacts with the bacteria (Dizaj et al., 2014; Huh & Kwon, 2011; Seil & Webster, 2012). In this manner, not only nanoparticles, but also nanostructured systems seem to have a potential use in the preparation of a new generation of antimicrobial agents.

Ones of the most explored nanostructured systems in the search of new antimicrobial systems are mesoporous silica nanoparticles (MSNs). MSNs are characterized by exhibiting a high stability, large specific surface area and volume, controllable size, easy surface functionalization, high biocompatibility and poorer hemolytic activity than their non-porous counterparts (Al Shamsi et al., 2010; Aznar et al., 2016; Botequim et al., 2012; Pérez-Esteve et al., 2014; Slowing et al., 2008; Tang et al., 2012; Zhao et al., 2011). Due to these properties some authors have reported the use of loaded and/or functionalized MSNs as antibacterial agents. Molina-Manso et al. (2012) used SBA-15 to encapsulate three different antimicrobial agents: vancomycin, rifampicin and linezolid. Park and coauthors encapsulated allyl isothiocyanate in a mesoporous silica particle reaching a bacteria growth management (Park et al., 2012). Bernardos et al. (2015) used

MCM-41 to encapsulate essential oils, achieving an important growth reduction of *Aspergillus niger* in comparison with non-encapsulated essential oils. More recently, Yu and coauthors described the use of poly(N-isopropylacrylamide)-gated Fe_3O_4-MSNs core shell nanoparticles for the temperature-triggered release of antibacterial enzyme lysozyme (Yu et al., 2015) and we stated the antimicrobial effect of caprylic acid incorporated in MSNs (Ruiz-Rico et al., 2015). Following an alternative approach, Li & Wang (2013) reported the use of lysozyme-coated MSNs as antibacterial agents, and Qi et al. (2013) used vancomycin-modified MSNs to kill pathogenic gram-positive bacteria. The same year, some of us reported the use of MCM-41 nanoparticles capped with ε-poly-l-lysine with high antibacterial activity against Gram-negative bacteria demonstrating the possibility of improving the antimicrobial effect of a molecule by functionalization on the surface of a suitable support (Mas et al., 2013).

Delving into this line, the goal of this work was to evaluate the effect of the concentration of the active groups provided by a really low effective antimicrobial molecule by means of their anchoring on the surface of a MSN on the antimicrobial activity against two of the most distributed food-borne pathogens; i.e. *Listeria monocytogenes* and *Escherichia coli*.

2. Materials and methods

2.1. Chemicals

Tetraethylorthosilicate (TEOS), *N*-cetyltrimethylammonium bromide (CTABr), sodium hydroxide (NaOH), *N*-(3-trimethoxysilylpropyl)diethylenetriamine (N3) and diethylenetriamine were provided by Sigma (Sigma-Aldrich, Madrid, Spain). *N*-3-(trimethoxysilyl)propyl ethylenediamine triacetic acid trisodium salt (C3) was provided by Fluorochem (Hadfield, UK).

2.2. *Mesoporous silica nanoparticles synthesis*

Nanoparticulated MCM-41 particles were synthesized by the procedure described by Ruiz-Rico et al. (2015). The molar ratio of the reagents was fixed at 1 TEOS:0.1 CTABr:0.27 NaOH:1000 H_2O. NaOH was added to the CTABr solution, and the solution temperature was adjusted to 95 °C. TEOS was then added dropwise to the surfactant solution. The mixture was allowed to stir for 3 h and yield a white precipitate. After synthesis, the solid was recovered by centrifugation, washed with distilled water, and air-dried at room temperature. The as-synthesized solid was calcined at 550 °C in an oxidant atmosphere for 5 h to remove the template phase.

2.3. *Functionalization of mesoporous silica nanoparticles*

The surfaces of bare nanoparticles were functionalized with *N*-(3-trimethoxysilylpropyl) diethylenetriamine (N3) or with *N*-[3-(trimethoxysilyl)propyl]ethylenediamine triacetic acid trisodium salt (C3) following a similar procedure to that described by Pérez-Esteve et al. (2014). To obtain amine-functionalized particles (**N3-N**), 1 g of MSNs was suspended in 40 mL of acetonitrile, and excess N3 (4.3 mL, 15.0 mmol/g) was added. To obtain carboxylate-functionalized particles (**C3-N**), 1 g of MSNs was suspended in 30 mL of water, and excess C3 (5.5 mL, 15.0 mmol/g) was added. Final mixtures were stirred for 5.5 h at room temperature. Finally, solids were filtered, washed with 30 mL of distilled water and dried at room temperature.

2.4. *Materials characterization*

Synthesized materials were characterized by standard techniques: transmission electron microscopy (TEM), field emission scanning electron microscopy (FESEM), particle size distribution, zeta potential and thermogravimetric analysis. TEM images were taken by a Philips CM10 (Philips

electronics, Eindhoven, The Netherlands), which operated at an acceleration voltage of 80 kV. FESEM images were acquired with a Zeiss Ultra 55 (Carl Zeiss NTS GmbH, Oberkochen, Germany) and observed in the secondary electron mode. The particle size distribution of the different MSNs was determined by Zetasizer Nano ZS instrument (Malvern Instruments, UK). For measurements, solids were dispersed in Ringer buffer (RB) (0.22% NaCl, 0.011% KCl, 0.012% $CaCl_2$ and 0.005% $NaHCO_3$ in distilled water). All the measurements were taken in triplicate on previously sonicated highly dilute dispersions. To determine the zeta potential of the bare and functionalized MSNs, a Zetasizer Nano ZS (Malvern Instruments, UK) was used. Samples were dispersed in RB at the 1 mg/mL concentration and were sonicated for 2 min to preclude aggregation. The zeta potential was calculated from the particle mobility values by applying the Smoluchowski model. The average of five recordings was reported as the zeta potential. The degree of functionalization of the different particles was determined by thermogravimetric analyses. Determinations were made on a TGA/SDTA 851e Mettler Toledo balance (Mettler Toledo Inc., Schwarzenbach, Switzerland), with a heating program that consisted in a heating ramp of 10 °C per minute from 273 to 373 K followed by an isothermal heating step at this temperature for 60 min in a nitrogen atmosphere (80 mL/min). Then, the program was allowed to continue with a dynamic heating segment from 373 to 1273 K in an oxidant atmosphere (air, 80 mL/min) and with an isothermal heating step at this temperature for 30 min.

2.5. Microbiological assays

Plate Count Agar (PCA) and Tryptic Soy Broth (TSB) were used to grow bacteria and to prepare inoculums. TSB and RB were used in the bacterial viability assays. Selective medium, Palcam Agar supplemented with polymyxin B, acriflavine and ceftazidime, and Tryptone Bile x-glucuronide (TBX) agar were used to grow the treated *Listeria monocytogenes* and *Escherichia coli*, respectively. All the media were provided by Scharlau (Barcelona, Spain).

L. monocytogenes (CECT 936) and *E. coli* (CECT 433) strains were obtained from the Colección Española de Cultivos Tipo (CECT; Valencia, Spain). Bacterial stocks were stored at 4 °C in PCA before use. Bacterial cells were grown aerobically in TSB at 37 °C for 24 h to obtain a cell concentration of approximately 1×10^8 cells/mL. For the assays in RB, the inoculum was centrifuged at 4,000 rpm for 5 min and the obtained bacteria pellet was resuspended in the buffer.

2.6. Viability assessment

The study of the influence of bare and functionalized MSNs on the viability of *L. monocytogenes* was tested within a range of concentrations between 0 and 0.15 mg of solid per mL of Ringer buffer. Otherwise, the 0-10 mg/mL range of the bare and functionalized MSNs was investigated for *E. coli*. In parallel, the influence of free amines (diethylenetriamine) was tested with a range of concentrations, which arranged from 0 to 3 mg/mL. Ringer buffer was used to ensure that the surface charge of particles was not influenced by the components of the solvent. All the treatments were set in triplicate. Positive and negative controls were included in all the assays.

Particle stock suspensions were prepared in RB and were sonicated in 3 cycles of 5 minutes to facilitate the suspension and preclude agglomerates. To achieve the final concentrations of particles, different volumes of particle suspension were added to 30 mL of RB in Erlenmeyer flasks. Finally, flasks were inoculated with 10 µL (*E. coli*) or 100 µL (*L. monocytogenes*) of washed inoculum and were incubated under orbital stirring (150 rpm) at 37 °C. Bacterial viability was quantified by preparing serial dilutions of the incubation mixtures and plating them on selective agar at 2 h of incubation. Plates were incubated at 37 °C for 24-48 h, and then the CFUs per milliliter were determined. These values were logarithmically transformed and expressed as $\log_{10}$ CFU/mL. The control positive values were used to quantify growth of microorganisms and to calculate the survival percentage of bacteria.

2.7. Detection of morphological changes in bacterial cells

To study the morphological changes in *L. monocytogenes* cells caused by MSNs treatment, TEM observations were made. The cells treated with bare and functionalized MSNs were collected at the end of the treatment by vacuum filtration (0.45 µm) under sterile conditions. Pellets were collected and fixed with 25 g/L glutaraldehyde solution for 24 h at 4 °C and were post-fixed with 20 g/L osmium tetroxide solution for 1.5 h. Cells were centrifuged and the pellet was collected after each process step.

After this process, cells were stabilized by mixing them with a low gelling temperature agarose solution (3%, p/v) at 30 °C, which facilitates fixation and embedding prior to TEM observation (Ortuño et al., 2014). Next the cells inserted in the solidified agar were cut into cubes (1 mm^3). These cubes were fixed with 25 g/L glutaraldehyde solution, post-fixed with 20 g/L osmium tetroxidesolution, dehydrated with 30 g/L, 50 g/L, 70 g/L ethanol and 100 g/L, contrasted with uranyl acetate solution (20 g/L) and embedded in epoxy resin (Durcupan, Sigma–Aldrich, St. Louis, MO, USA). The obtained blocks were cut by a Reichter-Jung ULTRACUT ultramicrotome (Leica Mycrosystems, Wetzlar, Germany). The obtained ultrathin sections (0.1 µm) were collected in copper grids and stained with 20 g/L acetate uranile and 40 g/L lead citrate to be observed in a JEOL JEM 2100F (JEOL Europe SAS, Croissy-sur-Seine, France) at 200 kV.

2.8. Determination of bacterial viability and agglomeration by fluorescence assay

A two-color fluorescent assay, LIVE/DEAD® BacLightTM (Life Technologies, Gaithersburg, MD, USA), was used to visualize viable and dead *L. monocytogenes* cells, according to Wheling et al. (2013). The kit provides a two-color assay of bacterial viability. SYTO 9 (green-fluorescent nucleic acid stain) labels all bacteria, with either intact or damaged membranes. In contrast, propidium iodide (red-fluorescent nucleic acid stain) penetrates only the bacteria with damaged

membranes, which causes a reduction in SYTO 9 stain fluorescence when both dyes are present.

The two provided dye components were mixed at a 1:1 ratio. Next 0.8 µL of SYTO 9/propidium iodide were added to 500 µL of the treated suspension, and were mixed and incubated for 10 min to facilitate the penetration of dyes. Then, 5 µL of stained bacteria were applied to poly-L-lysine-covered slides for immunofluorescence (Sigma-Aldrich, Madrid, Spain), and a coverslip was placed over the suspension and sealed. The preparation was incubated for 5-10 min at room temperature in the dark to allow bacteria to adhere to slides. Slides were then observed under an Olympus BX50 fluorescence microscope equipped with an Olympus DP71 camera and a BA515IF barrier filter.

2.9. WST-1 Cell viability assays

For the cell culture experiments, trypan blue solution (0.4%) cell culture grade and dimethyl sulfoxide (DMSO), phosphate buffered saline (PBS) and Dulbecco's Modified Eagle's medium (DMEM) with glucose, L-glutamine and pyruvate for cell culture were provided by Sigma-Aldrich (Poole, Dorset, UK). Mc Coy's 5a Medium and Keratinocyte Serum Free Medium, Fetal Bovine Serum (FBS) and trypsin were purchased from Gibco (Life Technologies, Madrid, Spain). Cell proliferation reagent WST-1 was purchased from Roche Applied Science (Barcelona, Spain).

HeLa human cervix adenocarcinoma and HEPG2 human liver carcinoma were grown in DMEM supplemented with 10% FBS. HCT116 human colon carcinoma cells were grown in McCoy's 5a Medium Modified supplemented with 10% FBS, HK2 homo sapiens kidney papilloma cells were grown in Keratinocyte Serum Free Medium supplemented with bovine pituitary extract and human recombinant epidermal growth factor. All these cells were purchased from the German Resource Centre for Biological Materials (DSMZ). Cells were maintained at 37 °C in an atmosphere of 5% carbon dioxide and 95% air and underwent passage twice a week.

Cells were placed in 96-well plates at a density of 1,000 cells per well. After 24 h, plates were incubated with the amine-functionalized MSNs or an equivalent amount of free polyamine at different concentrations at 37 °C for 24 h. After removing the solution that contained the MSNs, the MTT solution (200 mL, 1 mg/mL) was added and cells were incubated for another 3 h. When the MTT solution was removed, the purple formazan crystals were solubilized with DMSO (200 mL) and measured at 560 nm on a microplate reader (SPECTRAmax plus, Molecular Devices, Sunnyvale, CA, USA). Cytotoxicity was expressed as the percentage of cell viability.

2.10. Antimicrobial effect on a real food system

The developed **N3-N** nanoparticles were used to eliminate *L. monocytogenes* from apple nectar, which was purchased in a local supermarket. The particle stock suspension was prepared in sterile distilled water and was sonicated in 3 5-minute cycles to preclude agglomerates. Different particle suspension volumes were added to 30 mL of pasteurized apple nectar. Positive and negative controls were included in the assays. Samples were inoculated with 100 µL of washed inoculum and incubated under orbital stirring (150 rpm) at 37 °C. After 2 h of incubation, viable cell numbers were determined as $\log_{10}$ CFU/mL by the spread plate technique using selective media and incubated at 37 °C for 48 h.

2.11. Statistical analysis

Data were statistically processed using Statgraphics Centurion XVI (Statpoint Technologies, Inc., Warrenton, VA, USA). The influence of different MSNs on bacterial viability was analyzed by an analysis of variance (one-way ANOVA). The LSD procedure (least significant difference) was used to test for any differences between averages at the 5% significance level.

3. Results and discussion

3.1. Material characterization

Silica mesoporous nanoparticles were synthesized using *N*-cetyltrimethylammonium bromide (CTABr) as a template and tetraethylorthosilicate (TEOS) as a hydrolytic inorganic precursor (Ruiz-Rico et al., 2015). The solid was then calcined at 550 °C to obtain bare MSNs (**B-N**), which were further functionalized with either *N*-(3-trimethoxysilylpropyl) diethylenetriamine (N3) or *N*-[3-(trimethoxysilyl)propyl]ethylenediamine triacetic acid trisodium salt (C3), to include nanoparticles' positive and negative charges on the surface, respectively. This resulted in amine-functionalized (**N3-N**) and carboxylate-functionalized (**C3-N**) nanoparticles (Pérez-Esteve et al., 2014).

The morphology and structure of the silica mesoporous support were confirmed by field emission scanning electron microscopy (FESEM) and transmission electron microscopy (TEM). MSNs are porous nanospheres with a single-particle size of ca. 100 nm and channels of 2-3 nm which can be seen as alternate black and white stripes or as a pseudo hexagonal array of pore voids in TEM images (see Fig. 1A-B). The degree of functionalization of solids N3-N and C3-N was determined by thermogravimetric analyses. The amount of N3 anchored to MSNs was ca. 0.36 g/g solid, while the amount of anchored C3 was ca. 0.26 g/g solid. The larger quantity of polyamines than carboxylates might be related with the fact that C3 is a bulkier molecule than N3 (Pérez-Esteve et al., 2014).

The size distribution (Fig. 1C) and zeta potential (Fig. 1D) of bare and functionalized nanoparticles were determined in Ringer buffer (RB). Particle size fell within the 100-220 nm range for **B-N**, whereas the zeta potential was −23.5 mV. Particle size slightly decreased after functionalization, which was most likely due to the increased colloidal stability of the nanoparticles as a result of functionalization with charged groups, which resulted in zeta potential values of -44 mV and +43 mV for **C3-N** and **N3-N**, respectively.
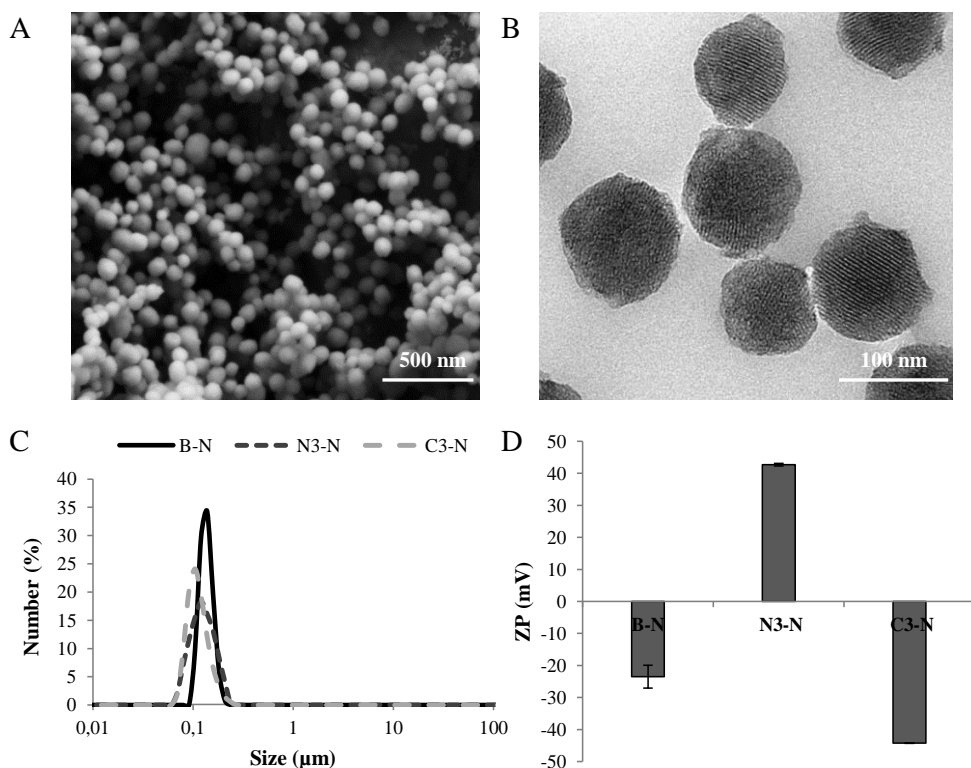
Figure 1. Material characterization of bare and functionalized MCM-41 nanoparticles. FESEM (A) and TEM (B) images of bare nanoparticles. The size distribution (C) and zeta potential (D) of bare and functionalized MSNs dispersed in RB.

3.2. Inhibitory activity of amine-functionalized nanoparticles

The use of polyamines as antimicrobial agents has been widely reported. The most important antimicrobials are the quaternary ammonium compounds with N-alkyl chain. The antimicrobial activity of these compounds involves an association between the positively charged quaternary nitrogen and the negatively charged head groups of acidic phospholipids in bacterial membranes which produces disruption of membrane integrity and leakage of cellular content (Buffet-Bataillon et al., 2012). They are commonly used as sanitizers in the food industry, but some

toxicological issues and microbial resistances have been reported (Aase et al., 2000; Thorsteinsson et al., 2003). Otherwise, primary and secondary amines are not considered effective antimicrobial agents. In this study, we assessed the antimicrobial activity of a secondary amine immobilized onto the surface of mesoporous silica nanoparticles. The antibacterial effect of amine-functionalized nanoparticles (**N3-N**) was tested by *in vitro* viability assays of bacterial suspensions of *L. monocytogenes*. In parallel, the antimicrobial activity of **B-N**, **C3-N** and free polyamine diethylenetriamine was also evaluated. Figure 2A displays the survival of *L. monocytogenes* after 2 h of treatment when these nanoparticles were used within the 0-150 μg/mL concentration range. The results showed that **B-N** and **C3-N** had no effect on bacteria. In contrast, **N3-N** completely inhibited microbial growth at a minimum bactericidal concentration (MBC) within the 10-50 μg/mL range. The effect of free diethylenetriamine was also studied. Microbial growth was totally inhibited at a concentration as high as 2 mg/mL. In order to compare the antibacterial effect of amines alone and when attached to MSNs, Figure 2B shows the survival of *L. monocytogenes* according to the polyamine concentration for free diethylenetriamine and solid **N3-N**. As it can be observed, **N3-N** was approximately 100 times more effective as an antibacterial agent than the free polyamine against *L. monocytogenes*.

This remarkable antibacterial efficacy was most likely due to an "enhanced concentration effect" operative in **N3-N**, which boosted attractive electrostatic forces between the negatively charged bacteria and positively charged particles functionalized with amines (Huang et al., 2010; Zhan et al., 2014). Given the high local concentration of amines in nanoparticles, the interaction of the functionalized nanoparticles with the bacterial membrane of the cells was probably most effective, and resulted in improved cell structure damage (*vide infra*).
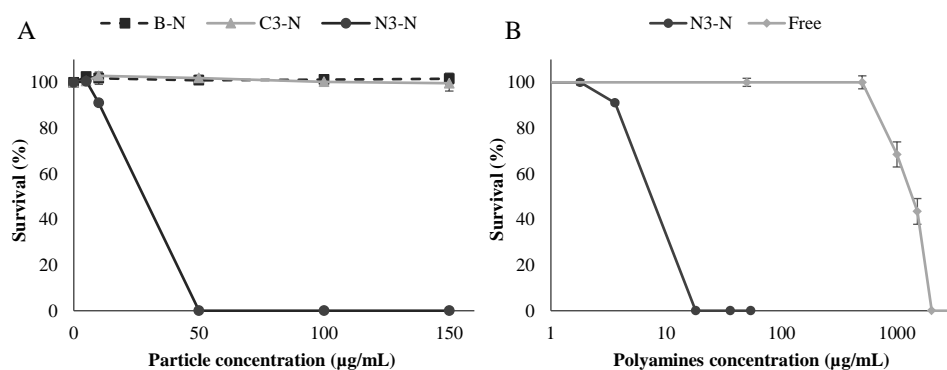
Figure 2. *L. monocytogenes* survival after incubation with bare and functionalized nanoparticles according to nanoparticle concentration (A) and *L. monocytogenes* survival after incubation with free polyamine diethylenetriamine and **N3-N** according to polyamine concentration (B) (means and standard deviations, n = 3).

After establishing the antimicrobial activity of **N3-N** for *L. monocytogenes*, we also investigated the effect of articles on the survival of the gram-negative bacteria *E. coli*. Figure 3 shows the survival of *E. coli* after 2 h of treatment when bare and amine-functionalized MSNs (i.e. **N3-N**) and free diethylenetriamine were used. In this case, large amounts of **N3-N** (10 mg/mL) were required to completely inhibit microbial growth. In contrast, free polyamine had a bactericidal effect at a low concentration (0.2 mg/mL), which clearly made a difference between the sensitivity of *L. monocytogenes* and *E. coli*. This effect was probably due to the dissimilarities in the structure and composition of bacterial cell walls. The cell wall of gram-positive bacteria contains a thick layer of peptidoglycan (10 nm), which is attached to teichoic acids. Otherwise, gram-negative bacteria have a thin peptidoglycan layer (2-3 nm), a periplasmic space and an outer membrane that contain lipopolysaccharides, phospholipids and proteins, particularly porins, embedded in the membrane (Hajipour et al., 2012). Porin channels on the outer membrane of gram-negative bacteria provide essential pathways for the controlled transport of ions, nutrients and metabolites in and out of the cell (Bolla

et al., 2011). Indeed the remarkable bactericidal effect of free diethylenetriamine against *E. coli* was probably due to the passive diffusion of polyamines through porins (Ritchie et al., 1987) and/or to the inhibition of porin-mediated fluxes by polyamines to reduce the permeation of nutrients across the outer membrane and to hinder bacterial growth. This has been previously reported for linear polyamines such as spermine and cadaverine (Vega et al., 1996). However, such bactericidal activity apparently reduces drastically for *E. coli* when polyamine is attached to MSNs.
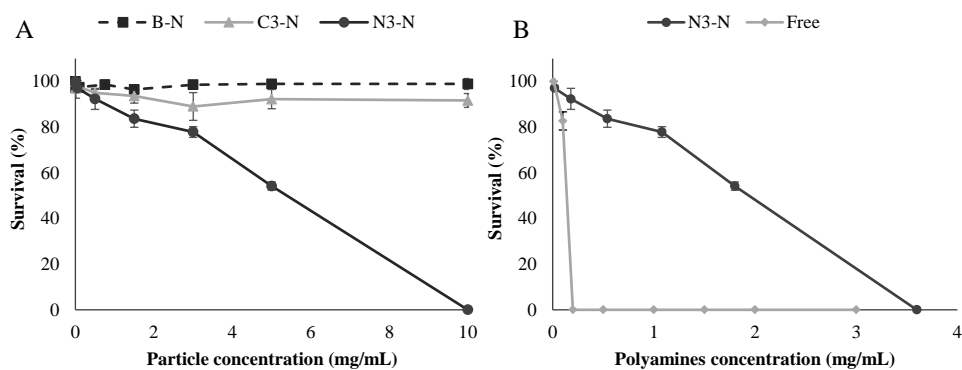
Figure 3. *E. coli* survival after incubation with bare and functionalized nanoparticles **N3-N** or **C3-N** according to nanoparticle concentration (A) and *E. coli* survival after incubation with free polyamine diethylenetriamine and **N3-N** according to polyamine concentration (B) (means and standard deviations, n = 3).

3.3. Morphological changes in L. monocytogenes treated with bare and functionalized nanoparticles

In order to assess the hypothesis of the concentration effect of **N3-N** on *L. monocytogenes*, the morphological changes of this bacterium in the presence of bare and functionalized MSNs were studied by TEM. The bacteria treated with **B-N** showed the typical rod-shaped morphology of a bacterium with a complete

cytoplasm and inner material surrounded by an intact cell membrane and cell wall (Fig. 4A-B). These results agree with the bacterial viability results (see Fig. 2) and with previous studies (Ruiz-Rico et al., 2015; Qi et al., 2013; Wehling et al., 2013; Yu et al., 2015). The cells treated with nanoparticles functionalized with carboxylates (**C3-N**) are shown in Fig. 4C-D, where both the bacterial cell wall and cell membrane appeared complete, but with roughness on some surface areas. Moreover, empty regions were observed in the cytoplasm, which could be produced by the aggregation or precipitation of internal cell components. Despite these morphological changes, bacterial viability was not affected by the presence of **C3-N** (see Fig. 2), which indicates that bacteria might be able to repair this sub-lethal cell damage and maintain their viability. Finally, the TEM images of the cells treated with nanoparticles functionalized with amines (**N3-N**) are seen in Fig. 4E-F. Here, bacteria cells showed severe damage, disruption of cell envelope integrity and leakage of cellular contents. These observations clearly agree with the above-described bacterial inhibition (see Fig. 2) and with the fluorescence microscopy results (*vide infra*).
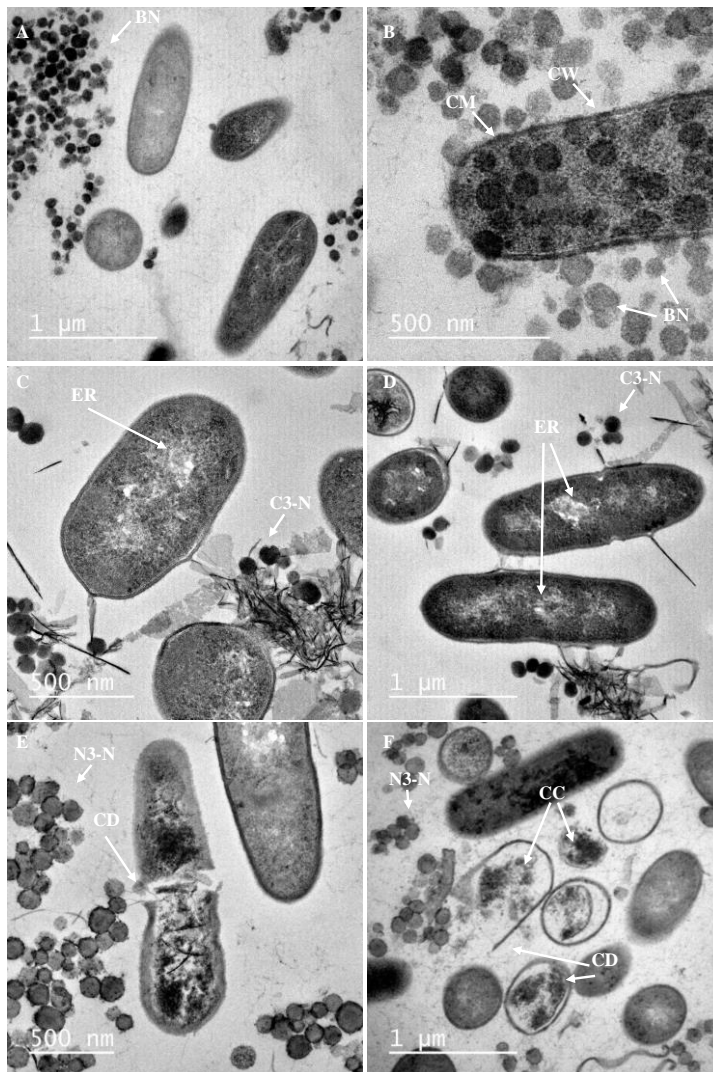
Figure 4. TEM micrographs by the ultrathin sectioning of *L. monocytogenes*. Images A and B represent cells in the presence of bare nanoparticles; images C and D show cells treated with C3-functionalized nanoparticles; and images E and F show cells in the presence of N3-functionalized nanoparticles. BN: bare MCM-41nanoparticules; CW: cell wall; CM: cell membrane; ER: empty regions; C3-N: carboxylate-functionalized nanoparticles; N3-N: amine-functionalized nanoparticles; CC: cytoplasmic content; CD: cell wall and membrane damage.

3.4. *Bacterial viability and agglomeration evaluation*

Besides TEM assays, studies conducted with a two-color fluorescent LIVE/DEAD® BacLightTM assay visualized viable and dead *L. monocytogenes* cells in the presence and absence of **N3-N** nanoparticles. Figure 5A shows bacteria in the absence of **N3-N**. All the *L. monocytogenes* bacteria are green-colored, which implies that cells were viable and membranes remained intact. Figure 5B shows bacteria in the presence of **N3-N**. When **N3-N** nanoparticles were in suspension, cell aggregation was evident, and was most likely favored by the presence of positively charged nanoparticles. Red-colored cells were scattered among green cells, which indicates cell damage, and eventually bacterial death (Wehling et al., 2013). Mechanism of action could be attributed to the polyamines corona. The gram-positive *L. monocytogenes* cell surface possesses a net negative electrostatic charge by virtue of the ionized phosphoryl and carboxylate substituent on outer cell envelope macromolecules, which are exposed to the extracellular environment (Hajipour et al., 2012). In contrast, amine-functionalized MSNs possess a positive zeta potential (see Fig. 1D). Therefore, the bacterium-particle interaction driven by attractive electrostatic interactions is expected to occur (Huang et al., 2010; Singh et al., 2011; Zhan et al., 2014). This binding between the bacterial cell wall and the amine-functionalized MSNs allowed the local concentration of amines on the bacterial surface to increase, and consequently the disruption of the cell membrane, and eventually bacterial cell death (Li & Wang, 2013; Qi et al., 2013).
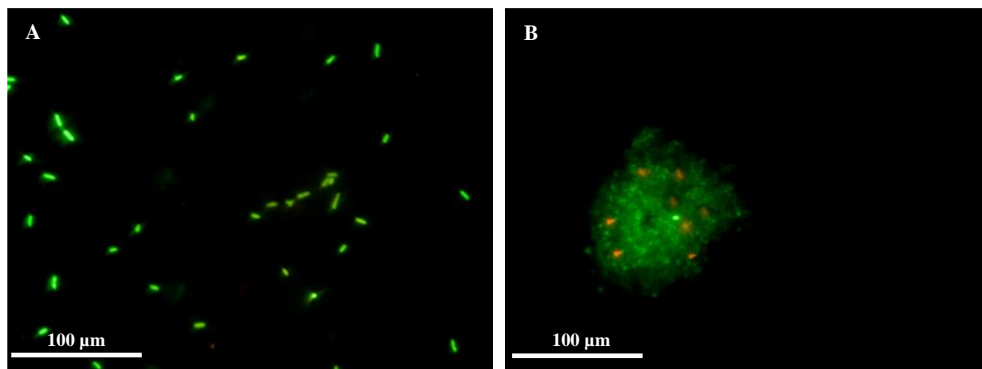
Figure 5. Fluorescence images of the untreated *L. monocytogenes* (A) and the cells treated after 2 h of incubation with **N3-N** (B). The study was performed by the two-color fluorescent LIVE/DEAD® BacLightTM assay, used to visualize viable (green) and dead (red) bacteria.

3.5. *In vitro biocompatibility tests*

Once the antimicrobial activity of the amine-functionalized MSNs was established, the biocompatibility of the **N3-N** solid and free polyamine to human cells was tested by WST-1 tests (Figure 6).
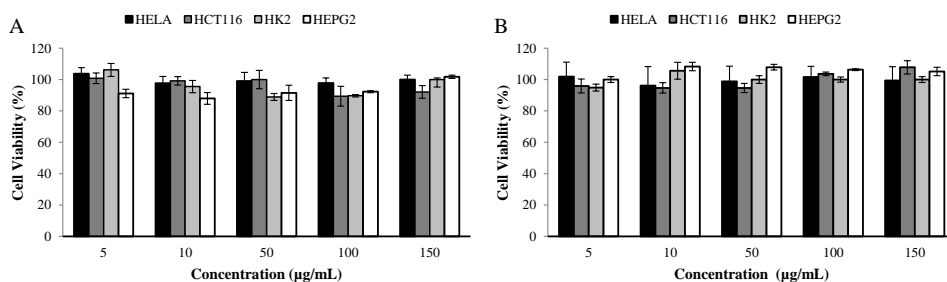
Figure 6. WST-1 cell viability assay. HeLa (black), HCT116 (dark grey), HK2 (light grey), and HEPG2 (white) cells treated with amine-functionalized nanoparticles **N3-N** (A) and the equivalent amount of free polyamine (B).

As seen in Figure 6, no significant cytotoxicity of the **N3-N** nanoparticles, or an equivalent amount of free polyamine to human colon carcinoma cells (HCT116), human liver carcinoma cells (HEPG2), human kidney epithelial cells (HK2) and human cervix carcinoma cells (HeLa) cells, even at concentration as high as 150 µg/mL, was observed.

3.6. Antimicrobial activity of amine-functionalized nanoparticles in a real food system

Listeria monocytogenes is one of the most important food-borne pathogens, being responsible of a serious infection called listeriosis (Gandhi & Chikindas, 2007). This bacterium is widely distributed in the environment and is generally associated with dairy products and juices, meat products, smoked fish and raw fruits and vegetables (McLauchlin et al., 2004). It can survive and grow over a wide range of environmental conditions such as refrigeration temperatures, low pH and high salt concentration (Carpentier & Cerf, 2011).

Microbial populations in apple juice can be inactivated by heat treatment such as pasteurization, however, potential concerns with alteration in composition and flavor properties of thermally processed fruit juices exist (Baskaran et al., 2010; Palgan et al., 2011). Moreover, commonly used preservatives such as potassium sorbate and sodium benzoate could be genotoxic and produce allergy problems (Zengin et al., 2011). Therefore, new technologies to prevent the spoilage and guarantee the safety of food products are needed.

The bactericidal ability of the amine-functionalized nanoparticles towards *L. monocytogenes* in a real food system (apple nectar) was investigated. The microbial growth results after 2 h of incubation in the presence of **N3-N** are shown in Figure 7. The **N3-N** concentrations within the 1-4 mg/mL range had a clearly antibacterial effect for *L. monocytogenes*, and resulted in a remarkable complete bacteria inhibition at the **N3-N** concentration of 4 mg/mL.
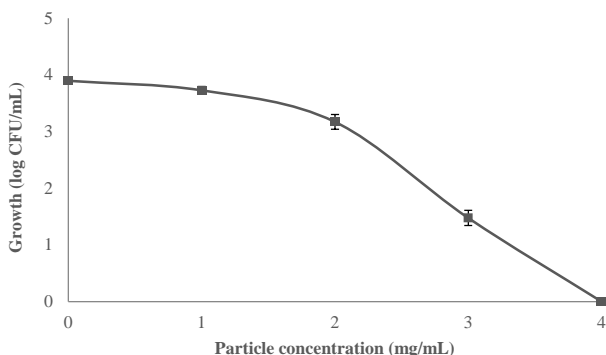
Figure 7. Microbial growth of *L. monocytogenes* in apple nectar after incubation with **N3-N** according to particle concentration (means and standard deviations, n = 3).

4. Conclusions

The simple attachment of polyamines to the surface of MSNs enabled us to obtain nanoparticles with a high local concentration of positive charges on the surface of particles. These amine-functionalized nanoparticles exhibited enhanced bactericidal activity, which was 100 fold greater than free polyamine diethylenetriamine against *L. monocytogenes*. The possible mechanism of action was most likely due to the combination of attractive binding forces between the positive amine corona on the surface of nanoparticles and the negatively charged bacteria membrane. These results showed that simple amine-functionalized MSNs acted as effective antimicrobial "nanobullets" against gram-positive pathogens like *L. monocytogenes* in both saline solution and food matrix. Moreover, functionalized nanoparticles are not toxic to human cells. These findings suggest that amine-immobilized nanoparticles can be used as new antimicrobial nanodevices for diverse applications. Our study also suggested that simple functionalized nanoparticles can have a tremendous impact on bacterial viability, which opens the door to the development of new antimicrobial agents based on organic-inorganic hybrid nanosystems.

Acknowledgements

References

Aase, B., Sundheim, G., Langsrud, S., & Rørvik, L.M. (2000). Occurrence of and a possible mechanism for resistance to a quaternary ammonium compound in *Listeria monocytogenes*. *International Journal of Food Microbiology*, 62(1), 57-63.

Al Shamsi, M., Al Samri, M.T., Al-Salam, S., Conca, W., Shaban, S., Benedict, S., Tariq, S., Biradar, A.V., Penefsky, H.S., Asefa, T., & Souid, A.K. (2010). Biocompatibility of calcined mesoporous silica particles with cellular bioenergetics in murine tissues. *Chemical Research in Toxicology*, *23*, 1796-1805.

Aznar, E., Oroval, M., Pascual, L., Murguía, J.R., Martínez-Máñez, R., & Sancenón, F. (2016) Gated materials for on-command release of guest molecules. *Chemical Reviews, 116*, 561-718.

Baskaran, S. A., Amalaradjou, M. A. R., Hoagland, T., & Venkitanarayanan, K. (2010). Inactivation of *Escherichia coli* O157: H7 in apple juice and apple cider by trans-cinnamaldehyde *International Journal of Food Microbiology*, 141(1), 126-129.

Bernardos, A., Marina, T., Žáček, P., Pérez-Esteve, E., Martínez-Mañez, R., Lhotka, M., Kourimská, L., Pulkrávek, J., & Klouček, P. (2015). Antifungal effect of essential oil components against *Aspergillus niger* when loaded into silica mesoporous supports. *Journal of the Science of Food and Agriculture, 95*, 2824–2831.

Bolla, J.M., Alibert-Franco, S., Handzlik, J., Chevalier, J., Mahamoud, A., Boyer, G., Kieć-Kononowicz, K., & Pagès, J.M. (2011). Strategies for bypassing the membrane barrier in multidrug resistant Gram-negative bacteria. *FEBS Letters, 585*(11), 1682-1690.

Botequim, D., Maia, J., Lino, M.M.F, Lopes, L.M.F, Simoes, P.N., Ilharco, L.M., & Ferreira, L. (2012). Nanoparticles and surfaces presenting antifungal, antibacterial and antiviral properties. *Langmuir, 28*(20), 7646-7656.

Buffet-Bataillon, S., Tattevin, P., Bonnaure-Mallet, M., & Jolivet-Gougeon, A. (2012). Emergence of resistance to antibacterial agents: the role of quaternary ammonium compounds—a critical review. *International Journal of Antimicrobial Agents*, 39(5), 381-389.

Capeletti, L.B., de Oliveira, L.F., Gonçalves, K.D.A., de Oliveira, J.F.A., Saito, Â., Kobarg, J., & Cardoso, M.B. (2014). Tailored silica–antibiotic nanoparticles: overcoming bacterial resistance with low cytotoxicity. *Langmuir, 30*, 7456-7464.

Carpentier, B., & Cerf, O. (2011). Review-Persistence of *Listeria monocytogenes* in food industry equipment and premises. *International Journal of Food Microbiology*, 145(1), 1-8.

Dizaj, S.M., Lotfipour, F., Barzegar-Jalali, M., Zarrintan, M.H., & Adibkia, K. (2014). Antimicrobial activity of the metals and metal oxide nanoparticles. *Materials Science and Engineering: C, 44*, 278–284.

Gandhi, M., & Chikindas, M. L. (2007). Listeria: a food-borne pathogen that knows how to survive. *International Journal of Food Microbiology*, 113(1), 1-15.

Hajipour, M.J., Fromm, K.M., Ashkarran, A.A., de Aberasturi, D.J., de Larramendi, I.R., Rojo, T., Serpooshan, V., Parak, W.J., & Mahmoudi, M. (2012). Antibacterial properties of nanoparticles. *Trends in Biotechnology, 30*(10), 499-511.

Huang, Y.F., Wang, Y.F., & Yan, X.P. (2010). Amine-functionalized magnetic nanoparticles for rapid capture and removal of bacterial pathogens. *Environmental Science & Technology, 44*(20), 7908-7913.

Huh, A.J., & Kwon, Y.J. (2011). "Nanoantibiotics": a new paradigm for treating infectious diseases using nanomaterials in the antibiotics resistant era. *Journal of Controlled Release, 156*(2), 128-145.

Li, L.L., & Wang, H. (2013). Enzyme-coated mesoporous silica nanoparticles as efficient antibacterial agents in vivo. *Advanced Healthcare Materials, 2*(10), 1351-1360.

Mas, N., Galiana, I., Mondragón, L., Aznar, E., Climent, E., Cabedo, N., Sancenón, F., Murguía, J.R., Martínez-Máñez, R., Marcos, M.D., & Amorós, P. (2013). Enhanced efficacy and broadening of antibacterial action of drugs via the use of capped mesoporous nanoparticles. *Chemistry - A European Journal, 19(*34), 11167-11171.

McLauchlin, J., Mitchell, R. T., Smerdon, W. J., & Jewell, K. (2004). *Listeria monocytogenes* and listeriosis: a review of hazard characterisation for use in microbiological risk assessment of foods. *International Journal of Food Microbiology*, 92(1), 15-33.

Molina-Manso, D., Manzano, M., Doadrio, J.C., Del Prado, G., Ortiz-Pérez, A., Vallet-Regí, M., Gómez-Barrena, E., & Esteban, J. (2012). Usefulness of SBA-15 mesoporous ceramics as a delivery system for vancomycin, rifampicin and linezolid: a preliminary report. *International Journal of Antimicrobial Agents, 40*(3), 252-256.

Ortuño, C., Quiles, A., & Benedito, J. (2014). Inactivation kinetics and cell morphology of E. coli and *S. cerevisiae* treated with ultrasound-assisted supercritical CO_2. *Food Research International, 62*, 955-964.

Palgan, I., Caminiti, I. M., Muñoz, A., Noci, F., Whyte, P., Morgan, D.J., Cronin, D.A., & Lyng, J.G. (2011). Effectiveness of high intensity light pulses (HILP) treatments for the control of *Escherichia coli* and *Listeria innocua* in apple juice, orange juice and milk. *Food Microbiology*, 28(1), 14-20.

Park, S.Y., Barton, M., & Pendleton, P. (2012). Controlled release of allyl isothiocyanate for bacteria growth management. *Food Control, 23*(2), 478-484.

Pérez-Esteve, E., Oliver, L., García, L., Nieuwland, M., de Jongh, H.H., Martínez-Máñez, R., & Barat, J.M. (2014). Incorporation of mesoporous silica particles in gelatine gels: effect of particle type and surface modification on physical properties. *Langmuir, 30*, 6970-6979.

Qi, G., Li, L., Yu, F., & Wang, H. (2013). Vancomycin-modified mesoporous silica nanoparticles for selective recognition and killing of pathogenic gram-positive bacteria over macrophage-like cells. *ACS Applied Materials & Interfaces, 5*(21), 10874-10881.

Ritchie, R.J., & Gibson, J. (1987). Permeability of ammonia and amines in *Rhodobacter sphaeroides* and *Bacillus firmus*. *Archives of Biochemistry and Biophysics, 258*(2), 332-341.

Ruiz-Rico, M., Fuentes, C., Pérez-Esteve, E., Jiménez-Belenguer, A.I., Quiles, A., Marcos, M.D., Martínez-Máñez, R., & Barat, J.M. (2015). Bactericidal activity of caprylic acid entrapped in mesoporous silica nanoparticles. *Food Control, 56*, 77-85.

Seil, J. T., & Webster, T. J. (2012). Antimicrobial applications of nanotechnology: methods and literature. *International Journal of Nanomedicine*, 7, 2767-2781.

Singh, S., Barick, K.C., & Bahadur, D. (2011). Surface engineered magnetic nanoparticles for removal of toxic metal ions and bacterial pathogens. *Journal of Hazardous Materials, 192*(3), 1539-1547.

Slowing, I.I., Vivero-Escoto, J.L., Wu, C.W., & Lin, V.S.Y. (2008). Mesoporous silica nanoparticles as controlled release drug delivery and gene transfection carriers. *Advanced Drug Delivery Reviews, 60*, 1278-1288.

Tang, F., Li, L., & Chen, D. (2012). Mesoporous silica nanoparticles: synthesis, biocompatibility and drug delivery. *Advanced Materials, 24*(12), 1504-1534.

Thorsteinsson, T., Másson, M., Kristinsson, K. G., Hjálmarsdóttir, M. A., Hilmarsson, H., & Loftsson, T. (2003). Soft antimicrobial agents: synthesis and activity of labile environmentally friendly long chain quaternary ammonium compounds. *Journal of Medicinal Chemistry,* 46(19), 4173-4181.

Vega, A.D., & Delcour, A.H. (1996). Polyamines decrease *Escherichia coli* outer membrane permeability. *Journal of Bacteriology, 178*(13), 3715-3721.

Wehling, J., Volkmann, E., Grieb, T., Rosenauer, A., Maas, M., Treccani, L., Rezwan, K. (2013). A critical study: Assessment of the effect of silica particles from 15 to 500 nm on bacterial viability. *Environmental Pollution, 176*, 292-299.

Yu, E., Galiana, I., Martínez-Máñez, R., Stroeve, P., Marcos, M.D., Aznar, E., Sancenón, F., Murguía, J.R., & Amorós, P. (2015). Poly (N-isopropylacrylamide)-gated Fe_3O_4/SiO_2 core shell nanoparticles with expanded mesoporous structures for the temperature triggered release of lysozyme. *Colloids and Surfaces B: Biointerfaces, 135*, 652-660.

Zengin, N., Yüzbaşıoğlu, D., Ünal, F., Yılmaz, S., & Aksoy, H. (2011). The evaluation of the genotoxicity of two food preservatives: sodium benzoate and potassium benzoate. *Food and Chemical Toxicology,* 49(4), 763-769.

Zhan, S., Yang, Y., Shen, Z., Shan, J., Li, Y., Yang, S., & Zhu, D. (2014). Efficient removal of pathogenic bacteria and viruses by multifunctional amine-modified magnetic nanoparticles. *Journal of Hazardous Materials, 274,* 115-123.

Zhao, Y., Sun, X., Zhang, G., Trewyn, B.G., Slowing, I.I., & Lin, V.S.Y. (2011). Interaction of mesoporous silica nanoparticles with human red blood cell membranes: size and surface effects. *ACS nano, 5*(2), 1366-1375.

5.4. Enhanced antimicrobial activity of essential oil components immobilized on silica particles

María Ruiz-Rico[a*], Édgar Pérez-Esteve[a], Andrea Bernardos[b,c], Félix Sancenón[b,c], Ramón Martínez-Máñez[b,c], María D. Marcos[b,c], José M. Barat[a]

[a] Grupo de Investigación e Innovación Alimentaria. Departamento de Tecnología de Alimentos, Universitat Politècnica de València. Camino de Vera s/n, 46022, Valencia, Spain

[b] Instituto Interuniversitario de Investigación de Reconocimiento Molecular y Desarrollo Tecnológico (IDM), Unidad Mixta Universitat Politècnica de València – Universitat de València. Departamento de Química, Universitat Politècnica de València, Camino de Vera s/n, 46022, Valencia, Spain

[c] CIBER de Bioingeniería, Biomateriales y Nanomedicina (CIBER-BBN)

Abstract

The antimicrobial activity of essential oils components (EOCs) is well-known. However, their high volatility and powerful aroma limit their application in the formulation of a wide range of food products. In this context, the antimicrobial activity of carvacrol, eugenol, thymol and vanillin grafted onto the surface of three silica supports with different morphologies, textural properties and chemical reactivities (silica-fumed, amorphous silica and MCM-41) was evaluated herein. Materials characterization revealed a good immobilization yield and all the devices showed a micro-scale particle size. Immobilization greatly enhanced the antimicrobial activity of the essential oil components against *Listeria innocua* and *Escherichia coli* compared to free components. The incorporation of EOCs immobilized on silica particles into pasteurized milk inoculated with *L. innocua* demonstrated their effectiveness not only for *in vitro* conditions, but also in a real food system.

Keywords: carvacrol, eugenol, *Listeria innocua*, thymol, vanillin, immobilization, silica support.

1. Introduction

New techniques to prevent food spoilage and to guarantee food safety have rapidly and innovatively developed in recent years as a result of the current inadequacy of traditional antimicrobial methods and the growing spread of antibiotic resistant strains of bacteria and fungi (Zengin et al., 2011; Capeletti et al., 2014). Some new tendencies in this field include the use of naturally-occurring antimicrobial compounds, e.g., plant metabolites. Essential oils (EOs), lipophilic extracts of bioactive compounds with antimicrobial activity against several pathogens and food-borne microorganisms have grown the most in research publications and industrial applications (Darvishi et al., 2013; Hyldgaard et al., 2012; Si et al., 2006).

The antimicrobial activity of EOs has been attributed to their phenolic compounds and their interaction with microbial cell membranes, which cause the leakage of ions and cytoplasmic content, and can thus lead to cellular breakdown (Burt, 2004). Despite the described antimicrobial behavior, the direct application of EOs to food products has several limitations: strong sensory properties (odor and flavor) (Nostro & Papalia, 2012), high volatility (Majeed et al., 2015), poor solubility (Burt, 2004), degradability (Turek & Stintzing, 2013) and potential toxicity (Smith et al., 2005). Moreover, the concentration of an essential oil component (EOC) needed to inhibit microbial growth in a food system is higher than in *in vitro* studies. This is not due only to interactions with food matrix components (Hyldgaard et al., 2012; Jo et al., 2015), but also to difficulties in their dispersion in the food water phase (Weiss et al., 2009).

Hence research has focused on the development of technologies, such as encapsulation or immobilization, to improve the functionality of natural antimicrobials (Weiss et al., 2009).

Regarding encapsulation, different organic delivery systems, including emulsions, liposomes, or polymer and protein capsules, have been used to encapsulate EOs for their later application directly or after incorporation to films

or coatings for food preservation purposes (Guarda et al., 2011; Higueras et al., 2014; Ravichandran et al., 2011; Ribes et al., 2016).

Besides traditional organic matrices, new inorganic materials (i.e. porous siliceous materials) have been used as supports to prepare antimicrobial devices through the encapsulation of a payload molecule in the voids of porous silica particles. Entrapment of antimicrobial compounds in these materials can also protect bioactive substances from environmental stress, mask undesirable sensory properties, prevent interactions with food components, and achieve the controlled release of the antimicrobial compound at the site of action. Bearing in mind these features, different naturally-occurring antimicrobial compounds, such as allyl isothiocyanate (Park et al., 2011; Park & Pendleton, 2012; Park et al., 2012; Siahaan et al., 2013), caprylic acid (Ruiz-Rico et al., 2015), lysozyme (Yu et al., 2015), and EOCs that include allyl isothiocyanate,carvacrol, cinnamaldehyde, diallyldisulfide, eugenol, thymol and thymoquinone (Bernardos et al., 2015; Janatova et al., 2015), have been encapsulated in mesoporous silica supports. It is noteworthy that all these studies have managed to preserve or enhance the inhibitory effect of bioactive compounds.

Apart from voids capable of entrapping active compounds, siliceous materials present a large surface capable of reacting with organic molecules, and of creating hybrid organic-inorganic systems where silica materials act as a support and organic molecules create a functional layer on the support's surface. Based on this approach, Li & Wang (2013) reported lysozyme-coated mesoporous silica nanoparticles that exhibited efficient enhanced antibacterial activity against E. coli both *in vitro* and *in vivo*. Qi et al. (2013) used vancomycin-modified mesoporous silica nanoparticles to kill pathogenic gram-positive bacteria. Pędziwiatr-Werbicka et al. (2014) synthesized fatty acids functionalized mesoporous silica particles with relative antimicrobial activity. Despite these promising results, the preparation of antimicrobial devices from EOs by this innovative approach has not yet been explored as far as we know.

Accordingly, this study aimed to design a collection of antimicrobial devices based on anchoring several volatile EOCs (carvacrol, eugenol, thymol and vanillin) to the surface of three types of silica particles with different surface areas, textural properties and chemical reactivities (silica-fumed, MCM-41 and amorphous silica), and to evaluate their antimicrobial activity against some food-borne pathogens, e.g., *Listeria innocua* and *Escherichia coli*, compared with that of free bioactive compounds.

2. Materials and methods

2.1. Chemicals

N-cetyltrimethylammonium bromide (CTABr), sodium hydroxide (NaOH), triethanolamine (TEAH$_3$), tetraethylorthosilicate (TEOS), (3-Aminopropyl)triethoxysilane (APTES), trimethylamine, paraformaldehyde, diethyl ether, chloroform, n-butanone, carvacrol, eugenol and thymol were provided by Sigma-Aldrich (Madrid, Spain). Vanillin was purchased from Ventós (Barcelona, Spain). Acetonitrile, HCl, MgSO$_4$, KOH, H$_2$SO$_4$ and microbiological media grade were provided by Scharlab (Barcelona, Spain). Fumed silica (FS) nanoparticles (AEROSIL® 200) were purchased from Evonik Industries (Essen, Germany) and amorphous silica (AS) microparticles (SYLYSIA® SY350/FCP) were provided by Silysiamont (Milano, Italy).

2.2. Mesoporous silica particles synthesis

Microparticulated MCM-41 particles were synthesized following the so-called "atrane route", where CTABr was used as the structure-directing agent. The molar ratio of the reagents was fixed at 7 TEAH$_3$: 2 TEOS:0.52 CTABr:0.5 NaOH:180 H$_2$O. CTABr was added to a TEAH$_3$ and NaOH solution, which contained TEOS at 118 °C. After dissolving CTABr in the solution, water was slowly added along with vigorous stirring at 70 °C to form a white suspension. This mixture was aged at 100 °C for

24 h. Following synthesis, the solid was recovered, washed with deionized water and dried at 70 °C. The as-synthesized microparticles were calcined at 550 °C in an oxidant atmosphere for 5 h to remove the template phase (Ruiz-Rico et al., 2016).

2.3.   Preparation of the antimicrobial devices

A three-step synthetic procedure was followed to prepare the antimicrobial devices (see Scheme 1).
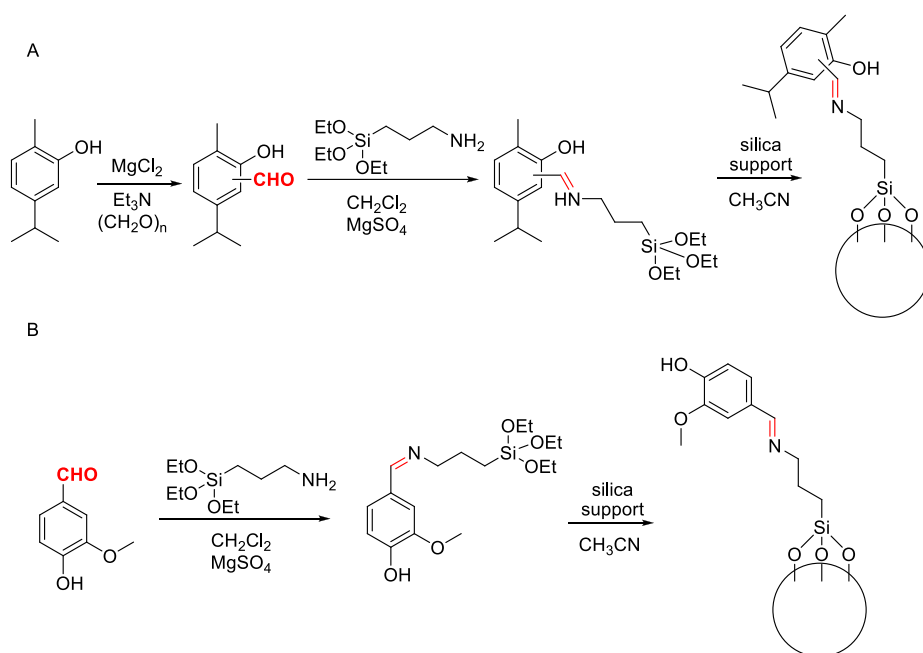
Scheme 1. Representation of the synthesis procedure of the antimicrobial devices. A. The three-step synthesis of the carvacrol, eugenol and thymol immobilized systems (carvacrol provided as an example). Step 1. Aldehyde derivatization. Step 2. Alkoxysilane derivatization. Step 3. Anchoring to the silica support (Fumed Silica, MCM-41 or Amorphous silica). B. The two-step synthesis of the vanillin immobilized systems. Step 1. Alkoxysilane derivatization. Step 2. Anchoring to the silica support (Fumed Silica, MCM-41 or Amorphous silica).

In the first step, carvacrol, eugenol and thymol were transformed into aldehydes derivatives. In a second step, the aldehydes of carvacrol, eugenol and thymol, and pure vanillin were reacted with 3-aminopropyltriethoxysilane (APTES) to yield the corresponding alkoxysilane derivatives. Further anchorage of the four silane derivatives to the external surface of three different inorganic scaffolds (FS, MCM-41 and AS particles, third step) resulted in the preparation of the final 12 solids.

2.3.1. Preparing the EOC aldehyde derivatives

The aldehyde derivatives of carvacrol, eugenol and thymol were synthesized for the purpose of adding a second reactive moiety capable of reacting with the amine group of alkoxysilane, and of maintaining hydroxyl group free of the compounds whose presence is critical for the antibacterial activity (Ben Arfa et al., 2006; Gill & Holley, 2006). Presence of an own aldehyde group in vanillin structure avoided this step.

The carvacrol and thymol aldehydes were synthesized by formylation an ortho position to the hydroxyl group. In a typical synthesis, 150 mL of acetonitrile, 40 mmol of carvacrol or thymol, 150 mmol of trimethylamine and 40 mmol of anhydrous $MgSO_4$ were placed inside a round-bottomed flask. The mixture was placed in an argon atmosphere and stirred for 15 min at room temperature. Afterward, 270 mmol of paraformaldehyde were added and the reaction mixture was refluxed for 3.5 h at 83 ºC. The mixture was then allowed to cool at room temperature. The solution was acidified with 5% HCl solution (320 mL) and stirred for 30 min in an inert atmosphere. Finally, the organic portion was extracted with diethyl ether and volatiles were removed under reduced pressure to obtain the carvacrol or thymol aldehyde.

Eugenol aldehyde was synthesized using a general Reimer–Tiemann reaction. Next 150 mL of water were heated at 80 °C in a round-bottomed flask, and 22 mmol of eugenol were dissolved in the water. When the temperature had fallen

to 60 °C, 400 mmol of KOH and 88 mmol of chloroform were added. As the reaction was exothermic, chloroform was added at a rate of 1 mL/h over a 7-hour period for safety reasons. The reaction mixture was kept at 60 ºC for a further 8-hour period. Then the solution was acidified with 10 % H_2SO_4 solution. The organic portion was extracted with n-butanone and volatiles were removed under reduced pressure.

2.3.2. Preparing the EOC-alkoxysilane derivatives

To facilitate the covalent anchoring of the four EOCs to silica supports the corresponding EOCs-alcoxysilane derivatives were synthesized. For this purpose, 2 mL of the carvacrol, thymol or eugenol and unmodified vanillin aldehydes were reacted with 2.3 mL (10 mmol) of 3-aminopropyltriethoxysilane (APTES) in the presence of dichloromethane (20 mL) and $MgSO_4$. The mixture was stirred in reflux for 1 h to be then filtered and evaporated under reduced pressure to give a transparent liquid. The reaction yield was calculated by ^{1}H NMR in a Bruker AV400 spectrometer (Bruker Daltonik GmbH, Bremen, Germany) which operated at room temperature.

2.3.3. Synthesis of the EOC-functionalized silica particles

The EOC-alkoxysilane derivatives were attached to three different silica particles: commercial fumed silica (FS) nanoparticles, synthesized MCM-41 microparticles and commercial amorphous silica (AS) microparticles.

In a typical synthesis, 1 g of bare particles was suspended in 40 mL of acetonitrile in a round-bottomed flask in an inert atmosphere. Then the excess of alkoxysilane derivative was added and the final mixture was stirred for 5.5 h at room temperature. Finally, the solids were filtered off, washed with acetonitrile and distilled water, and dried at room temperature in vacuum for 12 h.

2.4. Materials Characterization

Bare and functionalized silica supports were characterized by standard techniques: morphological analysis, particle size distribution, zeta potential and determination of the degree of functionalization. A morphological analysis was performed by field emission scanning electron microscopy (FESEM) observations. FESEM images were acquired by a Zeiss Ultra 55 (Carl Zeiss NTS GmbH, Oberkochen, Germany) and observed in the secondary electron mode. Particle size distribution was determined by a Malvern Mastersizer 2000 (Malvern Instruments, UK). To take measurements, solids were dispersed in tryptic soy broth (TSB). All the measurements were taken in triplicate on previously sonicated highly dilute dispersions. To determine the zeta potential, a Zetasizer Nano ZS (Malvern Instruments, UK) was used. Solids were dispersed in TSB at the 1 mg/mL concentration and were sonicated for 2 min to preclude aggregation. The zeta potential was calculated from the particle mobility values by applying the Smoluchowski model. The degree of functionalization of the different particles was determined by thermogravimetric analyses (TGA) and elemental analysis. TGA determinations were made on a TGA/SDTA 851e Mettler Toledo balance (Mettler Toledo Inc., Schwarzenbach, Switzerland), with a heating program that consisted in a heating ramp of 10 °C per minute from 273 to 373 K, followed by an isothermal heating step at this temperature for 60 min in a nitrogen atmosphere (80 mL/min). Then the program was allowed to continue with a dynamic heating segment from 373 to 1273 K in an oxidant atmosphere (air, 80 mL/min) and with an isothermal heating step at this temperature for 30 min. The bulk density of the different silica supports was determined by pouring around 20 g of support into a 100-mL measuring cylinder and tapping 10 times on a flat wooden platform. The volume occupied by the sample was recorded. The mass of the empty and filled measuring cylinders, and the final volume occupied by each sample, was noted. Bulk density was expressed as the mass/volume ratio (g/cm^3). The data acquired from the different characterization techniques were used to calculate the number of particles/g of solid, EOC content/g of particle and the EOC density on the

particles' surface. The number of particles per gram of solid was calculated according to Eq. 1. The content of the EOCs (determined by the TGA and elemental analysis) and the mean average particle size (determined by laser diffraction) values were used to estimate the number of EOC molecules/g solid (Eq. 2). The surface area was taken into account to calculate the density of EOCs on the particles' surface (Eq. 3).

Number of particles/g solid = 1 / ((particle's volume (cm^3) x density (g/cm^3)))   (Eq. 1)

EOC molecules/g solid = (α_{EOC} (g/g solid) / molecular weight (g/mol)) x 6.023 x 10^{23} (Eq. 2)

EOC density ($molec/nm^2$) = EOC molecules (molec/g solid) / surface area (nm^2/g solid)   (Eq. 3)

2.5. Microbiological Assays

Strains *L. innocua* (CECT 910) and *E. coli* K12 (CECT 433) were obtained from the Colección Española de Cultivos Tipo (CECT; Valencia, Spain). Bacterial stocks were stored at 4 ºC in plate count agar (PCA) before use. Cell from a colony of *L. innocua* or *E. coli* grown on PCA were transferred to 10 mL of TSB and were incubated at 37 ºC for 24 h to obtain an inoculum with a density of approximately 1 x 10^8 cells/mL of broth.

2.5.1.   Antimicrobial susceptibility assays

The antimicrobial activity of EOCs, both free and immobilized on silica particles, was determined by the macrodilution method. Different ranges of concentrations were tested for each EOC according to bibliographical data (Belda-Galbis et al., 2014; Burt, 2004; Cava-Roda et al., 2012; Guarda et al., 2011). Equivalent amounts of immobilized EOCs were calculated according to results obtained when characterizing the degree of functionalization (*vide infra*). The EOC stock solution in dimethyl sulfoxide (DMSO) or the particles stock suspension in TSB (functionalized fumed silica, MCM-41 and amorphous silica particles) was

prepared. To achieve the final concentrations of the free or immobilized bioactive compounds, different volumes of stock suspensions were added to 15 mL of TSB in Erlenmeyer flasks. Then flasks were inoculated with 5 or 50 µL of inoculum for *E. coli* and *L. innocua*, respectively, to provide an initial cell density of approximately 10^5 CFU/mL, and were incubated with orbital stirring (150 rpm) at 37 °C for 24 h. All the treatments were set in triplicate. Positive and negative controls were included in all the assays. The positive control indicated the bacterial growth profile with absence of treatment, while the negative control confirmed lack of contamination by the addition of treatment.

After incubation, viable cell numbers were determined as colony-forming units (CFU) by the spread plate technique using selective media (Palcam agar supplemented with polymyxin B, acriflavine and ceftazidime for *L. innocua*; Tryptone Bile X-glucuronide (TBX) agar for *E. coli*) and were incubated at 37 °C for 24 h (*E. coli*) or 48 h (*L. innocua*). These values were logarithmically transformed and expressed as $\log_{10}$ CFU/mL.

2.5.2.   Antimicrobial effect of EOCs on a real food system

The capability of the free and MCM-41 immobilized thymol and vanillin to control *L. innocua* growth in pasteurized skimmed milk was evaluated by simulating 7-days refrigeration storage. Equivalent concentrations of free and immobilized EOCs (0.05, 0.25 and 0.5 mg/mL for thymol; 0.5, 0.75 and 1 mg/mL for vanillin) were added to 15 mL of sterilized milk and were then inoculated with 10^2 CFU/mL of the microorganism. Samples were stored with stirring at 4 °C for 7 days. On days 0, 1, 3, 5, and 7, samples were taken and counted by the spread plate technique (see Section 2.5.1. for details). Positive and negative controls were included in the assays.

2.6. Statistical analysis

Data were statistically processed using Statgraphics Centurion XVI (Statpoint Technologies, Inc., Warrenton, VA, USA). The influence of different supports and concentrations of treatments on bacterial viability was analyzed by an analysis of variance (multifactor ANOVA). The LSD (least significant difference) procedure was used to test differences between averages at the 5% significance level.

Multiple regression analyses with the stepwise removal procedure were performed to study the relationship between different variables (EOC type, support type, EOC concentration, particle concentration, number of particles, mean size, zeta potential, EOC content and EOC density on particles' surface) and the dependent variable (bacterial growth) in the antimicrobial susceptibility assays. For the analysis, EOC type and support type were introduced as dummy variables (Fuentes et al., 2008).

3. Results and discussion

3.1. Designing the antimicrobial devices

Four EOCs were used in this study: carvacrol (a major component of oregano plants), eugenol (a major component of clove and cinnamon oil), thymol (a major component of thyme plants) and vanillin (a primary component of vanilla bean extracts). They all were selected for their recognized antimicrobial properties (Burt, 2004; Hyldgaard et al., 2012), them being a "generally recognized as safe" (GRAS) component, and for their restricted use in certain food industry applications as a result of limited water solubility and/or intense spicy/medicinal/sweet aroma, which justifies anchoring to mask their sensory properties (Shah et al., 2012).

Three different silica particles were selected as the inorganic support: amorphous silica, MCM-41 and fumed silica. Amorphous silica particles are non crystalline structures of silicon dioxide produced in different sizes, which are

widely used in cosmetics (sun creams), dentistry (toothpaste), paints, and food and animal feed additives (Uboldi et al., 2012). These particles are considered GRAS, an authorized additive in Europe and E-551-classified (Contado et al., 2013). MCM-41 is a mesoporous material with a hierarchical structure developed firstly by Mobil Oil Corporation researchers. These particles have been widely used in applications in the food sector, where they can be used as catalysts in the synthesis of nutrients and bioactive molecules (Márquez-Ávarezet al., 2004), in sensor technology (Climentet al., 2009), and also as carriers to design smart delivery systems (Pérez-Esteve et al., 2015). Finally, fumed silica are microscopic droplets of amorphous silica with a branched chainlike primary structure that consists of fused SiO_2 nanoparticles that agglomerate in three-dimensional secondary and tertiary particles (Walls et al., 2000). Fumed silica particles have an extremely low bulk density, a large surface area and, above all, high chemical reactivity.

The efficiency of the alkoxysilane derivation process was evaluated by the ^{1}H NMR analysis. For all the EOCs, the product yield estimated from the ^{1}H NMR spectra was 20-40%.

3.2. Characterizing the EOC-functionalized silica particles

The morphological characterization of the bare and EOC-functionalized silica particles by field emission scanning electron microscopy (FESEM) is shown in Figure 1. For materials characterization, the silica particles functionalized with thymol were chosen as reference supports. Bare fumed silica appears as an irregular-shaped sponge-like structure, probably formed by the aggregation of primary particles (reported particle size of 12 nm). Bare MCM-41 particles are seen as dense microparticles with a clear hexagonal morphology and a mean single-particle size of ca. 4 μm. Finally, amorphous silica is shown as being sphere-like with a rough morphology, similar to fumed silica supports. In all cases, the appearance of particles did not change after the functionalization process.

As synthesized   **Thymol-functionalized**
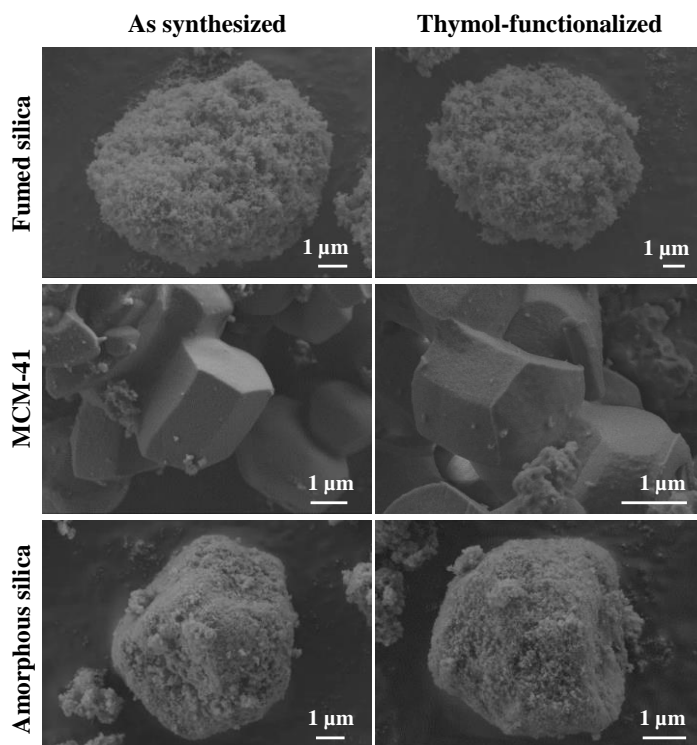
Figure 1. Characterization of particle size and particle shape by the FESEM of the bare and thymol-functionalized fumed silica, MCM-41 and amorphous silica materials.

The particle size distribution of the bare and functionalized materials in the presence of the culture broth used in the microbiological assays is shown in Table 1. The bare fumed silica particles showed a mean size distribution within the nanoscale range, which suggests the disaggregation of the sponge-like structures observed by FESEM. After the functionalization with the EOCs, particle size remained on the microscale, which suggests that the formation of an organic layer on the surface of particles stabilizes the original clusters. The bare MCM-41 particles displayed a similar size distribution to that determined by the FESEM analysis. The immobilization of EOCs on the MCM-41 surface increased the mean particle size. Finally, the bare amorphous silica materials showed a similar size

distribution on the microscale, which was in accordance with those determined by FESEM observations. After functionalization, size heterogeneously increased.

Table 1. The particle size and zeta potential of the different bare and EOC-immobilized silica particles in TSB (means and standard deviations, n=3).

Support	Immobilization	Size distribution d(0.5) (µm)	Zeta potential (mV)
Fumed silica	Bare	0.099±0.027	-14.0±2.6
	Carvacrol	5.407±0.121	-14.5±0.7
	Eugenol	5.232±0.330	-11.8±1.2
	Thymol	5.763±0.912	-13.4±1.2
	Vanillin	4.916±0.591	-10.4±2.1
MCM-41	Bare	1.414±0.019	-12.1±1.1
	Carvacrol	2.871±0.207	-10.1±0.4
	Eugenol	2.306±0.629	-11.1±0.8
	Thymol	2.282±0.158	-10.4±2.1
	Vanillin	2.551±0.337	-11.2±1.7
Amorphous silica	Bare	3.265±0.441	-11.4±0.6
	Carvacrol	4.853±0.581	-15.8±1.3
	Eugenol	8.694±0.795	-14.2±0.8
	Thymol	3.441±0.842	-14.8±0.6
	Vanillin	6.146±0.411	-8.45±0.7

Aggregation tendency can be explained by their zeta-potential values (Table 1), which fell within the instability range (-30 mV to +30 mV) so that the interaction between particles and some culture broth components were expected to form aggregation clusters (Ruiz-Rico et al., 2015). These data suggest that all

the functionalized particles presented a microscale size range. Hence these supports were unable to be endocytosed by bacteria and the whole antimicrobial effect was due to the bacteria that came into contact with the particle's surface.

The contents of EOCs (carvacrol, eugenol, thymol and vanillin) and APTES attached to the different solids (fumed silica, MCM-41 and amorphous silica) were determined by elemental and thermogravimetric analyses (see Table 2). These values were used to calculate the amount of the different solids required to evaluate the equivalent concentrations of the free and immobilized EOCs.

Table 2. Content (α) in grams of EOCs and APTES per gram of SiO_2 for the solids of fumed silica (FS), mesoporous silica (MCM-41) and amorphous silica (AS).

	Carvacrol		Eugenol		Thymol		Vanillin	
	α_{EOC} (g/g SiO_2)	α_{APTES} (g/g SiO_2)	α_{EOC} (g/g SiO_2)	α_{APTES} (g/g SiO_2)	α_{EOC} (g/g SiO_2)	α_{APTES} (g/g SiO_2)	α_{EOC} (g/g SiO_2)	α_{APTES} (g/g SiO_2)
FS	0.0084	0.0661	0.0499	0.1343	0.0072	0.0819	0.0886	0.0618
MCM-41	0.0181	0.1464	0.0652	0.1750	0.0758	0.1596	0.1886	0.1158
AS	0.0368	0.1015	0.0585	0.1274	0.0149	0.0994	0.0838	0.0640

3.3. Antimicrobial activity of the EOC-functionalized silica particles against *L. innocua*

The antimicrobial activity of the free and developed immobilized EOCs was established by determining the bacterial growth of two food-borne microorganisms by representing an example of gram-positive (*L. innocua*) and gram-negative bacteria (*E. coli*). Different ranges of concentrations were tested for each EOC in line with the literature (Belda-Galbis et al., 2014; Burt, 2004; Cava-Roda et al., 2012; Guarda et al., 2011). Figure 2 shows the bacterial count of *L. innocua* after 24 h of treatment with free and immobilized carvacrol, eugenol, thymol and vanillin. The inoculated initial microbial density is shown as a dotted

black line in the graphs, and allows us to distinguish if presence of the free or immobilized EOCs at different concentrations triggered a bacteriostatic or bactericide effect, or not, after 24 h of incubation.

For carvacrol (Figure 2A), addition of the free molecule to the culture broth within the 0.001-0.025 mg/mL range provoked very low antimicrobial activity (ca. 2-5% of reduced growth). However, the immobilization of EOCs on the three silica supports led to a reduction of between 2-6 logarithmic cycles of *L. innocua* at the same concentrations. At higher concentrations, the antimicrobial effect of the free carvacrol increased with the amount of added EOC, and reached total microbial growth inhibition at concentrations that equaled or were higher than 0.15 mg/mL. These results agree with previous studies, which have reported that treatment with 0.2 mg/mL of carvacrol brought about a reduction of 3 logarithmic cycles of *L. monocytogenes* after 5 h of treatment (Ait-Ouazzou et al., 2012). After immobilization, the minimum bactericidal concentration (MBC) was halved (0.075 mg/mL) when carvacrol was immobilized on the FS support, which demonstrates the positive effect of immobilization at both low and high concentrations.

Eugenol (Fig. 2B) affected *L. innocua* growth at higher concentrations than carvacrol; 1 mg/mL of free eugenol reduced the microorganism to undetectable levels, which is in accordance with the study of Gill and Holley (2006). The EOC displayed significantly greater antimicrobial activity after immobilization on MCM-41 and FS supports at low concentrations. Indeed, concentrations over 0.025 mg/mL and 0.3 mg/mL for the eugenol immobilized on the FS and MCM-41 supports, respectively, had a bactericidal effect. Despite this improvement, the MBC value remained at the same level. The eugenol-immobilized AS support progressively reduced the growth rate and had a bacteriostatic effect rather than bactericidal activity.

Thymol immobilization was the most remarkable enhancement of the antimicrobial effect. While addition of the free molecule at concentrations between 0.01 and 0.075 mg/mL only provoked reduced growth at about 1-3%, addition of immobilized thymol increased the antimicrobial effect, with a

bactericidal effect that fell within the 0.004-0.012 mg/mL range for the different supports. In fact MBC was established at 0.05 mg/mL for the thymol-functionalized FS and 0.075 mg/L for the thymol immobilized on the MCM-41 and AS particles. Addition of the free molecule did not reach the MBC within the whole range of concentrations studied in accordance with the results reported by Xiao et al. (2011), who stated that 0.02 mg/mL of thymol was able to reduce, but not inhibit, the microbial growth of *Listeria monocytogenes* in a growth medium. It should be taken into account that although thymol and carvacrol are isomers, the bactericidal effect of the two free compounds differed. While free carvacrol exhibited an MBC of 0.15 mg/mL, the MBC was not reached by free thymol, not even at concentrations of 0.2 mg/mL. After immobilization, the antimicrobial of both isomers was similar (an MBC of 0.05-0.075 mg/mL), which implies a more marked improvement of the antimicrobial activity of thymol.

Finally, vanillin had to be added at high concentrations to have an antimicrobial effect like that indicated in Figure 2D and in previous studies (Cava-Roda et al. 2012; Fitzgerald et al., 2004). In fact at free vanillin concentration of 2 mg/mL, only a reduction of 4.5 logarithmic cycles was achieved. Despite the poor antimicrobial activity of the free molecule, immobilization of vanillin on silica supports improved its antimicrobial activity on all the supports. Complete inhibition of *L. innocua* was accomplished after the treatment with 2 mg/mL of vanillin immobilized on the MCM-41 particles.
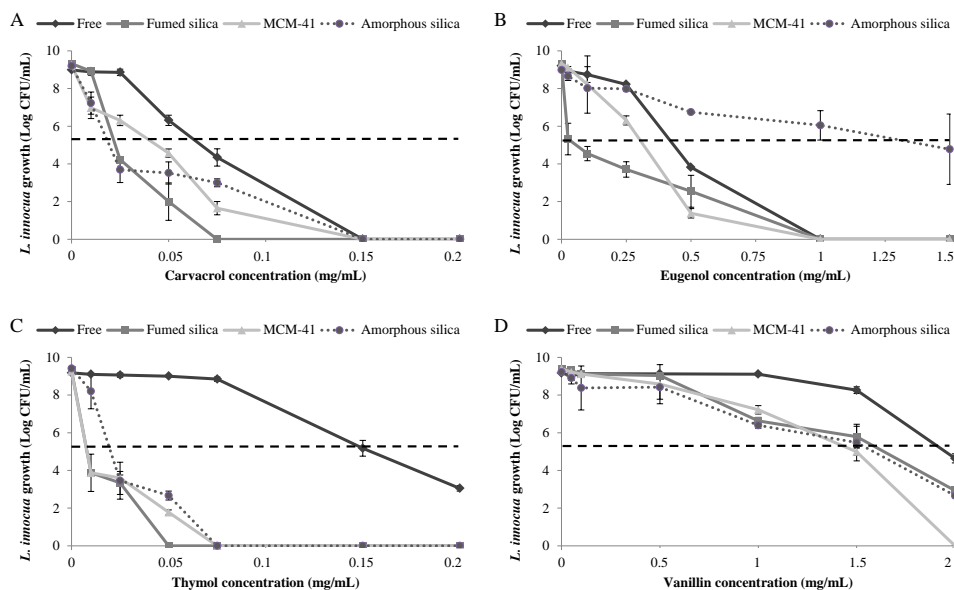
Figure 2. Growth (log$_{10}$ CFU/mL) of *L. innocua* after incubation with free and immobilized carvacrol (A), eugenol (B), thymol (C) and vanillin (D) according to the EOC concentration (means and standard deviations, n=3).

After demonstrating the effect of the immobilization of EOCs on reducing bacterial growth, a multiple regression analysis was performed to study the influence of the independent variables (EOC type, support type, EOC concentration, particle concentration, number of particles, mean size, zeta potential, EOC content and EOC density on the particles' surface) on the bacterial count. Table 3 shows the multiple linear regression model for the bacterial count for each EOC used. The R-Squared statistics indicates that the model fit explained 91.57% of variability in the bacterial count. As seen in the table, the statistical analysis confirmed the significant effect of EOC type, particle concentration, zeta potential and EOC density on bacterial growth, and how thymol was the most effective bioactive compound. Other independent variables did not appear to have any significant effect on microorganism inhibition, despite them being related to some significant independent variables (i.e. EOC density depended on

EOC content and mean particle size which, in turn, depended on zeta potential and type of solid). According to these data, the amount of particles and the EOC anchored to particles significantly determined the studied support's antimicrobial activity.

Table 3. Multiple linear regression models for bacterial growth ($\log_{10}$ CFU/mL) in the antimicrobial susceptibility assay of *L. innocua* according to the EOC (p < 0.001). Particle concentration (PC), Zeta potential (ZP), EOC density (ED).

EOC	Multiple linear regression model
Carvacrol	$\log_{10}$ CFU/mL = - 0.166*PC -0.444*ZP + 0.108*ED
Eugenol	$\log_{10}$ CFU/mL = - 0.166*PC -0.444*ZP + 0.108*ED
Thymol	$\log_{10}$ CFU/mL = -3.007 - 0.166*PC -0.444*ZP + 0.108*ED
Vanillin	$\log_{10}$ CFU/mL = - 0.166*PC -0.444*ZP + 0.108*ED

3.4. Antimicrobial activity of the EOC-functionalized silica particles against E. coli

Following the same procedure for *L. innocua*, the antimicrobial activity of the four free and immobilized EOCs included herein was tested against *E. coli*. As reported by other authors, *E. coli* was resistant to the treatment with carvacrol and vanillin at the higher concentrations studied (0.2 mg/mL for carvacrol; 2 mg/mL for vanillin) (Ait-Ouazzou et al., 2012; Guarda et al., 2011; Cava-Roda et al., 2012). Conversely to *L. innocua*, in which the poor effectiveness of these two free molecules significantly improved after immobilization on silica supports, immobilization did not lead to significant antimicrobial improvements against this bacterium (data not shown).

Conversely, strong *E. coli* growth inhibition took place after adding the immobilized eugenol and thymol to the growth broth. Figure 3A shows the bacterial count of *E. coli* after incubation with the free and immobilized eugenol.

As observed, addition of the free molecule at concentrations between 0.025 and 0.25 mg/mL only reduced the growth rate. In contrast, the treatment with 0.25 mg/mL of eugenol immobilized on MCM-41 and FS had a bactericidal effect with bacterial counts of 3.64 ± 0.40 and 4.45 ± 0.01 $\log_{10}$ CFU/mL for the eugenol-functionalized FS particles and MCM-41 particles, respectively. The MBC of free eugenol was established as 0.5 mg/mL in accordance with other studies (Dušan et al., 2006), whereas a concentration within the range of 1-1.5 mg/mL of immobilized EOC was needed to achieve total microorganism inhibition, except for the AS support.

The antimicrobial effect of thymol against *E. coli* is shown in Figure 3B. Neither free nor immobilized thymol caused any growth inhibition at the 0.01-0.05 mg/mL concentrations. However, high concentrations (0.075-0.2 mg/mL) of immobilized thymol on the MCM-41 and AS supports displayed improved antimicrobial activity compared to the free bioactive compound. So whereas the use of free thymol did not cause 100% growth inhibition at any of the tested concentrations, an MBC of 0.15 and 0.2 mg/mL was found for the immobilized thymol in the MCM-41 and amorphous silica particles.
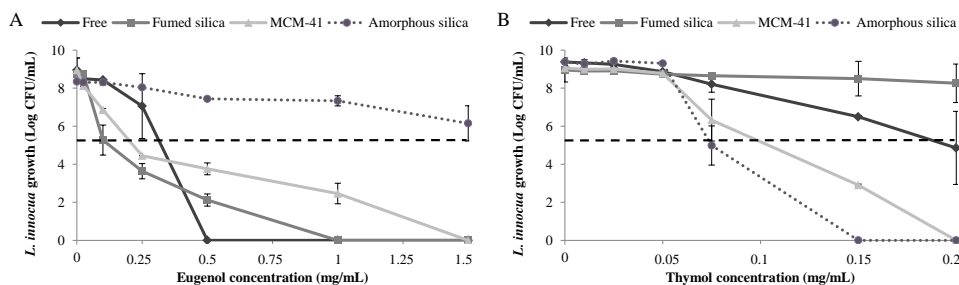

Figure 3. Growth ($\log_{10}$ CFU/mL) of *E. coli* after incubation with the free and immobilized eugenol (A) and thymol (B) according to EOC concentration (means and standard deviations, n=3).

It has been generally established that gram-positive bacteria are more sensitive than gram-negative ones when different EOCs are used (Ait-Ouazzou et al., 2012; Burt, 2004; Guarda et al., 2011). This behavior agrees with the results obtained herein. The poorer sensitivity of gram-negative bacteria to the action of the different EOCs could be due to differences in the structure and permeability of the bacterial cell membrane, such as the outer membrane that surrounds these microorganisms restricting the diffusion of hydrophobic compounds (Guarda et al., 2011).

According to several authors, the mechanism of action of EOCs on bacteria cells is based on the alteration of the cellular envelope of microorganisms. EOCs disrupt the cellular membrane with morphology modifications and cell permeabilization, cause pH homeostasis alterations, leakage of inorganic ions and loss of membrane potential, and inhibit cellular respiration and perturb lipid fractions of bacterial cytoplasmic membranes (Ait-Ouazzou et al., 2013; Fitzgerald et al., 2004; Gill & Holley, 2006). The simultaneous presence of a free hydroxyl group, a delocalized electron system in the molecule and a hydrophobic character that allows membrane accumulation appear essential for the antimicrobial activity of these EOCs (Ben Arfa et al., 2006; Nostro & Papalia, 2012).

A multiple regression analysis was also performed to study the influence of the independent variables (EOC type, support type, EOC concentration, particle concentration, number of particles, mean size, zeta potential, EOC content and EOC density on particles' surface) on *E. coli* growth. Table 4 shows the multiple linear regression model for the two EOC (R^2 = 96.86%). In this case, the significant independent variables were EOC type, EOC support, mean size, zeta potential and number of particles. The significant variables differed from the *L. innocua* results, but the statistical results were consistent between microorganisms; i.e., particle concentration, zeta potential and mean size determine number of particles. The support type also had a significant influence for the eugenol-functionalized solids, where FS particles were the most effective. The regression model indicated that the smaller the particle size, the lower the bacterial count. A large number of

particles in suspension enhanced the antimicrobial effect because the probability of a particle coming into contact with bacterial cells was higher.

Table 4. Multiple linear regression models for bacterial growth ($\log_{10}$ CFU/mL) in the antimicrobial susceptibility assay of *E. coli* according to the EOC (p < 0.001). Fumed silica (FS), Mean size (MS), Zeta potential (ZP), Particle number (PN).

EOC	Multiple linear regression model
Eugenol	Log_{10} CFU/mL = -2.542 - 5.115*FS + 0.551*MS - 0.654*ZP - 3.037 x 10^{-11}*PN
Thymol	Log_{10} CFU/mL = 0.551*MS - 0.654*ZP - 3.037 x 10^{-11}*PN

3.5. Antimicrobial effect of EOCs on a real food system

Finally, in order to assess the antimicrobial activity of the developed supports against *L. innocua* in real food, the antimicrobial activity of two solids that exhibited the greatest antibacterial activity was tested in pasteurized skimmed milk. Drinking pasteurized milk has been associated with some outbreaks of listeriosis due to recontamination after heat treatment (Cava-Roda et al., 2012). *Listeria* is able to grow under refrigeration and to survive in freezing environments (Gandhi & Chikindas, 2007). Therefore, the combined use of antimicrobials with refrigerated storage can be a suitable approach to prevent pathogen bacteria from proliferating in milk (Belda-Galbis et al., 2014).

Figure 5 shows the microbial growth of *L. innocua* inoculated in pasteurized skimmed milk (control) and milk after incorporating the free and MCM-41 immobilized thymol and vanillin. Presence of a lower free thymol concentration (0.05 mg/mL) in inoculated milk did not appear to have a significant inhibitory effect compared to the positive control. The ineffectiveness of this thymol level agrees with previous studies, such as Xiao et al. (2011), which showed no effect after 0.04 mg/mL of thymol treatment on reduced fat milk. Higher concentrations displayed bacteriostatic activity over time, which improved with increasing EOC

concentrations. Similar results were obtained for the treatment with the thymol-functionalized solid, particularly for the highest concentration (0.5 mg/mL). The antimicrobial activity of vanillin (Fig. 5B) was slower than the *in vitro* results due to the incubation conditions (4 ºC) and the food matrix composition. Nevertheless, immobilized vanillin displayed better antimicrobial activity than the free compound, which allowed microorganisms to grow. Low immobilized-vanillin concentrations had a bacteriostatic effect, whereas the highest concentration (1 mg/mL) reduced microbial growth by 1.5 logarithmic cycles on incubation day 3.

The differences to the *in vitro* results were caused mainly by refrigerated storage and the interaction with some food matrix components. The literature establishes that bactericidal concentrations increase for lower temperatures, probably due to the activation of the stress response in hostile environments. Microorganisms modify their membrane composition to increase their cold tolerance, so EOC resistance may also increase (Belda-Galbis et al., 2014). EOC can also interact with hydrophobic constituents (lipids and proteins) of complex food systems, such as milk, with diminished antimicrobial effectiveness (Cava-Roda et al., 2012; Shah et al., 2012).
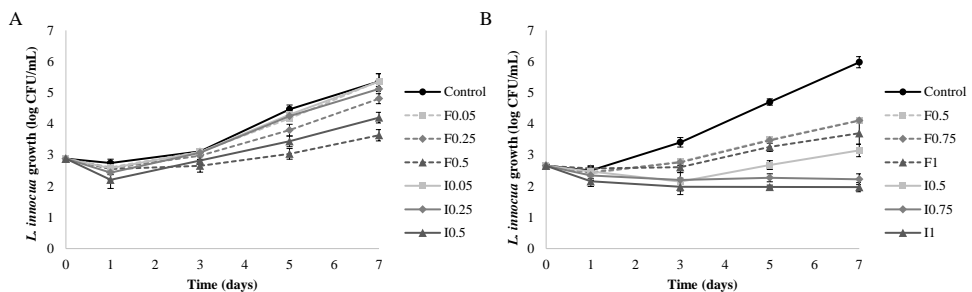

Figure 4. Microbial growth of *L. innocua* in skimmed milk with free and immobilized thymol (A) and vanillin (B) during 7 storage days at refrigeration temperatures (means and standard deviations, n=3).

4. Conclusions

We report herein the synthesis, characterization and evaluation of a collection of 12 antimicrobial devices based on anchoring carvacrol, eugenol, thymol and vanillin to the surface of silica supports of different particle sizes, and with distinct textural properties and chemical reactivities. Preserving the antimicrobial activity of EOCs allowed us to conclude that the proposed immobilization methodology allowed the functional hydroxyl moiety of carvacrol, eugenol, thymol and vanillin to be preserved. Despite the fact that different EOC-silica support combinations yielded distinct antimicrobial activity, the antimicrobial effect against *L. innocua* and *E. coli* of all the EOCs-functionalized supports improved compared to free compounds. These results suggest that the immobilization of EOCs onto silica supports might be considered a novel strategy to develop a new generation of antimicrobial systems that may not only enhance the antimicrobial activity of EOs, but also mask their characteristic odor/taste.

Acknowledgements

References

Ait-Ouazzou, A., Espina, L., Gelaw, T. K., Lamo-Castellví, S., Pagán, R., & García-Gonzalo, D. (2013). New insights in mechanisms of bacterial inactivation by carvacrol. *Journal of applied microbiology, 114*(1), 173-185.

Belda-Galbis, C.M., Leufven, A., Martínez, A., & Rodrigo, D. (2014). Predictive microbiology quantification of the antimicrobial effect of carvacrol. *Journal of Food Engineering, 141*, 37-43.

Ben Arfa, A., Combes, S., Preziosi-Belloy, L., Gontard, N., & Chalier, P. (2006). Antimicrobial activity of carvacrol related to its chemical structure. *Letters in Applied Microbiology*, *43*(2), 149-154.

Bernardos, A., Marina, T., Žáček, P., Pérez-Esteve, É., Martínez-Mañez, R., Lhotka, M., Kouřimská, L., Pulkrábek, J., & Klouček, P. (2015). Antifungal effect of essential oil components against *Aspergillus niger* when loaded into silica mesoporous supports. *Journal of the Science of Food and Agriculture, 95*, 2824–2831.

Burt, S. (2004). Essential oils: Their antimicrobial properties and potential applications in food – A review. *International Journal of Food Microbiology, 94*, 223–253.

Capeletti, L.B., de Oliveira, L.F., Gonçalves, K.D.A., de Oliveira, J.F.A., Saito, Â., Kobarg, J., & Cardoso, M.B. (2014). Tailored Silica-Antibiotic Nanoparticles: Overcoming Bacterial Resistance with Low Cytotoxicity. *Langmuir, 30*, 7456–7464.

Cava-Roda, R.M., Taboada-Rodríguez, A., Valverde-Franco, M.T., & Marín-Iniesta, F. (2012). Antimicrobial activity of vanillin and mixtures with cinnamon and clove essential oils in controlling *Listeria monocytogenes* and *Escherichia coli* O157: H7 in milk. *Food and Bioprocess Technology, 5*(6), 2120-2131.

Climent, E., Marcos, M.D., Martínez-Máñez, R., Sancenón, F., Soto, J., Rurack, K., & Amorós, P. (2009). The determination of methylmercury in real samples using organically capped mesoporous inorganic materials capable of signal amplification. *Angewandte Chemie, 121*(45), 8671-8674.

Contado, C., Ravani, L., & Passarella, M. (2013). Size characterization by sedimentation field flow fractionation of silica particles used as food additives. *Analytica chimica acta, 788*, 183-192.

Darvishi, E., Omidi, M., Bushehri, A.A.S., Golshani, A., & Smith, M.L. (2013). The antifungal eugenol perturbs dual aromatic and branched-chain amino acid permeases in the cytoplasmic membrane of yeast. *PloS one, 8*(10), e76028.

Dušan, F., Marián, S., Katarína, D., & Dobroslava, B. (2006). Essential oils—their antimicrobial activity against *Escherichia coli* and effect on intestinal cell viability. *Toxicology in vitro, 20*(8), 1435-1445.

European Commission. Regulations: commission implementing regulation (EU) No 872/2012. Official Journal of the European Union, L: Legislation 2012, 55, 24.

Fitzgerald, D.J., Stratford, M., Gasson, M.J., Ueckert, J., Bos, A., & Narbad, A. (2004). Mode of antimicrobial action of vanillin against *Escherichia coli*, *Lactobacillus plantarum* and *Listeria innocua. Journal of applied microbiology*, 97(1), 104-113.

Fuentes, A., Barat, J.M., Fernández-Segovia, I., Serra, J.A. (2008). Study of sea bass (*Dicentrarchus labrax L.*) salting process: Kinetic and thermodynamic control. *Food Control, 8*(19), 757-763.

Friedman, M. (2014). Chemistry and multibeneficial bioactivities of carvacrol (4-isopropyl- 2-methylphenol), a component of essential oils produced by aromatic plants and spices. *Journal of Agricultural & Food Chemistry, 62*, 7652–7670.

Gandhi, M., & Chikindas, L. (2007). Listeria: a foodborne pathogen that knows how to survive. *International Journal of Food Microbiology, 113*, 1-15.

Gill, A.O., & Holley, R.A. (2006). Disruption of *Escherichia coli*, *Listeria monocytogenes* and *Lactobacillus sakei* cellular membranes by plant oil aromatics. *International journal of food microbiology, 108*(1), 1-9.

Guarda, A., Rubilar, J.F., Miltz, J., & Galotto, M.J. (2011). The antimicrobial activity of microencapsulated thymol and carvacrol. *International journal of food microbiology, 146*(2), 144-150.

Higueras, L., López-Carballo, G., Hernández-Muñoz, P., Catalá, R., & Gavara, R. (2014). Antimicrobial packaging of chicken fillets based on the release of carvacrol from chitosan/cyclodextrin films. *International journal of food microbiology, 188*, 53-59.

Hyldgaard, M., Mygind, T., & Meyer, R.L. (2012). Essential oils in food preservation: mode of action, synergies, and interactions with food matrix components. *Frontiers in microbiology, 3*(12), 1-24.

Janatova, A., Bernardos, A., Smid, J., Frankova, A., Lhotka, M., Kourimská, L., Pulkrabeka, J., & Kloucek, P (2015) Long-term antifungal activity of volatile essential oil components released from mesoporous silica materials. *Industrial Crops and Products, 67*, 216–220.

Jo, Y.J., Chun, J.Y., Kwon, Y.J., Min, S.G., Hong, G.P., & Choi, M.J. (2015). Physical and antimicrobial properties of trans-cinnamaldehyde nanoemulsions in water melon juice. *LWT - Food Science and Technology, 60*, 444-451.

Li, L.L. & Wang, H. (2013). Enzyme-coated mesoporous silica nanoparticles as efficient antibacterial agents *in vivo*. *Advanced Healthcare Materials, 2*(10), 1351-1360.

Majeed, H., Bian, Y.Y., Ali, B., Jamil, A., Majeed, U., Khan, Q.F., Iqbal, K.J., Shoemaker, C.F., & Fang, Z. (2015). Essential oil encapsulations: uses, procedures, and trends. *RSC Advances, 5*(72), 58449-58463.

Márquez-Alvarez, C., Sastre, E., & Pérez-Pariente, J. (2004). Solid catalysts for the synthesis of fatty esters of glycerol, polyglycerols and sorbitol from renewable resources. *Topics in Catalysis, 27*(1-4), 105-117.

Nostro, A., & Papalia, T. (2012). Antimicrobial activity of carvacrol: current progress and future prospectives. *Recent patents on anti-infective drug discovery, 7*(1), 28-35.

Park, S.Y., & Pendleton, P. (2012). Mesoporous silica SBA-15 for natural antimicrobial delivery. *Powder Technology, 223*, 77-82.

Park, S.Y., Barton, M. & Pendleton, P. (2012). Controlled release of allyl isothiocyanate for bacteria growth management. *Food Control, 23*(2), 478-484.

Park, S.Y., Barton, M., & Pendleton, P. (2011). Mesoporous silica as a natural antimicrobial carrier. *Colloids and Surfaces A: Physicochemical and Engineering Aspects, 385*(1), 256-261.

Pędziwiatr-Werbicka, E., Miłowska, K., Podlas, M., Marcinkowska, M., Ferenc, M., Brahmi, Y., Katir, N., Majoral, J.P., Felczak, A., Boruszewka, A., Lisowska, K., Bryszewska, M., & El Kadib, A. (2014). Oleochemical-tethered SBA-15-type silicates with tunable nanoscopic order, carboxylic surface, and hydrophobic framework: cellular toxicity, hemolysis, and antibacterial activity. *Chemistry-A European Journal, 20*(31), 9596-9606.

Pérez-Esteve, É., Ruiz-Rico, M., Martínez-Máñez, R., & Barat, J.M. (2015). Mesoporous silica-based supports for the controlled and targeted release of bioactive molecules in the gastrointestinal tract. *Journal of food science*, *80*(11), E2504-E2516.

Qi, G., Li, L., Yu, F., & Wang, H. (2013). Vancomycin-modified mesoporous silica nanoparticles for selective recognition and killing of pathogenic gram-positive bacteria over macrophage-like cells. *ACS applied materials & interfaces, 5*(21), 10874-10881.

Ravichandran, M., Hettiarachchy, N.S., Ganesh, V., Ricke, S.C., & Singh, S. (2011). Enhancement of antimicrobial activities of naturally occurring phenolic compounds by nanoscale delivery against *Listeria monocytogenes*, *Escherichia coli* O157: H7 and *Salmonella Typhimurium* in broth and chicken meat system. *Journal of Food Safety, 31*(4), 462-471.

Ribes, S., Fuentes, A., Talens, P., & Barat, J.M. (2016). Use of oil-in-water emulsions to control fungal deterioration of strawberry jams. *Food Chemistry, 211*, 92-99.

Ruiz-Rico, M., Daubenschüz, H., Pérez-Esteve, É., Marcos, M. D., Amorós, P., Martínez-Máñez, R., & Barat, J. M. (2016). Protective effect of mesoporous silica particles on encapsulated folates. *European Journal of Pharmaceutics and Biopharmaceutics, 105*, 9-17.

Ruiz-Rico, M., Fuentes, C., Pérez-Esteve, É., Jiménez-Belenguer, A.I., Quiles, A., Marcos, M.D., Martínez-Máñez, R., & Barat, J.M. (2015). Bactericidal activity of caprylic acid entrapped in mesoporous silica nanoparticles. *Food Control, 56*, 77-85.

Shah, B., Davidson, P. M., & Zhong, Q. (2012). Nanocapsular dispersion of thymol for enhanced dispersibility and increased antimicrobial effectiveness against *Escherichia coli* O157: H7 and *Listeria monocytogenes* in model food systems. *Applied and environmental microbiology, 78*(23), 8448-8453.

Si, W., Gong, J., Tsao, R., Zhou, T., Yu, H., Poppe, C., Johnson, R., & Du, Z. (2006). Antimicrobial activity of essential oils and structurally related synthetic food additives towards selected pathogenic and beneficial gut bacteria. *Journal of Applied Microbiology, 100*(2), 296-305.

Siahaan, E.A., Meillisa, A., Woo, H. C., Lee, C.W., Han, J.H., & Chun, B.S. (2013). Controlled release of allyl isothiocyanate from brown algae *Laminaria japonica* and mesoporous silica MCM-41 for inhibiting food-borne bacteria. *Food Science and Biotechnology, 22*(1), 19-24.

Smith, R.L., Cohen, S.M., Doull, J., Feron, V.J., Goodman, J.I., Marnett, L.J., Portoghese, P.S., Waddell, W.J., Wagner, B.M., Hall, R.L., Higley, N.A., Lucas-Gavin, C., & Adams, T.B. (2005). A procedure for the safety evaluation of natural flavor complexes used as ingredients in food: essential oils. *Food and chemical toxicology, 43*(3), 345-363.

Suntres, Z.E., Coccimiglio, J., & Alipour, M. (2015). The bioactivity and toxicological actions of carvacrol. *Critical reviews in food science and nutrition, 55*(3), 304-318.

Turek, C., & Stintzing, F.C. (2013). Stability of essential oils: a review. *Comprehensive Reviews in Food Science and Food Safety, 12*(1), 40-53.

Uboldi, C., Giudetti, G., Broggi, F., Gilliland, D., Ponti, J., & Rossi, F. (2012). Amorphous silica nanoparticles do not induce cytotoxicity, cell transformation or genotoxicity in Balb/3T3 mouse fibroblasts. *Mutation Research/Genetic Toxicology and Environmental Mutagenesis*, *745*(1), 11-20.

Walls, H.J., Zhou, J., Yerian, J.A., Fedkiw, P.S., Khan, S.A., Stowe, M.K., & Baker, G.L. (2000). Fumed silica-based composite polymer electrolytes: synthesis, rheology, and electrochemistry. *Journal of Power Sources*, *89*(2), 156-162.

Weiss, J., Gaysinsky, S., Davidson, M., & McClements, D.J. (2009). Nanostructured encapsulation systems: food antimicrobials. *Global issues in food science and technology, 1*, 425-479.

Xiao, D., Davidson, P.M., & Zhong, Q. (2011). Spray-dried zein capsules with coencapsulated nisin and thymol as antimicrobial delivery system for enhanced antilisterial properties. *Journal of agricultural and food chemistry, 59*(13), 7393-7404.

Zengin, N., Yüzbaşıoğlu, D., Ünal, F., Yılmaz, S., & Aksoy, H. (2011). The evaluation of the genotoxicity of two food preservatives: sodium benzoate and potassium benzoate. *Food and Chemical Toxicology, 49*(4), 763-769.

6. GENERAL DISCUSSION

While the present PhD thesis was underway, nano- and microstructured materials were used to solve two of the main current problems of the food industry: a) protecting labile bioactive molecules under food processing conditions and b) enhancing the antimicrobial properties of naturally-occurring compounds. Bearing in mind these two ideas, the general objective of the present PhD thesis was to enhance the stability of one of the most instable water soluble vitamins (folates) and to develop new antimicrobials agents based on encapsulation and attachment to a surface of large amounts of bioactive molecules. Both approaches share the use of mesoporous silica materials as inorganic supports for the encapsulation of bioactive molecules and/or the provider of a reactive surface capable of anchoring organic molecules.

Despite the common nature of the chemical principles that both approaches involve, the objectives and results were divided into two different chapters to offer a better understanding of the goals, methodology and relevant findings. Chapter 1 deals with the use of amine-functionalized mesoporous silica microparticles for folates encapsulation. Chapter 2 addresses the use of silica supports to encapsulate or anchor antimicrobial molecules. Both these chapters were divided into different research articles. In this way, throughout both chapters and the five resulting articles, the findings of all the studies carried out to assess the general objective of this thesis are discussed in detail. Hence this section aims to sequentially and relatedly discuss all the results in order to address the issue holistically.

Mesoporous silica materials have proved remarkably potential in the design of efficient smart delivery systems for biomedical, agriculture and food sciences. These materials present mesopores of between 2 and 50 nm that confer them a great loading capacity. Moreover, the surface of mesoporous silica particles has a high concentration of structural defects that come the form of silanol groups (Si-OH), which can easily react with trialkoxysilane derivatives in order to create hybrid organic–inorganic materials. These remarkable features have led to the

development of "molecular gates" capable of hindering or allowing cargo delivery at a controlled rate according to a target external stimulus.

In particular, changes in pH along the gastrointestinal tract were used in this thesis as stimuli to trigger the release of folates. Folate intake should be accurately regulated to assure that the required level is obtained, but is not overdosed by consuming supplements or fortified food due to problems associated with unmetabolized folic acid accumulating in blood. Thus 5-formyltetrahydrofolate and folic acid were entrapped in amine-functionalized mesoporous silica microparticles that were tightly capped at pH 2, but displayed sustained delivery at a neutral pH. The gated system mechanism is based on the combination of low folate solubility at a low pH, the gating effect of the polyamines anchored to the surface of mesoporous materials due to electrostatic repulsions, and the interaction between the polyammonium moieties and anionic species of the buffer. After stating the controlled release, the stability of the free and entrapped vitamins after an acidic pH, high temperature and light exposure was studied (**Article 1**). Both encapsulated vitamins were highly preserved in the acidic environment by the pH-responsive gated material. Encapsulated 5-formyltetrahydrofolate showed better stability than free vitamer after exposure to high temperature. In addition, the mesoporous support enhanced folic acid stability to visible and ultraviolet light stress. In general, the designed encapsulation strategy better protected vitamers than the well-known addition of antioxidants such as ascorbic acid.

In a second step (**Article 2**), the capability of the smart delivery system to modulate folic acid bioaccessibility in a real context was evaluated by incorporating the support into fruit juices and simulating human digestion. The folic acid delivery results confirmed that the release was hindered during the simulated pass through the stomach, but addition of the simulated intestinal fluid caused sustained delivery with a maximum value of 84 μg of FA per mg of solid at 4 h of digestion. The encapsulation system allowed us to achieve the dietary reference intake of folates with a small amount (ca. 5 mg) of the mesoporous

support. In addition, the ability of the encapsulation system to enhance entrapped folic acid stability after food production and storage simulation was assessed. The results showed improved stability of the free and entrapped folic acid in orange juice compared with apple juice given the presence of ascorbic acid in citrus juice. Nevertheless, the encapsulation system protected the vitamin against heat treatment, photodegradation and storage to a greater extent for the apple juice samples, in which ascorbic acid content is negligible.

Therefore, the results obtained in Articles 1 and 2 (Chapter 1) confirmed the suitability of mesoporous silica particles as a support for folate encapsulation and protection in not only buffer systems, but also in real fortified beverages (i.e. fruit juices), and with further advantages than other reported encapsulation systems, e.g., controlled vitamin release and, thus, bioaccessibility at the site of action.

In order to evaluate silica particles' ability to develop a new generation of antimicrobial agents capable of reverting the problems of current synthetic biopesticides, two alternatives were proposed: encapsulation of molecules with antimicrobial properties in the voids of silica particles; anchoring organic molecules to the surface of particles.

Following the first approach, **Article 3** studied the encapsulation of naturally-occurring antimicrobial compound caprylic acid in mesoporous silica nanoparticles to maintain antimicrobial activity, and to control the delivery of fatty acid and mask its unpleasant organoleptic properties. The delivery results displayed a burst release of fatty acid at the beginning, with maximum release after 3 h of particle suspension in the nutrient broth. The bacterial viability assays showed the biocompatibility of unloaded nanoparticles with microorganisms and bacterial inhibition with the free and encapsulated caprylic acid. In general, fatty acid was more effective against gram-positive microorganisms than for gram-negative bacteria. The antibacterial activity of free and entrapped caprylic acid against *E. coli* remained within the same range (18.5–20 mM), but the minimum bactericidal concentration of the encapsulated caprylic acid slightly increased for *S. enterica* (20–22.5 mM), *S. aureus* and *L. monocytogenes* (18.5–20 mM) compared with the

free fatty acid. The transmission electronic microscopy images of the bacterial cells treated with caprylic acid-loaded nanoparticles showed cell envelope disintegration, which confirmed the bactericidal effect of fatty acid.

Having established the suitability of mesoporous silica particles to create antimicrobial agents due to their loading capacity, the possibility of immobilizing antimicrobial compounds on the surface of silica particles was studied in Articles 4 and 5. Antimicrobial "nanobullets", based on amine-functionalized mesoporous silica nanoparticles, were evaluated in **Article 4**. The immobilization of large amount of polyamines (ca. 0.36 g/g solid) in the silica support generated particles with highly positively charged surfaces that completely inhibited the microbial growth of *L. monocytogenes* and *E. coli*. The minimum bactericidal concentration of the nanodevice was approximately 100-fold lower than that of the free diethylenetriamine for *L. monocytogenes*. Microscopy observations showed cell aggregation and cell envelope damage, which finally resulted in bacterial cell death. This outstanding enhancement of the antibacterial effect was probably the combination of bacterium-particle aggregation favored by attractive electrostatic interactions between the positively charged nanoparticles and the negatively charged bacteria, and then the polyamines corona given the high local concentration of amines in the nanoparticles attached to the bacterial surface. In this study, the cell viability assays on HCT116, HEPG2, HK2 and HeLa cells indicated that all the cell lines exhibited a high level of cell viability after treatment with the amine-functionalized nanoparticles, which confirmed the biocompatibility of the proposed antimicrobial agent. Thus antimicrobial "nanobullets" were incorporated into apple nectar contaminated with *L. monocytogenes* to confirm their antimicrobial effect in a real food matrix.

In a later step, essential oil components carvacrol, eugenol, thymol and vanillin were immobilized in three silica supports (fumed silica, mesoporous silica and amorphous silica) to create antimicrobial agents with improved features compared with the free substances (**Article 5**). The bioactive compounds had been previously derivatized to covalently immobilize them on the surface of the

supports that preserved functional hydroxyl moiety, whose presence is critical for their antimicrobial activity. The bacterial susceptibility results revealed inhibitory activity maintenance against *L. innocua* and *E. coli* compared with the treatment with the free essential oil components. In fact, the immobilization of the essential oil components enhanced bactericidal activity for the functionalized supports. Finally, some of the antimicrobial solids (thymol and vanillin immobilized in mesoporous silica microparticles) were incorporated into pasteurized skimmed milk contaminated with *L. innocua* to assess their potential application to prevent microbial growth in food products in combination with refrigerated storage. The results showed the improved effect of immobilized vanillin in comparison with the free vanillin, with a maximum reduction of 1.5 logarithmic cycles after 3 storage days.

The development of new antimicrobial agents based on the encapsulation or immobilization of naturally-occurring antimicrobial substances allowed compounds with recognized bactericidal properties to be used, but with limited application due to their sensorial features (odor and flavor). Additionally, the obtained solids displayed antimicrobial activity preservation and a greatly enhanced inhibitory effect in some cases, which led to the required amount of antimicrobial to be reduced.

Despite the advantages described for the proposed devices, applying nanotechnology to the agri-food sector is still a relatively new concept given issues of product labeling, potential health risks, and lack of unifying regulations. Currently there are major gaps in our knowledge about nanomaterials in the food sector that need further research. First, a clear strict definition of nanoparticles is needed. Validated methods for the *in situ* detection and characterization of nanomaterials in complex food matrices should be developed by ideally using relatively easy procedures with equipment that is currently available in most laboratories. Precise toxicology and absorption, metabolism, distribution and excretion profile studies should be conducted. The long-term health consequences of ingesting nanoparticles via food have to be investigated.

Accurate risk assessment methodologies should be provided by scientific organizations. Finally, adequate regulations on nanotechnology applications for food and related products should be developed by the regulatory authorities. Once these limitations have been solved, approved nanomaterials might be used as safely technologies in the food industry to make the most of their excellent antimicrobial properties.

7. CONCLUSIONS AND PERSPECTIVES

Conclusions

- Amine-functionalized mesoporous silica microparticles of the MCM-41 family capable of modifying folates bioaccessibility during *in vitro* digestion as a result of changes in pH have been successfully synthesized and characterized.

- Developed smart delivery systems are able to improve the stability of folic acid and folates while exposed to different pH values, high temperature, and visible and ultraviolet light. Protective action has been demonstrated not only in an *in vitro* liquid matrix (buffer), but also in real liquid food (fruit juices).

- Amine-gated mesoporous silica particles have the potential to act as vitamin-based smart delivery systems that offer new opportunities for the development of novel functional food.

- Three different antimicrobial agents, based on the use of silica supports as either a suitable encapsulating matrix or a suitable surface to anchor organic molecules have been prepared, characterized and evaluated.

- Caprylic acid encapsulation in mesoporous silica nanoparticles shows the preservation of the bactericidal activity of fatty acid after encapsulation within a similar range to the free compound. In addition, encapsulation would avoid problems related with unpleasant sensory properties of fatty acid, interaction with food matrices and could be used as a smart delivery system after incorporating molecular gates.

- The decoration of the external surface of mesoporous silica nanoparticles with polyamines creates particles with a highly positively charged surface, which are able to act as highly effective antimicrobial "nanobullets" against the two food-borne microorganisms (*L. innocua* and *E. coli*) with no toxicity for human cells.

- The covalent anchoring of four different essential oil components to the external surface of different porous silica particles allows the development of

antimicrobial devices, which increases the bactericidal effect of an equivalent amount of the free active principles, and odor perception is masked.

- The incorporation of amine-functionalized particles into fruit nectar and the incorporation of essential oil components immobilized to porous silica particles into skimmed milk have revealed the potential application of these antimicrobial devices to prevent microbial growth in food products.

Perspectives

- These results can be extrapolated to the encapsulation and protection of other bioactive compounds of nutritional interest.

- The *in vivo* evaluation of the developed smart delivery systems can be performed to study the bioaccessibility of folates in a real system, the acute and chronic toxicity of delivery supports, the effect of particles on the environment, and the stability of the supports in food matrices.

- The possible future development related with antimicrobials is the design of antimicrobial surfaces or new antimicrobial particles based on food-grade materials, such as cellulose, or other naturally-occurring antimicrobial compounds.

8. APPENDICES

Appendix I. Abbreviations and Acronyms

^{1}H NMR	^{1}H nuclear magnetic resonance
AA	Ascorbic acid
Ag	Silver
ANOVA	Analysis of variance
AMS	Anionic-templated mesoporous silica material
APTES	(3-Aminopropyl)triethoxysilane
AS	Amorphous silica particles
Au	Gold
ATP	Adenosine triphosphate
B-N	Bare nanoparticles
BET	Brunauer, Emmett and Teller model
BJH	Barret, Joyner and Halenda model
BMP-7	Bone morphogenetic protein-7
C3	*N*-3-(trimethoxysilyl)propyl ethylenediamine triacetic acid trisodium salt
C3-N	Carboxylate-functionalized particles
CA	Caprylic acid
CaCl$_2$	Calcium chloride
CaO	Calcium oxide
CC	Cytoplasmic content
CD	Cell wall and membrane damage
CECT	Colección Española de Cultivos Tipo
CeO$_2$	Cerium oxide
CFU	Colony-forming unit
CH$_3$OH	Methanol
CLSI	Clinical and Laboratory Standards Institute
CM	Cell membrane
CTABr	*N*-cetyltrimethylammonium bromide
Cu	Cooper
CuO	Cooper oxide
CW	Cell wall
DDAB	Didodecyldimethylammonium bromide
DLS	Dynamic Light Scattering
DMEM	Dulbecco's modified eagle's medium
DMSO	Dimethyl sulfoxide
DNA	Deoxyribonucleic acid
DRI	Dietary Reference Intake
DSMZ	German Resource Centre for Biological Material

231

ε-PL	ε-poly-L-lysine
EFSA	European Food Safety Authority
EOs	Essential oils
EOCs	Essential oil components
ER	Empty regions
E-FA	Encapsulated folic acid
E-FO	Encapsulated 5-formyltetrahydrofolate
FA	Folic acid
FBS	Fetal Bovine Serum
FDA	Food and Drug Administration
Fe_2O_3/Fe_3O_4	Iron Oxide
FESEM	Field Emission Scanning Electron Microscopy
FFAs	Free fatty acids
FO	5-formyltetrahydrofolate
F-FA	Free folic acid
F-FO	Free 5-formyltetrahydrofolate
FS	Fumed silica particles
FSM	Folded Sheet Mesoporous Materials
GC-MS	Gas chromatography–mass spectrometry
GRAS	Generally Recognized As Safe
H_2SO_4	Sulfuric acid
HCl	Hydrochloric acid
HCT116	Human colon carcinoma cells
HeLa	Human cervix carcinoma cells
HEPG2	Human liver carcinoma cells
HMS	Hexagonal Mesoporous Silica
HK2	Human kidney epithelial cells
HPLC	High liquid performance chromatography
IUPAC	International Union of Pure and Applied Chemistry
KCl	Potassium chloride
KIT	Korea Advanced Institute of Science and Technology material
KOH	Potassium hydroxide
log	Logarithm
LSD	Least significant difference
Lys	Lysozyme
MBC	Minimum bactericidal concentration
MCM	Mobil Composition of Matter
MgO	Magnesium oxide
$MgSO_4$	Magnesium sulfate
MSNs	Mesoporous silica nanoparticles

MSPs	Mesoporous silica particles
MSU	Michigan State University material
N0	Calcined nanoparticles
N1	Caprylic acid loaded nanoparticles
N3	*N*-(3-trimethoxysilylpropyl)diethylenetriamine
N3-N	Amine-functionalized nanoparticles
NaCl	Sodium chloride
NAD	Nicotinamide adenine dinucleotide
NADPH	Nicotinamide adenine dinucleotide phosphate
NaHCO$_3$	Sodium bicarbonate
NaOH	Sodium hydroxide
NFM	Nanoporous folic-acid templated material
NPs	Nanoparticles
Na$_2$HPO$_4$	Sodium phosphate dibasic
NaH$_2$PO$_4$	Sodium phosphate monobasic
PAA	Peracetic acid
PBS	Phosphate Buffer Solution
PCA	Plate count agar
PLGA	Poly (DL-lactide-co-glycolide)
PMOs	Periodic Mesoporous Organosilicas
PSD	Particle size distribution
PXRD	Powder X-ray diffraction
RB	Ringer buffer
ROS	Reactive oxygen species
SBA	Santa Barbara Amorphous material
SBET	BET surface area
SiO$_2$	Silicon dioxide
TBAHS	Tetrabutylammonium hydrogen sulfate
TBX	Tryptone bile x-glucuronide agar
TEAH$_3$	Triethanolamine
TEM	Transmission electron microscopy
TEOS	Tetraethylorthosilicate
TGA	Thermogravimetric analysis
TiO$_2$	Titanium dioxide
tRNA	Transfer ribonucleic acid
TSB	Tryptic soy broth
TUD	Technische Universiteit Delft material
UV	Ultraviolet
UVM	Universidad Valencia Material
ZnO	Zinc oxide

Appendix II. List of Publications included in this thesis

Ruiz-Rico, M., Fuentes, C., Pérez-Esteve, É., Jiménez-Belenguer, A.I., Quiles, A., Marcos, M.D., Martínez-Máñez, R., & Barat, J.M. (2015). Bactericidal activity of caprylic acid entrapped in mesoporous silica nanoparticles. *Food Control, 56,* 77-85.

Ruiz-Rico, M., Daubenschüz, H., Pérez-Esteve, É., Marcos, M.D., Amorós, P., Martínez-Máñez, R., & Barat, J.M. (2016). Protective effect of mesoporous silica particles on encapsulated folates. *European Journal of Pharmaceutics and Biopharmaceutics*, 105, 9-17.

Pérez-Esteve, É., **Ruiz-Rico, M.**, Martínez-Máñez, R., & Barat, J.M. (2016). Mesoporous silica particles as encapsulation and delivery systems for food ingredients and nutraceuticals. In: Sen, S., & Pathak, Y. (Eds) Nanotechnology in Nutraceuticals: Production to Consumption. CRC Press, 397–438.

Ruiz-Rico, M., Pérez-Esteve, É., & Barat, J. M. Use of nanotechnology as an antimicrobial tool in the food sector. In: Dhawan, A., Shanker, R., Singh, S., Kumar, A. (Ed.) Nanobiotechnology: Human Health and the Environment. CRC Press, *In press*.

Ruiz-Rico, M., Pérez-Esteve, É., Lerma-García, M.J., Marcos, M.D., Martínez-Máñez, R., & Barat, J.M. (2017). Protection of folic acid through encapsulation in mesoporous silica particles included in fruit juices. *Food Chemistry,* 218, 471-478.

Ruiz-Rico, M., Pérez-Esteve, É., de la Torre, C., Jiménez-Belenguer, A.I., Quiles, A., Marcos, M.D., Martínez-Máñez, R., & Barat, J.M. Towards the development of powerful antimicrobial "nanobullets" based on functionalized mesoporous silica particles. *Submitted to Biotechnology & Bioengineering*.

Ruiz-Rico, M., Pérez-Esteve, É., Bernardos, A., Sancenón, F., Martínez-Máñez, R., Marcos, M.D., & Barat, J.M. Enhanced antimicrobial activity of essential oil components immobilized in silica particles. *Submitted to International Journal of Antimicrobial Agents.*

Appendix III. Other scientific publications

Pérez-Esteve, É., **Ruiz-Rico, M**., de la Torre, C., Llorca, E., Sancenón, F., Amorós, P., Martínez-Máñez, R., Marcos, M. D., & Barat, J. M. (2016). Stability of different mesoporous silica particles during an *in vitro* digestion. *Microporous and mesoporous materials, 230,* 196-207.

Pérez-Esteve, É., **Ruiz-Rico, M**., de la Torre, C., Villaescusa, L. A., Sancenón, F., Marcos, M. D., Amorós, P., Martínez-Máñez, R., Barat, & J. M. (2016). Encapsulation of folic acid in different silica porous supports: a comparative study. *Food Chemistry, 196,* 66-75*.*

Pérez-Esteve, É., **Ruiz-Rico, M**., Fuentes, A., Marcos, M. D., Sancenón, F., Martínez-Máñez, R., & Barat, J. M. (2016). Enrichment of stirred yoghurts with folic acid encapsulated in pH-responsive mesoporous silica particles: Bioaccessibility modulation and physico-chemical characterization. *LWT-Food Science and Technology, 72,* 351-360.

Pérez-Esteve, É., **Ruiz-Rico, M**., Martínez-Máñez, R., & Barat, J. M. (2015). Mesoporous silica based supports for controlled and targeted release of bioactive molecules in the gastrointestinal tract. *Journal of Food Science. 80(11),* E2504-E2516.

Gutiérrez-Guzmán, N., Fernández-Segovia, I., Fuentes, A., **Ruiz-Rico, M.**, Barat, J.M. (2015). Physico-chemical and microbiological changes in commercial tilapia (*Oreochromis niloticus*) during cold storage*. VITAE, 22*(2), 140-147.

Zaragozá, P., Fuentes, A., **Ruiz-Rico, M.**, Vivancos, J.L., Fernández-Segovia, I., Ros-Lis, J.V., Barat, J.M., Martínez-Máñez, R. (2015). Development of a colorimetric sensor array for squid spoilage assessment. *Food Chemistry, 175*, 315-321.

Ruiz-Rico, M., Fuentes, A., Masot, R., Alcañiz, M., Fernández-Segovia, I., Barat, J.M. (2013). Use of the voltammetric tongue in fresh cod *(Gadus morhua)* quality assessment*. Innovative Food Science and Emerging Technologies*, 18, 256-263.

Fuentes, A., Masot, R., Fernández-Segovia, I., **Ruiz-Rico, M.**, Alcañiz, M., Barat, J.M. (2013). Differentiation between fresh and frozen-thawed sea bream (*Sparus aurata*) using impedance spectroscopy techniques. *Innovative Food Science and Emerging Technologies*, 19, 210-217.

Appendix IV. Book chapters

Ruiz-Rico, M., Pérez-Esteve, É., Jiménez-Belenguer, A., Ferrús, M. A., Martínez-Mañez, R., & Barat, J. M. (2015) Bactericidal effect of encapsulated caprylic acid on *Listeria monocytogenes*. In: Méndez-Vilas, A. (Ed.). *Multidisciplinary Approaches for Studying and Combating Microbial Pathogens*. Brown Walker Press (pp. 63-67).

Appendix V. Patents

Barat, J.M.; Marcos, M.D.; Martínez-Máñez, R.; Pérez-Esteve, E.; **Ruiz-Rico, M.;** Sancenón, F. Sistema antimicrobiano (Nº DE SOLICITUD: P201531075). Fecha de concesión: 16/06/2016.